Imperial College London

The mechanisms by which ANP32 proteins support the influenza polymerase

Bhakti D. Mistry

Supervised by Professor Wendy Barclay
Department of Virology
Faculty of Medicine

Submitted for degree of Doctor of Philosophy

Declaration of originality

I confirm that all work presented in this thesis, except where clearly stated, is my own. Any material from other sources has been acknowledged and a licence has been obtained for use of all figures from outside sources where permission was necessary.

Copyright declaration

‘The copyright of this thesis rests with the author. Unless otherwise indicated, its contents are licensed under a Creative Commons Attribution-Non Commercial 4.0 International Licence (CC BY-NC).

Under this licence, you may copy an redistribute the material in any medium or format. You may also create and distribute modified versions of the work. This is on the condition that: you credit the author and do not use it, or any derivative work, for a commercial purpose.

When reusing or sharing this work, ensure you make the licence terms clear to others by naming the licence and linking to the licence text. Where a work has been adapted, you should indicate that the work has been changed and describe those changes.

Please seek permission from the copyright holder for uses of this work that are not included in this licence or permitted under UK Copyright Law’.

Acknowledgments

Firstly, I would like to thank my supervisor, Professor Wendy Barclay. Thank you for all of the support, guidance and encouragement you have given to me over the past three years. I feel very lucky to have worked for such an intelligent, passionate and kind PI.

Thank you to all of the Barclay lab, both past and present members. I couldn't have asked for better people to work alongside. You have helped me to grow as a scientist and made my time here enjoyable. To Daniel for your motivation and 80% successful SWC, to Rebecca for always knowing the answer to every question, to Jocelyn for always smiling despite certain assays misbehaving, to Rob for all your endless support and to all of the ANP team for their ideas and discussions. Special thanks to Jason for being a great teacher and for all your help and advice throughout.

I would also like to thank my collaborators, Adam Cawte and David Rueda for all their help with the microscopy as well as Stuart Armstrong and Julian Hiscox for all their work on the mass spectrometry experiments.

Thank you to my family and friends especially to my parents, Rachna, Anand and Neil. I couldn't have done this without all your support, understanding and freshly cooked meals.

And finally, thank you to the Wellcome trust for funding my PhD, the Microbiology Society for funding my visits to several conferences and to Imperial College for hosting me.

Abstract

Influenza A naturally resides asymptomatically in wild aquatic birds. However, cross over into humans can occur and may result in a pandemic if the virus adapts for efficient replication and transmission between immunologically naïve human hosts. Fortunately, pandemics occur infrequently due to the existence of host range barriers. Poor replication of the influenza genome in the human cell nucleus is one of the main barriers that restricts avian origin influenza virus. The most common mutation which can overcome this block is the E627K mutation in the PB2 subunit of the trimeric influenza polymerase complex. Both the absence of a compatible positive factor or the presence of an inhibitory factor in human hosts have been proposed to explain why a polymerase bearing a glutamic acid at position 627 of PB2 is restricted in human cells.

Avian ANP32A has been identified as a host factor which can support the activity of an avian origin viral polymerase. However, this polymerase is not compatible with the shorter human orthologues of this protein, human ANP32A and ANP32B. Since these human proteins have been implicated in supporting the activity of a human adapted influenza polymerase, it is hypothesised that the PB2 E627K mutation is an adaptation towards utilising huANP32A and -B.

In this study we investigate how the ANP32A proteins are able to support polymerase activity and why species differences in this protein determine its compatibility with polymerases bearing different mutations. This was primarily examined by assessing differences in the interactions between specific ANP32A proteins and viral polymerases. We found that the

interactions with trimeric polymerase complex were dependent on the species of ANP32A. These interactions were stabilised at inactive ribonucleoproteins, but dissociated as replication of the viral genome occurred. However, using multiple methods, we concluded that the ability of viral polymerase to co-opt ANP32A was determined by more than differences in interactions alone.

As ANP32A can act as an adapter protein in some cases, we also investigated whether the interactome of the polymerase differed in the presence or absence of avian ANP32A. We further explored the impact of two human proteins, SRPK1 and importin α7, which differed in their interaction with avian origin polymerase when chicken ANP32A was co-expressed.

Finally, we visualised the viral polymerase by overexpression of PA-GFP in human cells and observed differences between an avian origin polymerase and that with humanising mutations. Specifically, the avian origin polymerase appeared to form speckles in the nucleus of human cells. We explored the requirements for formation of these speckles as well as their relationship with ANP32A.

This study has allowed us to gain insight into the mechanism by which ANP32A can support influenza virus polymerase. This was explored via several avenues, which led to the identification of other host factors which may affect polymerase activity. Overall, these data have enhanced our understanding of host restriction of influenza virus polymerase and the interplay between host and viral factors.

Table of Contents

Declaration of originality **2**

Copyright declaration **2**

Acknowledgements **3**

Abstract **4**

Table of contents **6**

List of figures 12

List of Tables 15

Acronyms and abbreviations 16

Chapter 1: Introduction **19**

1.1 Influenza virus 19

1.2 Classification and nomenclature 20

1.3 Host Reservoirs and Pandemics 20

1.4 Virion structure 25

1.5 Influenza A Virus Life Cycle 29

1.5.1 Cell entry 30

1.5.2 Nuclear entry 30

1.5.3 RNA synthesis 31

1.5.4 Nuclear export 33

1.5.5 Packaging and budding of new virions 34

1.6 RNP Structure 35
1.6.1 Viral Promoter 35
1.6.2 Viral Polymerase 37
1.6.3 Viral Nucleoprotein 40
1.7 Transcription and replication 40
1.7.1 Transcription 41
1.7.2 cRNA synthesis 43
1.7.3 vRNA synthesis 44
1.7.4 Regulation between transcription and replication 45
1.8 Host restriction 50
1.8.1 HA 50
1.8.2 NA 51
1.8.3 NP 51
1.8.4 NEP 52
1.8.5 Polymerase 53
1.8.5.1 DDX17 56
1.8.5.2 RIG-I 57
1.8.5.3 Importin-α proteins 57
1.9 ANP32 58
1.9.1 Structure 58
1.9.2 Family 60
1.9.3 Endogenous functions and roles in disease 60
1.9.3.1 mRNA export 61

1.9.3.2 PP2A inhibition 61

1.9.3.3 Development 62

1.9.3.4 Transcriptional regulation 62

1.9.3.5 Apoptosis 64

1.9.3.6 Organelle transport 65

1.9.4 The role of ANP32 in influenza A 65

1.9.5 Association of ANP32 with other viruses 69

1.10 Thesis aims and objectives 70

Chapter 2: Characterising interactions between ANP32A and the viral polymerase 72

2.1 Introduction 72

2.2 Results 73

2.2.1 Development of a split luciferase complementation assay to measure interactions 73

2.2.2 chANP32A binds to the trimeric polymerase to a greater extent than huANP32A 79

2.2.3 The interaction between ANP32A and the polymerase occurs in the nucleus of human cells 87

2.2.4 The 33 amino acids in chANP32A are responsible for the greater interaction with polymerase compared to huANP32A 89

2.2.5 Binding of chANP32A to the polymerase involves the 627 domain 91

2.2.6 Function of ANP32A is not determined by extent of binding to the trimeric polymerase 93

2.2.7 Interactions between the polymerase and ANP32A are stabilised at RNPs 98

2.2.8 Interactions between the polymerase and ANP32A subside when the polymerase is active 101

2.2.9 Promoter mutations that overcome host range restriction of viral polymerase do not negate the requirement for ANP32A 104

2.2.10 ANP32A interacts with NP 106

2.2.11 chANP32A is able to increase replication independently of NP 109

2.3 Discussion 110

Chapter 3: A mass spectrometry screen to identify differences in the interactome of AIV polymerase in the presence or absence of chANP32A, or due to adaptive mutations in the polymerase 116

3.1 Introduction 116

3.2 Results 118

3.2.1 Differences in the interactome of AIV polymerase in the presence or absence of chANP32A or human adapted polymerase 118

3.2.2 Characterisation of the role of SRPK1 in influenza polymerase activity 127

3.2.2.1 Validation of mass spectrometry results- SRPK1 127

3.2.2.2 SRPK1 interacts with the trimeric polymerase complex and with PB2 alone 129

3.2.2.3 SRPK1 does not interact with ANP32A 130

3.2.2.4 shRNA mediated knockdown of SRPK1 reduces polymerase activity 131

3.2.2.5 SRPK1 can support the activity of several influenza A polymerases 133

3.2.2.6 SRPK1 is localised in the nucleus and cytoplasm 134

3.2.3 Characterisation of the role of Importin α7 in influenza polymerase activity 136

3.2.3.1 Validation of mass spectrometry results-Importin α7 136

3.2.3.2 Importin α7 is coprecipitated with ANP32A 138

3.2.3.3 Knockdown of importin α7 does not affect entry of ANP32A into the nucleus 139

3.2.3.4 Effect of importin α7 on polymerase activity 141

3.3 Discussion 144

Chapter 4: Differences between nuclear location of avian and human adapted viral polymerases visualised by widefield microscopy 151

4.1 Introduction 151

4.2 Results..... 153

4.2.1 An avian origin polymerase forms speckles in the nuclei of human cells 153

4.2.2 The trimeric polymerase complex is the minimal requirement for formation of speckles 156

4.2.3 chANP32A decreases the proportion of speckled nuclei in cells expressing IAV polymerase 158

4.2.4 Reconstituted AIV polymerase from a different viral subtype also forms speckles in the nucleus of human cells 160

4.2.5 chANP32A 1-208 can affect the likelihood of speckled nuclei forming.....162

4.2.6 The human adapted viral polymerase forms speckles in the absence of huANP32A and -B 163

4.2.7 Speckles in avian cells expressing the AIV polymerase form less frequently 167

4.2.8 The formation of speckles negatively correlates with replication efficiency directed by different PB2 mutants 169

4.2.9 The speckles do not colocalise with previously described nuclear bodies 171

4.3 Discussion 172

Chapter 5: Discussion and Summary 177

Chapter 6: Materials and Methods 190

6.1 Materials 190

6.1.1 Cell lines 190

6.1.2 Antibodies 190

6.1.3 Plasmids 193

6.1.4 Oligonucleotides 203

6.1.5 Buffers 212

6.2 Methods 214

6.2.1 Cloning 214

6.2.2 Cell culture, transfections and complementation assays 219

6.2.3 RNA extraction and qRTPCR 223

6.2.4 shRNA induced silencing 224

6.2.5 Co-immunoprecipitations, western blotting and mass spectrometry 225

6.2.6 Immunofluorescence 230

6.2.7 Statistical analysis 232

References 233

Appendices 258

Appendix A 258

Appendix B 270

List of figures

Fig 1: Influenza virus hosts 21

Fig 2: Composition of pandemic strains 24

Fig 3: Structure of the influenza A virion 27

Fig 4: Influenza A life cycle 29

Fig 5: Influenza A genomic RNA synthesis 32

Fig 6: vRNP structure 36

Fig 7: Proposed structures of the vRNA promoter 37

Fig 8: Structure of Bat Influenza A polymerase with vRNA promoter 38

Fig 9: Glutamic acid at position 672 disrupts an area of positive charge 54

Fig 10: Structure of ANP32A LRR domain 59

Fig 11: ANP32 sequence alignment 68

Fig 12: Schematic of split luciferase complementation assay 75

Fig 13: Interactions between polymerase subunits can be measured using the split luciferase complementation assay 78

Fig 14: Interactions between polymerase subunits and chANP2A can be measured using the split luciferase complementation assay 80

Fig 15: $PB1_{luc1}$ and $chANP32A_{luc2}$ are functional proteins 82

Fig 16: chANP32A binds to the influenza polymerase to a greater extent than huANP32A 84

Fig 17: Interactions between the polymerase and ANP32A require the whole trimeric polymerase complex 86

Fig 18: Interactions between the polymerase and ANP32A occur in the nucleus of human cells..... 88
Fig 19: The 33 amino acids in chANP32A contribute to greater binding with polymerase compared to huANP32A..... 90
Fig 20: Binding of chANP32A involves the 627 domain of PB2 92
Fig 21: Interactions between chANP32A and the polymerase do not correlate with function 94
Fig 22: Differences in interactions between ANP32A and the polymerase do not explain function 96
Fig 23: The influenza polymerase can adopt multiple conformations 99
Fig 24: Interaction between ANP32A and polymerase is stabilised at RNP..... 100
Fig 25: Interaction between ANP32A and polymerase decreases when polymerase is active 102
Fig 26: ANP32A is required to replicate a template with mutations at 3’5’8..... 105
Fig 27: ANP32A interacts with NP..... 107
Fig 28: Viral polymerase disrupts the interaction between chANP32A and NP 108
Fig 29: chANP32A can rescue activity of the polymerase independently of NP..... 109
Fig 30: Mass spectrometry experimental condition..... 118
Fig 31: The PA-GFP fusion protein is functional 119
Fig 32: Comparison of protein abundances between conditions..... 121
Fig 33: Hypothetical models relating to mass spectrometry results..... 123
Fig 34: Identification of proteins coprecipitated with AIV polymerase which changed in abundance depending on the presence of chANP32A 124
Fig 35: Validation of binding pattern of SRPK1 revealed by mass spectrometry..... 128

Fig 36: SRPK1 interacts with the trimeric polymerase and to PB2 alone 129

Fig 37: SRPK1 does not coprecipitate with ANP32A-flag 130

Fig 38: shRNA mediated knockdown of SRPK1 reduces viral polymerase activity 132

Fig 39: Knockdown of SRPK1 reduces activity of various influenza A polymerases..... 133

Fig 40: Localisation of SRPK1 135

Fig 41: Validation of binding pattern of importin α7 revealed by mass spectrometry..... 137

Fig 42: Importin α7 coprecipitates with ANP32A-flag 138

Fig 43: knockdown of importin α7 does not affect subcellular distribution of ANP32A..... 140

Fig 44: Functional effects of importin α7 on polymerase activity..... 142

Fig 45: Speckles can be observed in cells expressing AIV polymerase 155

Fig 46: The trimeric polymerase is the minimum requirement for speckle formation..... 157

Fig 47: chANP32A decreases the proportion of speckled nuclei in cells expressing AIV polymerase 159

Fig 48: UDL viral polymerase displays same speckled pattern as 5092 viral polymerase 161

Fig 49: chANP32A1-208 decreases the proportion of speckled nuclei in cells expressing AIV 162

Fig 50: Influenza polymerase forms speckles in eHAP1 double knockout cells..... 164

Fig 51: Speckles in avian cells are observed less frequently 168

Fig 52: Other humanising mutations in PB2 affect speckle formation..... 170

Fig 53: Polymerase speckles do not colocalise with other known nuclear bodies 171

Fig 54: Model for the role of the avian specific 33 amino acids in chANP32A in preventing inhibition of AIV polymerase 184

List of tables

Table 1: Influenza A core proteins 28

Table 2: Host factors which support the influenza A polymerase 47

Table 3: Plasmids constructed for split luciferase complementation assays 76

Table 4: Predicted SUMOylation sites on SRPK1 126

Table 5: Cell lines used in this study 190

Table 6: Primary antibodies used in this study 190

Table 7: Secondary antibodies used in this study 192

Table 8: Main plasmids used in this study 193

Table 9: Oligonucleotides used in this study 203

Table 10: Buffers used in this study 212

Acronyms and Abbreviations

50-92	A/Turkey/England/50-92/91
aa	Amino acid
AIV	Avian influenza virus
ANP32A	Acidic leucine rich nuclear phosphoprotein 32 family member A
ANP32B	Acidic leucine rich nuclear phosphoprotein 32 family member B
ANP32E	Acidic leucine rich nuclear phosphoprotein 32 family member E
BSA	Bovine serum albumin
bp	basepair
cDNA	Complementary DNA
chANP32A	Chicken ANP32A
chANP32B	Chicken ANP32B
cRNA	Complementary RNA
cRNP	Complementary ribonucleoprotein
DDX17	Dead box helicase 17
DMEM	Dulbecco's modified eagle medium
DNA	Deoxyribonucleic acid
DNAJC7	DNAJ Heat shock protein family Member C7
Eng195	A/England/195/09
Gluc	Gaussia Luciferase
HA	Haemagglutinin
HEK 293T	Human embryonic kidney cells 293T
huANP32A	Human ANP32A
huANP32B	Human ANP32B
huANP32E	Human ANP32E
IAV	Influenza A virus
IFIT5	Interferon-induced protein with tetratricopeptide repeats 5
IMDM	Iscove's modified Dulbecco's medium
IN	Input
INHAT	Inhibitor of acetyl transferase

ISG	Interferon stimulated gene
kDa	Kilodalton
LCAR	Low complexity acidic region
LRR	Leucine rich repeat
M1	Matrix protein 1
M2	Matrix protein 2
mRNA	Messenger RNA
NA	Neuraminidase
NCR	Non-coding region
NEP	Nuclear export protein
NES	Nuclear export signal
NLS	Nuclear localisation signal
NP	Nucleoprotein
NS1	Non-structural protein 1
nt	Nucleotide
PA	Polymerase acidic protein
PD	Pulldown
PIAS2	Protein inhibitor of activated STAT 2
PIAS4	Protein inhibitor of activated STAT 4
PB1	Polymerase basic protein 1
PB2	Polymerase basic protein 2
PBS	Phosphate buffered saline
PCR	Polymerase chain reaction
RIG-I	Retinoic acid inducible gene I
RNA	Ribonucleic acid
RNP	Ribonucleoprotein
shRNA	Short hairpin RNA
SIM	SUMO interacting motif
siRNA	Short interfering RNA
SRPK1	Serine-Arginine rich protein kinase 1
Tky/05	A/turkey/Turkey/05/2005
TUFM	Elongaltion factor Tu, mitochondrial

UDL	A/chicken/Pakistan/UDL-01/2008
UTR	Untranslated region
Vic	A/Victoria/3/1975
vRNA	viral RNA
vRNP	viral ribonucleoprotein
WHO	World Health Oragnisation
WT	Wildtype

Chapter 1: Introduction

1.1 Influenza virus

Influenza viruses belong to the family of Orthomyxoviridae, which can be divided into seven genera; Influenza A, Influenza B, Influenza C, Influenza D, Isavirus, Thogotovirus and Quaranjavirus. Influenza viruses are respiratory pathogens responsible for seasonal epidemics and occasional pandemics. Symptoms of influenza virus infections include fever, headaches, coughing and malaise, with the severity of illness ranging from mild to fatal (WHO, 2018). The earliest reports of influenza like symptoms were in 412 BC in Ancient Greece. The first accepted pandemic was in 1580, although the virus was not isolated in a laboratory until 1932 (Potter, 2001). Infection by influenza virus continues to be a significant health burden with the World Health Organisation estimating 3-5 million severe cases and 290000-650000 deaths per year due to seasonal epidemics (WHO, 2018). Emergence of pandemic strains have resulted in significant mortality, and the threat of future pandemics remains almost an inevitability. Influenza is a rapidly evolving virus requiring the need for constantly updated vaccines and the development of new drugs.

1.2 Classification and Nomenclature

Influenza A viruses are characterised depending on the subtype of the haemagglutinin (HA) and neuraminidase (NA) glycoproteins, found on their surface. 18 HA (H1-H18) and 11 NA (N1-N11) subtypes have so far been discovered. H1-H16 and N1-N9 viruses have been isolated from wild aquatic birds, with some subtypes also infecting other species (Long *et al.,* 2019). H17-H18 and N10-N11 have so far only been isolated from bats (Tong *et al.,* 2012; Tong *et al.,* 2013). Influenza B viruses are divided into lineages. Viruses from the B/Yamagata and B/Victoria lineages currently circulate in humans.

The accepted nomenclature for influenza viruses is as follows; influenza type, species in which it was isolated (not included if isolated from humans), location, isolate number, year of isolation, HA and NA subtype (for influenza A virus only). For example, A/Turkey/England/50-92/91 (H5N1) denotes isolate 50-92 of an influenza A virus isolated from a turkey in England in 1991, with H5 and N1 surface glycoproteins.

1.3 Host Reservoirs and Pandemics

Influenza viruses infect a wide range of hosts **(Fig 1)** (Long *et al.,* 2019). The natural reservoir of influenza A viruses are wild aquatic birds, but these viruses can infect a wide range of species including humans. (Long *et al.,* 2019). Influenza B and C mainly infect humans, although infection by influenza C is not considered to be a significant health burden. Influenza D has been isolated from cattle, pigs and goats. Serological evidence suggests that influenza D is able to infect humans in close contact with these animals, however human to human

transmission has not been reported (White *et al.,* 2016). Zoonosis of influenza A viruses have been the cause of all major pandemics in the last century and the potential of further zoonosis events of influenza A viruses remains the most prominent threat. (Long *et al.,* 2019).

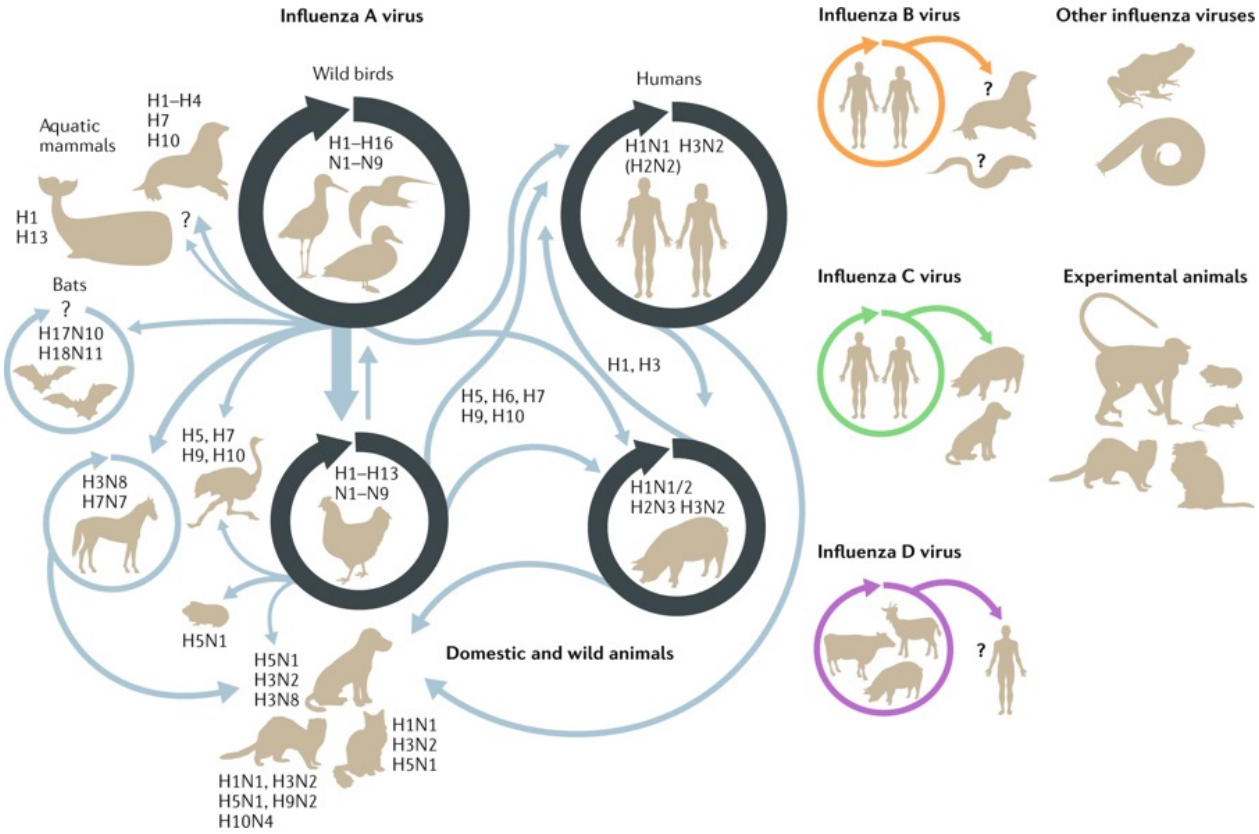


Fig 1: Influenza virus hosts

Image from Long *et al.,* 2019. The main reservoir of influenza A H1-H16 and N1-N9 subtypes are wild birds. However, these viruses can also infect many other species, although adaptive mutations may need to be acquired to do so (blue arrows). Circles represent instances where specific subtypes have become established in a population. The main reservoir of influenza B and C is humans, although infection in other species has been reported. Influenza D viruses infect cattle, goats and pigs. It is not clear whether they can infect humans. Influenza like RNA has also been isolated from Wuhan Asiatic toads and spiny eels, although the genera of this has not been identified. Macaques, guinea pigs, mice, ferrets and marmosets have been used for experimental purposes.

The influenza A genome consists of single stranded, negative sense RNA, separated into eight segments which encode ten core proteins (described in section 1.4) (Bouvier and Palese, 2008). Influenza A evolution is driven by both antigenic drift and antigenic shift. Antigenic drift refers to the occurrence of mutations in the viral genome, whilst antigenic shift refers to the re-assortment of viral gene segments made possible by co-infection of cells by more than one virus. Introduction of an antigenically novel virus, which has acquired sufficient mammalian adaptive mutations, into the human population, can result in a pandemic. Following the emergence of pandemic strains, these viruses continue to circulate as seasonal influenza, often displacing the previous seasonal influenza strain. Seasonal influenza strains continue to undergo antigenic drift, hence the requirement for annually updated influenza A vaccines (Long *et al.,* 2019).

Since 1900, there have been four major pandemics. The most severe was the 1918 'Spanish flu' pandemic, caused by a H1N1 influenza strain. This strain killed 50-100 million people, most of who were healthy young adults. Evidence suggests that all segments from this pandemic virus were of avian origin, although there is controversy surrounding this (Neumann and Kawaoka, 2015).

Re-assortment between the resulting seasonal H1N1 influenza strain and a H2N2 avian strain caused the 1957 'Asian flu' pandemic. This virus was formed of the HA, NA and PB1 segments of the avian influenza virus whilst the other five segments were retained from the circulating H1N1 virus strain (Neumann and Kawaoka, 2015).

The H3N2 'Hong Kong flu' pandemic occurred in 1968. Again, this was formed by re-assortment between the circulating H2N2 strain and a virus of avian origin. In this case, the

virus was composed of the HA and PB1 segments from the avian strain and retained the remaining six segments from the circulating H2N2 influenza strain (Neumann and Kawaoka, 2015).

In 1977, a H1N1 strain emerged. This virus had similarities to that which was circulating in the 1950s, however the origin of this virus remains unknown (Nakajima *et al.,* 1978). Both the H3N2 virus and H1N1 viruses circulated in the human population until 2009, when the H1N1 'Swine flu' pandemic virus strain emerged. This H1N1 virus was the result of multiple re-assortment events. First, re-assortment between the human H3N2 virus, a North American avian virus and classical swine virus resulted in a H3N2 triple re-assortant. This virus subsequently re-assorted with a classical swine virus to form a H1N2 virus. Finally, this virus re-assorted with a Eurasian avian like swine virus to form the 2009 H1N1 pandemic strain. This virus was composed of NA and M segments from the Eurasian swine strain and retained the other six segments from the H1N2 virus. This virus displaced the previously circulating H1N1 seasonal strain, but the H3N2 strain remained in circulation. These two viruses as well as two influenza B viruses, currently circulate in the human population (Neumann and Kawaoka, 2015; Tscherne and Garcia-Sastre, 2011). The emergence and composition of the pandemic strains from the 20th and 21st centuries are illustrated in **Fig 2.**

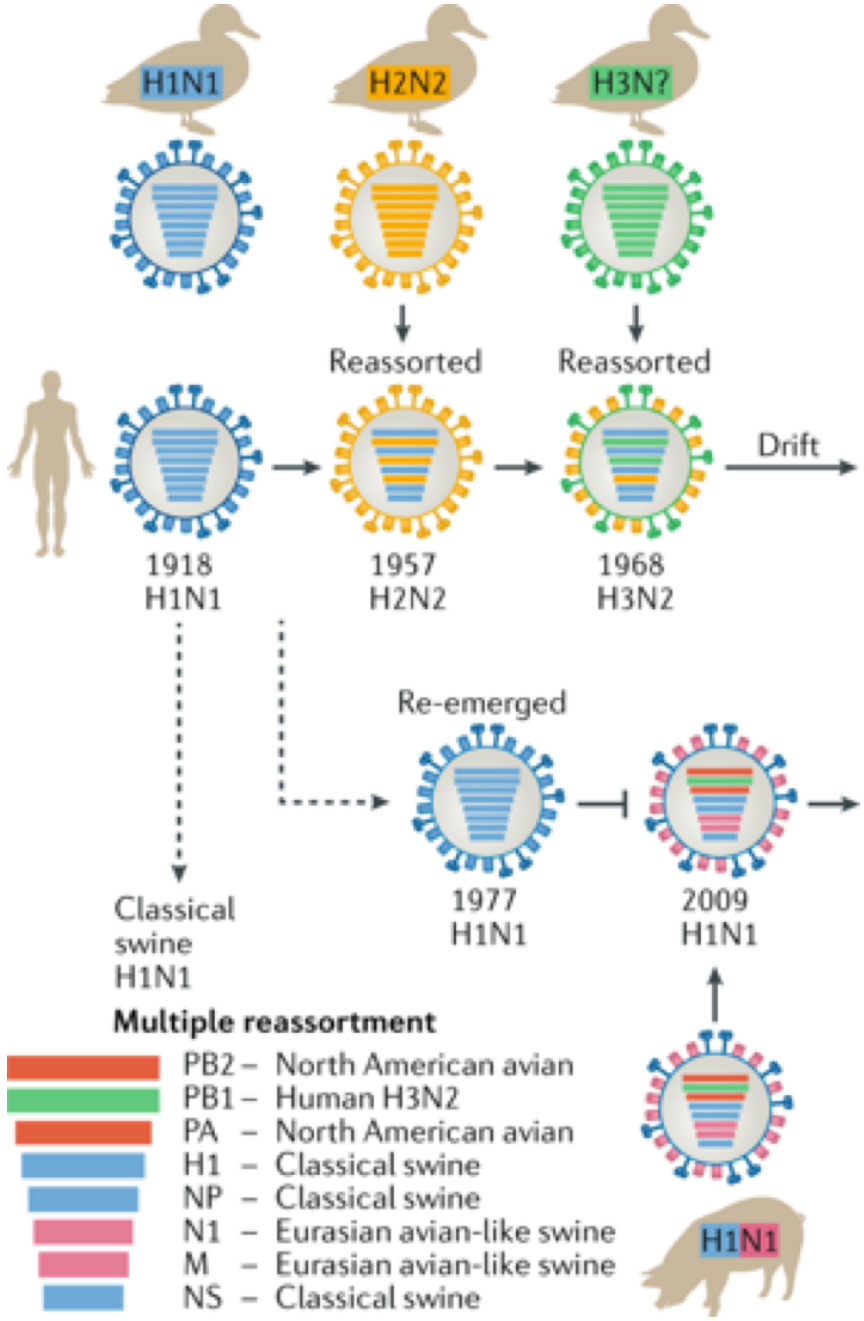


Fig 2: Composition of pandemic strains

Image from Long *et al.,* 2019. All segments of the 1918 pandemic H1N1 virus were thought to originate from an avian source. Re-assortment of segments from this virus and H2N2 avian strain resulted in the 1957 H2N2 pandemic virus. Re-assortment of this virus with a H3 avian strain resulted in the 1968 H3N2 pandemic virus strain. In 1977, a H1N1 strain similar to that from the 1950s emerged. Multiple re-assortment events resulted in the 2009 pandemic H1N1 strain. The origins of each segment are illustrated. The H3N2 and H1N1 influenza A strains (along with two influenza B viruses) currently circulate in the human population, but continue to undergo antigenic drift.

The most recent threats to the human population are highly pathogenic H5N1 and low pathogenic H7N9 viruses, which circulate in avian species (Sutton, 2018). The first case of H5N1 in humans was reported in 1997 in Hong Kong. Since then a total of 860 cases have been confirmed with 454 deaths, equating to a fatality rate of over 50 % (WHO, 2018).

The first emergence of H7N9 in humans was reported in 2013 in China. Since then, there have been 1567 cases and 615 deaths in over 16 different countries, culminating in an approximately 40 % fatality rate. There have also been sporadic cases of H6, H7 and H9 as well as some swine viruses jumping into humans (WHO, 2018)

So far, transmission has been due to close contact with poultry. Although cases of human to human transmission have been reported, the ability to sustain human transmission has not yet been acquired by these viruses. However, several studies have revealed that as few as five mutations in A/Indonesia/5/2005 (H5N1) may allow airborne transmission between ferrets (Herfst *et al.,* 2012; Linster *et al.,* 2014).

1.4 Virion Structure

Influenza A is a pleomorphic virus which can display both spherical or filamentous morphologies. Typically, spherical virions are 100 nm in diameter and filamentous virions can be 30 μm in length (Badham and Rossman, 2016). The advantages of a particular morphology are not clear.

The influenza structure is illustrated in **Fig 3.** Influenza A is an enveloped virus. This envelope is acquired from host cells during budding and contains three essential viral proteins; haemagglutinin (HA), neuraminidase (NA) and matrix 2 protein (M2). HA is the most abundant, followed by NA then M2. Beneath the envelope lies a coat produced by oligomerisation of viral matrix 1 protein (M1). The eight viral genome segments, which encode the ten core viral proteins, are contained within the virion. Each negative sense viral RNA (vRNA) is bound at the promoter region by the heterotrimeric polymerase complex consisting of polymerase basic 1 (PB1), polymerase basic 2 (PB2) and polymerase acidic (PA) proteins. The remaining vRNA is encapsidated with nucleoprotein (NP) in a helical structure. Each structure is known as a viral ribonucleoprotein (vRNP). Non-structural protein 1 (NS1) and nuclear export protein (NEP) are also found within the virion (Hutchinson *et al.,* 2014). The size and functions of each core protein are described in **Table 1**. Virions also comprise many host factors, incorporated from the host cell during budding (Hutchinson *et al.,* 2014; Shaw et al., 2008). In addition to the ten core proteins, various accessory proteins encoded by the viral gene segments have also been discovered. These include PB2-S1 (Yamayoshi et al., 2016), PB1-N40 (Wise et al., 2009), PB1-F2 (Chen et al., 2001), PA-X (Jagger et al., 2012), PA-N155 (Muramoto et al. ,2013), PA-N128 (Muramoto et al. ,2013), M3 (Lamb et al., 1981), M4 (Shih et al., 1998), M42 (Wise et al., 2012), NS3 (Selman et al., 2012) and NEG8 (Zhirnov et al., 2007). Many of these proteins are formed by translation from alternative start sites due to leaky ribosome scanning. PB1-F2 is implicated in cell death and pathogenesis (Chen et al., 2001; Zamarin et al., 2006). PA-X functions to inhibit cellular gene expression as well as modulating the host response to infection (Jagger et al., 2012). The function of the other accessory proteins remains largely unknown.

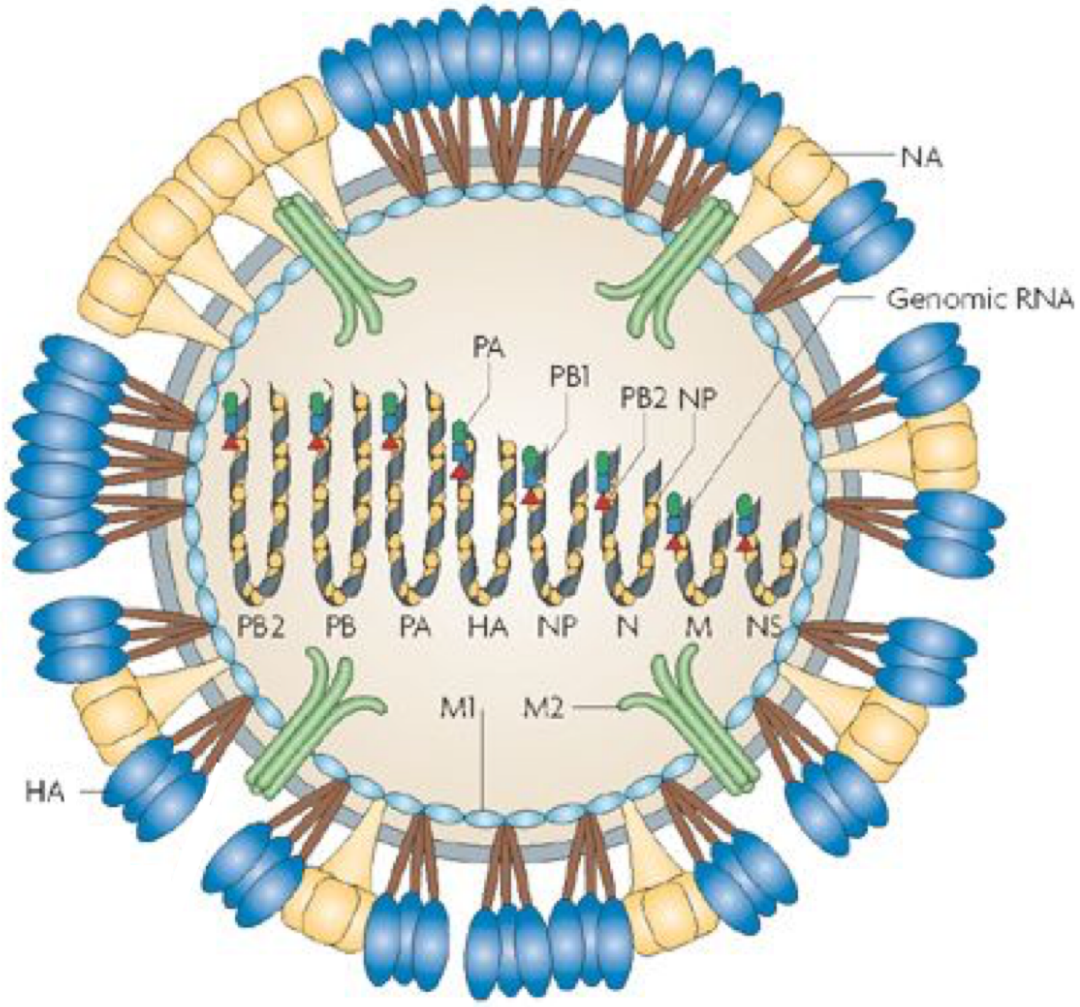


Fig 3: Structure of the influenza A virion

Image adapted from Karlsson Hedestam *et al.,* 2008. HA, NA and M2 are embedded in the lipid envelope acquired from host cells. Underneath lies a layer of oligomerised M1. Negative sense genomic RNA is encapsidated by NP and bound at promoters by the heterotrimeric polymerase complex consisting of PB1, PB2 and PA. Each segment encodes at least one core protein and may also encode various accessory proteins.

Segment	Segment Length (nucleotides)	Protein	Protein Length (Amino acids)	Function
1	2341	PB2	759	Polymerase subunit, recognises cap structures on host mRNAs
2	2341	PB1	757	Polymerase subunit, possesses catalytic activity
3	2233	PA	716	Polymerase subunit, cleaves cap off host mRNAs
4	1778	HA	550	Surface glycoprotein, binds to sialic acid residues on the cell surface
5	1565	NP	498	Coats vRNA and cRNA within v- and cRNPs, respectively, promotes nuclear import of vRNPs
6	1413	NA	454	Surface glycoprotein, cleaves sialic acid residues at cell surface to allow virus release
7	1027	M1	252	Forms scaffold inside virion and binds vRNPs, involved in vRNP export, budding
		M2	97	Proton channel required for release of vRNPs from M1, membrane scission
8	890	NS1	230	Interferon antagonist
		NEP/NS2	121	Replication, vRNP export

Table 1: Influenza A core proteins. Adapted from Bouvier and Palese, 2011. Summary of the size and function of the core proteins encoded by the eight segments of Influenza A virus. Lengths based on A/Puerto Rico/8/1934 (H1N1).

1.5 Influenza A Virus Life Cycle

A summary of the influenza A virus life cycle is described below and illustrated in **Fig 4.**

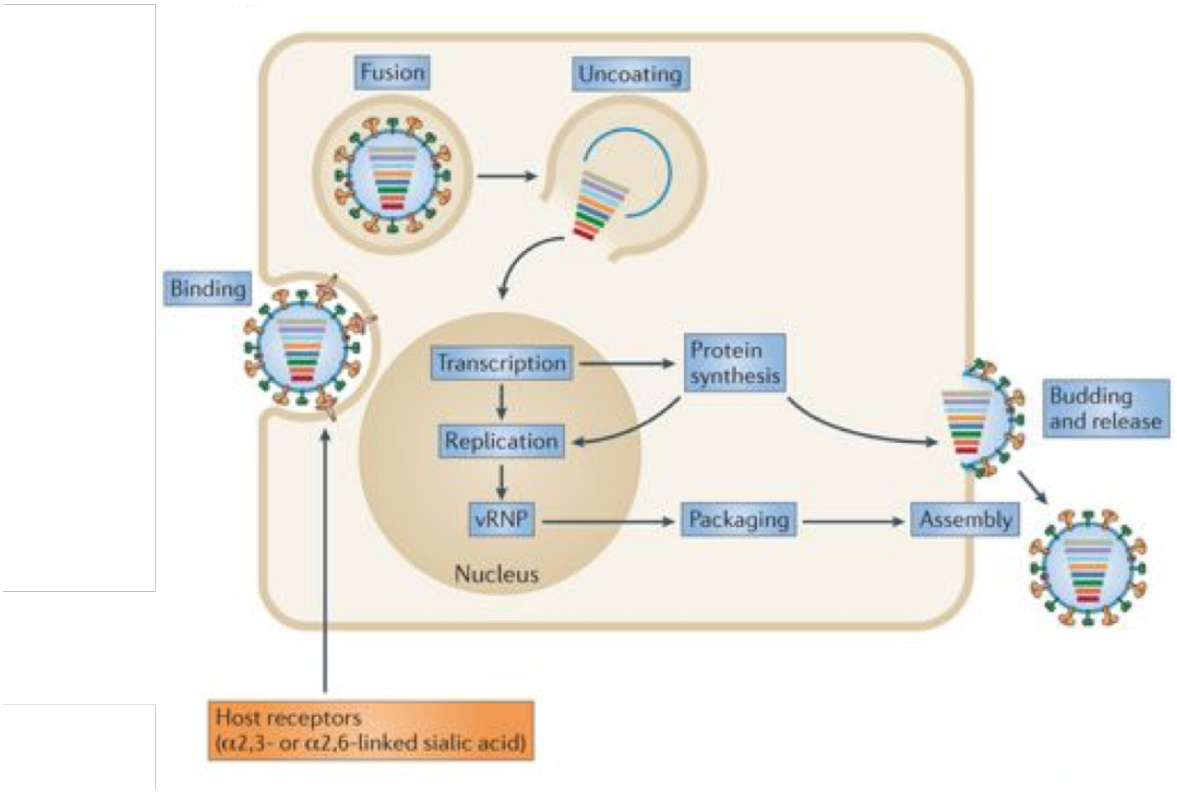


Fig 4: Influenza A life cycle
Image adapted from Shi *et al.,* 2014. Binding is mediated by interactions between viral haemagglutinin and sialic acid receptors on host cells Sialic acid residues can be either α2,3 or α2,6 linked to the penultimate galactose. Once endocytosed, acidification of the endosome causes fusion between the host and viral membranes resulting in the creation of a pore. Acidification of the viral particle mediated by M2 enable release of the vRNPs into the cytoplasm. vRNPs are translocated into the nucleus where the genome is transcribed and replicated. mRNA is translated into proteins. HA, NA and M2 are translocated to the cell membrane, whilst the rest of the proteins re-enter the nucleus to allow formation of progeny vRNPs. These vRNPs can undergo further replication or exit the nucleus to be packaged into a new virion. Budding of progeny virions occurs at the cell membrane and the virions are released from the cell by NA, which cleaves sialic acid residues.

1.5.1 Cell entry

The first step in the influenza A life cycle is attachment to host cells. This is mediated by interactions between HA molecules on the viral surface and sialic acid moieties on the surface of host cells (reviewed in Bouvier and Palese, 2008). Sialic acids are found at the termini of many glycoproteins or glycolipids and may be linked to galactose via its carbon-2 to either carbon-3 or carbon-6, giving rise to α2,3 or α2,6 linkages, respectively. The nature of these linkages is one of the determinants of host range (discussed in section 1.8.1) (Long *et al.,* 2019). Following binding, the virus is internalised. Internalisation is thought to be primarily carried out by clathrin mediated endocytosis (Matlin *et al.,* 1981), although macropinocytosis (Rossman *et al.,* 2012) and clathrin independent endocytosis (Sieczkarski and Whittaker, 2002) have also been shown to occur. These processes can be regulated by signalling pathways involving Ca^{2+} and as such it has been demonstrated that binding of HA to sialyated voltage dependent Ca^{2+} channels triggers an influx of Ca^{2+} into the cell, initiating internalisation (Fujioka *et al.,* 2013; Fujioka *et al.,* 2018).

1.5.2 Nuclear entry

The acidic environment of the endosome triggers a conformational change in the HA molecule, resulting in exposure of the hydrophobic fusion peptide. This peptide mediates the fusion of the viral and endosomal membranes creating a pore to allow release of vRNPs from the endosome. Before they are released however, the M2 channel must pump protons from the endosome into the viral particle in order to disrupt interactions between M1 and vRNPs and allow their release (Martin and Helenius, 1991b). The initial release of vRNPs from the M1 coat is mediated by HDAC6 and cellular motor proteins including myosin II and actin

filaments (Banerjee *et al.,* 2014). Transportin-1 interacts with an NLS on M1, which is exposed upon acidification. This interaction removes any M1 still bound to vRNPs to allow separation of the vRNPs from one another (Miyake *et al.,* 2019).

Unlike many RNA viruses, influenza A replicates in the nucleus of host cells. Therefore, the vRNPs released from virions must make their way from the cytoplasm into the nucleus. The nuclear membrane contains nuclear pore complexes, which allow passive diffusion of small proteins (Paine *et al.,* 1975). However, vRNPs must utilise host proteins to be actively imported into the nucleus. Although all protein components of the vRNP harbour nuclear localization sequences (NLS) (Li *et al.,* 2015), transport of vRNPs into the nucleus is mediated by an NLS at the N terminus of NP via binding to importin α proteins which in turn binds to importin β proteins. (O'Neill *et al.,* 1995).

1.5.3 RNA synthesis

Once in the nucleus, the vRNA is transcribed by the resident viral polymerase within the vRNP to generate mRNA **(Fig 5)**. Transcription is a primer dependent process. This primer is acquired by binding and cleavage of host mRNAs by the viral polymerase in a process termed 'cap snatching' (Bouloy *et al.,* 1978). Elongation continues until the polymerase reaches a stretch of five to seven uracil residues. This causes stuttering of the polymerase and subsequent formation of a polyadenylated tail (Poon *et al.,* 1999).

The influenza A viral polymerase also carries out replication of the vRNA **(Fig 5)**. This is achieved through a cRNA intermediate. Unlike transcription, replication does not require a primer and occurs *de novo*. The cRNA generated is an exact complement of the vRNA. cRNA are incorporated into cRNPs, similar to vRNPs, before being synthesised back into vRNA (te

Velthuis *et al.,* 2016b; York *et al.,* 2013). It is thought that synthesis of vRNA from cRNA requires the presence of multiple viral polymerase complexes (Jorba *et al.,* 2009; York *et al.,* 2013). A more detailed description of transcription and replication can be found in section 1.7.

The viral mRNA synthesised is translocated to the cytoplasm and translated into viral proteins using host cell machinery. These proteins are then imported back into the nucleus to aid further replication or to be packaged into new virions. Reformation of the heterotrimeric polymerase complex occurs in the nucleus. PB2 is imported back into the nucleus by binding to importin α proteins, whereas PB1 and PA are thought to be imported as a dimer in a RanBP5 dependent manner (Deng *et al.,* 2005; Fodor and Smith, 2004). An alternative model suggests that PB1 and PB2 are imported as a dimer whilst bound to Hsp90 (Naito *et al.,* 2007b).

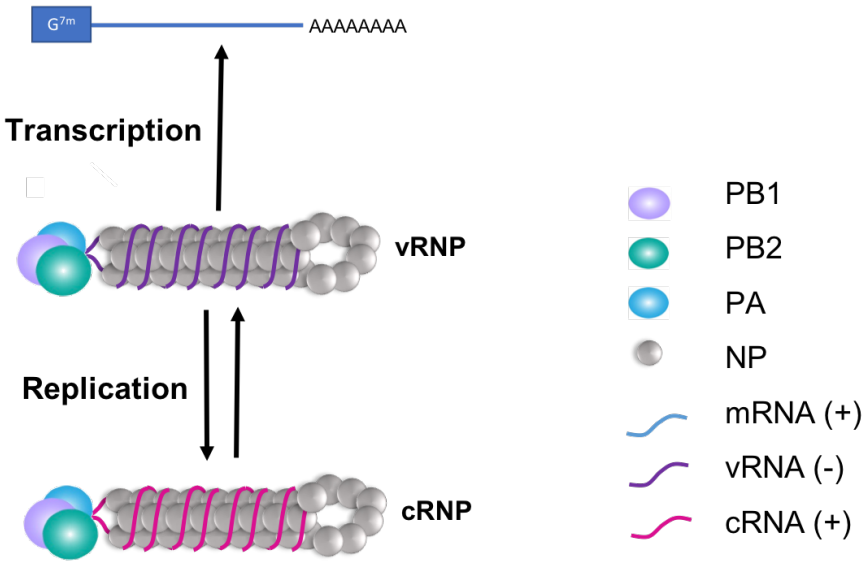


Fig 5: Influenza A genomic RNA synthesis
Image partly adapted from Cauldwell *et al.,* 2014. The influenza polymerase transcribes negative sense vRNA to produce positive sense mRNA. The 5' end of the mRNA contains a cap structure obtained from host mRNAs and a polyadenylated tail at its 3' end formed by stuttering of the viral polymerase. The viral polymerase also replicates vRNA, via a positive sense cRNA intermediate. The 5' and 3' promoters of both vRNA and cRNA are bound by the viral polymerase, whilst the remaining RNA is bound to NP to form vRNPs or CRNPs.

1.5.4 Nuclear export

In order to be packaged into new virions, the vRNPs must first be exported out of the nucleus. Although NP does harbour a nuclear export signal (NES), export of vRNPs requires both M1 and NEP (Bui *et al.,* 2000; Martin and Helenius, 1991a; O'Neill *et al.,* 1998). In the 'daisy chain' model of vRNP export, vRNPs are bound to M1, which are in turn bound to NEP. Binding of NEP to the nuclear export protein, CRM1, through two NES motifs at its N terminus, facilitates export. A subsequent study indicated that the C terminus of NEP binds simultaneously to both M1 and polymerase subunits within the vRNP and that this interaction is required for stabilisation of the interactions between M1 and NP (Brunotte *et al.,* 2014). The interaction between M1 and NP also prevents re-entry of vRNPs into the nucleus (Whittaker *et al.,* 1996). Although the mechanism by which this occurs is unknown, one possibility is that M1 blocks the NLS on NP, preventing it from being recognised by importin α proteins.

It is currently unclear how the timing of export of vRNPs is regulated. Several studies have shown temporal regulation of synthesis of specific viral segments. Preferential synthesis of NS1 and NP occur early in infection, whereas preferential synthesis of HA, NA and M1 occurs later during infection (Shapiro *et al.,* 1987; Smith and Hay, 1982). Furthermore, NEP is generated though splicing of NS1 using a suboptimal splice site, resulting in only gradual accumulation of NEP as infection progresses. (Chua *et al.,* 2013). Early synthesis of NS1 and NP may allow evasion of the innate immune response and efficient replication, respectively. As infection progresses, accumulation of M1 and NEP may favour vRNP export. Moreover, accumulation of HA at the cell membrane can activate MAPK signalling pathways which enhance vRNP export, further supporting the idea that temporal regulation of viral protein synthesis may regulate the timing of export (Marjuki *et al.,* 2006).

After exiting the nucleus, the vRNPs must find their way to the plasma membrane at sites of HA, NA and M2 accumulation (Leser and Lamb, 2005). vRNPs accumulates at microtubule organising centres near the nucleus and travel to the plasma membrane using the microtubule network, whilst bound to Rab11 endosomes (Amorim *et al.,* 2011). However, a study by Nturibi *et al.,* demonstrated that multicycle replication of influenza A virus could still occur in the absence of intact microtubules suggesting that other mechanisms of vRNP transport may also exist (Nturibi *et al.,* 2017).

1.5.5 Packaging and budding of new virions

An infectious virion must contain one copy of each of the eight viral segments. It is unclear how this is achieved, however two models have been proposed. The first model suggests that packaging of vRNPs occurs at random and those that happen to contain all eight segments go on to achieve productive infection. Other evidence suggests that packaging of vRNPs is a regulated process. Each segment comprises a unique bipartite packaging signal enabling specific incorporation of each segment into the virion (Hutchinson *et al.,* 2010). Further evidence for this model comes from electron microscopy studies in which the eight segments can be visualised forming a 1 + 7 arrangement (Noda *et al.,* 2006). Interestingly, virions which were generated without HA using a reverse genetics system were still shown to form the 1 + 7 arrangement. These virions incorporated rRNA into an RNP like structure in place of the HA vRNP suggesting that this arrangement is important for budding. (Noda *et al.,* 2018). Although it is not known how this forms, RNA-RNA interactions between different segments have been observed (Gavazzi *et al.,* 2013).

Budding occurs from sites of HA, NA and M2 protein within the plasma membrane. These sites are usually enriched with sphingolipids and cholesterol (Leser and Lamb, 2005). Accumulation of HA and NA at these sites contributes to initiation of budding whilst M2 contributes mainly to membrane scission. Underneath the membrane, the vRNP bound M1 proteins form a layer through interactions with HA and NA cytoplasmic tails. M1 is also thought to form interactions with M2 (Rossman *et al.,* 2011).

Finally, in order for the progeny virions to be released, NA must cleave sialic acids to prevent HA from binding to that same cell and allow infection of other cells (Reviewed in Dou *et al.,* 2018).

1.6 RNP Structure

1.6.1 Viral Promoter

Each of the eight vRNA segments are bound by the heterotrimeric viral polymerase and multiple NP proteins to form vRNP complexes **(Fig 6)**. Flanking the coding nucleotides of each segment are non-coding regions. Within this, the terminal 13 nucleotides from the 5' end and 12 nucleotides from the 3' end, constitute the viral promoter. These nucleotides, which are partially complementary, are conserved between segments and are bound by the viral polymerase (Ferhadian *et al.,* 2018). Several structures of the vRNA promoter region have been proposed **(Fig 7)**. Hsu et al proposed that the terminal vRNA ends form a panhandle structure whereby the complementary nucleotides form base pairs (Hsu *et al.,* 1987). Fodor et al., subsequently proposed the fork model whereby base-pairing occurs between the noncoding regions, however the extreme termini of the vRNA are single stranded (Fodor *et*

al., 1994). Next, Flick et al., proposed the corkscrew model whereby small stem loops are formed by the terminal nucleotides, followed by base-pairing between the two noncoding regions (Flick *et al.,* 1996). A crystal structure in which the polymerase was shown bound to vRNA revealed that the vRNA forms a corkscrew-like structure whereby the 5' terminus forms a step loop, termed the 5' 'hook', but the 3' strand remains single stranded (Pflug *et al.,* 2014). It is believed that in the absence of polymerase, the promoter forms a panhandle structure, whereas upon binding to polymerase it adopts the corkscrew-like hook structure (Noble *et al.,* 2011; Pflug *et al.,* 2014).

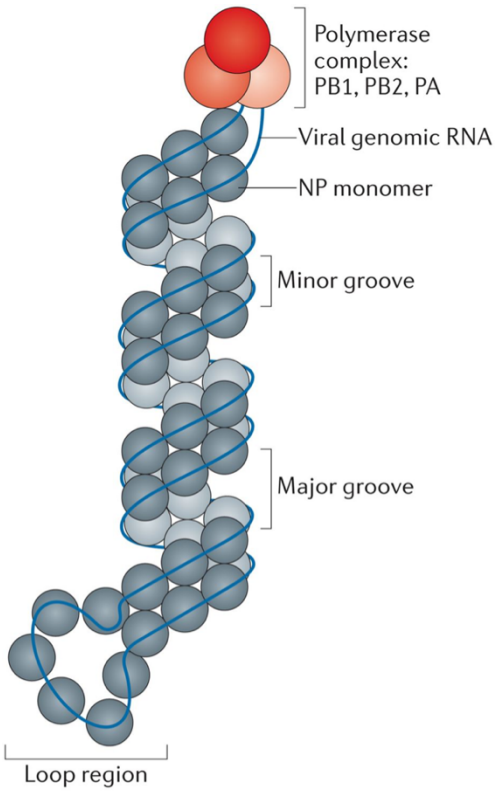


Fig 6: vRNP structure
Image from Eisfeld *et al.,* 2015. vRNPs consist of genomic RNA bound by the heterotrimeric polymerase complex at the promoter region. The remaining RNA is encapsidated by NP. Contacts between NP monomers promote formation of an antiparallel double helix, resulting in minor and major grooves and a loop at the far end of the structure.

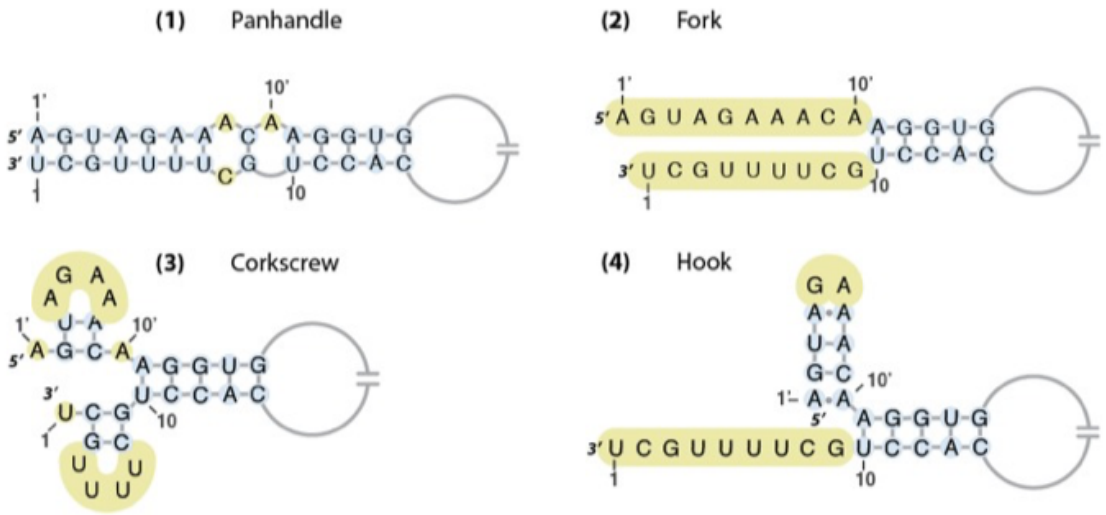


Fig 7: Proposed structures of the vRNA promoter
Image adapted from Ferhadian *et al.,* 2018. Illustrations of the proposed structures of the influenza A vRNA promoter. Nucleotides highlighted in blue are double stranded regions, those highlighted in yellow represent unpaired nucleotides.

1.6.2 Viral Polymerase

The influenza A viral polymerase is a heterotrimer of approximately 270 kDa composed of PB1, PB2 and PA subunits. Human influenza A polymerase is known to be difficult to purify, but structures have been solved for bat influenza A virus **(Fig 8)** as well as human influenza B and C (Hengrung *et al.,* 2015; Pflug *et al.,* 2014; Reich *et al.,* 2014; Reich *et al.,* 2017; Thierry *et al.,* 2016). These structures reveal distinct domains within each protein in the complex **(Fig 8)**.

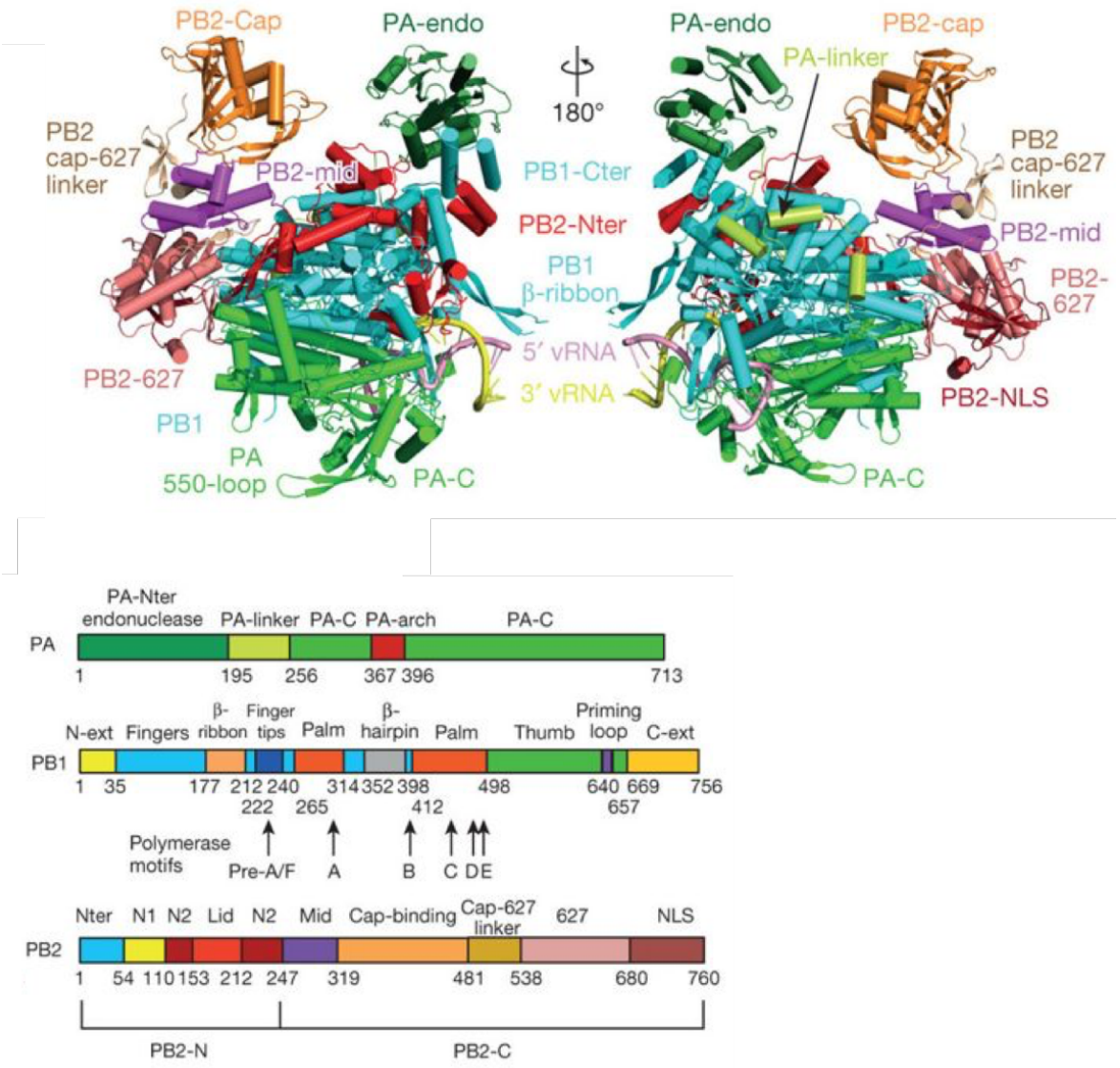


Fig 8: Structure of Bat Influenza A polymerase with vRNA promoter

Image from Pflug *et al.,* 2014. Crystal structure of the bat influenza A polymerase bound to promoter vRNA viewed from two angles. Schematic of domains within each subunit of the polymerase are illustrated below. The same colour code is used in the ribbon structure and schematic apart from the PA-C, which is all green, PB1 which is all cyan and PB2-N, which is all red in the ribbon structure.

PA encompasses two main domains, an N terminal endonuclease domain and a C terminal domain. These domains are positioned on opposite sides of the PB1 subunit, with a linker region wrapping around PB1 and connecting the two domains (Pflug et al., 2014).

The PB1 subunit possesses the catalytic activity and has been observed to form a right-handed fold, which is characteristic of RNA dependent RNA polymerases. This fold consists of finger, fingertip, palm and thumb domains within which lie the well conserved Pre-A (also called F) and A-E motifs (Pflug et al., 2014). N and C terminal extensions are responsible for interactions with PA and PB2, respectively. The β-hairpin highlighted in Fig 8 is associated with binding the 5' vRNA template, whereas residues in the C terminal extension are involved in binding the 3' vRNA template. A priming loop required for cRNA synthesis is formed of an anti-parallel β-loop which exists within the thumb domain (Pflug et al., 2014 and te Velthuis *et al.,* 2016b).

The PB2 subunit consists of a series of modules at its N terminus followed by the cap binding domain, which is separated from the host determinant 627 domain by a linker. Following the 627 domain is the NLS domain (Pflug et al., 2014).

Interestingly, the polymerase has been shown to undergo conformational changes dependent on whether influenza viral-like RNA is bound and whether this is in the positive or negative sense (Hengrung *et al.,* 2015; Pflug *et al.,* 2014; Reich *et al.,* 2014; Reich *et al.,* 2017; Thierry *et al.,* 2016). This suggests that the polymerase is a dynamic structure and different conformations may be stabilised when carrying out specific processes or when binding to particular host or viral factors.

1.6.3 Viral Nucleoprotein

The internal region of the vRNP structure forms an anti-parallel double helix, which is stabilized through interactions between NP monomers (Arranz *et al.,* 2012; Moeller *et al.,* 2012). NP coats the RNA through interactions involving the phosphate backbone of vRNA and multiple residues within NP (Elton *et al.,* 1999), with one NP molecule for approximately every 24 nucleotides (Ortega *et al.,* 2000). Since the vRNA within vRNPs is sensitive to RNase degradation, it is believed that vRNA lies on the outside of vRNPs (Baudin *et al.,* 1994). NP is also able to bind viral polymerase subunits and is thought to function as an elongation factor (Biswas *et al.,* 1998; Honda *et al.,* 1998; Vidic *et al.,* 2016).

Oligomerization of NP requires interactions between the tail loop of one monomer and a groove in the body domain of the adjacent NP monomer (Ye *et al.,* 2006). Regulation by phosphorylation of Ser 165 within the tail binding groove of NP determines whether NP is able to forms oligomers (Turrell *et al.,* 2015). Phosphorylation and dephosphorylation by PKC-δ and CDC25B, respectively, are implicated in this regulation (Cui *et al.,* 2018; Mondal *et al.,* 2017).

1.7 Transcription and replication

The influenza A viral polymerase carries out both transcription and replication of its genome. As with every other stage in the virus life cycle, transcription and replication of the influenza genome requires the help of many host factors. The section below details the mechanisms of transcription and replication, including some of the main host factors known to facilitate

these processes. A comprehensive list of host factors which have been implicated in functionally aiding these processes is included in **Table 2**.

1.7.1 Transcription

Synthesis of viral mRNA requires a primer which is acquired from 7-methyl guanosine capped host mRNAs through a process known as 'cap snatching' (Bouloy *et al.,* 1978; te Velthuis *et al.,* 2016a). Cap snatching requires a close association with host RNA Polymerase II (RNAPII). The C terminal domain (CTD) of RNAPII consists of 52 heptad repeats. Differential phosphorylation of serine residues within these repeats occurs at different points during transcription of host mRNAs. Specifically, phosphorylation of Ser5 is most prominent during initiation, whereas phosphorylation of Ser2 occurs mostly during elongation (Komarnitsky *et al.,* 2000). The viral polymerase associates with the phospho-Ser5 form of RNAPII through interactions involving two binding sites within PA (Lukarska *et al.,* 2017).

Cap snatching results from binding of host capped mRNAs by the PB2 cap binding domain, followed by cleavage 10-15 nucleotides downstream of this by the PA endonuclease domain. Caps from host snRNAs and snoRNAs are preferentially used, although this may be as a consequence of their high abundance (Gu *et al.,* 2015; Sikora *et al.,* 2017). Structural studies reveal that cap snatching is likely to occur whilst the polymerase exists in a pre-initiation state, which permits alignment of the PB2 cap binding and PA endonuclease domains. The cleaved primer is then inserted into the PB1 catalytic site through the product exit channel, a process which requires rotation of the PB2 cap binding domain (Reich *et al.,* 2014). Rotation of the cap binding domain also shields the bound primer from further cleavage by the PA endonuclease domain (Reich *et al.,* 2014). The 3' end of the vRNA template is simultaneously

inserted into the active site through an unknown mechanism (te Velthuis *et al.,* 2016a). Transcription is initiated by addition of either a G or C residue to the primer, which is complementary to the C (at position 2) or G (at position 3) of the vRNA template (Beaton *et al.,* 1981). Elongation is carried out, presumably through local dissociation and re-association of NP molecules to vRNA as it passes through the catalytic core of the polymerase. Emergence of the growing mRNA strand is thought to terminate interactions between the cap and cap binding domain of PB2 (te Velthuis *et al.,* 2016a).

Like host mRNAs, viral mRNA is polyadenylated. A poly adenylated tail is generated by a stuttering mechanism which occurs at a stretch of five-seven uracil residues near the 5' end of the vRNA (Poon *et al.,* 1999). It is thought that strong associations between the 5' terminus and the polymerase facilitate this process (Pflug *et al.,* 2017). SFPQ/PSF was shown to aid polyadenylation of viral mRNAs since knockdown of this protein resulted in production of non-polyadenylated transcripts or those with shorter polyadenylated tails. Consequently, silencing of this gene also resulted in reduced viral titers (Landeras-Bueno *et al.,* 2011). However, a different study showed silencing of this gene increased viral titers suggesting that it may play different roles under different conditions and for different viruses. (Bortz *et al.,* 2011).

Capped viral mRNAs are bound by nuclear cap binding proteins to be processed and translated by host cell machinery (Bier *et al.,* 2011; Yangueez *et al.,* 2011). This is further assisted by inhibition of host gene expression by viral NS1 and PA-X proteins, which results in preferential processing of viral mRNAs by host machinery (Jagger *et al.,* 2012; Khaperskyy *et al.,* 2015; Khaperskyy *et al.,* 2016).

Splicing occurs on NS1, M1 and in some cases PB2 transcripts (Bouvier and Palese, 2008; Yamayoshi *et al.,* 2016). Host splicing factors are essential for this process. In particular, RED, SMU1, SF2/ASF, NS1-binding protein and hnRNP K are known to facilitate this process (Fournier *et al.,* 2014; Mor *et al.,* 2016; Shih and Krug, 1996; Tsai *et al.,* 2013).

1.7.2 cRNA synthesis

Replication is carried out in two stages. vRNA is first synthesised into cRNA, which is incorporated into cRNPs, similar to vRNPs (York *et al.,* 2013). The cRNA is then used as a template for vRNA synthesis. Unlike mRNA synthesis, replication occurs *de novo*, that is independently of a primer (Hay *et al.,* 1982). For the synthesis of cRNA from vRNA, terminal initiation takes place whereby the 3' vRNA is transferred into the active site of PB1 and a pppApG dinucleotide is incorporated onto the U and C nucleotides at position 1 and 2 of the 3' vRNA terminus, respectively (Deng *et al.,* 2006). Compared to transcription initiation which includes use of a primer, this method of initiation is much less efficient (te Velthuis *et al.,* 2016b). However, the priming loop of PB1 is able to stabilise the initiation complex. Truncation or mutation of the priming loop reduces the efficiency of cRNA synthesis by 10 fold highlighting the importance of this structure (te Velthuis *et al.,* 2016b). Once the dinucleotide is in place, elongation occurs and the newly synthesised cRNA is bound by another polymerase complex, as well as NP molecules to form a cRNP (York *et al.,* 2013). The minichromosome maintenance (MCM) complex, a helicase involved in DNA replication, stimulates the progression from initiation to elongation via an interaction with PA (Kawaguchi *et al.,* 2007). In order to produce a full copy of the vRNA, the tight association between the 5' hook of vRNA and the polymerase must to be overcome. The mechanism by which this occurs and how polyadenylation is avoided is not clear (te Velthuis *et al.,* 2016a).

1.7.3 vRNA synthesis

Synthesis of vRNA from cRNA also occurs *de novo*. The 3' end of cRNA is inserted into the polymerase active site, but unlike cRNA synthesis, vRNA synthesis is initiated at positions 4 and 5 of the 3' end of cRNA, in a process termed internal initiation. Here, a pppApG dinucleotide is templated by the U and C nucleotides at position 4 and 5, respectively. The dinucleotide is then realigned to the U and C at positions 1 and 2 (Deng *et al.,* 2006). It is not clear why this 'prime and realign' method is used, however it is more energetically favourable than terminal initiation and as such does not require presence of the priming loop (te Velthuis *et al.,* 2016b).

In vitro studies have indicated that cRNA synthesis can be carried out by the resident polymerase on the vRNP (Vreede and Brownlee, 2007). However, there is some controversy as to whether this is the case for vRNA synthesis. Jorba *et al* proposed a model whereby the 3' end of the cRNA is inserted into the active site of a separate viral polymerase and it is this *trans*-acting polymerase which performs vRNA synthesis. In this model, an additional polymerase would also be required to bind to the newly synthesised vRNA (Jorba *et al.,* 2009). A study by York *et al* provided evidence for a *trans*-activating polymerase. In this model, an additional polymerase is needed to stimulate vRNA synthesis, however this polymerase was not required to be catalytically active in order to perform this function (York *et al.,* 2013). It is hypothesised that binding of the *trans*-activating polymerase to the resident polymerase could induce a conformational change in the resident polymerase enabling insertion of the 3' cRNA into the active site or stabilising initiation. The *trans*-activating polymerase may also bind to the newly synthesised vRNA as it emerges from the catalytic core of the resident polymerase.

Host factors ANP32A and -B are able to stimulate vRNA synthesis *in vitro* (Sugiyama *et al.,* 2015). An interaction between ANP32A and B and viral polymerase has been identified (Bradel-Tretheway *et al.,* 2010; Sugiyama *et al.,* 2015; Watanabe *et al.,* 2014), however the exact mechanisms by which these proteins function remains unclear. ANP32 proteins are discussed further in section 1.9.

As well as host proteins, viral proteins have also been implicated in this step. Although NEP is mainly known for its role in export of vRNPs, there is increasing evidence to suggest it also plays a role in polymerase activity (Robb *et al.,* 2009). In particular, NEP is involved in the generation of small viral RNAs (svRNAs) which resemble the 5' termini of vRNA. These 22-27nt svRNAs stimulate the synthesis of cRNA to vRNA though an interaction with PA, which may alter its conformation to create a replication competent polymerase (Perez *et al.,* 2010; Perez *et al.,* 2012).

1.7.4 Regulation between transcription and replication

It is unclear what determines whether the viral polymerase carries out transcription or replication of the vRNA. mRNA can be detected early during infection, whereas cRNA accumulates later (Engelhardt *et al.,* 2006). It was therefore proposed that the polymerase undergoes a 'switch' from transcription to replication, a process in which NP has been implicated (Portela and Digard, 2002). Vreede *et al*., opposed the idea of a 'switch' and suggested that both mRNA and cRNA are synthesised from the beginning of infection. However, until sufficient amounts of NP and polymerase are generated from the mRNA, the cRNA cannot be stabilised and is likely degraded. Once sufficient amounts of these proteins are produced, this cRNA can be stabilised and more easily detected (Vreede *et al.,* 2004).

However, this model is still not able to explain how the polymerase regulates which process it is going to carry out. It is possible that binding to different host or viral factors may regulate this.

Although binding of viral polymerase to host RNAPII is required for transcription, in the late stages of infection, the viral polymerase complex (not that within vRNPs) has been shown to contribute to degradation of the large subunit of RNAPII (Martinez-Alonso *et al.,* 2016; Vreede and Fodor, 2010). Degradation of RNAPII prevents expression of antiviral genes. Moreover, since RNAPII is not required for viral genome replication, this degradation may be linked to the switch between transcription and replication.

The presence of svRNAs has also been implicated in this switch and is thought to promote replication (Perez *et al.,* 2010). An attractive hypothesis is that the activity of the polymerase is regulated by the relative amounts of particular host or viral factors which may be regulated either temporally or spatially. For example, early association with RNAPII puts the viral polymerase in close contact with proteins required for transcription and splicing. As cRNA begins to accumulate, the amount of svRNAs increase, whilst the amount of RNAPII decreases, altogether promoting replication. The spatial distribution of the polymerase within the nucleus may allow the viral polymerase to be in close association with different host factors required to promote the different activities.

Host factor	Role	Reference
NP chaperones		
UAP56	Binds to NP, may act as chaperone facilitating formation of NP-RNA complexes	Momose *et al.,* 2001
Tat-SF-1	Binds to NP, may act as chaperone facilitating formation of NP-RNA complexes	Naito *et al.,* 2007a
Prp18	Binds to NP, may act as chaperone facilitating formation of NP-RNA complexes to promote elongation	Minakuchi *et al.,* 2017
FMRP	Binds to NP, may act as chaperone facilitating formation of NP-RNA complexes	Zhou *et al.,* 2014
NP Post Translational Modifications		
PKCδ	Phosphorylates NP, binds to PB2, regulates RNP assembly	Mondal *et al.,* 2017
CDC25B	Dephosphorylates NP to facilitate oligomerisation and RNP assembly	Cui *et al.,* 2018
CNOT4	Ubiquitination of NP, hypothesised to facilitate NP-RNA binding	Lin *et al*., 2017
GCN5	Acetylation of NP, knockdown of this protein reduces polymerase activity, but mechanism is unknown	Hatakeyama *et al.,* 2018
Polymerase Chaperones		
LYAR	Promotes assembly of RNPs	Yang *et al.,* 2018
Hsp70	Interacts with PB1 and PB2, possible chaperone for PB2	Manzoor *et al.,* 2014
Hsp90	Chaperone for viral polymerase subunits	Naito *et al.,* 2007b
CCT	Chaperone for PB2	Fislova *et al.,* 2010
DnaJ/Hsp40	Chaperone for viral polymerase subunits	Cao *et al.,* 2014

IncRNA-PAAN	Associates with PA, facilitates assembly of viral heterotrimeric polymerase complex	Wang *et al.,* 2018
Transcription		
RNA polymerase II	Source of caps for cap snatching which is essential for viral transcription	Engelhardt *et al.,* 2005
CyclinT1/CDK9	Promotes interaction between polII and viral polymerase	Zhang *et al.,* 2010
RRP1B	Promotes binding of viral polymerase to host capped RNAs	Su *et al.,* 2015
RNA exosome components	Facilitates capsnatching	Rialdi *et al.,* 2017
CHD1	Facilitates viral primary transcription	Marcos-Villar *et al.,* 2016
NXP2	Facilitates viral transcription	Ver *et al.,* 2015
Acetyl coA	Binds PB2 cap binding domain, implicated in viral transcription	Hatakeyama *et al.,* 2014
SFPQ/PSF	Facilitates polyadenylation of viral transcripts	Landeras-Bueno *et al.,* 2011
cRNA Synthesis		
MCM	Helicase activity facilitates elongation during cRNA synthesis	Kawaguchi *et al.,* 2007
vRNA Synthesis		
ANP32A	Facilitates cRNA to vRNA synthesis, implicated in host restriction	Sugiyama *et al.,* 2015
ANP32B	Facilitates cRNA to vRNA synthesis, implicated in host restriction	Sugiyama *et al.,* 2015 Watanabe *et al.,* 2014
JNK	Facilitates vRNA synthesis	Zhang *et al.,* 2016
Exact Function Unclear		
Importin α proteins	Roles in replication by an unknown mechanism, also has roles in nuclear	Hudjetz *et al.,* 2012 Gabriel *et al.,* 2008

	import of vRNPs, PB2 and NP. Implicated in host restriction	
DDX17	Binds to polymerase, knockdown resulted in reduced polymerase activity, implicated in host restriction	Bortz *et al.,* 2011
DR1	Suppresses IFN-β production late in infection, facilitating viral replication. May have other roles independent of IFN-β production which directly affects viral replication at earlier time points	Hsu *et al.,* 2015
hnRNP A2/B1	Binds to NP, knockdown of hnRNP A2/B1 resulted in reduced polymerase activity	Chang *et al.,* 2017
PP6	Interacts with PB1 and PB2, knockdown of PP6 resulted in reduced polymerase activity	York *et al.,* 2014
ZBTB25	Binds NP and PB2, knockdown resulted in reduced polymerase activity	Chen *et al.,* 2017
hCLE	Binds to viral polymerase, knockdown of hCLE resulted in reduced polymerase activity	Rodriguez *et al.,* 2011

Table 2: Host factors which support the influenza A polymerase
List of host factors have been shown to functionally support the influenza A polymerase in human cells.

1.8 Host restriction

The natural reservoir of influenza A viruses are wild aquatic birds, where the virus resides asymptomatically. However, transmission of a novel avian influenza virus into humans can result in a pandemic. Fortunately, pandemics are infrequent since transmission of avian influenza into humans is inefficient and usually leads to dead end infections. If a virus is to be able to replicate and be capable of sustained transmission between humans, the virus must acquire the necessary adaptive mutations to overcome the multiple host range barriers that exist in the new host.

This section highlights some of the main host range barriers that exist and the ways in which influenza A viruses have adapted to overcome them. The main focus of this section will be on the restriction in replication of the influenza A genome.

1.8.1 HA

Entry into host cells represents one of the main barriers restricting infection of avian influenza viruses in human cells. HA binds to sialic acids at the end of glycoproteins and glycolipids on the cell surface. Carbon-2 of sialic acid moieties can be linked to the penultimate galactose via either their carbon-3 or carbon-6 giving rise to α2,3 or α2,6 linkages, respectively. Avian influenza A viruses typically bind α2,3 linked sialic acids. However, ciliated epithelia in the human upper respiratory tract display α2,6 linked sialic acids and therefore the virus must adapt to be able to infect these cells (Long *et al.,* 2019). Studies have revealed that E190D and D225G mutations in the HA of H1 viruses and Q226L and G228S mutations in H2 and H3 viruses are able to alter the binding preference from avian to human (Matrosovich *et al.,*

2000). It has also been proposed that soluble α2,3 linked receptors found in the human airway may act as decoy receptors (Cauldwell *et al.,* 2014). Although only H1, H2 and H3 viruses have so far been the only viruses capable of sustained transmission in the human population, it has been shown that H7N9 viruses are capable of binding in the upper respiratory tract (van Riel *et al.,* 2013). Furthermore, a study which engineered already known humanising mutations into H5 viruses showed that these mutations contribute to transmissibility, although other mutations may also be required (Herfst *et al.,* 2012). However, it is not only the linkage of the terminal sialic acids which affects binding. Addition of functional groups as well as branching of the receptor can also affect binding of HA (Long *et al.,* 2019; Peng *et al.,* 2017).

1.8.2 NA

HA binds sialic acid receptors to enter cells, whereas NA cleaves sialic acid receptors to allow release of virions from the cell. Therefore, the infectivity and transmission of a virus depends on a balance between the two proteins. NA consists of a head domain, which encompasses the cleavage activity and a stalk domain. Deletions in the stalk enhance replication in chickens, however a longer stalk is required for efficient aerosol transmission between ferrets (Blumenkrantz *et al.,* 2013; Hoffmann *et al.,* 2012).

1.8.3 NP

Virus replication can be inhibited by the interferon regulated protein, MxA. Whereas chicken Mx proteins do not inhibit influenza replication, human MxA is able to target influenza A viruses of avian origin (Benfield *et al.,* 2008; Dittmann *et al.,* 2008). Adaptive mutations in NP can overcome this restriction, however they bear a fitness cost (Goetz *et al.,* 2016; Mänz *et al.,* 2013).

Adaptive mutations in NP can also affect nuclear import. The NP N319K mutation enhances its binding with importin α1, resulting in increased nuclear accumulation of NP in mammalian cells and consequently, increased viral growth. This mutation did not affect binding to importin α1 or nuclear accumulation of NP in avian cells (Gabriel *et al.,* 2008). A subsequent study showed that this adaptive mutation also mediated a switch between dependence on importin α3 for avian viruses to importin α7 for human adapted viruses in human cells (Gabriel *et al.,* 2011).

1.8.4 NEP

Although NEP is well known for its role in nuclear export of vRNPs, NEP is also able to stimulate polymerase activity (Mänz *et al.,* 2012). The C terminus of NEP harbours the polymerase enhancing activity, whilst the N terminus functions as a regulatory domain (Reuther *et al.,* 2014). Binding of the two domains maintains NEP in a closed conformation and renders it incapable of supporting polymerase activity. An open conformation exposes the C terminus enabling support of polymerase activity. It has been hypothesised that replication in avian hosts, which occurs at between 39-42 °C, encourages an open conformation, whereas replication in human hosts which occurs at 34 °C, favours the closed conformation. Adaptive mutations in NEP which lower the affinity between the two domains facilitate formation of an open conformation in human hosts, enhancing polymerase activity (Reuther *et al.,* 2014). These mutations, such as the M16I mutation, have been found in various strains which have retained avian signatures such as PB2 627E (described below), but are able to replicate in human hosts. Examples include the 2009 pandemic H1N1 virus and H5N1 viruses isolated from human hosts (Mänz *et al.,* 2012; Reuther *et al.,* 2014). It is not

clear how NEP stimulates polymerase activity, but an interaction between the C terminus of NEP with PB1 and PB2 has been shown (Mänz *et al.,* 2012).

1.8.5 Polymerase

Mammalian adaptive mutations have been identified in all three polymerase subunits (Cauldwell *et al.,* 2014). Mutations in PB2 have been the most studied and are well known for overcoming host range restriction of the viral polymerase (Almond, 1977). These include the PB2 D701N mutation, which along with NP N319K enhances binding to importin α1 to facilitate import of vRNPs into the nucleus of mammalian cells (Gabriel *et al.,* 2008). Position 701 lies close to an NLS and mutations in this residue may alter interactions within the complex, which in turn facilitates binding to importin-α proteins (Tarendeau *et al.,* 2007).

However, by far the most well-known PB2 adaptive mutation is the E627K mutation (Subbarao *et al.,* 1993). Viral replication in mammalian cells represents a significant host range barrier for influenza zoonosis (Long *et al.,* 2019). Specifically, PB2 627E containing polymerases are able to produce cRNPs, but these cannot be used as templates to efficiently synthesise vRNA (Mänz *et al.,* 2012). The single PB2 E627K mutation was shown to permit efficient replication in mammalian cells, where replication was otherwise limited. It enhances replication, virulence in mice and transmission between guinea pigs or ferrets (Chen *et al.,* 2007; Hatta *et al.,* 2001; Shinya *et al.,* 2004; Steel *et al.,* 2009). Whilst most avian influenza strains harbour glutamic acid at position 627, all strains circulating in humans in the 20th century contained lysine at this position. Interestingly, replication in avian cells does not depend on the identity of position 627. Both a glutamic acid or lysine residue can be tolerated with no obvious fitness cost.

Position 627 lies on a solvent exposed region of the polymerase complex, where it is surrounded by a basic patch of amino acids **(Fig 9)**. Although no structural changes are thought to occur as a consequence of the PB2 E627K mutation, presence of glutamic acid at this position disrupts the region of positive charge, where as a lysine at this position enhances it (Tarendeau *et al.,* 2008). Although the 2009 H1N1 pandemic virus retained 627E, it acquired PB2 G590S and Q591R mutations which allowed efficient replication in human cells. Position 591 lies adjacent to 627 and like E627K, the mutation renders it positively charged and therefore these mutations may support viral polymerase activity through similar mechanisms (Mehle and Doudna, 2009).

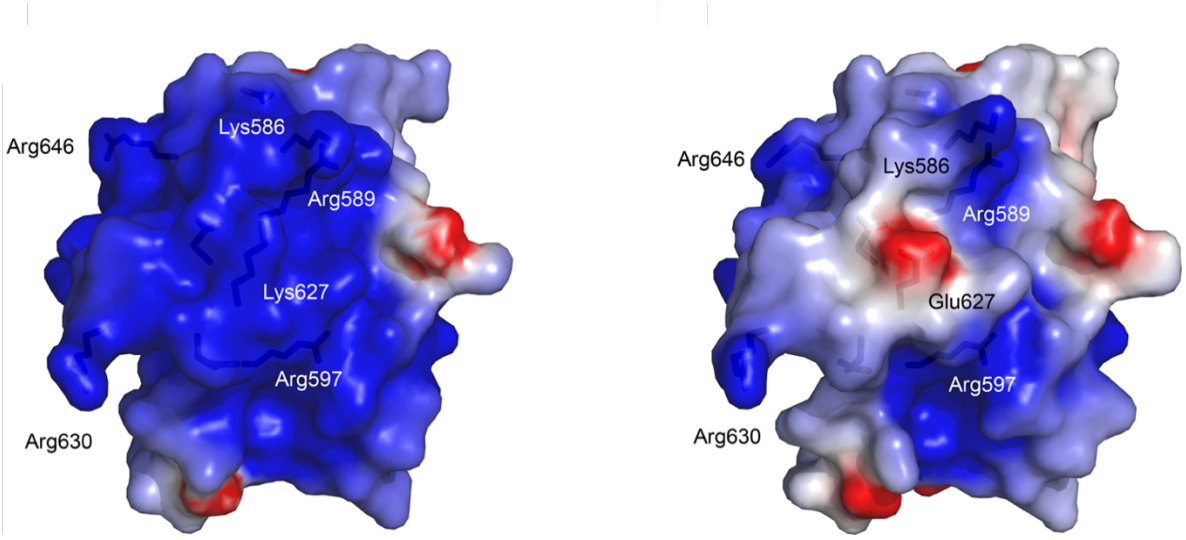


Fig 9: Glutamic acid at position 672 disrupts an area of positive charge
Image from Tarendeau *et al.,* 2008. Electrostatic surface potential of influenza polymerase containing 627K (left) or 627E (right). Positive electrostatic surface potentials represented in blue and negative electrostatic surface potentials represented in red.

Introduction of mutations in the 3' vRNA promoter region, G3A, U5C and C8U, can also overcome the restriction and enhance avian adapted polymerase activity in human cells (Crescenzo-Chaigne *et al.,* 2002; Neumann and Hobom, 1995). Although these mutations increase complementarity within the panhandle structure, it is the specific sequence that is important rather than the complementarity (Paterson *et al.,* 2014). This indicates that the way in which the polymerase binds to the promoters may be important. However, exactly how the PB2 E627K mutation is able to overcome the host restriction imposed in mammalian cells is unclear.

Differences in temperature between hosts was proposed to contribute to this adaptation. Replication of avian influenza viruses occurs at approximately 41 °C in the gastrointestinal tract of birds. However, the temperature of the human upper respiratory tract is approximately 33 °C. It was shown that the PB2 E627K mutation was able to enhance polymerase activity at lower temperatures, suggesting that temperature partly accounts for the restriction (Massin *et al.,* 2001). However, the restriction was still present even at higher temperatures demonstrating that other factors may also contribute (Massin *et al.,* 2001).

Previous studies have suggested that the PB2 E627K mutation enhances an interaction between PB2 and NP, which in turn enhances polymerase activity (Labadie *et al.,* 2007; Ng *et al.,* 2012). However, a subsequent study disputed these findings and revealed that the increased coprecipitation of PB2-NP complexes seen was an indirect consequence of enhanced replication (Cauldwell *et al.,* 2013). It has also been demonstrated that the restriction in replication is independent of NP (Paterson *et al.,* 2014).

Interestingly, purified avian polymerases are not restricted *in vitro* suggesting that the restriction seen in cells may involve specific host factors and/or limitations in the spatial distribution of the polymerase complex within the cell (Aggarwal *et al.,* 2011). Furthermore, given that position 627 lies on a surface exposed region of the polymerase, differing interactions with host factors seems likely (Tarendeau *et al.,* 2008). By fusion of avian and human cells, Mehle and Doudna presented evidence for the existence of an inhibitory factor in human cells which was restricting the PB2 627E polymerase (Mehle and Doudna, 2008). Using a similar heterokaryon assay, Moncorgé et al showed that fusion of human cells with increasing numbers of avian cells increased polymerase activity of the PB2 627E polymerase in human cells (Moncorgé *et al.,* 2010). This suggests that the avian adapted polymerase is restricted in human cells due to the absence of a compatible stimulatory factor which usually facilitates replication in avian cells. Both inhibitory and stimulatory host factors have been implicated in host range. These include DDX17 (Bortz *et al.,* 2011), RIG-I (Weber *et al.,* 2015), the α-importins (Hudjetz *et al.,* 2012), TUFM (Kuo *et al.,* 2017) and most recently, ANP32A (Long *et al.,* 2016) (ANP32 is discussed in detail in section 1.9).

1.8.5.1 DDX17

Using an siRNA screen, DDX17, an RNA helicase, was identified as a factor which supports activity of the influenza A viral polymerase. In avian cells, it was shown that avian DDX17 supported the activity of both avian and human adapted viral polymerases. However, siRNA mediated knockdown of DDX17 in human cells caused a decrease in polymerase activity of a polymerase bearing 627K, but resulted in an increase in polymerase activity of that bearing 627E. An interaction between DDX17 and both polymerases could be detected. This suggests

that DDX17 in human cells may inhibit the activity of the polymerase, unless it undergoes the E627K mutation (Bortz *et al.,* 2011).

1.8.5.2 RIG-I

A different study proposed that incoming vRNPs are inhibited by RIG-I in the cytoplasm by binding to panhandle structures formed by the terminal ends of the vRNA. Interactions between PB2 627K polymerase and NP were shown to be stronger than that with PB2 627E, resulting in less recognition and inhibition by RIG-I for the human adapted polymerase. Although RIG-I is not found in chickens, homologues are found in ducks, geese and pigeons. In these organisms, PB2 627E containing polymerases are able to replicate, suggesting inhibition by RIG-I may not be the primary determinant of the PB2 E627K mutation (Weber *et al.,* 2015).

1.8.5.3 Importin-α proteins

The importin-α proteins have also been implicated in host range. siRNA mediated knockdown of importin-α1 and -α7 resulted in a reduction in polymerase activity of a PB2 627K containing polymerase but not 627E (Hudjetz *et al.,* 2012). Subsequent studies have also shown a specific dependency of human adapted viral polymerases on importin-α7 (Bertram *et al.,* 2017). Interestingly, analysis of the mRNA expression levels of various importins in human nasal mucosa indicates that importin-α7 is significantly more abundant than importin-α1 or -α3 in these cells (Ninpan *et al.,* 2016). This may introduce a selective pressure which encourages avian viruses to adapt to using importin-α7.

Although the main role of importin-α proteins is to import proteins into the nucleus, its complete function in supporting viral polymerase activity is unclear. Mutations in the NLS of PB2 reduced nuclear accumulation of the protein somewhat and caused a reduction in polymerase activity. However, replacement of the NLS with an exogenous NLS allowed complete nuclear accumulation of PB2, but could not rescue polymerase activity, suggesting that the importins-α's may serve a function beyond nuclear import (Resa-Infante *et al.,* 2008).

1.9 ANP32

Acidic (leucine rich) nuclear phosphoprotein 32 kDa (ANP32) proteins are essential for influenza A viral polymerase activity and are heavily implicated in host range restriction (Long *et al.,* 2016; Sugiyama *et al.,* 2015). Human ANP32 (huANP32) family members have been ascribed various functions within the cell and as such are associated with a number of diseases. Since the same proteins have been discovered a number of times, they are known by multiple names. ANP32A is also known as pp32, LANP or PHAPI. ANP32B is also known as APRIL, PHAPI2 or SSP29. This section describes the structure and function of ANP32 proteins as well as their association with influenza A.

1.9.1 Structure

ANP32 proteins consist of multiple leucine rich repeats (LRR) followed by a low complexity acidic region (LCAR). NMR resolved solution structures of the LRR domain of both ANP32A and -B as well as crystal structures of the LRR of ANP32A have been solved **(Fig 10)**. All four structures align well with one another, although the higher resolution structure reported by Zamora-Caballero *et al.,* shows a slight change in the first α-helix compared to the others (de

Chiara *et al*., 2008; Huyton *et al*., 2007; Tochio *et al*., 2010; Zamora-Caballero *et al.,* 2015). These structures revealed an N terminal α-helix, followed by 5 LRR domains and a C terminal cap structure (de Chiara *et al*., 2008; Huyton *et al*., 2007; Tochio *et al*., 2010; Zamora-Caballero *et al.,* 2015). LRRs are 20-29 amino acid motifs, often involved in protein-protein interactions. The LRR domains of ANP32A and B follow the SDS22-like subfamily consensus sequence LxxLxxLxLxxNxIxxLx-x (when 'x' is any residue and '-' indicates a possible insertion) (Kobe *et al*., 2001). The five LRRs form a horseshoe like structure, with the concave face lined with β-strands and the convex surface mainly composed of α-helices. It is the concave face, which has been shown to be involved in many protein-protein interactions (de Chiara *et al*., 2008; Huyton *et al*., 2007; Tochio *et al*., 2010). Following the C terminal cap is a more flexible central region containing multiple phosphorylation sites. The LCAR domain of huANP32 proteins consist of 60-75% glutamic acid and aspartic acid residues, making them incredibly negatively charged. An NLS motif can also be found near the C terminus of the LCAR domain.

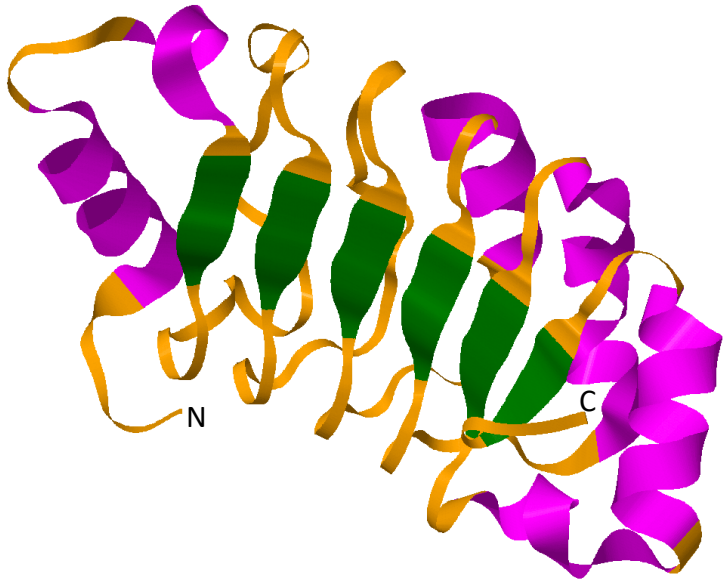


Fig 10: Structure of ANP32A LRR domain
Ribbon representation of the structure of human ANP32A LRR domain. α-helices are represented in magenta, β-strands are represented in green. Image created using Geneious version 6. PDB: 4XOS. (Zamora-Caballero *et al.,* 2015).

1.9.2 Family

ANP32 proteins belong to the superfamily of LRR containing proteins. Proteins with a similar sequence to ANP32 have been annotated in the animal, plant and protist kingdoms (Matilla & Radrizzani, 2005). It has been proposed that eight ANP32 family members exist in humans, ANP32A-H (Matilla & Radrizzani, 2005). Of these, ANP32A, -B and -E are conserved between vertebrates and are the most well studied. A splice variant of ANP32B also exists which has a shorter LCAR domain and lacks an NLS (Matilla & Radrizzani, 2005). ANP32C and -D genes are intronless and their endogenous expression and attributed functions are debatable (Reilly *et al*., 2014).

1.9.3 Endogenous functions and roles in disease

A variety of functions have been proposed for the members of the huANP32 family of proteins and as a consequence they have been implicated in several diseases. Some of these roles are shared by different members of the family, while others are specific to a particular member. The proteins can also have apposing roles. The diversity of these functions is enhanced by the fact that in different cell types and under different conditions, ANP32 proteins can be found in different subcellular locations. For example, the presence of reactive oxygen species triggers the translocation of ANP32A from the cytoplasm into the nucleus in K562 cells (Martinvalet *et al*., 2005). Phosphorylation of ANP32B at T244 results in translocation of ANP32B from the nucleus to the cytoplasm (Fries *et al*., 2007). The proteins contain a nuclear localising signal (NLS) at their C terminus and also three predicted nuclear export signals (NES) on their LRR domain. The majority of studies find ANP32 proteins are either nuclear, cytoplasmic or both (Reilly *et al.,* 2014). However, ANP32A has also been found to be secreted

by hepatocellular carcinoma cells (Chang *et al*., 2010) and also proposed to be found on the cell membrane where it can act as a receptor for the V3 loop of gp120 on HIV particles (Callebaut *et al*., 1998). The ANP32 proteins exist as monomers, but one study reported ANP32A forming a trimer as well as dimers and this oligomerisation was mediated by the LRR domain of the protein (Ulitzur *et al*., 1977a).

Some of the functions attributed to huANP32A, -B and -E are highlighted below:

1.9.3.1 mRNA export

Both the LRR and LCAR domains of ANP32 have the capability of binding to proteins and as such huANP32 proteins can act as adapters within protein complexes. For example, both huANP32A and -B can act as adapter proteins between the RNA binding protein, huR, and the nuclear export protein, CRM1. Through this complex they are involved in the nuclear export of AU-rich element (ARE) containing mRNAs. The interaction between huR and huANP32A involves the RNA recognition motif 3 domain of huR and the LCAR domain of huANP32A. It is thought that CRM1 binds to the LRR domain of huANP32A, most likely through its NES (Brennan *et al*., 2000). Some mRNAs are exported by complexes containing specific huANP32 members. For example, CD83 mRNA can be exported into the cytoplasm by huANP32B but not huANP32A and this is regulated by phosphorylation of huANP32B (Fries *et al*., 2007).

1.9.3.2 PP2A inhibition

Both huANP32A and ANP32E can inhibit the activity of protein phosphatase 2A (PP2A) (Li *et al*., 1995; Radrizzani *et al*., 2001). The interaction between the catalytic domain of PP2A and ANP32A was mapped to residues 1-120 of the LRR domain of ANP32A (Chen *et al*., 2008).

Despite the sequence similarity, ANP32B does not share this function (Sun *et al*., 2006). PP2A plays a key role in regulating phosphorylation in the human brain and as such, deregulation of PP2A is associated with neurodegenerative diseases such as Alzheimer's. In this way, ANP32A may be implicated in Alzheimer's disease through inhibition of PP2A leading to the hyperphosphorylation of tau (Chen *et al*., 2008; Tsujio *et al*., 2005).

1.9.3.3 Development

ANP32E is thought to have a role in cerebellar development as its expression is changed throughout this process (Radrizzani *et al*., 2001). However, mice lacking ANP32E did not have any strong defects (Reilly *et al*., 2010). Mice completely lacking ANP32A were also viable (Opal *et al*., 2004). Knocking out ANP32B on the other hand, was highly lethal. Those mice who survived harboured defects in a range of organs and also became more sensitive to knockout of ANP32A (Reilly *et al*., 2011). This suggests that ANP32B is the most important member of the family with regards to development, but that ANP32A and ANP32B may share some redundant roles. Recently, conditional ANP32B knockout mice have been generated. These mice were viable, but exhibited a dysregulated immune response implicating ANP32B in autoimmune diseases (Chemnitz *et al.,* 2019).

1.9.3.4 Transcriptional regulation

huANP32A forms part of the inhibitor of acetyltransferase (INHAT) complex with SET/Taf-Iβ and Taf-Iα. The INHAT complex is able to repress transcription by blocking acetylation of lysine residues on histone tails, ensuring that DNA remains tightly bound to the histones. An interaction between ANP32A and histones is required for this function and this interaction was mapped to residues 151-180 of ANP32A. Alone, ANP32A shows a preference for binding

histone H2B and H3, whereas as part of the INHAT complex, the strongest interactions were with histones H3 and H4 (Seo *et al*., 2002). Interestingly, mouse models for Alzheimer's disease show reduced histone acetylation and accumulation of ANP32A in parts of the brain involved in memory. Knocking down ANP32A in these mice was able to rescue their memory and learning compared to controls (Chai *et al*., 2017). Despite its association with the INHAT complex, huANP32A has also been shown to promote the transcription of several interferon stimulated genes (ISGs) through the recruitment of STAT1 and STAT2 to ISG promoters (Kadota *et al*., 2011).

ANP32A has long been known to bind to Ataxin-1, the protein mutated in spinocerebellar ataxia type 1 (Matilla *et al*., 1997). The importance of this interaction was revealed in a study by Cventanovic *et al*. ANP32A interacts with EF4 and this complex repressed transcription. EF4 is displaced by Ataxin-1 leading changes in transcriptional regulation (Cventanovic *et al*., 2007).

huANP32B can bind to all core histones via its LCAR domain and specifically to histone H3 and H4 via its LRR domain (Tochio *et al*., 2010). huANP32B can act as a histone chaperone facilitating the incorporation of histones into DNA (Munemasa *et al*., 2008). Furthermore, huANP32B can bind to and inhibit the activity of the transcription factor, KLF5 (Munemasa *et al*., 2008). Using these methods, huANP32B acts a transcriptional repressor. Like huANP32B, huANP32E also acts as a histone chaperone. Specifically, it is involved in the removal of histone H2A.Z from nucleosomes by binding to H2A.Z using a unique sequence on its LCAR domain, which is not present in huANP32A or -B (Obri *et al*., 2014).

1.9.3.5 Apoptosis

Many studies implicate ANP32 proteins in regulation of cell survival and apoptosis (Reilly *et al.,* 2014). huANP32A, -B and -E promote apoptosis by activating caspase-9 (Jiang *et al*., 2003). Both the central and LCAR domains of huANP32A are needed for its apoptotic activity (Pan *et al*., 2009). huANP32A can also aid apoptosis through its involvement in the SET complex. As well as huANP32A, the SET complex includes the DNase, NM23-HI, as well as three substrates of Granzyme A including SET, which inhibits NM23-HI. Cleavage of SET by Granzyme A results in activation of the DNase and consequently, apoptosis (Martinvalet *et al*., 2005).

In other studies, contrasting data shows ANP32A can promote cell survival and proliferation (Cui *et al*., 2008; Chang *et al*., 2010). ANP32B was shown to inhibit caspase 3 and act as an inhibitor of apoptosis (Shen *et al*., 2010; Sun *et al*., 2006).

Due to these roles in regulating apoptosis, ANP32 proteins have frequently been associated with cancer. Elevated levels of ANP32A have been found in hepatocellular carcinoma cells (Zhu *et al*., 2010), prostate cancer cells (Kadkol *et al*., 1998), colorectal cancer cells (Yan *et al*., 2017) and acute myeloid leukaemia cells (Yang *et al*., 2018). High levels of ANP32B and -E have also been associated with poor prognosis (Reilly *et al*., 2011; Xiong *et al*., 2018). On the other hand, other studies have attributed tumor suppressive function to ANP32A and these were mapped to residues 150-174 (Bai *et al*., 2001; Brody *et al*., 1999; Chen *et al*., 1996).

1.9.3.6 Organelle transport

ANP32A can bind to microtubule associated proteins via their tubulin binding domain (Ulitzer *et al*., 1997b). This interaction likely involves the LCAR domain of ANP32A (Ulitzer *et al*., 1997a). The exact mechanisms by which this effects organelle transport Is unclear.

1.9.4 The role of ANP32 in influenza A

Over the past few years, the contribution of ANP32 proteins to host range of the viral polymerase has been increasingly studied. In the first study which implicated ANP32 proteins in host range, Long *et al*., used a radiation hybrid library of hamster cells containing different regions of chicken chromosomes to identify which chicken genes were required to support the activity of an avian origin viral polymerase in these mammalian cells. Chicken ANP32A (chANP32A) was identified from these experiments (Long *et al.,* 2016). Exogenous expression of chANP32A in HEK 293T cells was able to rescue the activity of a PB2 627E containing polymerase, which is otherwise restricted in these cells (Long *et al.,* 2016). Knockdown of chANP32A in avian cells also resulted in reduced viral polymerase activity verifying its function in supporting the activity of the avian origin viral polymerase (Long *et al.,* 2016).

Compared to its human orthologues, chANP32A harbours an additional 33 amino acids in between its LRR and LCAR domains. 27 of these amino acids come from a partial duplication of exon 4, whereas the first 6 amino acids are unique. These 33 amino acids were shown to be essential for chANP32A's ability to support the avian adapted viral polymerase as removal of these amino acids prevented rescue in human cells. Furthermore, addition of these 33 amino acids into huANP32A or -B rendered these proteins capable of supporting the activity of a PB2 627E containing polymerase, which they previously were unable to do (Long *et al.,*

2016). A subsequent study showed that the first six of these 33 amino acids are most important for function and proposed that it may bind to a SUMOylated host or viral factor (Domingues and Hale, 2017). However, splice variants of chANP32A lacking the first four of these 33 amino acids are still able to support activity of the avian origin polymerase, albeit more than ten times less than with the full 33 amino acid insertion (Baker *et al.,* 2018). Transcripts lacking the additional 33 amino acids altogether also exist in avian species. The proportion of each of these three isoforms of avian ANP32A differs between different avian species, but whether this affects their susceptibility to infection is unclear (Baker *et al.,* 2018).

A role for huANP32A and -B in supporting the activity of a human adapted polymerase, such as that which contains the PB2 627K signature, has been shown (Staller *et al., in* review; Sugiyama *et al.,* 2015; Watanabe *et al.,* 2014; Zhang *et al.,* 2019). It has therefore been hypothesised that differences in ANP32 proteins between species may be a driver of adaptive mutations in the viral polymerase. In line with this, sequence alignment of ANP32 proteins revealed that avian species, excluding ratites, harbour the longer ANP32A sequence **(Fig 11)**. Interestingly, ostriches which possess a shorter ANP32A, like mammals, select for the PB2 E627K mutation upon virus infection (Shinya *et al.,* 2009). Furthermore, ANP32A lacking the additional 33 amino acids was shown to be the predominant isoform in the swan goose (>70%) (Baker *et al.,* 2018). Isolation of avian virus from the closely related bar headed goose showed the PB2 627K signature, suggesting that the proportion of particular isoforms of avian ANP32A in different avian species may induce a selection pressure on the virus (Chen *et al.,* 2005).

huANP32A and -B are thought to play essential and redundant roles in supporting human viral polymerase activity (Staller *et al., in* review; Zhang *et al.,* 2019). Avian ANP32B does not

harbour the additional 33 amino acids and therefore cannot support avian adapted viral polymerase activity (Long *et al.,* 2016). In fact, human adapted viral polymerase also appears to rely entirely on avian ANP32A and not avian ANP32B for activity in avian cells (Long *et al*., in press). Amino acids 129I and 130N in the LRR region of chANP32B were found to be responsible for the inability to support viral polymerase activity (Long *et al.,* in press; Zhang *et al.,* 2019). A role for ANP32E proteins has not yet been studied.

An interaction between ANP32 proteins and the viral polymerase has been shown (Baker *et al.,* 2018; Bradel-Thetheway *et al.,* 2011; Domingues and Hale, 2017; Sugiyama *et al.,* 2015; Wei *et al.,* 2019). ANP32B has also been identified as a host protein binding to viral NA (Watanabe *et al.,* 2014). However, the exact mechanisms by which ANP32 proteins support polymerase activity remains to be elucidated. Long *et al*., showed that nuclear accumulation of PB2 is not affected by expression of chANP32A (Long *et al.,* 2016). A study by Sugiyama *et al*., revealed that huANP32A and -B can stimulate synthesis of vRNA from a cRNA template *in vitro* (Sugiyama *et al.,* 2015). Exactly how ANP32 proteins function, why differences in the proteins between species underlie host range and whether there is a link with other proteins implicated in host range of the viral polymerase is currently unclear.

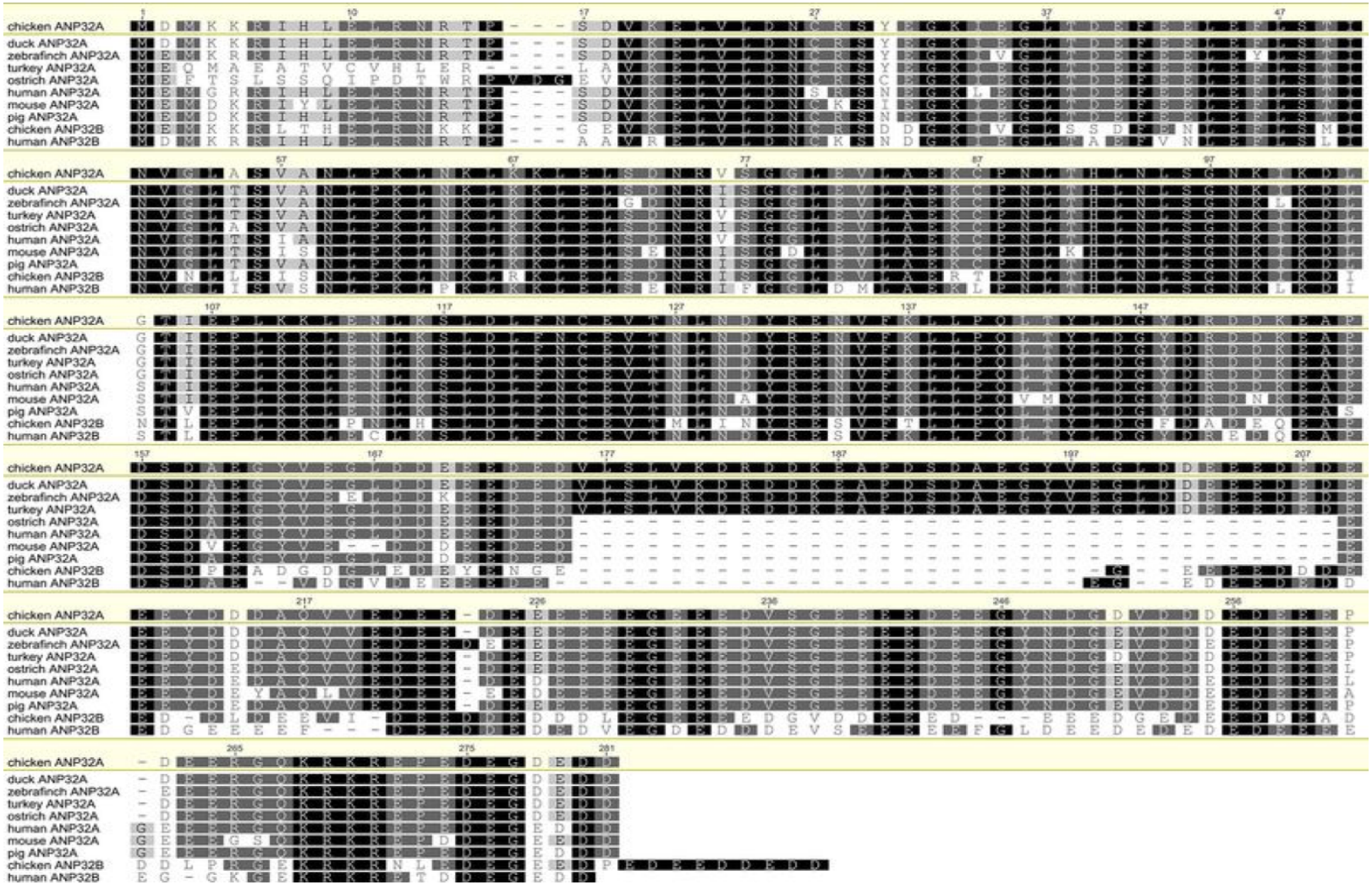


Fig 11: ANP32 sequence alignment

Image from Long *et al.,* 2016. ANP32 proteins from the named species were aligned and compared to chANP32A using Geneious R6 software. Gaps are represented by dashes. Degree of amino acid sequence identity is represented as black (100% identity) to white (<60 % identity).

1.9.5 Association of ANP32 with other viruses

Aside from influenza virus, huANP32A and -B have also been implicated in the pathogenesis of several other viruses. huANP32A was found to bind to the Ebola VP24 protein (Garcia-Dorival *et al*., 2014) as well as several proteins encoded by adeno virus (Higashino *et al*., 2005; Harada *et al*., 2002; Xue *et al*., 2005). In particular, binding of huANP32A to adeno virus encoded protein, E4orf6, was found to be needed for the export of several protooncogenes, in association with huR (Higashino *et al*., 2005). huR is an RNA binding protein involved in nuclear to cytoplasmic shuttling of mRNAs. It is able to carry out this process through interactions with huANP32A and -B, which act as adapter proteins between huR and the nuclear export protein, CRM1. In this way, both huANP32A and -B are also involved in the export of foamy virus mRNAs (Bodem *et al*., 2011). siRNA mediated knockdown of these proteins resulted in reduced cytoplasmic accumulation of foamy virus mRNAs (Bodem *et al*., 2011). huANP32B has also been implicated in nuclear to cytoplasmic shuttling during Nipah virus infection. It can bind to the M protein of both Nipah and Hendra viruses, however the functional relevance of this is currently unclear (Bauer *et al.*, 2014). Finally, huANP32A and -B have both been implicated in the replication of adeno-associated virus. They have been shown to bind to the viral Rep68 protein. This interaction was mapped to the LCAR domain of ANP32 and was necessary for its function in supporting replication (Pegoraro *et al*., 2006).

1.10 Thesis aims and objectives

ANP32 proteins are co-opted by influenza A to enable efficient replication of its genome. The activity of an avian origin viral polymerase is restricted in human cells. This is due to incompatibilities with huANP32A and -B. A 33 amino acid insertion present in chANP32A, but not huANP32A or -B accounts for this incompatibility. Mutations in PB2, such as the well-known PB2 E627K mutation, overcome the restriction in human cells and are able to utilise huANP32A and -B for their activity. It is therefore hypothesised that species differences in ANP32 proteins may drive the adaptive mutations. How ANP32 proteins support the activity of the polymerase and why species differences in ANP32 determine whether they can be co-opted by particular viral polymerases is unclear. The aims of this thesis are outlined below:

Chapter 2

- Develop an assay to quantify interactions
- Characterise interactions between ANP32A and the viral polymerase
- Investigate whether differences in interactions can explain why avian origin viral polymerases are compatible with chANP32A, but not huANP32A

Chapter 3

- Uncover differences in the interactome of the avian origin viral polymerase in the presence or absence of chANP32A
- Further characterise proteins that have been identified to determine whether they support the activity of the polymerase and whether this function is associated with ANP32A

Chapter 4

- Investigate whether any differences between the avian origin viral polymerase and that with the PB2 E627K mutation can be observed using microscopy
- Investigate the association of these differences with ANP32A

Chapter 2: Characterising interactions between ANP32A and the viral polymerase

2.1 Introduction

Replication of influenza A viruses relies on the hijack of host cell machinery. Each host species presents a different environment to the virus and therefore the virus must adapt to overcome any host range barriers which exist. Replication of the viral genome by an avian origin viral polymerase is restricted in human cells (Long *et al*., 2019). The most common mammalian adaptive mutation which is able to overcome this restriction is the PB2 E627K mutation (Subbarao *et al*., 1993). Position 627 lies on a surface exposed region of the polymerase and therefore mutations at this position may affect interactions with host cell factors (Tarendeau *et al*., 2008).

It is proposed that the avian origin polymerase is restricted in human cells due to incompatibilities with the host factors huANP32A and -B that are essential for viral replcation (Long *et al*., 2016). On the other hand, viral polymerases with mammalian adapting mutations such as PB2 E627K are able to utilise huANP32A and -B to support their activity (Sugiyama *et al*., 2015; Watanabe *et al*., 2014). chANP32A is required for viral polymerase activity in avian cells and exogenous expression of chANP32A in human cells can overcome the restriction imposed on avian origin viral polymerases (Long *et al*., 2016). chANP32A harbours an additional 33 amino acids in between its LRR and LCAR domains, which the human

orthologues of this protein do not possess. It is therefore hypothesised that species differences in ANP32 proteins may drive adaptive mutations such as PB2 E627K (Long *et al*., 2016).

In this chapter, we investigate whether differences in interactions between ch- or huANP32A with the viral polymerase explain why the avian origin viral polymerase is unable to co-opt huANP32A. To do this, we developed a split luciferase assay to quantify protein:protein interactions. We explore which parts of the proteins are involved in these interactions and how these interactions are affected by the addition of RNA or NP, altogether with the aim of gaining a further understanding of the mechanisms by which ANP32 proteins support the influenza polymerase.

2.2 Results

2.2.1 Development of a split luciferase complementation assay to measure interactions

Influenza A must exploit host factors at each stage of its replication cycle. It achieves this through interactions between viral and host proteins, and therefore the measurement of these interactions is an integral part of understanding how the virus is able to replicate. Protein-protein interactions can be studied using a variety of methods. In order to study protein-protein interactions quantitatively, we developed a split luciferase complementation assay based on that described by Cassonnet *et al*., 2011. This assay takes advantage of the ability of the *Gaussia* luciferase (Gluc) enzyme to be reconstituted after being split into two parts, if the two fragments are bought into close proximity to one another. This can be

achieved by fusion of these fragments to two other proteins which interact. Addition of substrate can then be used to measure the interaction of these proteins using luminescence as the output **(Fig 12a)**. Gluc is used due to it sensitivity and its small size, which at just 19.9 kDa, limits potential interference with interactions between the proteins of interest. To create the system, the first 18 amino acids, making up the nuclear export signal of Gluc were removed and the remaining sequence cut between Gly109 and Glu110 (Cassonnet *et al*., 2011; Remy *et al,* 2006). Each fragment of Gluc was then fused to two potential interacting partners. Signals from samples including each individual tagged protein with the complementary Gluc fragment (which is not fused to a protein) are used to determine background signals. For all experiments carried out using this split luciferase complementation assay, the normalised luminescence ratio (NLR) was calculated, which is the signal derived from GLuc reconstituted by the interacting partners divided by the sum of the two controls **(Fig 12b)**. An NLR above 3.5 was counted as a true interaction (Cassonnet *et al.,* 2011). This system has previously been used to measure interactions between the subunits of different exogenously expressed influenza polymerase complexes as well as host-virus interactions (Li *et al.,* 2016; Munier *et al.,* 2013). Here we largely used to it investigate interactions between the influenza polymerase and ANP32A. The polymerase subunits used in this study were derived from the avian origin virus H5N1 A/Turkey/England/50-92/91 (50-92) or the human adapted virus H3N2 A/Victoria/3/75 (Vic).

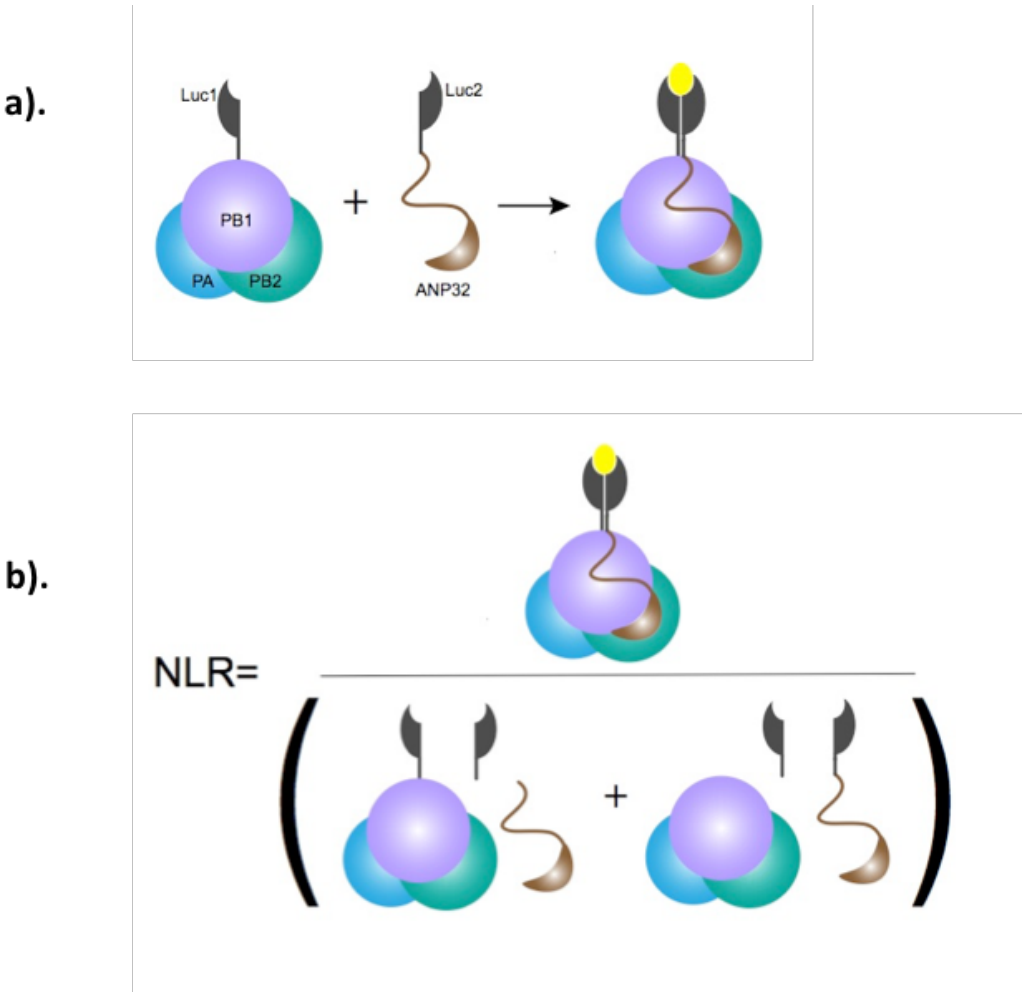


Fig 12: Schematic of split luciferase complementation assay
a). Interaction of binding partners which are both fused to the two halves of Gluc can be measured by the addition of substrate using bioluminescence. **b).** Calculation of NLR. The signal from the interacting partners is divided by the sum of the two controls, which are the signals measured from each individual interacting partner with the corresponding untagged Gluc fragment.

A list of all of the split luciferase constructs made is shown in **Table 3.** The Gluc halves were fused to the N- or C-terminus of the gene of interest by overlapping PCR. A linker sequence of AAAGGGGSGGGGS was inserted between the gene of interest and the Gluc fragment to allow greater structural flexibility. Inserts were then cloned into pCAGGS expression vectors and the correct sequence was verified by Sanger sequencing.

Construct	Virus
pCAGGS-PB1$_{luc1}$ pCAGGS-PB1D446Y$_{luc1}$ pCAGGS-$_{luc1}$PB2 pCAGGS-$_{luc1}$PB2 E627K pCAGGS-PB2$_{luc1}$ pCAGGS-PB2 E627K$_{luc1}$ pCAGGS-PB2$_{luc2}$ pCAGGS-PB2 E627K$_{luc2}$ pCAGGS-PA$_{luc1}$ pCAGGS-PA$_{luc2}$	A/Turkey/England/50-92/91 (H5N1)
pCAGGS-$_{luc1}$PB1 pCAGGS-PB1$_{luc1}$ pCAGGS-$_{luc1}$PB2 pCAGGS-$_{luc2}$PB2 pCAGGS-PB2$_{luc1}$ pCAGGS-PB2 627E$_{luc1}$ pCAGGS-PB2$_{luc2}$ pCAGGS-PB2 627E$_{luc2}$ pCAGGS-PA$_{luc1}$ pCAGGS-PA$_{luc2}$ pCAGGS-$_{luc1}$NP pCAGGS-NP$_{luc1}$	A/Victoria/3/75 (H3N2)
pCAGGS-chANP32A$_{luc2}$	N/A

pCAGGS-chANP32AΔ33$_{luc2}$ pCAGGS-huANP32A$_{luc2}$ pCAGGS-huANP32A+33$_{luc2}$ pCAGGS-Luc1 pCAGGS-Luc2	

Table 3: Plasmids constructed for split luciferase complementation assays

Since the three polymerase subunits of influenza A are known to form a trimer in the cell nucleus (Deng *et al.,* 2005; Detjen *et al.,* 1987), we first used the split luciferase complementation assay in HEK 293T cells to measure interactions between different combinations of the polymerase subunits to ensure the system would detect a known interaction. By testing all possible combinations of polymerase subunits, given the constructs made, we found that PA$_{luc1}$ in combination with PB2$_{luc2}$ gave the highest signal for both 50-92 and Vic polymerases **(Fig 13a and b).** The lowest signal was measured from $_{luc1}$PB2 in combination with PA$_{luc2}$. It is unclear using this method, whether the interactions measured are between subunits within the same polymerase trimer or between subunits residing in separate trimers that may themselves be forming dimers or higher order structures.

To ensure the signal measured between PA$_{luc1}$ and PB2$_{luc2}$ was specific, we carried out competition experiments using untagged polymerase subunits. Addition of increasing amounts of either untagged PA or untagged PB2, decreased the interaction between 50-92 PA$_{luc1}$ and PB2$_{luc2}$ in a dose dependent manner, suggesting that the signal measured is a specific measurement of the interaction between the polymerase subunits and not a consequence of random collisions **(Fig 13c and d)**.

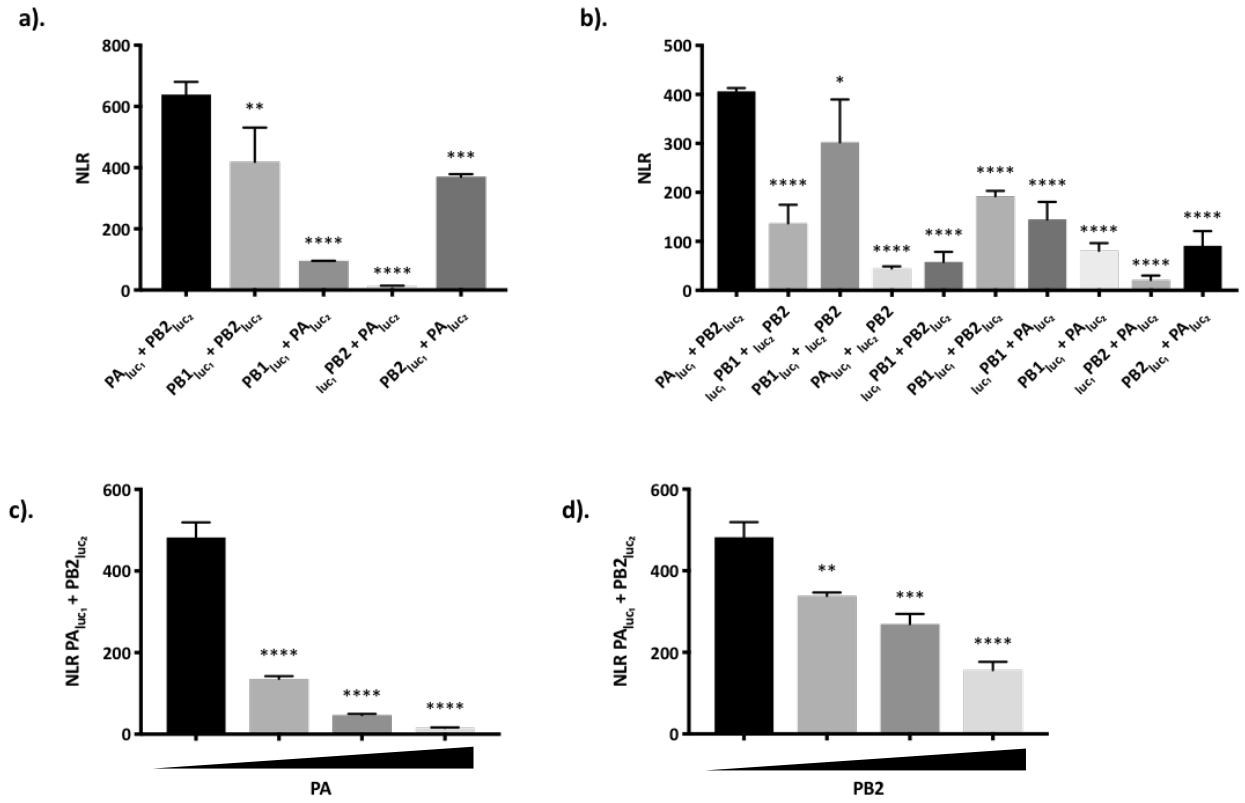


Fig 13: Interactions between polymerase subunits can be measured using the split luciferase complementation assay. HEK 293T cells were transfected with different combinations of complementary split luciferase constructs derived from either **a).** 50-92 or **b).** Vic polymerases. 25 ng of each construct was transfected. 25 ng of an untagged version of the remaining polymerase subunit was also transfected to allow formation of a trimeric polymerase complex. For **c** and **d,** 25ng of 50-92 PA$_{luc1}$, PB2$_{luc2}$ and PB1 were transfected into cells along with 0, 12.5, 25 or 50 ng of untagged **c).** PA or **d).** PB2. Total DNA was kept constant between samples using an empty vector. 24 hours after transfection, cells were lysed and Gluc activity measured and normalised to controls. Results shown are mean ± standard deviation from triplicate samples. Statistical significance was assessed by one-way ANOVA, comparisons made to sample with highest signal (PA$_{luc1}$ + PB2$_{luc2}$) for a) and b) or to 0ng additional PA or PB2 (black bar) for c) and d), *p<0.05, **p<0.01, ***p<0.001, ****p<0.0001. Results representative of three independent experiments.

2.2.2 chANP32A binds to the trimeric polymerase to a greater extent than huANP32A

We next used the split luciferase complementation assay to measure interactions between chANP32A and the influenza A polymerase. We chose to use the 50-92 polymerase for these experiments due to its avian origin. It was unknown where chANP32A might bind to the polymerase and therefore different luc1 tagged polymerase constructs were tested to determine which constructs best allowed the two Gluc fragments to reform and produce a signal when expressed in combination with chANP32A$_{luc2}$. In each case, untagged versions of the remaining polymerase subunits were also expressed to allow formation of a trimeric polymerase complex. The highest signal was measured between chANP32A$_{luc2}$ and PB1$_{luc1}$ **(Fig 14a)**. These constructs were therefore used for the majority of the following experiments, unless otherwise stated. To ensure the signal measured was due to a specific interaction between PB1$_{luc1}$ and chANP32A$_{luc2}$, we carried out competition assays. The addition of increasing amounts of untagged PB1 decreased the Gluc signal in a dose dependent manner **(Fig 14b).** Addition of increasing amounts of untagged chANP32A also decreased the signal in a dose dependent manner **(Fig 14c)**, indicating that the signal measured was due to a specific interaction.

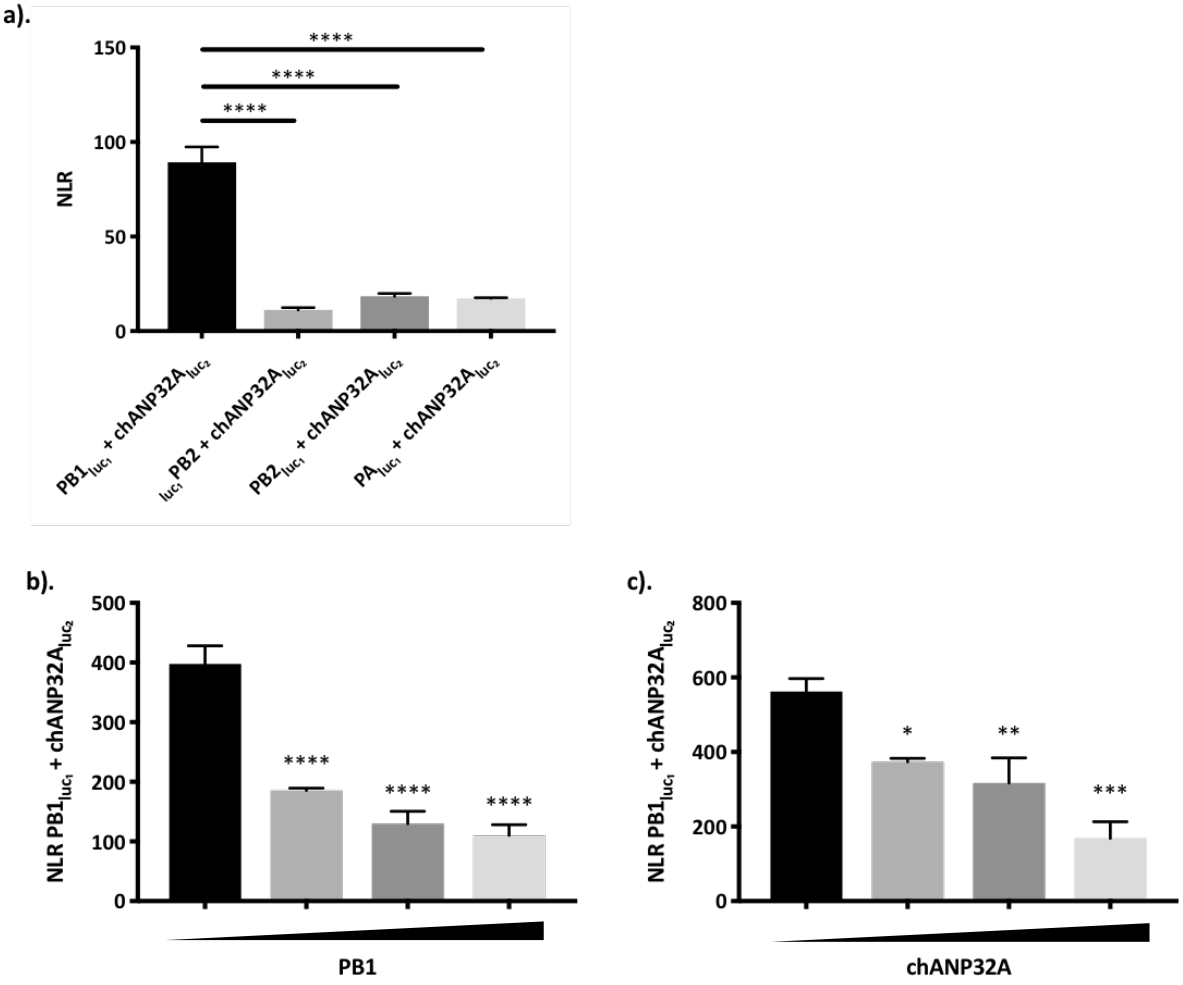


Fig 14: Interactions between polymerase subunits and chANP2A can be measured using the split luciferase complementation assay. a). HEK 293T cells were transfected with 12.5 ng chANP32A$_{luc2}$ as well as various Gluc tagged polymerase subunits. Untagged versions of the remaining polymerase subunits were also expressed; 25 ng PB1 or PB2 or 12.5 ng PA was used. For **b** and **c,** 25 ng PB1$_{luc1}$, 12.5 ng chANP32A$_{luc2,}$ 25 ng PB2 and 12.5 ng PA was transfected into cells along with 0, 6.25, 12.5 or 25 ng of untagged **b).** PB1 or **c).** chANP32A. Total DNA was kept constant between samples using an empty vector. 24 hours after transfection, cells were lysed and Gluc activity measured and normalised to controls. Results shown are mean ± standard deviation from triplicate samples. Statistical significance was assessed by one-way ANOVA, comparisons made between all samples for a). and to 0ng additional PB1 or chANP32A (black bar) for b) and c), *p<0.05, **p<0.01, ***p<0.001, ****p<0.0001, non-significant comparisons not shown. Results representative of three independent experiments.

To ensure that a polymerase containing $PB1_{luc1}$ was still able to function and that $chANP32A_{luc2}$ was still able to support the activity of the polymerase containing the luc1 tagged PB1, a minigenome assay was carried out. In a minigenome assay, pCAGGS expression plasmids encoding the three polymerase subunits as well as NP are transfected into cells. A reporter plasmid encoding firefly luciferase, under the control of a polI promoter is also transfected into these cells. The firefly luciferase gene is flanked with the NS (segment 8) noncoding regions including the viral promoters, allowing the negative sense RNA transcribed by RNA polymerase I from the plasmid to be recognised, amplified and expressed by the reconstituted influenza polymerase. Finally, a pCAGGS plasmid encoding *Renilla* luciferase is also transfected into these cells to serve as an internal control. Sequential addition of substrates for firefly and *Renilla* luciferase is then used to measure activity using luminescence as an output.

$chANP32A_{luc2}$ was able to rescue the activity of an avian influenza polymerase containing $PB1_{luc1}$ in human cells indicating that neither luc fusion had prevented polymerase activity **(Fig 15)**. Mutation of PB2 at position 627 from a glutamic acid to a lysine residue is able to overcome the block in replication of an avian origin polymerase in human cells (Subbarao *et al.,* 1993). We therefore used a polymerase with this humanising mutation to further confirm that a polymerase containing $PB1_{luc1}$ is functional even in the absence of co-expressed chANP32A **(Fig 15)**. Since both *Renilla* luciferase and *Gaussia* luciferase share the same substrate, the *Renilla* luciferase control plasmid was not included in these experiments.

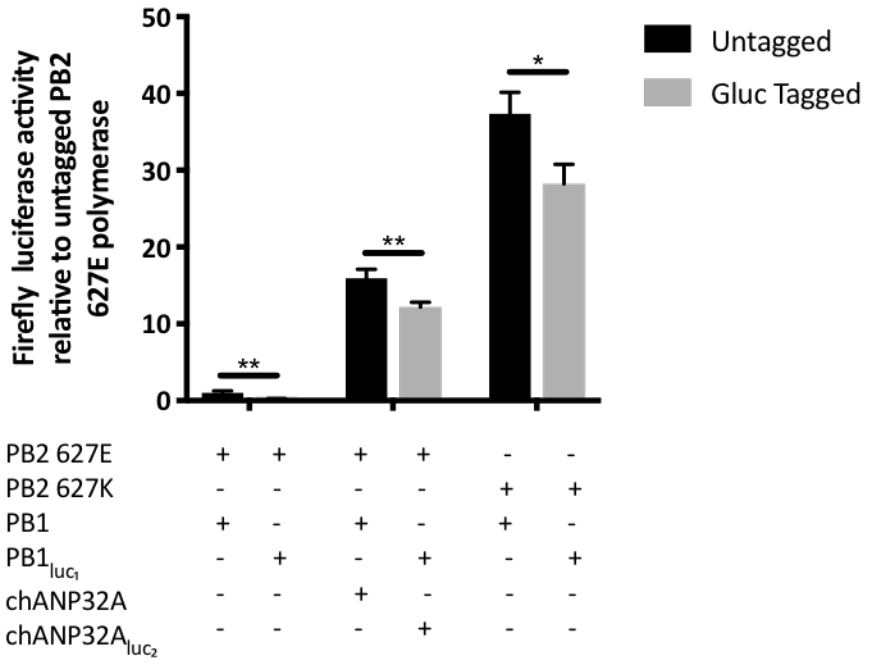


Fig 15: $PB1_{luc1}$ and $chANP32A_{luc2}$ are functional proteins.
HEK 293T cells were transfected with the avian 50-92 polymerase set including 20 ng $PB1_{luc1}$, 20 ng PB2 627E or 627K, 10 ng PA, 40 ng NP, 20 ng polI Firefly luciferase and either 10 ng empty plasmid or $chANP32A_{luc2}$. 24 hours after transfection cells were lysed and firefly luciferase activity measured. Results shown are mean ± standard deviation from triplicate samples and are plotted relative to the activity of a PB2 627E containing polymerase with no tagged constructs (left bar). Statistical significance was assessed by multiple t-tests, comparisons made to untagged samples (black bars) *p<0.05, **p<0.01. Results representative of three independent experiments.

It has been shown that the activity of an avian influenza virus (AIV) polymerase can be supported by chANP32A but not huANP32A (Long *et al.,* 2016). We hypothesised that this may be due to differences in interactions between the AIV polymerase and the two ANP32A proteins. Indeed, split luciferase complementation assays revealed that the interaction between huANP32A$_{luc2}$ and the AIV polymerase was significantly lower than with chANP32A$_{luc2}$ **(Fig 16a)**. To ensure that the lower signal observed with huANP32A$_{luc2}$ was not a result of a non-optimal steric orientation of the two luc fragments, we also tested the interaction of huANP32A$_{luc2}$ with several other luc tagged polymerase constructs. However, as with chANP32A$_{luc2}$, the highest signal was produced using PB1$_{luc1}$ **(Fig 16b).**

The differences in interaction of either ch- or huANP32A with AIV polymerase were further confirmed using a co-immunoprecipitation assay. HEK 293T cells were transfected with polymerase subunits as well as C terminally flag-tagged ch- or huANP32A. chANP32A-flag or huANP32A-flag were immunoprecipitated and coprecipitation of PB2 protein was probed for on a western blot. More PB2 was coprecipitated with chANP32A-flag than huANP32A-flag, confirming the pattern seen using the split luciferase complementation assay **(Fig 16c).**

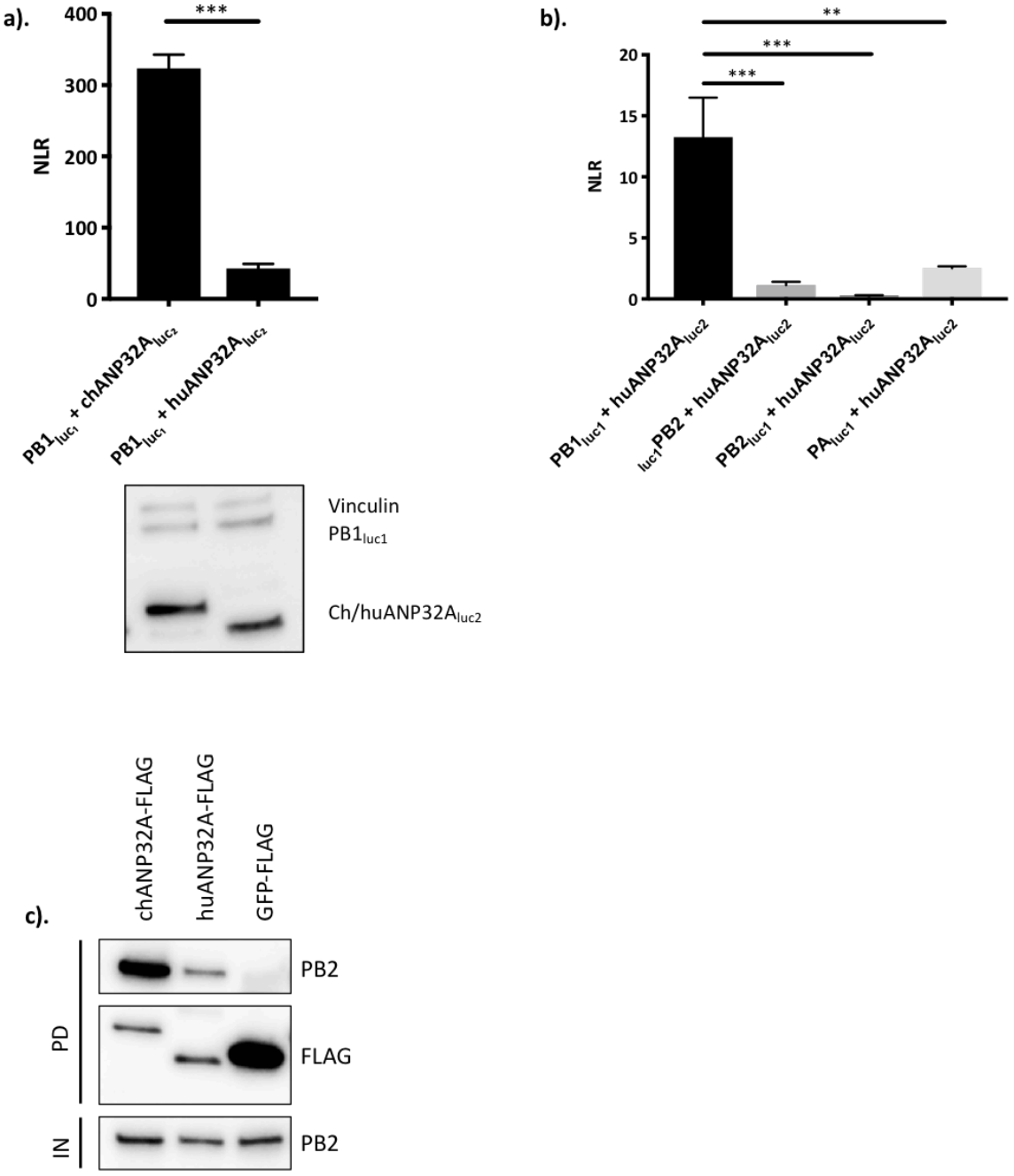


Fig 16: chANP32A binds to the influenza polymerase to a greater extent than huANP32A a). a). HEK 293T cells were transfected with 25 ng $PB1_{luc1}$, 25 ng PB2, 12.5 ng PA and 12.5 ng either $chANP32A_{luc2}$ or $huANP32A_{luc2}$. Gluc activity was measured 24 hours after transfection. Expression of proteins shown on western blot below. Anti-Gluc was used to detect Gluc tagged proteins. Statistical significance was assessed by unpaired students t-test ***p<0.001 **b).** 12.5 ng $huANP32A_{luc2}$ as well as various luc1 tagged polymerase subunits were transfected into cells. Untagged versions of the remaining polymerase subunits were also transfected; 25 ng PB1 or PB2 or 12.5 ng PA was used. Results shown are mean ± standard deviation from triplicate samples. Statistical significance assessed by one-way ANOVA, comparisons made between all conditions, **p<0.01, ***p<0.001, non-significant comparisons not shown **c).**

Cells were transfected with 3 μg PB1, 3 μg PB2, 1.5 μg PA and 1.5 μg chANP32A-FLAG, huANP32A-FLAG or GFP-FLAG. 30 hours after transfection, cells were lysed followed by flag immunoprecipitation and western blotting. Results representative of three independent experiments.

It has previously been shown that binding of huANP32A to the human influenza A viral polymerase strain A/WSN/33 requires the whole trimeric polymerase complex (Sugiyama *et al.,* 2015). To confirm this on an avian strain and test whether this also applies to the interaction between AIV polymerase and chANP32A, PB2 was omitted from the split luciferase assay. PB2 was chosen to be excluded since exclusion of PA may have resulted in re-localisation of $PB1_{luc1}$ (Deng *et al.,* 2005). Omission of PB2 abolished the luciferase signal between $PB1_{luc1}$ and $chANP32A_{luc2}$ **(Fig 17a)**. The weaker interaction between $huANP32A_{luc2}$ and the polymerase was also reduced **(Fig 17b)**. To ensure that neither ch- or huANP32A proteins bound to PB2 alone, a co-immunoprecipitation assay was carried. No interaction above background could be detected between PB2 and either chANP32A or huANP32A using this method **(Fig 17c)**.

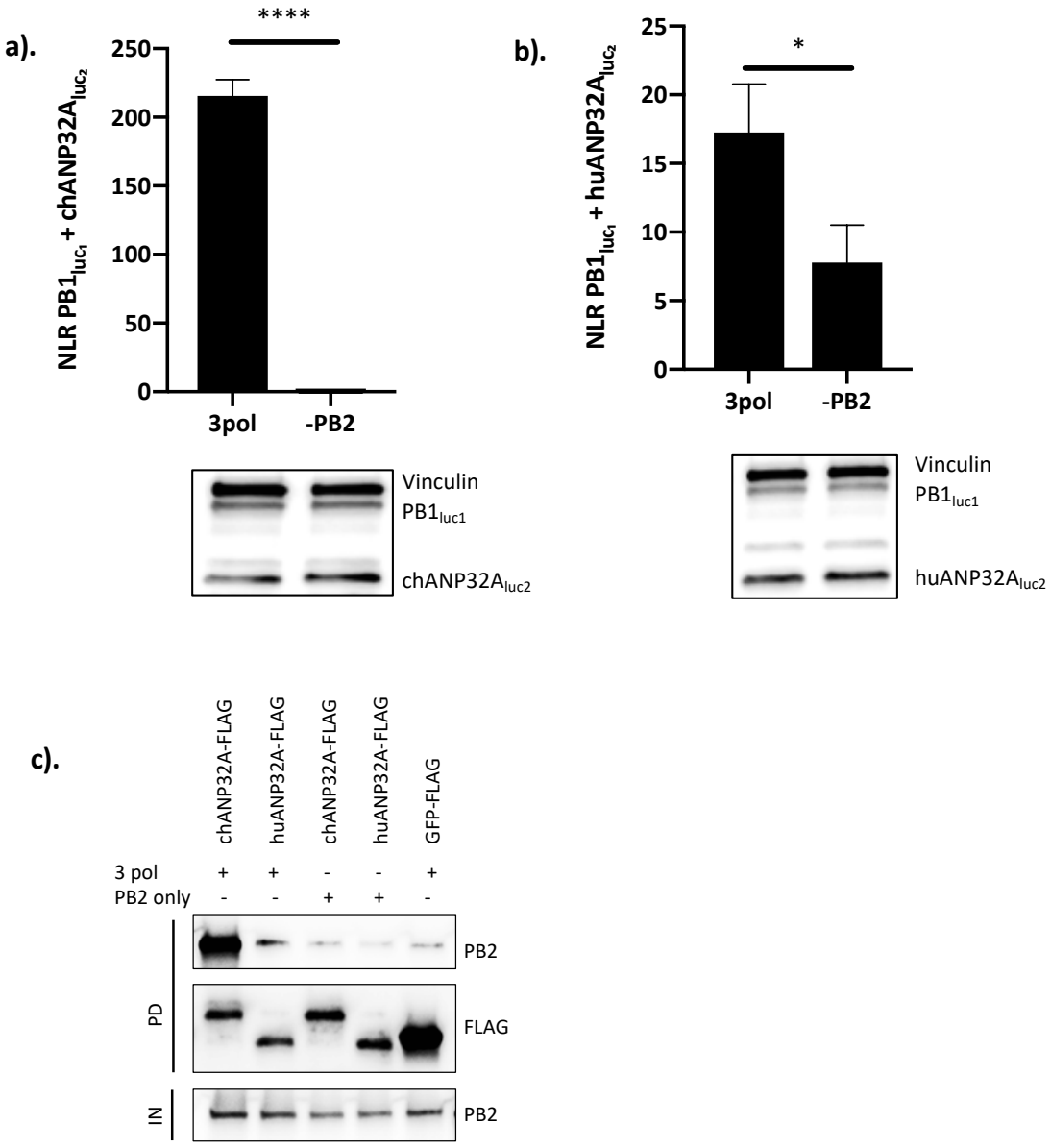


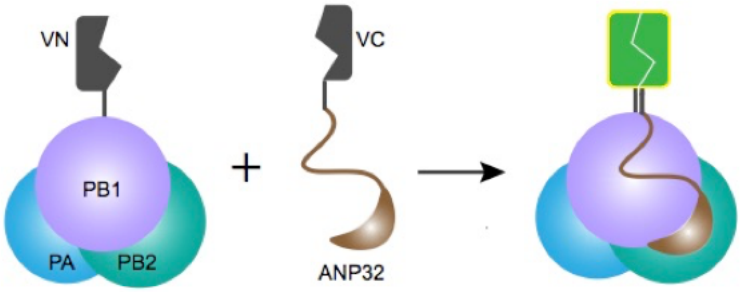
Fig 17: Interactions between the polymerase and ANP32A require the whole trimeric polymerase complex. HEK 293T cells were transfected with 25 ng $PB1_{luc1}$, 12.5 ng 12.5 ng PA, either 25ng PB2 or empty plasmid and **a).** $chANP32A_{luc2}$ or **b).** $huANP32A_{luc2}$. Gluc activity was measured 24 hours after transfection. Expression of proteins was confirmed by western blot analysis. Anti-Gluc was used to detect Gluc tagged proteins. Results shown are mean ± standard deviation from triplicate samples. Statistical significance was assessed by unpaired t-tests, comparisons made to 3pol, *p<0.05, ****p<0.0001. Results representative of three independent experiments **c).** All viral polymerase subunits or PB2 only were transfected into 293T cells with chANP32A-flag, huANP32A-flag or GFP-flag. 30 hours after transfection, flag was immunoprecipitated and co-precipitation of PB2 detected by western blotting. Fig 17c was repeated twice.

2.2.3 The interaction between ANP32A and the polymerase occurs in the nucleus of human cells

ANP32A is primarily a nuclear protein, however there have been some reports of its presence outside of the nucleus (reviewed in Reilly *et al.,* 2014). Since the influenza trimeric polymerase complex forms in the nucleus of host cells (Deng *et al.,* 2005), it is likely that the interaction between ANP32A and the polymerase complex also takes place in the nucleus. To prove this, bimolecular fluorescence complementation (BiFC) assays were carried out. Overlapping PCR was used to C-terminally tag 50-92 PB1 and both ANP32A proteins with each half of Venus fluorescent protein. Interaction of $PB1_{VN}$ with $ANP32A_{VC}$ should allow the two halves of Venus to reform producing a fluorescent signal which can be visualised *in situ* **(Fig 18a)**.

To visualise the interactions between ANP32A and the polymerase, HEK 293T cells were transfected with $PB1_{VN}$ and ch- or $huANP32A_{VC}$, as well as untagged PB2 and PA to ensure formation of a trimeric polymerase complex. 20 hours after transfection, the cells were fixed and visualised using confocal microscopy. It can be clearly seen that the interaction between the polymerase and both ch- and huANP32A occurs in the nucleus of these cells **(Fig 18b top panel).** Cells transfected with the two tagged constructs as well as PA, but omitting PB2 were used as a control. Only a very dim background signal was observed **(Fig 18b bottom panel).**

a).



b).

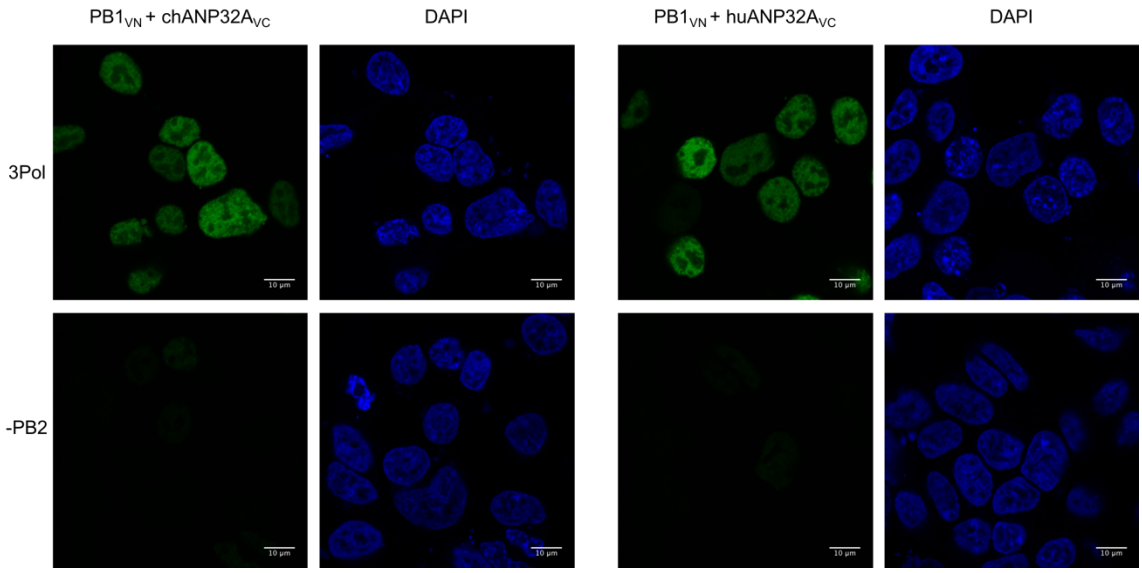


Fig 18: Interactions between the polymerase and ANP32A occur in the nucleus of human cells. a). Schematic of BiFC assay **b).** HEK 293T cells were transfected with 80 ng $PB1_{VN}$, 40 ng $chANP32A_{VC}$ or $huANP32A_{VC,}$ 40 ng PA and either 80 ng PB2 or empty plasmid. 20 hours after transfection, cells were lysed, fixed and stained with dapi. Images were taken using confocal microscopy. Scale bars represent 10 μm.

2.2.4 The 33 amino acids in chANP32A are responsible for the greater interaction with polymerase compared to huANP32A

Since the main sequence difference between chANP32A and huANP32A is the additional 33 amino acids present in the avian protein, we hypothesised that these 33 amino acids confer the greater binding of chANP32A with the polymerase. We engineered and tested a chANP32A$_{luc2}$ construct lacking the extra 33 amino acids (chANP32AΔ33$_{luc2}$). The interaction with the AIV polymerase decreased to levels similar to that seen for huANP32A$_{luc2}$. Insertion of the 33 amino acids into huANP32A (huANP32A+33$_{luc2}$) resulted in an increase in the interaction between huANP32A and the polymerase, indicating that the 33 amino acids are responsible for the enhanced binding of chANP32A with the AIV polymerase **(Fig 19a)**. This was also confirmed using a coimmunoprecipitation assay **(Fig 19b).**

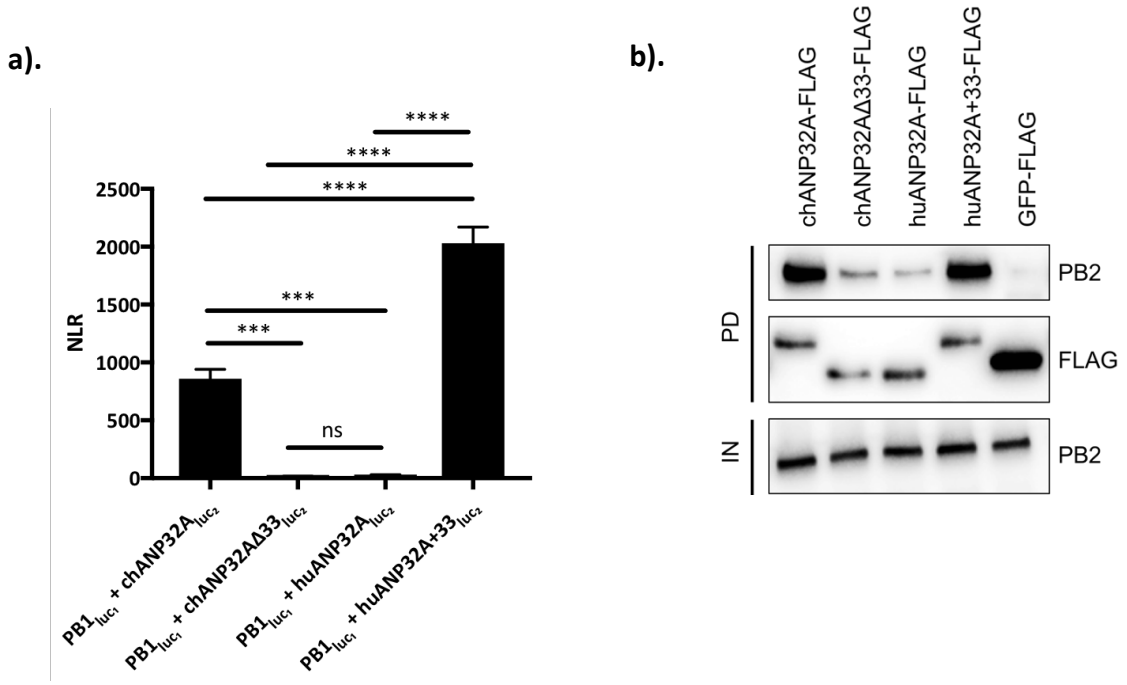


Fig 19: The 33 amino acids in chANP32A contribute to greater binding with polymerase compared to huANP32A a). HEK 293T cells were transfected with 25 ng $PB1_{luc1}$, 25 ng PB2, 12.5 ng PA and 12.5 ng of the appropriate $ANP32A_{luc2}$ construct. Gluc activity was measured 24 hours after transfection. Results shown are mean ± standard deviation from triplicate samples. Statistical significance was assessed by one-way ANOVA, comparisons made between each condition ns = non-significant, ***p<0.001, **** p<0.0001 **b).** Cells were transfected with 3 μg PB1, 3 μg PB2, 1.5 μg PA and 1.5 μg of the appropriate ANP32A-FLAG construct or GFP-FLAG. 30 hours after transfection, cells were lysed followed by flag immunoprecipitation and western blotting. Results representative of three independent experiments.

2.2.5 Binding of chANP32A to the polymerase involves the 627 domain

As previously mentioned, the most commonly occurring mutation in the polymerase which can overcome the restriction to AIV replication in mammalian cells is the PB2 E627K mutation. To investigate whether the 627 domain of PB2, in which position 627 resides, is necessary for the interaction with ch- and huANP32A, we generated a 50-92 PB2 construct lacking the 627 domain as previously described (Nilsson *et al*., 2017). It has previously been shown that this construct is able to fold correctly and form a complex with the other polymerase subunits (Nilsson *et al.,* 2017). In the absence of the 627 domain, the interaction between chANP32A and the AIV polymerase decreased in both split luciferase and co-immunoprecipitation assays **(Fig 20a and b).** In contrast, the interaction between huANP32A and the AIV polymerase remained unchanged in the absence of the PB2 627 domain **(Fig 20a and c).** This indicates that the enhanced interaction of polymerase with chANP32A, is mediated by the 627 domain of PB2. Since chANP32A harbours the extra 33 amino acids responsible for the strong interaction, which huANP32A does not possess, it is likely that it is these 33 amino acids which are necessary for the interaction involving the 627 domain.

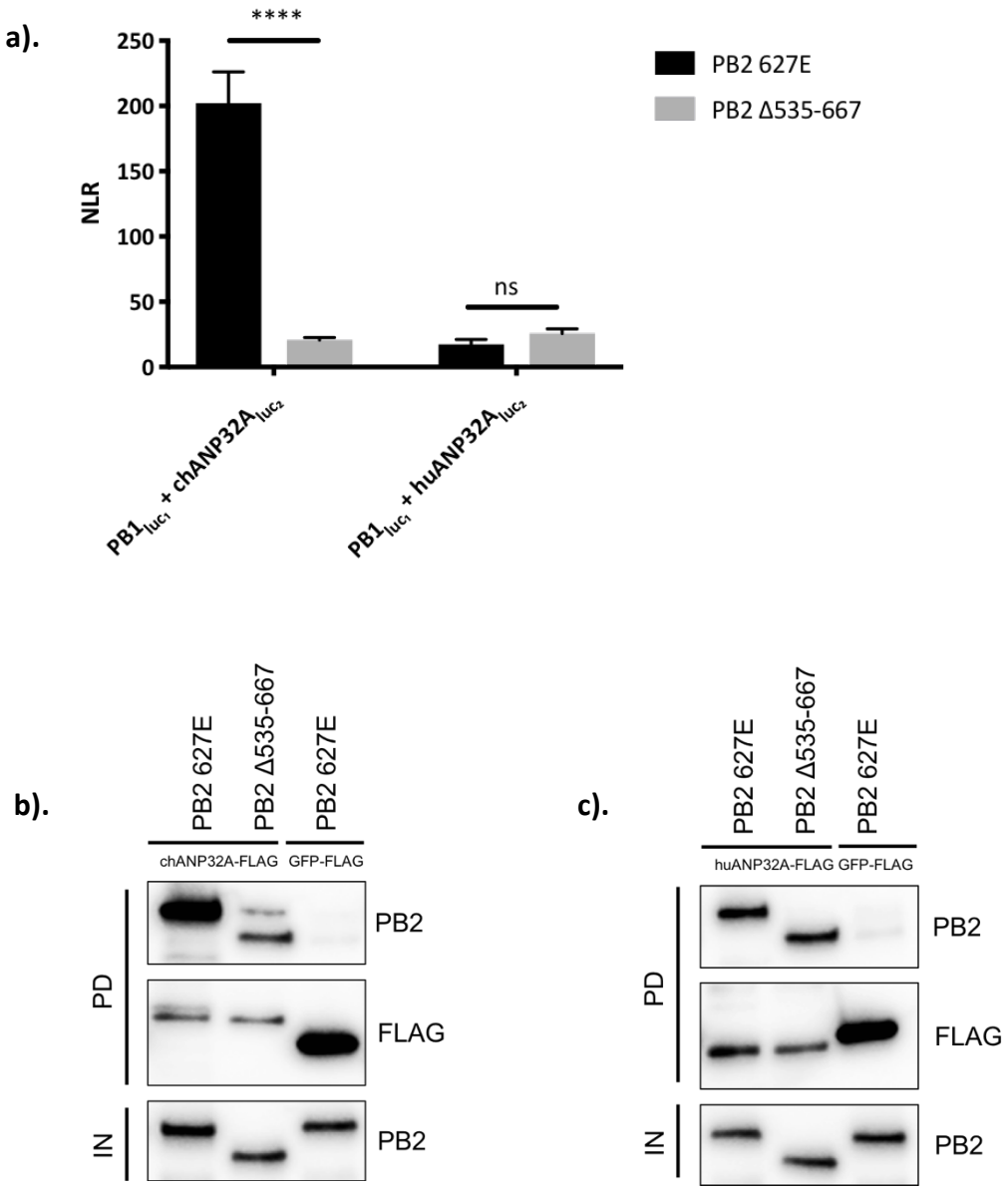


Fig 20: Binding of chANP32A involves the 627 domain of PB2 a). HEK 293T cells were transfected with 25 ng $PB1_{luc1}$, 12.5 ng PA, 12.5 ng either $chANP32A_{luc2}$ or $huANP32A_{luc2}$ and either WT PB2 or PB2Δ535-667. Gluc activity was measured 24 hours after transfection. Results shown are mean ± standard deviation from triplicate samples. Statistical significance was assessed by multiple t-tests, comparisons made to WT PB2 (black bars) ns = non significant, **** p<0.0001. For **b** and **c**, cells were transfected with 3 μg PB1, 3 μg WT PB2 or PB2Δ535-667, 1.5 μg PA and 1.5 μg of **b).** chANP32A-FLAG or **c).** huANP32A-FLAG or GFP-FLAG as indicated. 30 hours after transfection, cells were lysed followed by flag immunoprecipitation and western blotting. Results representative of three independent experiments.

2.2.6 Function of ANP32A is not determined by extent of binding to the trimeric polymerase

To further investigate which regions of chANP32A are required for the interaction with the AIV polymerase as well as for the functional rescue of AIV polymerase activity, we constructed several chANP32A mutants **(Fig 21a).** As described in **fig 19**, deletion of the 33 amino acids resulted in lower binding, as shown by a coimmunoprecipitation assay **(Fig 21b)**. Using a minigenome assay, we also saw that this loss of binding correlates with a reduction in its ability to support polymerase activity **(Fig 21c).** A naturally occurring splice variant of chANP32A lacks the first four of those 33 amino acids (chANP32AΔ4). Deletion of these four amino acids also resulted in decreased binding and function **(Fig 21b and c)**. However, although deletion of the entire LCAR domain (chANP32A 1-208) resulted in almost undetectable binding with the polymerase, chANP32A with this truncation was still able to support the activity of the polymerase, albeit it 63% less efficiently than full length chANP32A **(Fig 21b and c).** Altogether, this suggests that although chANP32A has a greater interaction with the polymerase than huANP32A, strong interaction alone is not sufficient for its function. Nevertheless, full length chANP32A is required for maximal polymerase activity.

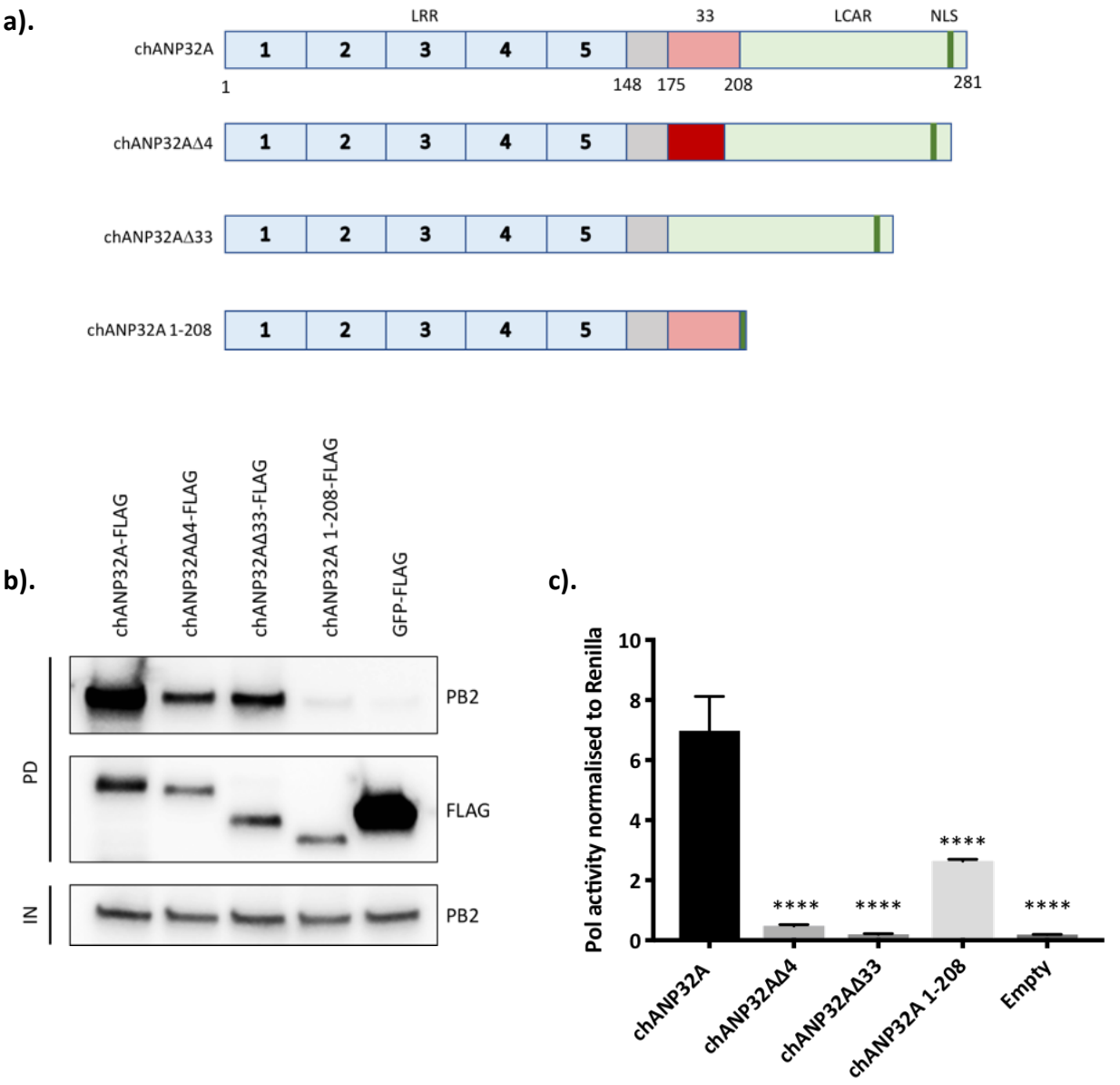
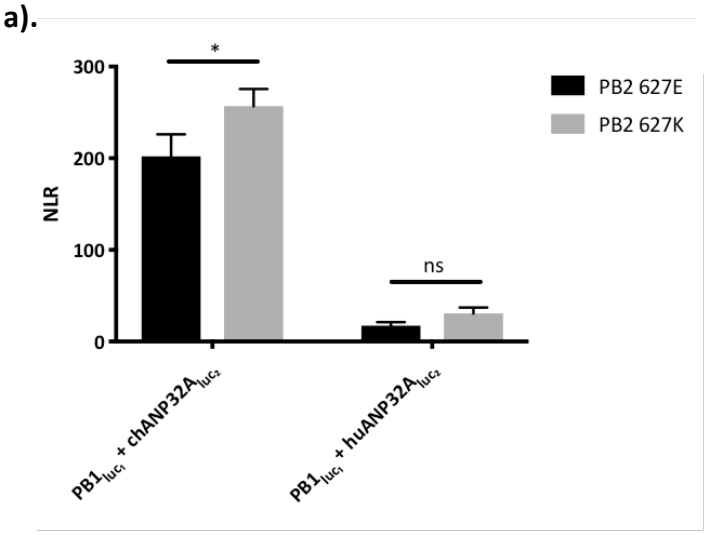
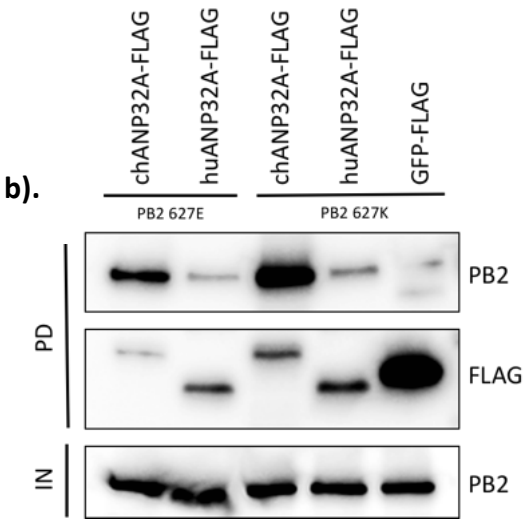
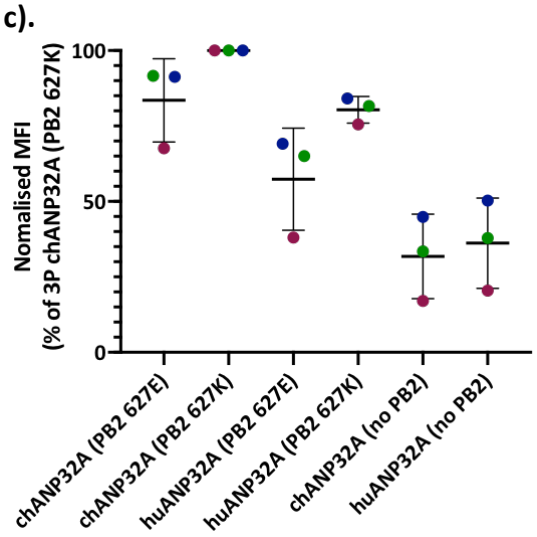


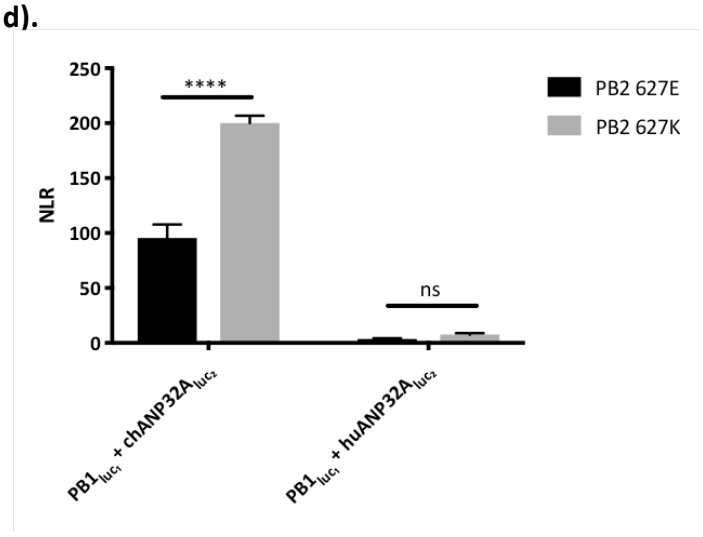
Fig 21: Interactions between chANP32A and the polymerase do not correlate with function **a).** Schematic of chANP32A mutants created. Plasmids cloned by Dr Jason Long. Top is full length chANP32A. chANP32AΔ4 lacks the first four of the avian specific 33 amino acid insertion. chANP32AΔ33 lacks the whole 33 amino acids. chANP32A 1-208 has a truncated LCAR domain. **b).** HEK 293T cells were transfected with 3μg PB1, 3μg PB2, 1.5 μg PA and 1.5μg of the appropriate chANP32A-FLAG mutant or GFP-FLAG. 30 hours after transfection, cells were lysed followed by flag immunoprecipitation and western blotting. **c).** Cells were transfected with 20 ng PB1, 20 ng PB2, 10 ng PA, 40 ng NP, 20 ng pol I Firefly luciferase and 10 ng *Renilla* luciferase as an internal control. 20 ng of the appropriate chANP32A mutant or an empty plasmid was also transfected. Results are normalised to *Renilla* luciferase. Results shown are mean ± standard deviation from triplicate samples. Statistical significance was assessed by one-way ANOVA, comparisons made to full length chANP32A (black bar) **** $p<0.0001$. Results representative of three independent experiments.

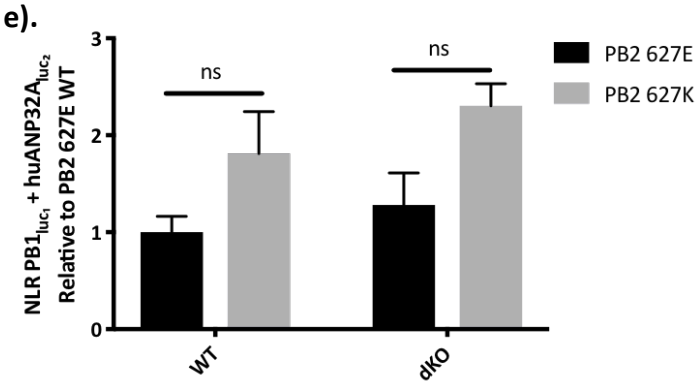
Several publications have shown that huANP32A and -B are host factors that support the activity of a human adapted influenza polymerase in human cells (Long *et al.,* 2016; Sugiyama *et al.,* 2015; Watanabe *et al.,* 2014). As previously mentioned, the E627K mutation in the PB2 subunit of the polymerase is able to overcome the restriction of AIV polymerase replication in human cells. We therefore investigated whether a 50-92 polymerase engineered to contain PB2 E627K showed a greater interaction with huANP32A. In split luciferase, coimmunoprecipitation and analysis of *in situ* BiFC assays by flow cytometry, it was revealed that, although there were slight increases in the interaction between huANP32A and the polymerase with PB2 627K compared to PB2 627E, these differences were not significant and the interaction did not reach the level of chANP32A **(Fig 22a, b and c).** The same pattern of binding was also seen using a human viral polymerase, Vic **(Fig 22d).** To ensure that endogenous levels of huANP32A or -B were not hindering the exogenously expressed huANP32A from binding to the polymerase, we assessed the polymerase:ANP32 interactions in human eHAP1 cells in which both huANP32A and -B have been knocked out using CRISPR-Cas9 (Staller *et al., in review*). In these cells, the ratio between the interactions when PB2 contained 627E or 627K remained similar to the wildtype cell line in both split luciferase and co-immunoprecipitation assays **(Fig 22e and f)**. This further suggests that the enhanced binding of AIV polymerase to chANP32A does not, on its own, explain the ability of the avian ANP32 proteins to support AIV polymerase function.


a).
*
300
200
100
0
NLR
ns
PB2 627E
PB2 627K
PB1luc1 + chANP32Aluc2
PB1luc1 + huANP32Aluc2


b).
chANP32A-FLAG
huANP32A-FLAG
chANP32A-FLAG
huANP32A-FLAG
GFP-FLAG
PB2 627E
PB2 627K
PD
IN
PB2
FLAG
PB2


c).
Nomalised MFI
(% of 3P chANP32A (PB2 627K)
100
50
0
chANP32A (PB2 627E)
chANP32A (PB2 627K)
huANP32A (PB2 627E)
huANP32A (PB2 627K)
chANP32A (no PB2)
huANP32A (no PB2)


d).
****
250
200
150
100
50
0
NLR
ns
PB2 627E
PB2 627K
PB1luc1 + chANP32Aluc2
PB1luc1 + huANP32Aluc2


e).
NLR PB1luc1 + huANP32Aluc2
Relative to PB2 627E WT
3
2
1
0
ns
ns
PB2 627E
PB2 627K
WT
dKO

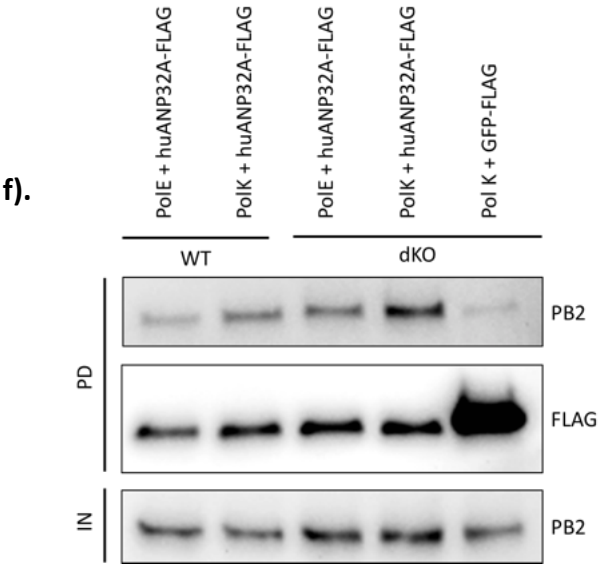

f).
PolE + huANP32A-FLAG
PolK + huANP32A-FLAG
PolE + huANP32A-FLAG
PolK + huANP32A-FLAG
Pol K + GFP-FLAG
WT
dKO
PD
IN
PB2
FLAG
PB2

Fig 22: Differences in interactions between ANP32A and the polymerase do not explain function. HEK 293T cells were transfected with 25 ng **a).** 5092 $PB1_{luc1}$ or **d).** Vic $PB1_{luc1,}$ 25 ng PB2 627E or PB2 627K, 12.5 ng PA and 12.5 ng $chANP32A_{luc1}$ or $huANP32A_{luc2}$. Gluc activity was measured 24 hours after transfection. Results shown are mean ± standard deviation from triplicate samples. Statistical significance was assessed by two-way ANOVA, comparisons between PB2 627E and PB2 627K ns = non significant, * p<0.05, **** p<0.0001. **b).** HEK 293T cells were transfected with 3ug 5092 PB1, 3ug PB2 627E or PB2 627K, 1.5 ug PA and 1.5ug of the appropriate ANP32A-FLAG or GFP-FLAG. 30 hours after transfection, cells were lysed followed by flag immunoprecipitation and western blotting. **c).** HEK 293T cells were transfected with 80 ng 5092 $PB1_{VN}$, 80 ng PB2 627E or PB2 627K, 40 ng PA and either 80 ng $chANP32A_{VC}$ or $huANP32A_{VC}$. PB2 was omitted in controls and compensated for using an empty plasmid. 20 hours after transfection, mean fluorescent intensity was measured using flow cytometry. Results from three independent experiments are plotted (each colour represents a different experiment) **e).** eHAP1 WT or dKO cells lacking human ANP32A and -B were transfected with 25ng $PB1_{luc1,}$ 25 ng PB2 627E or PB2 627K, 12.5 ng PA and 12.5 ng $huANP32A_{luc2}$. Gluc activity was measured 24 hours after transfection. Results shown are mean ± standard deviation from triplicate samples. Statistical significance was assessed by two-way ANOVA, results are plotted relative to signal from polymerase containing PB2 627E in WT cells (left bar), comparisons made to PB2 627E of each cell line. ns = non significant. **f).** eHAP1 WT or dKO cells were transfected with 3μg 5092 PB1, 3μg PB2 627E or PB2 627K, 1.5 μg PA and 1.5μg of huANP32A-FLAG or GFP-FLAG. 30 hours after transfection, cells were lysed followed by flag immunoprecipitation and western blotting. Results representative of three independent experiments.

2.2.7 Interactions between the polymerase and ANP32A are stabilised at RNPs

It is important to note that all of the binding experiments above were carried out using the reconstituted viral polymerase trimer alone, with no viral RNA species. However, a minigenome assay, which is used to assess function, also requires the presence of NP and an influenza viral-like RNA. Crystal structures have shown that the polymerase adopts different conformations when bound to a v- or cRNA promoter compared to an 'apo' polymerase with no influenza RNA bound (Hengrung *et al.,* 2015; Thierry *et al.,* 2016). In particular, the N-terminal endonuclease domain of PA and several domains at the C terminus of PB2 undergo a major shift depending on whether the polymerase is bound to vRNA **(Fig 23a and b)**. The C terminal domains of PB2 that shift include the 627 domain, where the host adaptive residue, 627 lies. We therefore explored whether binding of chANP32A to the polymerase altered when the polymerase formed part of an RNP. In order to do this, we carried out split luciferase assays as above, with the addition of a 1723 nt vRNA template expressed from a polI plasmid, which can be recognised by the reconstituted polymerase. Since it has been shown that processive replication on long RNA templates requires NP, these experiments were carried out in the absence of NP to prevent replication (Paterson *et al.,* 2014). Addition of the vRNA template resulted in an increase in the interaction between the AIV polymerase and chANP32A in a dose dependent manner **(Fig 24a)**. Similarly, addition of a cRNA template also increased the interaction between the AIV polymerase and chANP32A **(Fig 24b)**.

It was shown in section 2.2.6 that enhanced binding of ANP32A to the polymerase apoenzyme alone could not explain why chANP32A was able to support the activity of an AIV polymerase, but huANP32A could not. To investigate whether binding of huANP32A to polymerases within RNPs could shed light on this, we examined whether the patterns of binding of polymerases

with PB2 627E or K to huANP32A differed in the presence of vRNA or cRNA templates. We observed that the addition of either a 1723nt vRNA or cRNA template, resulted in increased interactions between the polymerase and huANP32A$_{luc2}$ regardless of the identity of amino acid at position 627 of PB2 **(Fig 24c and d)**.

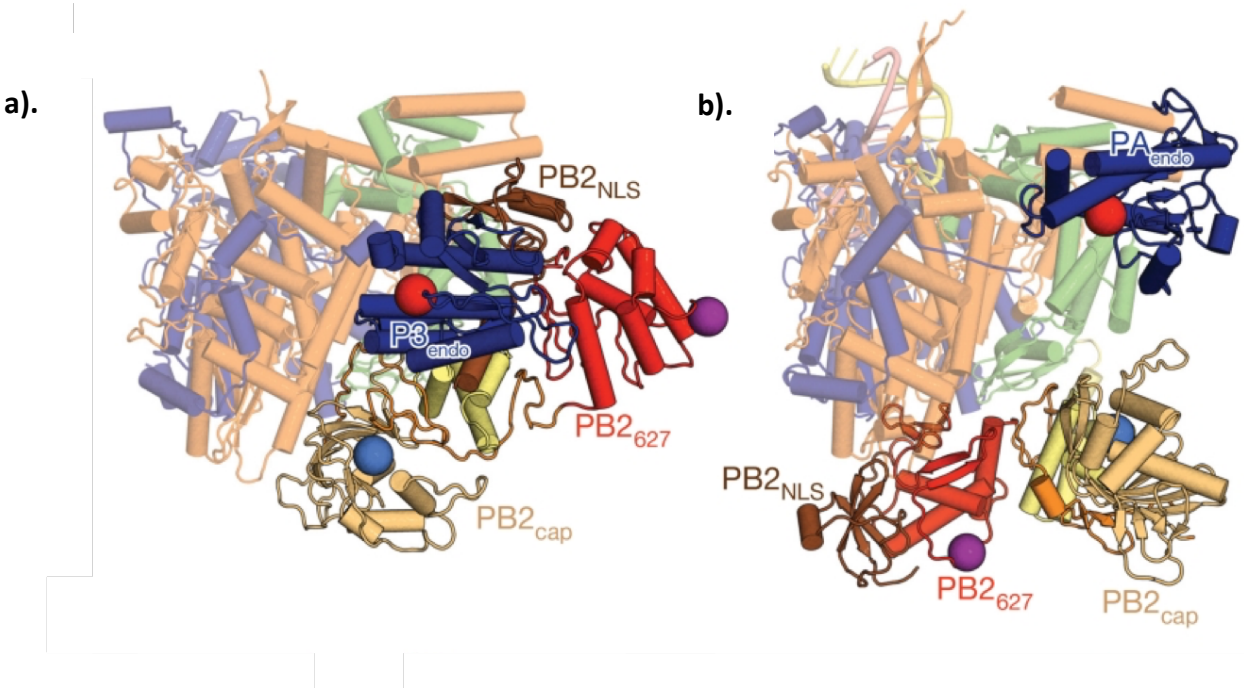


Fig 23: The influenza polymerase can adopt multiple conformations. a). Apo-influenza polymerase C. **b).** Promoter bound influenza polymerase A. PB1 is coloured orange, PB2 is coloured green and PA/P3 are coloured blue. Red sphere corresponds to the endonuclease active site, blue sphere is the cap binding pocket and red sphere is residue 627 of PB2 (or the equivalent residue 649 in the influenza C apo structure). Domains that do not change between structures are semi transparent, domains which do change are highlighted and labelled. (Hengrung *et al.,* 2015).

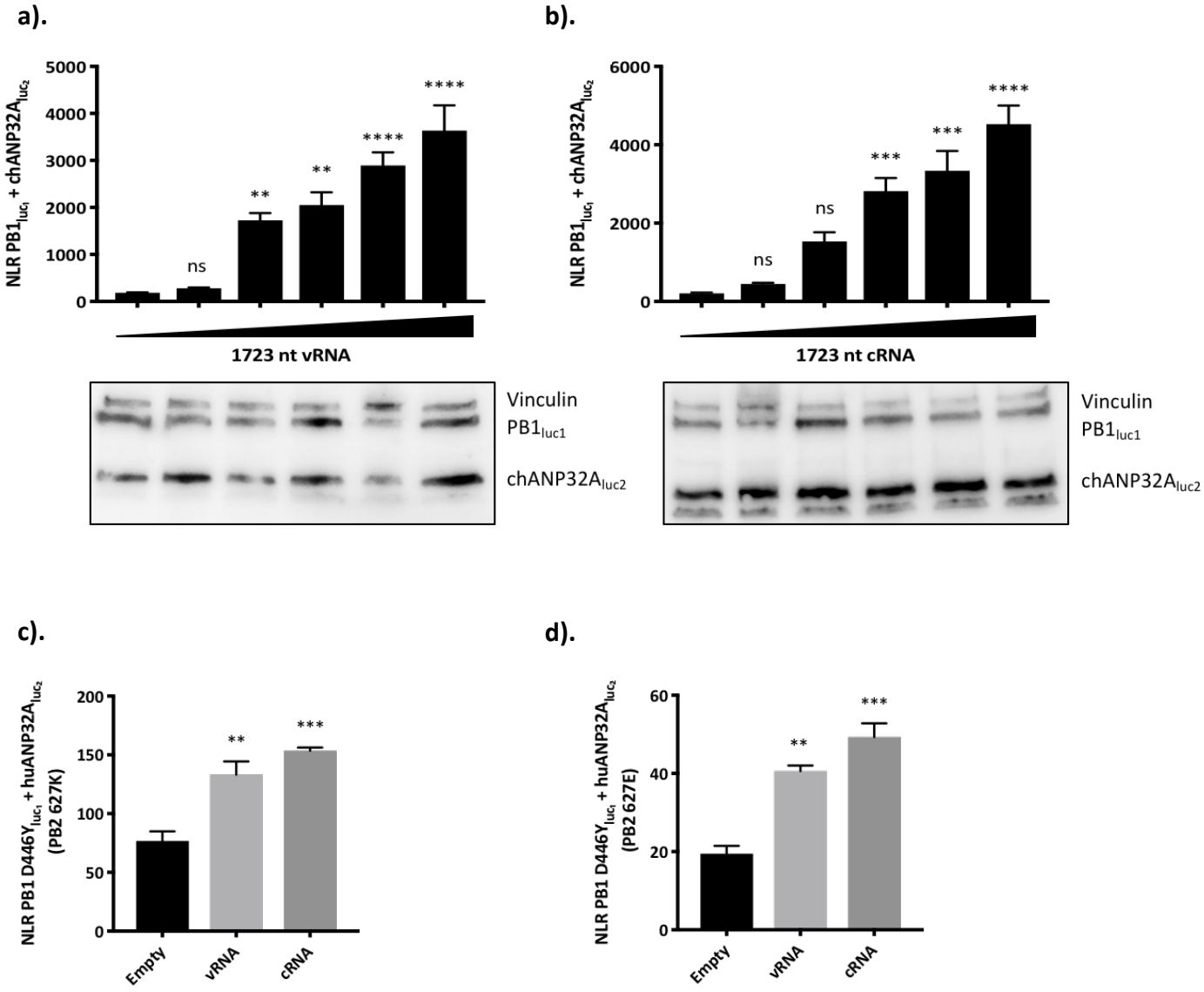


Fig 24: Interaction between ANP32A and polymerase is stabilised at RNPs. HEK 293T cells were transfected with 10 ng $PB1_{luc1}$, 10 ng PB2, 5 ng PA, 5 ng $chANP32A_{luc2}$ and 0 ng, 10 ng, 100 ng, 200 ng, 300 ng or 400 ng of **a).** 1723nt vRNA or **b).** 1723nt cRNA. For **c** and **d,** cells we transfected with 10 ng PB1 $D446Y_{luc1}$, 5 ng PA, 5 ng $huANP32A_{luc2,}$ 400 ng 1723 nt vRNA and 10 ng either **c).** PB2 627K or **d).** PB2 627E. Gluc activity was measured 24 hours after transfection. Expression of proteins was assessed by western blotting. Anti-Gluc antibody was used to detect all Gluc tagged proteins. Vinculin was used as a loading control. The bottom band occurs as a result of non-specific binding of the Gluc antibody. Results shown are mean ± standard deviation from triplicate samples. Statistical significance was assessed by one-way ANOVA, comparisons made to sample with no added RNA (left) ns = non-significant, ** p<0.01. *** p<0.001. **** p<0.0001. Results representative of three independent experiments.

2.2.8 Interactions between the polymerase and ANP32A subside when the polymerase is active

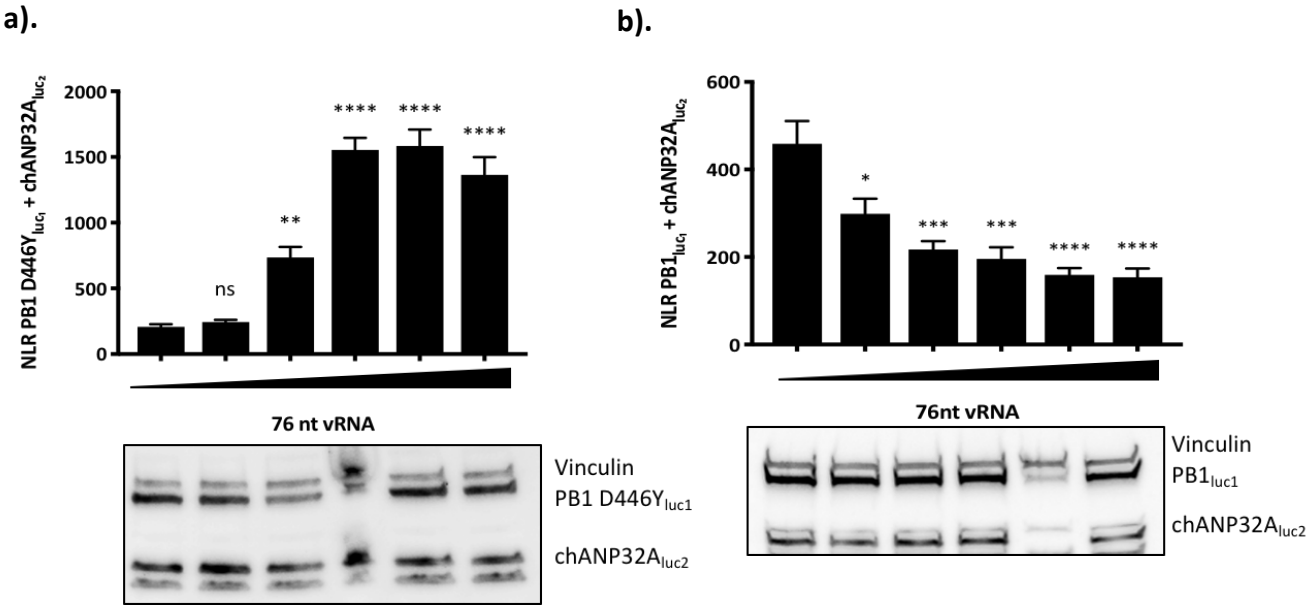
It has previously been shown that vRNA templates 76 nt in length do not require NP in order to be replicated, but replication of this template is still affected by the PB2 E627K mutation (Paterson *et al*, 2014). Using a $PB1_{luc1}$ engineered to contain a D446Y mutation in the SDD motif in the catalytical site of PB1, which renders it catalytically inactive (Biswas *et al.,* 1994), we again looked at the interaction with $chANP32A_{luc2}$, this time with the addition of a 76nt flu like RNA from a polI plasmid (Paterson *et al.,* 2014). The catalytically inactive PB1 was used to stabilise formation of the RNPs whilst also preventing the polymerase from replicating the RNA. As above, the addition of increasing amounts of the vRNA resulted in an increase in the interaction between the polymerase and $chANP32A_{luc2}$ in a dose dependent manner **(Fig 25a).**

Conversely, if an active $PB1_{luc1}$ was expressed, which allowed replication to take place, this resulted in a decrease in interaction between the polymerase and $chANP32A_{luc2}$ **(Fig 25b).** The same pattern was observed for the interaction between $huANP32A_{luc2}$ and a polymerase harbouring the PB2 E627K mutation **(Fig 25c)**. However, the pattern was different for interaction between $huANP32A_{luc2}$ and AIV polymerase with PB2 627E, which did not decrease significantly with the addition of 76 nt vRNA **(Fig 25d)**.

The decrease in signal could be due to dissociation of ANP32A from the polymerase complex. Alternatively, it could be caused by a conformational change in the polymerase as it binds to the RNA, resulting in the two halves of Gluc being too far apart or in an unsuitable orientation to be able to reform. To decipher this, we carried out a coimmunoprecipitation assay. Co-

precipitation of PB2 within an active polymerase with ANP32A-flag decreased with the addition of 76 nt vRNA **(Fig 25e).**

Altogether, this suggests that although ANP32A is able to bind to the trimeric polymerase complex, this binding is stabilised with polymerases which form part of RNPs. However, as the polymerase replicates the RNA, ANP32A dissociates. Whether the interaction between huANP32A and the AIV polymerase fails to dissociate as a result of the polymerase being unable to replicate the vRNA, or whether it fails to replicate as a result of a failure to dissociate is unclear.



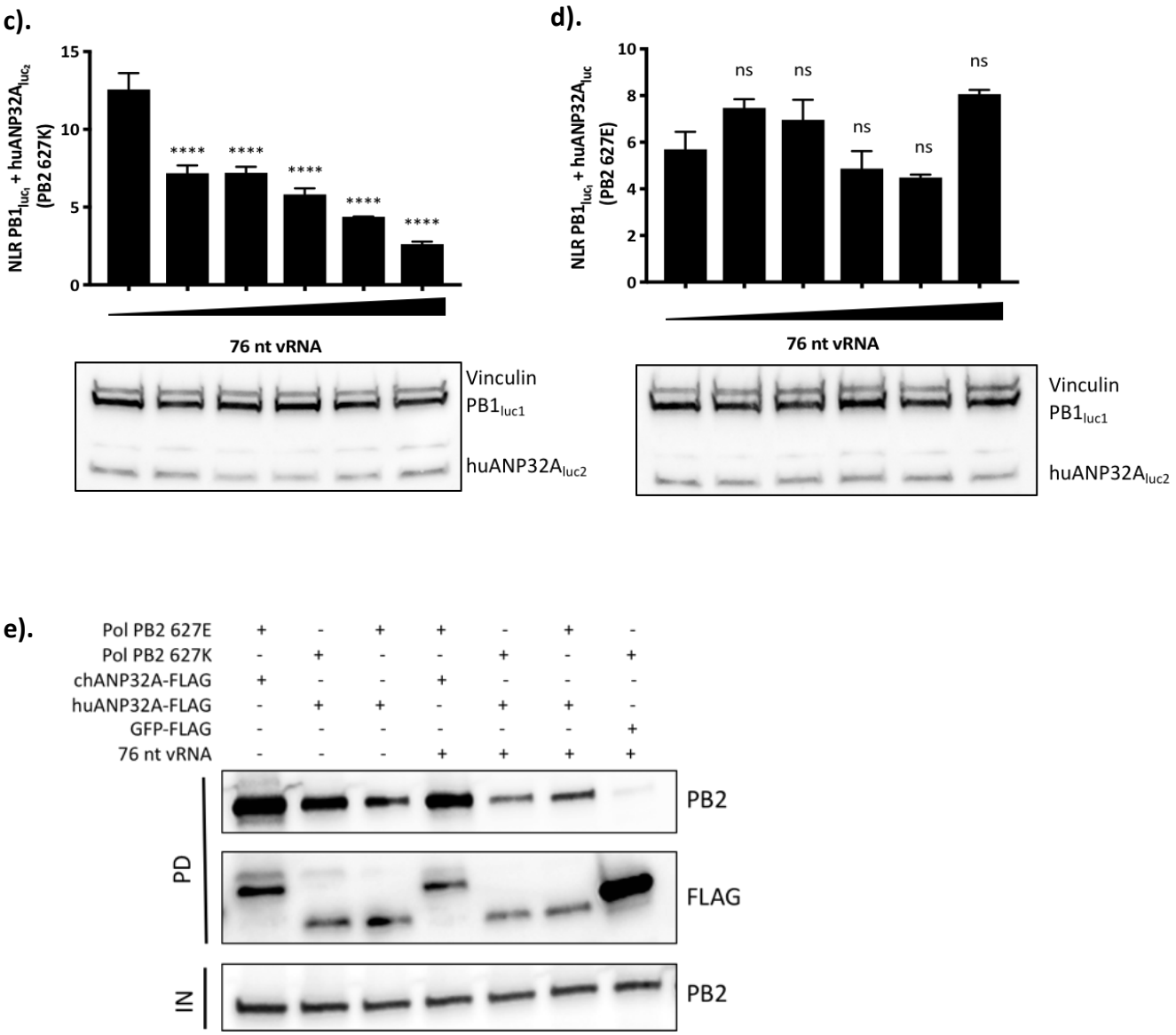


Fig 25: Interaction between ANP32A and polymerase decreases when polymerase is active. Split luciferase assays were carried out on HEK 293T cells transfected with 10 ng **a).** PB1 D446Y$_{luc1}$ or **b,c and d)**PB1$_{luc}$ as well as 5 ng PA and 0, 0.625, 1.25, 2.5, 5, or 10 ng polI 76 nt vRNA and either **a and b).** chANP32A$_{luc2}$ and PB2 627E, **c).** huANP32A$_{luc2}$ and PB2 627K or **d).** huANP32A$_{luc2}$ and PB2 627E. For **e).** Cells were transfected with 3 μg PB1, 3 μg PB2 627E or PB2 627K, 1.5 μg PA and 1.5 μg of chANP32A-FLAG, huANP32A-FLAG or GFP-FLAG as indicated. 750 ng polI 76nt vRNA was also transfected into the indicated samples. Total DNA was kept constant between samples by compensating with an empty vector. 30 hours after transfection, cells were lysed followed by flag immunoprecipitation and western blotting. Results shown are mean ± standard deviation from triplicate samples. Statistical significance was assessed by one-way ANOVA, comparisons made to sample with no added RNA (left) ns = non-significant, * p<0.05, ** p<0.01. *** p<0.001. **** p<0.0001. Results representative of three independent experiments.

2.2.9 Promoter mutations that overcome host range restriction of viral polymerase do not negate the requirement for ANP32A

It is clear that binding of ANP32A with viral polymerase is increased at assembled but inactive RNPs compared to apoenzyme. Interestingly, mutations in the promoter region of the RNA have been shown to be able to overcome the host restriction of AIV polymerase activity in a minigenome assay. Specifically, G3A, U5C and C8U mutations in the 3' promoter vRNA, which increase the complementarity with the 5' promoter strand, can relieve the restriction of AIV polymerase in human cells (Crescenzo-Chaigne *et al.,* 2002) **(Fig 26a)**. This effect was not due to an increase in the complementarity of the promoter region however, but instead due to the specific bases on the 3' promoter strand (Paterson *et al.,* 2014). Using an engineered vRNA with the 3'5'8' mutations as a template in a minigenome assay, it has previously been shown that chANP32A cannot further increase the polymerase activity of an AIV polymerase in human cells, suggesting that the promoter mutations and chANP32A may overcome the same barrier (Baker *et al.,* 2018).

Ongoing studies in our laboratory have shown that in eHAP1 cells edited by CRISPR to knockout expression of huANP32A and -B, polymerase activity of a human adapted polymerase is abolished (Staller *et al., in review*). Using these huANP32A and -B double knock out cells, we sought to investigate whether the polymerase would be able replicate a vRNA template with the 3'5'8 mutations. In a minigenome assay, no matter which vRNA template was used, neither a wild type AIV polymerase nor one bearing the PB2 E627K mutation was able to function in these cells **(Fig 26b and c)**. Interestingly, when using a vRNA template harbouring the 3'5'8 mutations, an AIV polymerase was rescued with huANP32A and -B more significantly than when the RNA did not contain these mutations **(Fig 26d).** This is in line with

the observation that in human cells, this mutated template is efficiently amplified by the AIV polymerase (Crescenzo-Chaigne *et al.,* 2002). Overall, this suggests that expression of ANP32 proteins are essential for polymerase function even if the vRNA template contains the 3'5'8 mutations. These promoter mutations may however, increase the compatibility of huANP32A and -B with an AIV polymerase.

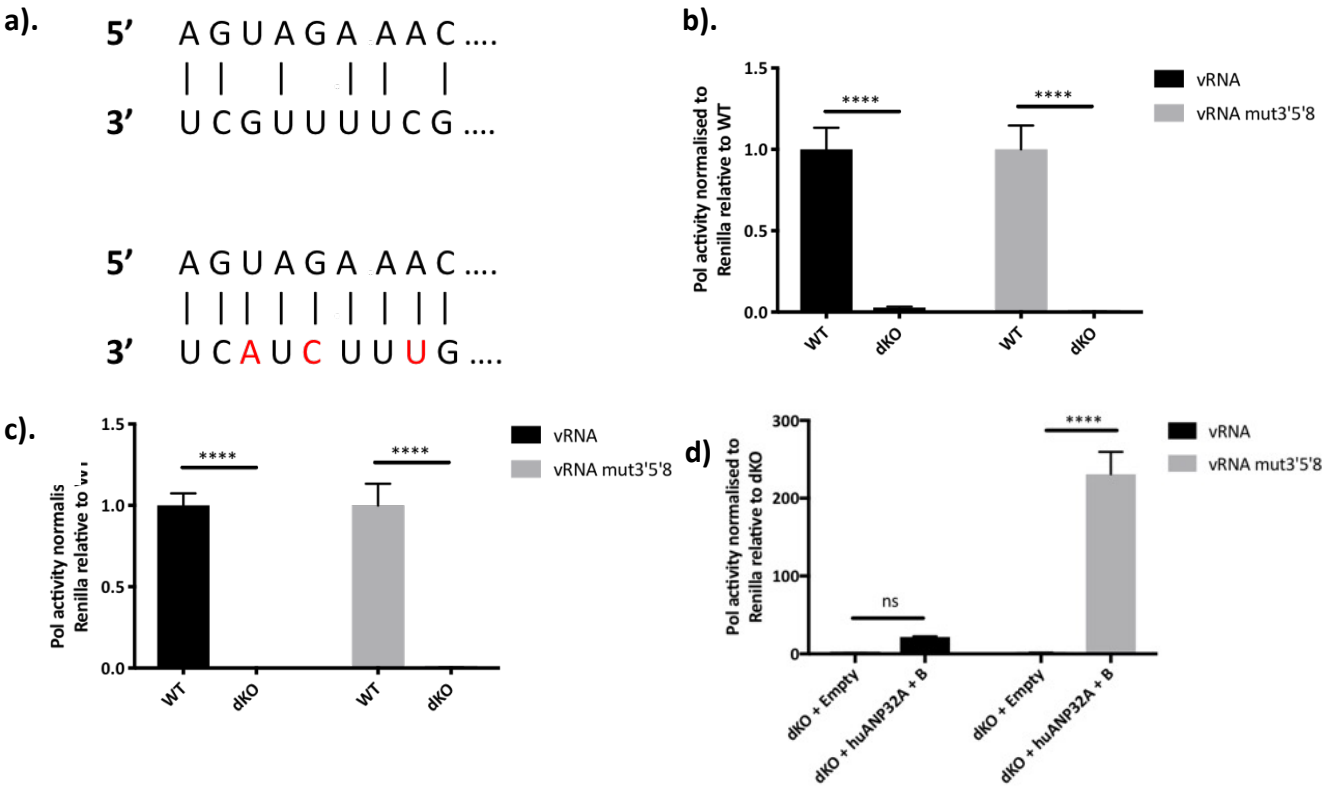


Fig 26: ANP32A is required to replicate a template with mutations at 3'5'8. a). WT and mutated vRNA promoter based on pan handle structure. Mutated residues in red. For b and c, eHAP1 WT or huANP32A and -B double knockout (dKO) cells were transfected with 5092 polymerase minigenome components including either **b).** PB2 627E or **c).** PB2 627K and either WT vRNA (black bars) or that with the 3'5'8 mutations (grey bars). **d).** dKO cells were transfected with minigenome components including either WT vRNA (black bars) or that with the 3'5'8 mutations (grey bars). Either 20 ng empty plasmid or 10 ng each of huANP32A and -B was transfected. Firefly luciferase activity was normalised to *Renilla* luciferase. Results shown are mean ± standard deviation from triplicate samples. Statistical significance was assessed by two-way ANOVA, comparisons made between each sample with the same vRNA template, ns = non-significant, ** $p<0.01$, **** $p<0.0001$. Results representative of three independent experiments.

2.2.10 ANP32A interacts with NP

ANP32 proteins bind to influenza polymerase in the absence of NP. However, NP was included in the minigenome assays described above that assessed function of polymerase in the presence of ANP32 proteins. It has been proposed that the PB2 E627K mutation may determine the stability of the interaction between the polymerase and NP (Labadie *et al.,* 2007; Ng *et al.,* 2012). We therefore also studied whether the role of ANP32A to support influenza polymerase function may involve NP.

We first investigated whether ANP32A could bind to NP. We performed a split luciferase assay with Vic NP_{luc1} and ch- or huANP32A$_{luc2}$. A signal could be observed with both ANP32A proteins **(Fig 27a).** 50-92 NP could also be coprecipitated with both chANP32A-flag and huANP32A-flag **(Fig 27b).** Since NP is positively charged and can bind to RNA, RNase was added to degrade cellular RNA. In the presence of RNase, the interaction between both ANP32A proteins and NP increased **(Fig 27c).** This is most likely because degradation of RNA released NP from an oligomeric state to monomers or dimers, making more NP units available to bind to ANP32A.

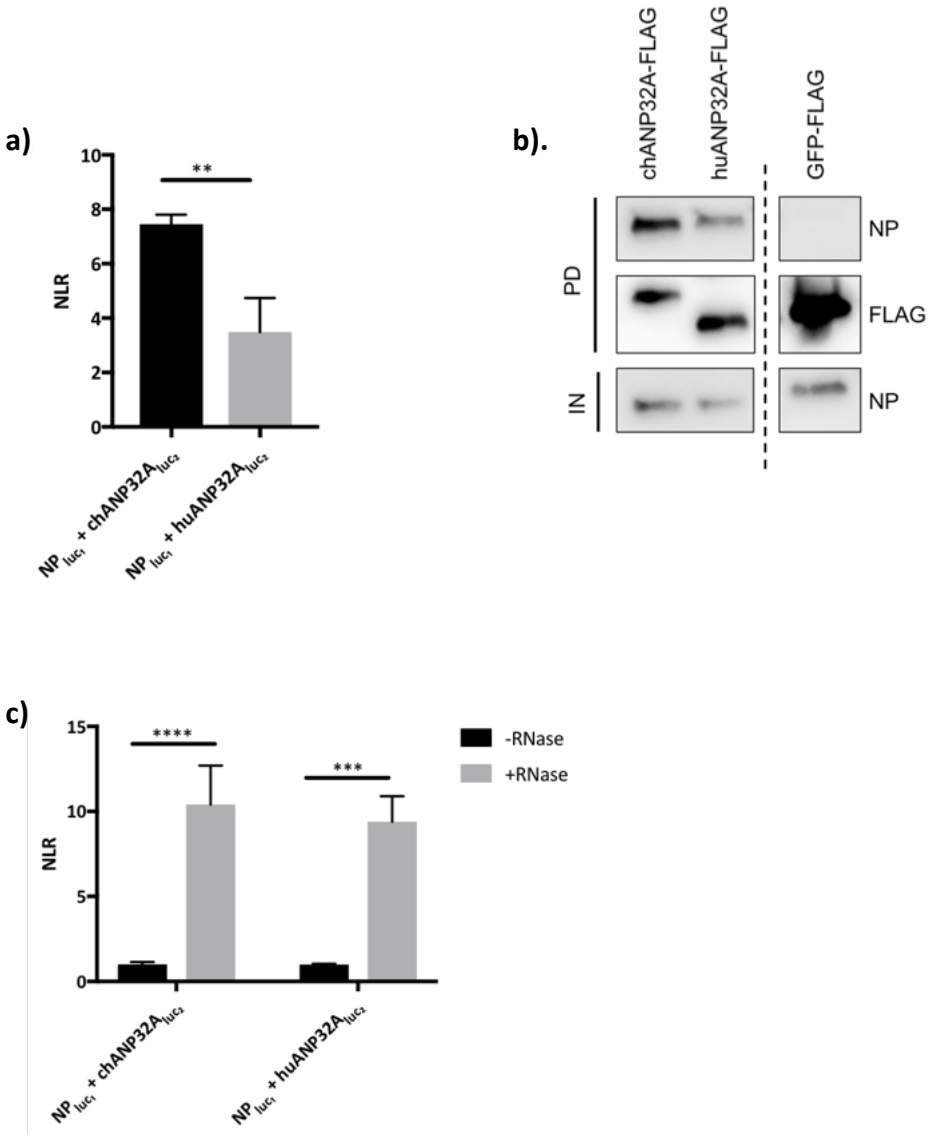


Fig 27: ANP32A interacts with NP. a). Split luciferase assays were carried out on 293T cells transfected with 20ng Vic NP_{luc1} + $chANP32A_{luc2}$ or $huANP32A_{luc2}$. Results shown are mean ± standard deviation from triplicate samples. Statistical significance was assessed by unpaired students t-test, ** p<0.01 **b).** Cells were transfected with 1.5 μg 50-92 NP and 1.5 μg chANP32A-FLAG, huANP32A-FLAG or GFP-FLAG as indicated. 30 hours after transfection, cells were lysed followed by flag immunoprecipitation and western blotting. Dotted line represents lanes cut out of western blot. **c).** Cells were transfected as in a). During lysis 10ug/ml RNase A was added to the lysate. Results shown are relative to no RNase, mean ± standard deviation from triplicate samples. Statistical significance was assessed by two-way ANOVA, comparisons made between no RNase and RNase, *** p<0.001, **** p<0.0001. Results representative of three independent experiments.

We next carried out competition assays between NP and the polymerase to determine whether ANP32A would preferentially bind to NP or the polymerase. The addition of increasing amounts of polymerase caused the interaction between chANP32A and NP to decrease in a dose dependent manner **(Fig 28a).** However, the addition of increasing amounts of NP, did not have such an effect on the interaction between chANP32A and the polymerase **(28b).** This suggests that chANP32A preferentially binds viral polymerase over NP.

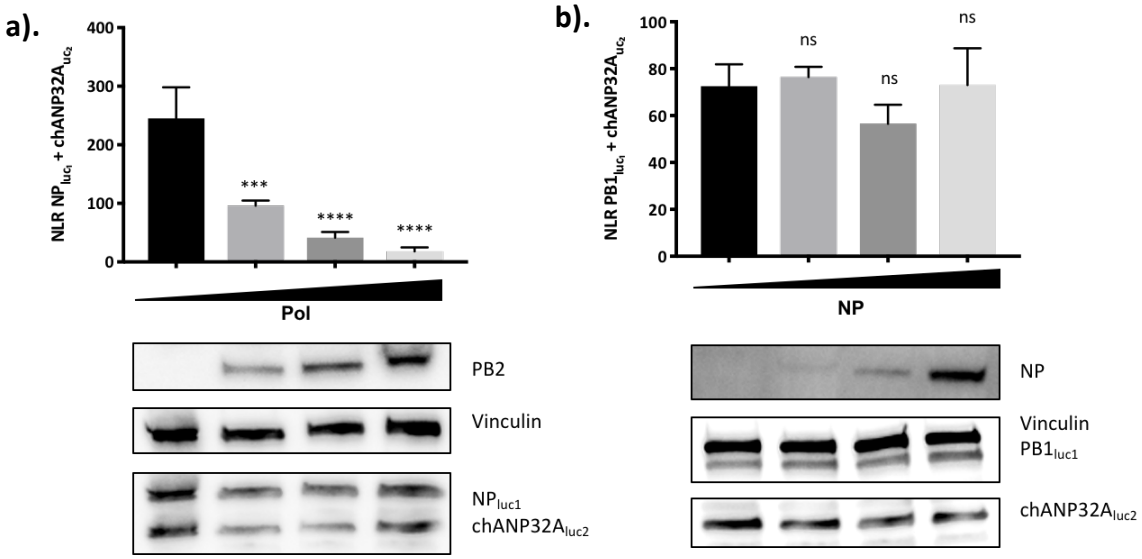


Fig 28: Viral polymerase disrupts the interaction between chANP32A and NP. 25 ng PB1$_{luc1}$, 12.5 ng chANP32A$_{luc2,}$ 25 ng PB2 and 12.5 ng PA were transfected into cells along with 0, 6.25, 12.5 or 25ng of untagged **a).** PB1, PB2 and PA or **b).** NP. Total DNA was kept constant between samples using an empty vector. Gluc activity was measured 24 hours after transfection. Western blots below show expression of proteins. Results shown are mean ± standard deviation from triplicate samples. Statistical significance was assessed by one-way ANOVA, comparisons made to sample with 0ng additional polymerase or NP (black bars), ns = non-significant, ***p<0.001, ****p<0.0001. Results representative of three independent experiments.

2.2.11 chANP32A is able to increase replication independently of NP

Since replication can be measured independently of NP when using a template of 76nt or less (Paterson *et al.,* 2014), we looked to see whether chANP32A could increase the polymerase activity of an avian origin polymerase on addition of this template. Using qRTPCR, we observed that the levels of vRNA increased approximately 2 fold in the presence of chANP32A, to a level similar to that attained when PB2 has 627K **(Fig 29).** vRNA did not increase in the presence of chANP32AΔ33 **(Fig 29).** Since chANP32A can still support the activity of the AIV polymerase in an assay which does not require NP, this suggests that the role of chANP32A is likely to be independent of NP. Since the polymerase with 627E is still restricted on a 76nt template, this also infers that the restriction is independent of NP (Paterson *et al.,* 2014).

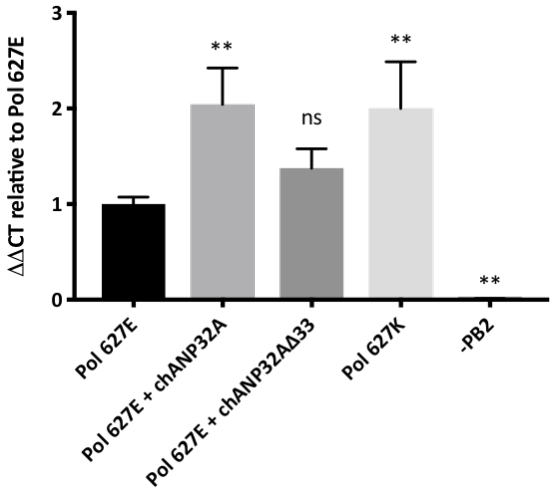


Fig 29: chANP32A can rescue activity of the polymerase independently of NP. 40 ng PB1, 40 ng PB2 627E, 627K or empty vector, 20 ng PA, 20 ng polI 76nt vRNA and either 40 ng empty plasmid, chANP32A or chANP32AΔ33 were transfected into HEK 293T cells. RNA was extracted after 24 hours and reverse transcribed to cDNA using primers specific for the 76nt vRNA, followed by qPCR. Results are normalised to 18S RNA. ΔΔCT plotted relative to Pol 627E (black bar). Results shown are mean ± standard deviation from triplicate samples. Statistical significance was assessed by one-way ANOVA, comparisons made to Pol 627E (black bar), ns+ non-significant, ***p*<0.01. Results representative of three independent experiments.

2.3 Discussion

In this chapter, we have used a split luciferase assay to quantify interactions between ch- or huANP32A and influenza A viral proteins. We have discovered that the interaction between chANP32A and the viral polymerase is much greater than that of huAN32A and this greater interaction is mediated by the 33 amino acid avian insertion in chANP32A and the 627 domain of PB2. We have also shown that the interaction between ANP32A and viral polymerase occurs in the nucleus of human cells. ANP32A can bind apo viral polymerases. These interactions are stabilised with inactive polymerases at RNPs and decrease when the polymerase is active.

Several studies have demonstrated an interaction between the viral polymerase and ANP32A using proteomics or coimmunoprecipitation assays (Baker *et al.,* 2018; Bradel Trethaway *et al.,* 2011; Domingues and Hale, 2017; Sugiyama *et al.,* 2015; Wei *et al.,* 2019). We used a split luciferase complementation system to compare interactions between the viral polymerase with different mutations and ANP32A from different species. Where interpretation of co-precipitation assays can sometimes be subjective, split luciferase assays enable quantification of interactions and assessment of statistical significance. Compared to other split protein systems, split *Gaussia* luciferase benefits from its small size, sensitivity and reversible nature (Remy *et al.,* 2006). A limitation of the split luciferase complementation assay however, is that it relies on a cooperative steric orientation of both luciferase halves. Therefore, experiments carried out in this chapter were also validated by performing co-immunoprecipitation experiments, the results of which aligned well to those from split luciferase assays. Both of these methods require lysis of cells which could affect interactions.

Therefore, we also used a BiFC assay in order to visualise these interactions *in situ*, in the nucleus of host cells. Furthermore, quantification of fluorescence from BIFC experiments by flow cytometry revealed similar trends as the other two methods, altogether providing a robust analysis of the interactions between ANP32A and the viral polymerase.

The aim of this chapter was to investigate whether differences in interactions could explain why AIV polymerases are unable to utilise huANP32A for their activity. Indeed, we found that the interaction between huANP32A and the AIV polymerase was much less than that of chANP32A and this was due to the absence of the 33 amino acid avian insertion. However, the interaction between a polymerase with the mammalian adaptive PB2 E627K mutation did not show a statistically significant increase in interaction with huANP32A compared to the PB2 627E polymerase, even though it is able to utilise huANP32A. This indicates that differences in interactions with the apo viral polymerase alone are not sufficient to explain how mammalian adaption of viral polymerase renders it compatible with huANP32A.

The interaction between huANP32A and the viral polymerase was not affected by removal of the PB2 627 domain. chANP32A lacking the 33 amino acids, and therefore similar to huANP32A, has previously been shown to bind to the 627 domain *in vitro* (Baker *et al.,* 2018). This discrepancy could be explained by other amino acids unique to chANP32A being involved in the interactions. Alternatively, huANP32A may bind to the PB2 627 domain, but binding to the heterotrimeric polymerase complex as a whole may not depend on this interaction. We mapped interactions with the 627 domain to the 33 amino acid region of chANP32A. The glutamic acid at position 627 is surrounded by positively charged residues (Tarendeau *et al.,* 2008). Interestingly, the restriction in polymerase activity can also be overcome by mutation to other positively charged or neutral residues (Chin *et al.,* 2014). The function of the 33

amino acids in chANP32A may therefore be to negate a restriction imposed by this negatively charged residue, and in the absence of the negative charge, huANP32A may stimulate polymerase activity.

Removal of the 33 amino acids insertion or the first four of these amino acids reduced both binding and function. The first six amino acids have previously been identified as a SUMO interacting motif (SIM), essential for the function of chANP32A (Domingues and Hale, 2017). Interestingly, co-precipitation of polymerase with chANP32A 1-208 could not be detected. This truncated protein was however, still able to support activity of the polymerase, albeit non-optimally. This intriguing finding may be resolved using techniques such as labelling of proximal proteins by fusion of APEX-2 to one of the interacting partners which could highlight transient interactions (Lam *et al.,* 2015). These results also confirm those seen previously (Domingues and Hale, 2017) and demonstrates that while the LCAR domain is most important for binding, the 33 amino acids are the most critical for the ability of chANP32A to support the AIV polymerase.

The viral polymerase is a dynamic structure and has been solved in distinctive conformations dependent on the presence of specific viral RNAs (Hengrung *et al.,* 2015; Pflug *et al.,* 2014; Reich *et al.,* 2014; Reich *et al.,* 2017; Thierry *et al.,* 2016). Compared to the apo polymerase, the presence of vRNA promoter causes the PA N-terminus and PB2 C-terminus to undergo a major shift (Hengrung *et al.,* 2015; Pflug *et al.,* 2014; Reich *et al.,* 2014). In this structure, the terminal 3' vRNA residues are not within the active site and so it is thought that this represents a 'pre-initiation' conformation (Reich *et al.,* 2014). Further shifts may need to take place in order to form an initiation competent conformation (Reich *et al.,* 2014; Reich *et al.,* 2017). The viral polymerase in complex with 5' cRNA, although similar to the apo structure,

represents yet another different conformation (Thierry *et al.,* 2016). It is hypothesised that different structures are in equilibrium (Thierry *et al.,* 2016) and therefore binding to host factors may stabilise a specific conformation required for a specific process. In line with this, we observed increased interactions between ANP32A and an inactive viral polymerase in the presence of viral RNA. This observation was also seen with splice variants of chANP32A (Baker *et al.,* 2018). Investigation into whether the interactions between chANP32A 1-208 and the avian origin polymerase also increase with the addition of viral RNA may explain how this truncated protein is able to exert its effect.

In vitro, huANP32A is able to stimulate the synthesis of vRNA from cRNA templates (Sugiyama *et al.,* 2015). vRNA synthesis differs from cRNA synthesis in several ways. cRNA synthesis initiates at position one of the 3' RNA whereas vRNA synthesis initiates at position four followed by realignment of the short dinucleotide primer back to position one. (Deng *et al.,* 2006). vRNA synthesis also requires *trans*-acting or *trans*-activating polymerases, which are not thought to be required for cRNA synthesis (Jorba *et al.,* 2009; York *et al.,* 2013). Furthermore, the binding affinity of viral polymerase to cRNA is weaker than to vRNA (Robb *et al.,* 2016). The two templates differ in their interactions with specific parts of the polymerase (Gonzalez and Ortin, 1999) and the conformation of the polymerase is dependent on which RNA is bound (Hengrung *et al.,* 2015; Pflug *et al.,* 2014; Reich *et al.,* 2014; Reich *et al.,* 2017; Thierry *et al.,* 2016). Therefore, ANP32A may act to stabilise polymerase binding to the RNA or perhaps induce an initiation competent conformation. Whether ANP32A exerts its effect directly to the resident polymerase or through *trans*-acting or *trans*-activating polymerase remains to be investigated.

In contrast to data presented here and that by Baker *et al.,* Sugiyama *et al.,* did not detect co-precipitation of NP with huANP32A or -B during viral infection, implying that ANP32 does not bind to RNPs (Sugiyama *et al.,* 2015). It is possible that the interaction is transient and therefore could not be detected using these conditions. In accordance with this, we demonstrate that interactions are reduced with an active viral polymerase. This was the case for chANP32A with an AIV polymerase and huANP32A with a polymerase bearing PB2 627K. Where huANP32A cannot support the activity of an avian origin polymerase, the interaction between these proteins did not significantly decrease. It is possible that the lack of dissociation of huANP32A may also contribute to the incompatibility between huANP32A and the AIV polymerase. One could speculate that transition to a particular conformation may trigger dissociation of ANP32A. Incompatibilities between huANP32A and an avian origin polymerase may result in a failure to undergo this transition.

G3A, U5C and C8U mutations in the 3' vRNA promoter are also able to overcome the restriction, further highlighting a role for polymerase-RNA interactions in the restriction in polymerase activity in human cells (Crescenzo-Chaigne *et al.,* 2002; Paterson *et al.,* 2014). It was previously shown that exogenous expression of chANP32A did not alter the activity of an avian origin polymerase in human cells if the viral RNA contained these mutations (Baker *et al.,* 2018). We show that huANP32A and -B are still essential for viral polymerase activity with the mutated promoter. However, an avian origin polymerase was more readily rescued by addition of huANP32A and -B if this mutated promoter RNA was used suggesting that these mutations may increase the compatibility of the polymerase with host factors such as huANP32A/B.

We also investigated the relationship between NP and ANP32A. huANP32 proteins have been implicated in the incorporation of histones into DNA (Munemasa *et al*., 2008). Since NP is a histone-like protein that associates with nuclei acid, ANP32 supporting viral polymerase activity by facilitating NP incorporation into RNPs was an attractive hypothesis. However, since chANP32A was still able to rescue the activity of an avian origin polymerase in an assay in which polymerase activity is measured independently of NP, it is probable that the function of chANP32A is also independent of NP. Furthermore, AIV polymerase is still restricted in activity in human cells in the absence of NP (Paterson *et al.,* 2014).

To summarise, we have characterized the interactions between ANP32A and the influenza A polymerase and provided an insight into where during the replication process these interactions may be important. To do this we developed a split luciferase complementation assay and this assay was subsequently used to screen for drugs which inhibit the interaction between the mammalian adaptive polymerase and huANP32A (Jocelyn Schreyer). Although interactions are important for the ability of chANP32A to overcome the restriction in viral polymerase activity to its full capacity, the mechanism by which it does this appears to be more complex than differences in interactions alone.

Chapter 3: A mass spectrometry screen to identify differences in the interactome of AIV polymerase in the presence or absence of chANP32A, or due to adaptive mutations in the polymerase

3.1 Introduction

The previous chapter demonstrated that interactions between chANP32A and AIV polymerase could not fully explain the function of chANP32A. It is clear however, that the additional 33 amino acids between the LRR and LCAR domains of the protein, and in particular the first four of these amino acids, are important for its function. It had previously been shown that these four amino acids are part of a sequence that resembles a SIM (Domingues and Hale, 2017). Glycine mutations at positions 1, 2, 4 and 5 of the 33 amino acids also resulted in reduced ability to support AIV polymerase activity and exogenous expression of huANP32A engineered to contain a SIM sequence from PIAS2 or PIAS4 could partially rescue the activity of AIV polymerase in human cells (Domingues and Hale, 2017). Furthermore, expression of SUMO proteases reduced the ability of chANP32A to support the AIV polymerase (Domingues and Hale, 2017). It could therefore be possible that the function of chANP32A is to chaperone

or stabilise another host factor, which may be SUMOylated, within the polymerase complex. Thus, we aimed to uncover this putative factor. To do this we carried out label free mass spectrometry to identify proteins which differed in their abundance in complex with the 50-92 AIV polymerase in the presence or absence of chANP32A. We also compared the polymerase interactome between the 50-92 AIV polymerase bearing either E or K at position 627 of the PB2 subunit. Using this approach, we identified 347 proteins which bound to the polymerase. Differences in abundance dependent on the presence of chANP32A was measured for 61 proteins. Of these, we chose to explore Serine-Arginine Protein Kinase 1 (SRPK1) and importin α7 further.

SRPK1 is involved in the phosphorylation and regulation of splicing factors, nuclear speckle reorganisation and cell cycle progression (Giannakouros *et al.,* 2011). It has previously been implicated in modulating the replication cycle of multiple viruses including SARS coronavirus, human papilloma virus and hepatitis B and C (Bell *et al.,* 2007; Daub *et al.,* 2002; Karakama *et al.,* 2010; Peng *et al.,* 2008).

Importin α7 mediates the nuclear import of its substrates via their NLS. There is a wealth of literature linking importin α proteins to influenza, including roles in host range. Importin α isoforms facilitate the entry of vRNPs into the nucleus as well as newly synthesised PB2 and NP (O'Neill *et al.,* 1995; Tarendeau *et al.,* 2007; Wang *et al.,* 1997). Roles aside from nuclear import have also been proposed (Hudjetz *et al.,* 2012; Resa-Infante *et al.,* 2008).

The mass spectrometry experiments presented here were carried out in collaboration with Dr Stuart Armstrong and Prof Julian Hiscox at the University of Liverpool.

3.2 Results

3.2.1 Differences in the interactome of AIV polymerase in the presence or absence of chANP32A or human adapted polymerase

We used label free LC-MS/MS to identify differences in the interactome of the 50-92 polymerase in the presence or absence of chANP32A. We also looked at the interactome of the 50-92 polymerase using PB2 which was engineered to contain the E627K mutation. In order to carry out the mass spectrometry experiments, HEK 293T cells were transfected with PA-GFP, PB1, either PB2 627E or PB2 627K and either chANP32A or an empty plasmid. GFP-flag was used as a negative control **(Fig 30)**. The PA-GFP or GFP-flag was immunoprecipitated from cell lysate using GFP-trap beads and the eluted sample was analysed using LC-MS/MS. Mass spectrometry experiments were carried out in duplicate.

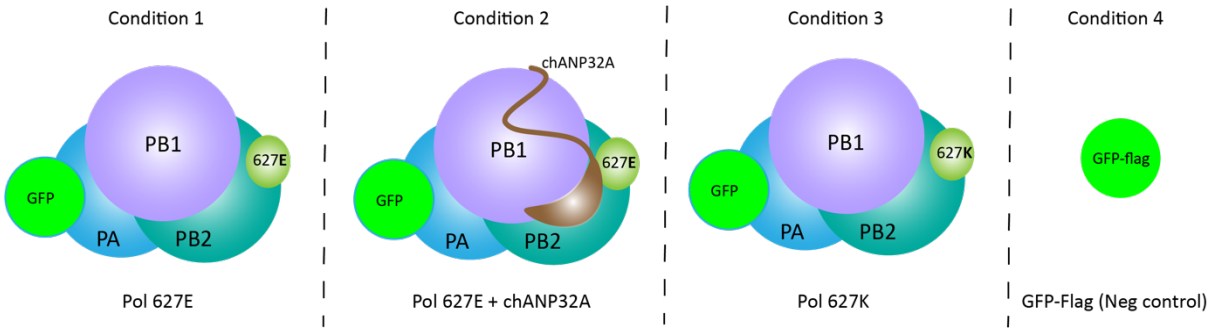


Fig 30: Mass spectrometry experimental conditions
Schematic of the conditions used for analysis by mass spectrometry. Condition 1: Polymerase harbouring PB2 627E. Condition 2: Polymerase harbouring PB2 627E with the addition of chANP32A. Condition 3: Polymerase harbouring PB2 627K. Condition 4: GFP-flag negative control. PA-GFP fusion protein was used in conditions 1-3. An empty vector was used to keep total amount of DNA transfected equal between conditions.

To ensure that PA-GFP was functional and that the GFP was not occluding binding of proteins needed to support viral polymerase activity, a minigenome assay was carried out using this construct. The ability of chANP32A to rescue activity of an AIV polymerase decreased by 25% when using PA-GFP compared to untagged PA. The activity of an avian or human adapted polymerase decreased by approximately 33% **(Fig 31)**. Although there were decreases in activity due to the GFP tag, substantial polymerase activity was maintained.

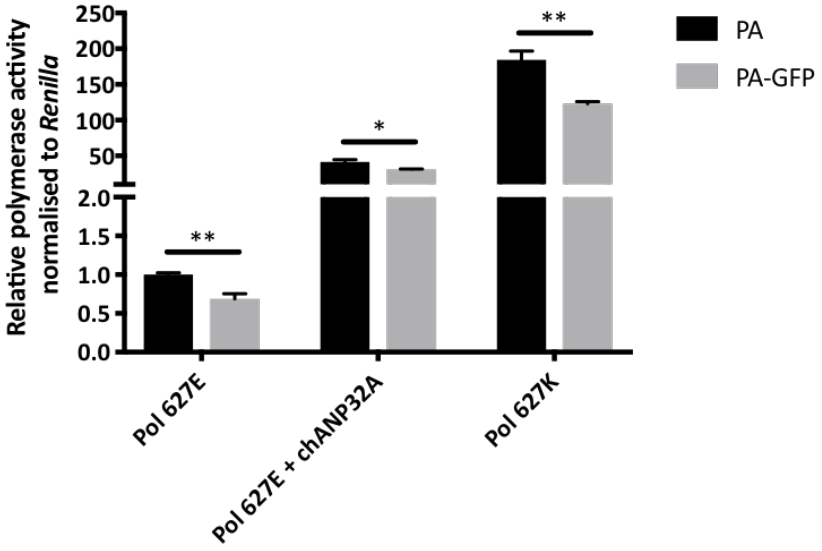


Fig 31: The PA-GFP fusion protein is functional
HEK 293T cells were transfected with pCAGGs expression vectors encoding PB1, PB2 627E or 627K, PA or PA-GFP, NP, chANP32A or an empty plasmid and *Renilla* luciferase. Polymerase activity was measured by expression of firefly luciferase from the polI mini genome plasmid. Results are normalised to *Renilla.* All results are plotted relative to Pol 627E with an untagged PA (left bar). Results shown are mean ± standard deviation from triplicate samples. Statistical significance was assessed by multiple t-tests *p<0.05, **p<0.01. Results representative of three independent experiments.

The results of the LC-MS/MS were analysed by Peaks software to identify the abundance of each protein present. The abundance of all proteins were normalised to that measured for PB1 since the PA-GFP-PB1 dimer is formed in all conditions. Proteins were only counted if they were at least ten times more abundant in a polymerase sample than in the GFP-flag negative control and if at least two unique peptides for that protein had been identified. After removal of all non-specific proteins, a total of 347 factors binding to the polymerase were revealed. A full list of the proteins identified in these experiments can be found in Appendix A. A comparison of the abundance of each protein in the different conditions was carried out **(Fig 32).** Abundance between proteins in each condition were counted as different if they were at least more than twice that of each other and only if this was true of both repeats. The identified proteins in each comparison are listed in Appendix B.

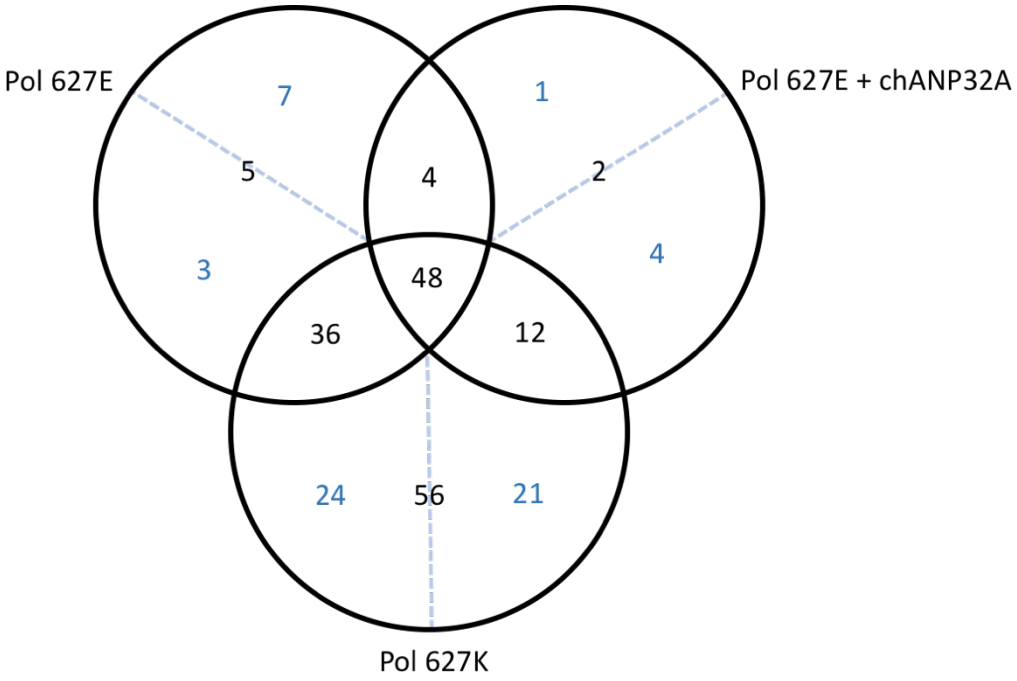


Fig 32: Comparison of protein abundances between conditions

Venn diagram showing number of proteins identified by mass spectrometry showing specific patterns of abundances between conditions. Abundances were calculated as the sum of the area under the peaks for each peptide and were normalised to the abundance of PB1, which was set to 100%. The central region denotes proteins with similar abundances between conditions. Regions with two overlapping circles represent proteins which are at least twice as abundant in both those conditions compared to the condition which is not involved in that overlap. Black numbers in non-overlapping regions (on dashed lines) represent proteins which were at least twice as abundant in that condition compared to both of the other two conditions. For example, there were 5 proteins which were more abundant in Pol 627E compared to both Pol 627E + chANP32A and Pol 627K. Blue numbers in non-overlapping regions represent proteins which were at least twice as abundant as one of the other conditions but not the other. For example, there were 7 proteins which were more abundant in Pol 627E compared to Pol 627E + chANP32A, but not pol K and there were 3 proteins more abundant in Pol 627E compared to Pol 627K but not pol 627E + chANP32A. Note that the figure only contains proteins where the abundance pattern was the same in both experimental repeats. Proteins showing differing patterns between experimental repeats were not included.

Since we hypothesised that the SIM motif of chANP32A allows the viral polymerase to be further associated with an unknown SUMOylated factor **(Fig 33a)**, we chose to focus on differences in host proteins binding to the pol 627E in the presence or absence of chANP32A **(Fig 34a)**. Overall, there were 15 proteins whose abundance were increased in the presence of chANP32A compared to when it was absent **(Fig 34b)**. SUMOplot prediction software revealed that all of these proteins apart from that encoded by *chtop* had sites which could be SUMOylated.

Another hypothesis is that chANP32A is able to occlude binding of an inhibitory factor to the AIV polymerase **(Fig 33b)**. We therefore also looked at which proteins decreased in their abundance with the AIV polymerase when chANP32A was present compared to when it was absent. Overall, there were 46 proteins co-precipitated with AIV whose abundance decreased in the presence of chANP32A **(Fig 34c)**.

It is possible that huANP32A supports the polymerase with PB2 627K in the same way that chANP32A is able to support the AIV polymerase, and therefore the same stimulatory factor may be recruited to the PB2 627K polymerase as the PB2 627E polymerase if chANP32A is also expressed **(Fig 33a)**. Alternatively, the E627K mutation may allow escape of an inhibitory factor which chANP32A can also prevent **(Fig 33b)**. Although we focussed mainly on changes in the abundance of proteins bound to the AIV polymerase depending on the presence of chANP32A, we also highlighted those proteins where a large change in binding pattern seen by the addition of chANP32A was mirrored by the viral polymerase with the PB2 E627K adaption **(Fig 34b and c)**.

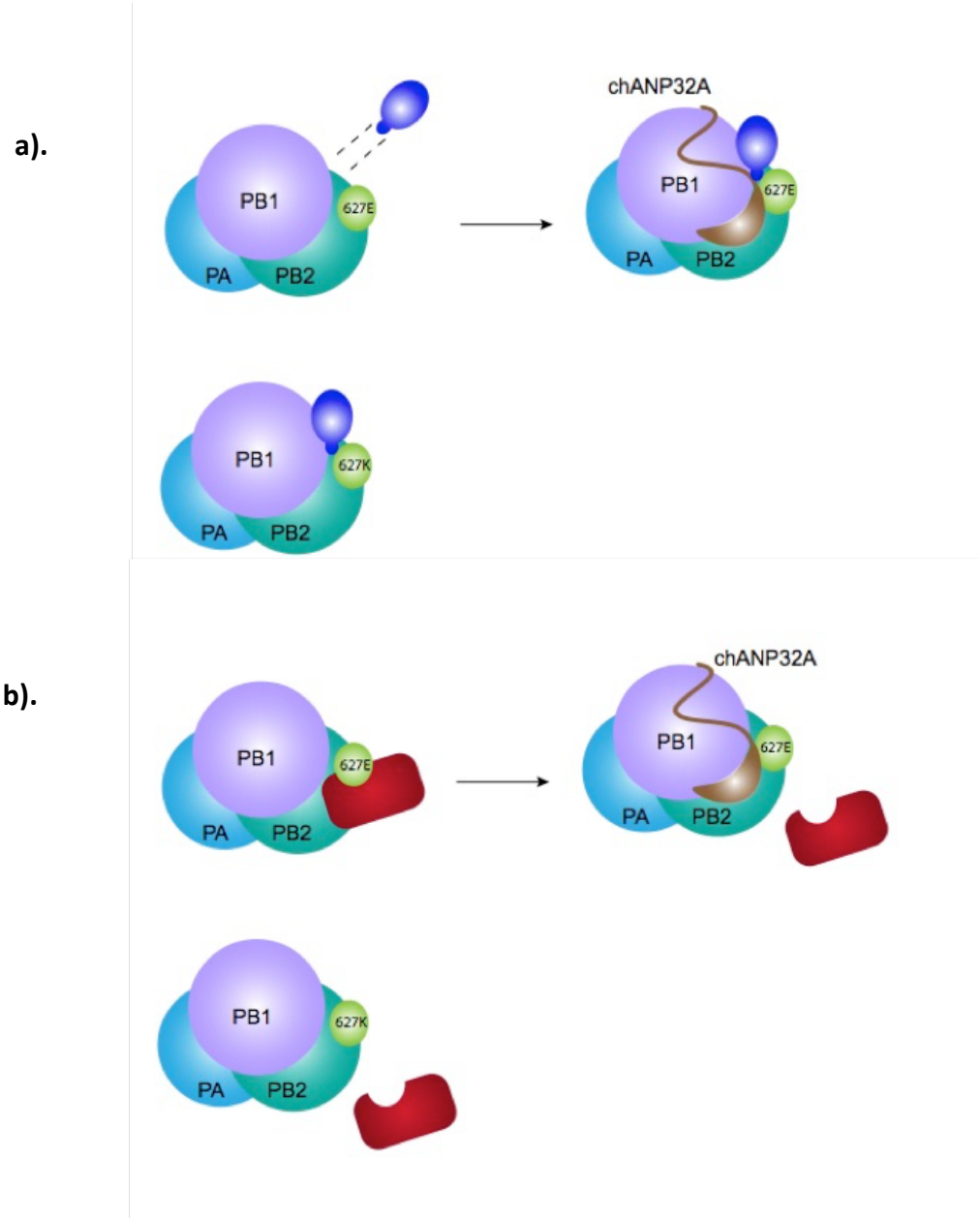


Fig 33: Hypothetical models relating to mass spectrometry results
a). chANP32A (brown) could stabilise binding of a SUMOylated host factor (blue) to AIV polymerase. In the absence of chANP32A, the interaction is less stable due to 627E. The E627K adaption allows binding of this stimulatory host factor. **b).** An inhibitory factor (red) binds to 627E and can be displaced by chANP32A. The E627K adaption escapes inhibition by this factor.

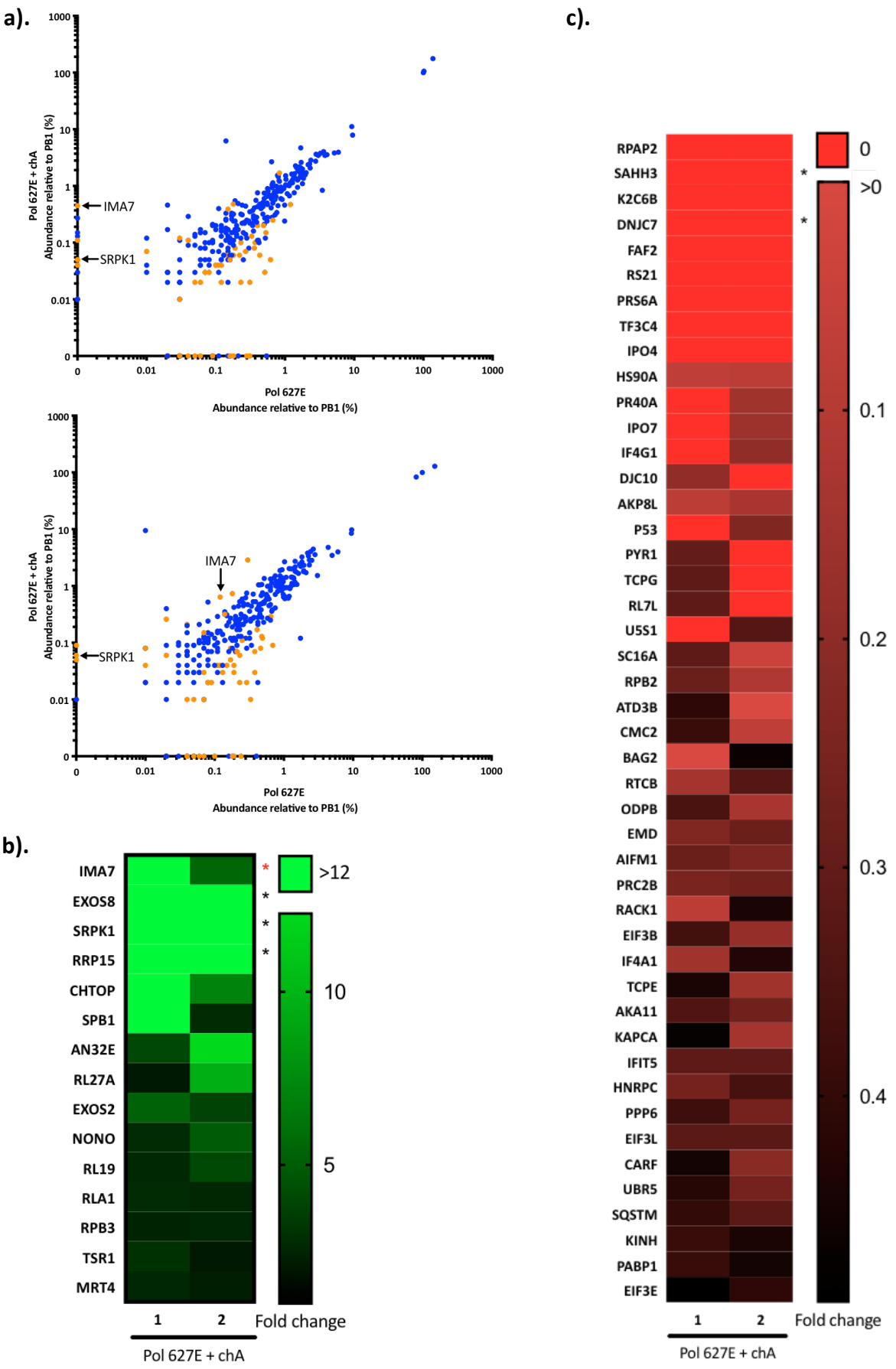

a).
Pol 627E + chA
Abundance relative to PB1 (%)
IMA7
SRPK1
Pol 627E
Abundance relative to PB1 (%)
b).
IMA7
EXOS8
SRPK1
RRP15
CHTOP
SPB1
AN32E
RL27A
EXOS2
NONO
RL19
RLA1
RPB3
TSR1
MRT4
>12
10
5
1
2
Fold change
Pol 627E + chA
c).
RPAP2
SAHH3
K2C6B
DNJC7
FAF2
RS21
PRS6A
TF3C4
IPO4
HS90A
PR40A
IPO7
IF4G1
DJC10
AKP8L
P53
PYR1
TCPG
RL7L
U5S1
SC16A
RPB2
ATD3B
CMC2
BAG2
RTCB
ODPB
EMD
AIFM1
PRC2B
RACK1
EIF3B
IF4A1
TCPE
AKA11
KAPCA
IFIT5
HNRPC
PPP6
EIF3L
CARF
UBR5
SQSTM
KINH
PABP1
EIF3E
0
>0
0.1
0.2
0.3
0.4
1
2
Fold change
Pol 627E + chA

Fig 34: Identification of proteins coprecipitated with AIV polymerase which changed in abundance depending on the presence of chANP32A. a). Abundance of proteins bound to the AIV polymerase in the presence or absence of chANP32A. All points are relative to the abundance of PB1, which was set at 100%. Abundance was calculated as the sum of the area under the curve for each peptide of a protein. Blue dots represent proteins which did not change in abundance, orange dots represent host proteins which changed in abundance depending on presence of chANP32A in both experiments. Graphs represent two separate experiments. Dots representing SRPK1 and IMA7 are labelled. **b).** Heatmap listing proteins which increased in abundance at least two fold when chANP32A was present compared to when it was absent in both experiments. Brighter green represents a larger change. Brightest green represents cases when the protein was not detected at all in the absence of chANP32A and therefore have values much above the rest. The highest point on the scale was set to 12. **c).** Heatmap listing proteins which decreased in abundance by at least half when chANP32A was present compared to when it was absent. Lighter red represents a larger change. Brightest red represents cases when the protein was not detected at all when chANP32A was present. 1 and 2 refer to experiment number. Proteins are ordered by highest average change between the two experiments to lowest. Scales represent fold change in relative abundance. * represents cases where addition of chANP32A and the PB2 E627K mutation changed the abundance of the host factor in the same way compared to polymerase with PB2 627E. This was only noted for those proteins where in at least one condition, the host factor was not detected at all. * represents host factors previously implicated in host range of influenza. Mass spectrometry experiments were carried out in duplicate.

Of the proteins identified in this proteomic experiment we chose to explore SRPK1 and importin α7 (denoted ima7) further. SRPK1 was chosen as an example of a putative positive factor whose binding to polymerase might be recruited by chANP32A. It showed one of the biggest differences in abundance between conditions, as well a high probability for SUMOylation **(Table 4)**. Importin α7 was also a putative positive factor and was chosen due to previous studies in the literature, which have linked this protein to host range of influenza (Resa-Infante and Gabriel, 2013).

No.	Position	Sequence	SUMOplot prediction score
1	K215	I**K**PE	0.94
2	K18	A**K**KD	0.79
3	K71	V**K**IG	0.76
4	K575	G**K**VP	0.57
5	K377	H**K**ED	0.52
6	K615	E**K**YE	0.5
7	K329	E**K**LE	0.5
8	K594	K**K**GD	0.48
9	K25	R**K**SE	0.44
10	K301	Q**K**RP	0.39
11	K103	G**K**KF	0.32
12	K85	R**K**LG	0.27
13	K506	H**K**HF	0.17

Table 4: Predicted SUMOylation sites on SRPK1
Sites within SRPK1 with the potential for SUMOylation as predicted by SUMOplot online software (Abgent). Sites listed in order of probability of SUMOylation.

3.2.2 Characterisation of the role of SRPK1 in influenza polymerase activity

3.2.2.1 Validation of mass spectrometry results- SRPK1

The results obtained by mass spectrometry indicated that SRPK1 did not bind to an avian origin polymerase in the absence of chANP32A, but did so when chANP32A was present or when the polymerase had a K at position 627 of PB2 **(Fig 35a)**. This could therefore suggest that chANP32A may bring in or stabilise SRPK1 in the polymerase complex. Without chANP32A, SRPK1 may not be able to bind stably to the polymerase unless it undergoes the PB2 E627K mutation. We therefore explored the relationship between SRPK1, the influenza polymerase and ANP32A further.

First, we aimed to validate the interaction pattern shown in the mass spectrometry experiments using immunoprecipitation followed by western blotting. To do this, we transfected HEK 293T cells with 50-92 PA-GFP, PB1, either PB2 627E or 627K and chANP32A or an empty vector. PA-GFP was immunoprecipitated and endogenous SRPK1 was probed for on a western blot. Although some binding between SRPK1 and a PB2 627E containing polymerase could be detected using this method, the overall pattern of greater binding when chANP32A was present or with a human adapted polymerase was confirmed, reflecting the results obtained by mass spectrometry **(Fig 35b)**.

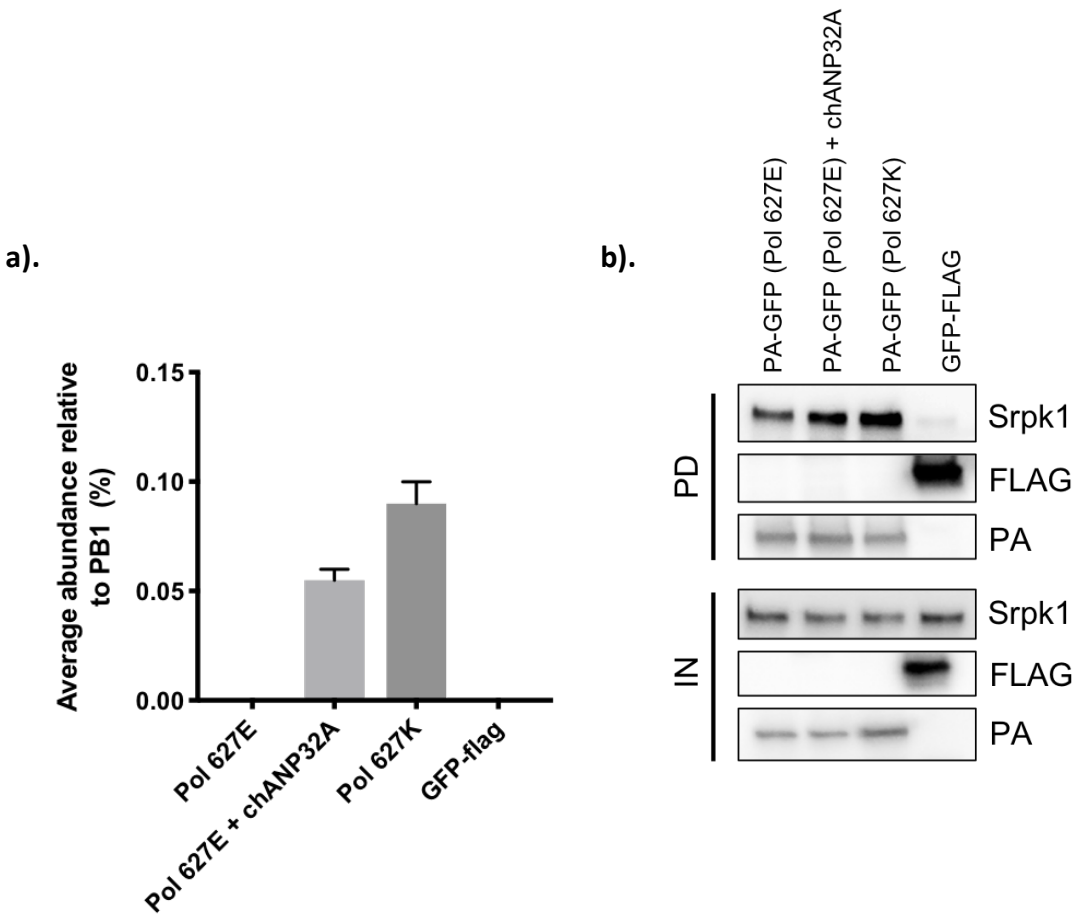


Fig 35: Validation of binding pattern of SRPK1 revealed by mass spectrometry
a). Average abundance of SRPK1 detected by mass spectrometry. Data are relative to abundance of PB1, which was set to 100%. **b).** HEK 293T cells were transfected with pCAGGs expression plasmids encoding PB1, PA-GFP, either PB2 627E or PB2 627K and chANP32 or an empty vector. GFP-flag was used as a negative control. 30 hours after transfection, PA-GFP was immunoprecipitated and endogenous SRPK1 probed for on a western blot. Co-immunoprecipitation assay was repeated twice.

3.2.2.2 SRPK1 interacts with the trimeric polymerase complex and with PB2 alone

Next, we wanted to determine which subunits of the polymerase were necessary for the interaction between the polymerase and SRPK1. To do this, co-precipitation of various polymerase components with SRPK1-Flag was tested. Interactions between SRPK1-Flag and the trimeric polymerase complex were detected, with greater binding observed between a polymerase containing PB2 627K compared to PB2 627 E as shown on the previous page **(Fig 36**, lanes 1 and 2**)**. Binding of SRPK1-Flag could not be detected with PB1 and PA or PA alone **(Fig 36**, lanes 3 and 4**)**, indicating that it is PB2 which determines whether an interaction takes place. SRPK1-Flag also bound PB2 alone, again with greater binding to PB2 627K compared to PB2 627E **(Fig 36**, lanes 5 and 6). Altogether this suggests, that SRPK1 can bind to the trimeric polymerase complex or PB2 alone and the degree of binding is determined by the nature of the amino acid at position 627 of PB2.

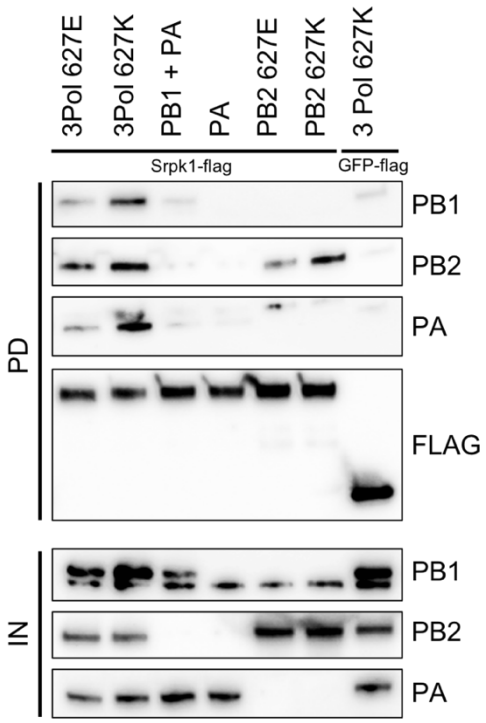


Fig 36: SRPK1 interacts with the trimeric polymerase and to PB2 alone
HEK 293T cells were transfected with pCAGGs expression plasmids encoding the three polymerase subunits including either PB2 627E or PB2 627K (lanes 1, 2 and 7), just PB1 and PA (lane 3), PA only (lane 4) or PB2 only (lanes 5 and 6). Samples were also transfected with either SRPK1-Flag (lanes 1-6) or GFP-Flag (lane 7). 30 hours after transfection, the flag tagged proteins were immunoprecipitated and polymerase components were probed for on a western blot. Bottom line in PB1 input box is due to unspecific binding of PB1 antibody. Results representative of two independent experiments.

3.2.2.3 SRPK1 does not interact with ANP32A

We showed in figure 35 that the interaction between the avian origin polymerase and SRPK1 increases in the presence of chANP32A. If the glutamic acid at position 627 of PB2 reduces the stability of the interaction of SRPK1 with polymerase, it could be that chANP32A is able to stabilise this. To determine whether chANP32A-flag or huANP32A-flag could bind to SRPK1 in the absence of polymerase, HEK 293T cells were transfected with the flag tagged ANP32A proteins and immunoprecipitated. Co-precipitation of endogenous SRPK1 was assessed using western blotting. Binding between SRPK1 and either chANP32A or huANP32A could not be detected **(Fig 37)**. However, this does not exclude an interaction between ANP32A and SRPK1 within the polymerase complex.

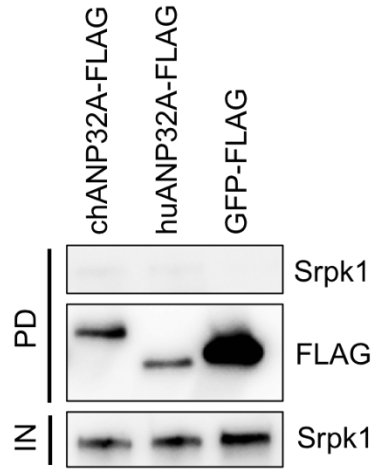


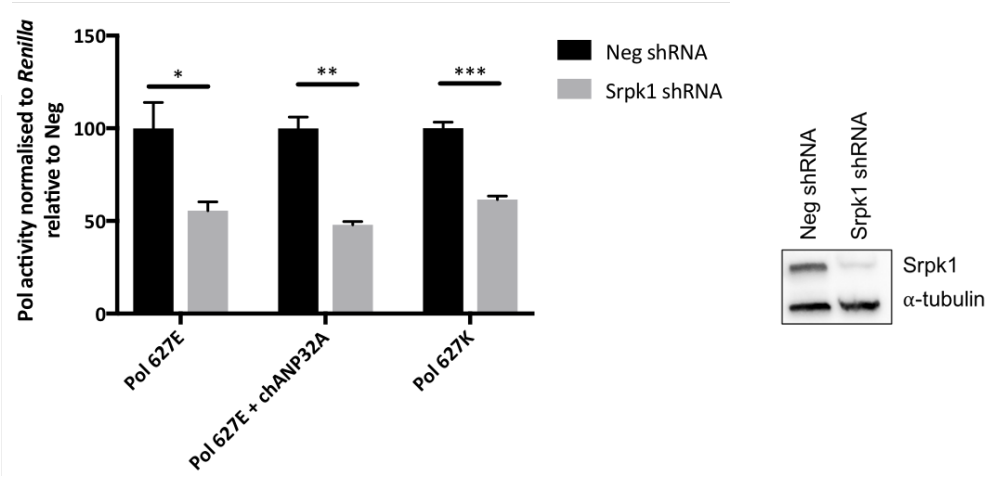
Fig 37: SRPK1 does not coprecipitate with ANP32A-flag
HEK 293T cells were transfected with either chANP32A-flag, huANP32A-flag or GFP-flag. 30 hours after transfection the flag tagged proteins were immunoprecipitated and coprecipitation of endogenous SRPK1 was probed for on a western blot. Representative of three independent experiments.

3.2.2.4 shRNA mediated knockdown of SRPK1 reduces polymerase activity

To assess the functional relevance of SRPK1 on polymerase activity, SRPK1 was knocked down using shRNA mediated silencing in HEK 293T cells and a minigenome assay was performed. Non-targeting shRNA (neg) treated cells were used as control cells. Even though SRPK1 displayed different binding patterns depending on the nature of the influenza polymerase, knockdown of SRPK1 caused a 50% reduction in polymerase activity, regardless of the identity of position 627 of PB2 and regardless of whether chANP32A was absent or present **(Fig 38a)**. This suggests that SRPK1 is a host factor which can support influenza polymerase activity, but that the low activity of an avian origin polymerase in human cells is not due to incompatibilities with SRPK1. Along with the binding assay in fig 37, this indicates that SRPK1 supports the polymerase independently of ANP32A proteins.

We also overexpressed SRPK1 in HEK 293T cells so see whether this would lead to an increase in polymerase activity. However, the activity of the polymerase remained unchanged compared to controls **(Fig 38b)**. This may be because the endogenous levels of SRPK1 are sufficient to support the polymerase to its maximum capacity.

a).



b).

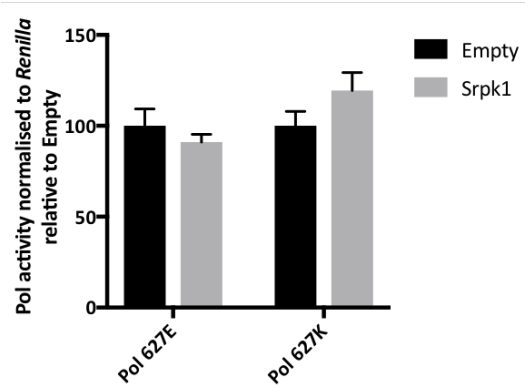


Fig 38: shRNA mediated knockdown of SRPK1 reduces viral polymerase activity

a). Control (neg) or SRPK1 shRNA 293T cells were transfected with pCAGGs expression plasmids encoding 50-92 PB1, PB2 627E or PB2 627K, PA, NP, either chANP32A or an empty plasmid and *Renilla* luciferase. The influenza A mini genome encoding firefly luciferase was used to measure polymerase activity. Results are normalised to *Renilla* luciferase and presented relative to neg shRNA cells, which were set to 100% for each condition. SRPK1 shRNA mediated knockdown was validated using western blotting (right). **b).** Components of the minigenome assay described in a). were transfected into HEK 293T cells. 100 ng of either SRPK1 or empty vector was also transfected into these cells. Polymerase activity was normalised to *Renilla* and plotted relative to empty (black bars), which were set to 100%. Results shown are mean ± standard deviation from triplicate samples. Statistical significance was assessed by multiple t-tests *p<0.05, **p<0.01, ***p<0.001. Non-significant changes are not indicated. Results representative of three independent experiments.

3.2.2.5 SRPK1 can support the activity of several influenza A polymerases

The results so far suggest that SRPK1 supports the activity of the 50-92 influenza polymerase regardless of other factors. Next, we measured polymerase activity from several different polymerases; H5N1 A/turkey/Turkey/05/2005 (Tky05), H9N2 A/chicken/Pakistan/UDL-01/2008 (UDL), pH1N1 A/England/195/2009 (Eng195), H3N2 A/Victoria/3/1975 (Vic) and H1N1 A/WSN/1933 (WSN). All of these viral polymerases naturally contain a lysine at position 627 apart from UDL and Eng195. Eng195, although retaining 627E, has other adaptive mutations which allow activity in human cells (Mehle and Doudna, 2009). UDL is an avian virus but was engineered to contain a lysine at position 627 to allow replication in this experiment. shRNA mediated knockdown of SRPK1 resulted in a reduction in polymerase activity of all polymerases tested by approximately 50% **(Fig 39)**. This reinforces the hypothesis that SRPK1 supports influenza polymerases of different host origins.

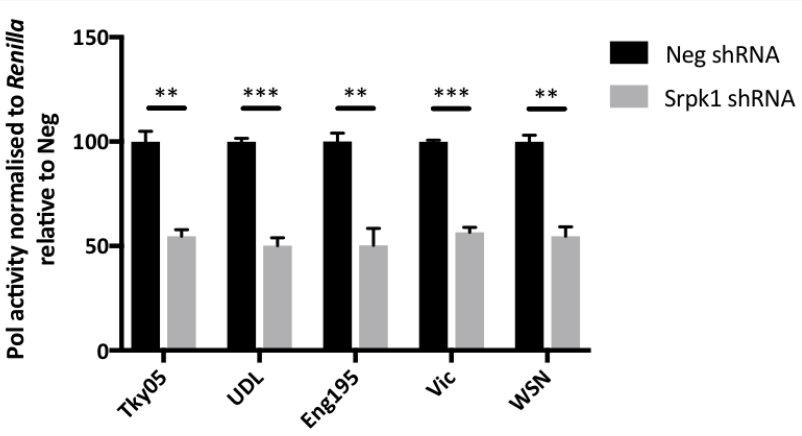


Fig 39: Knockdown of SRPK1 reduces activity of various influenza A polymerases
a). Control (neg) or SRPK1 shRNA HEK 293T cells were transfected with pCAGGs expression plasmids encoding PB1, PB2 627K, PA, NP from the indicated influenza A background as well as *Renilla* luciferase. The influenza mini genome encoding firefly luciferase was used to measure polymerase activity. Results are normalised to *Renilla* luciferase and represented relative to neg shRNA cells, which was set to 100% for each strain. Results shown are mean ± standard deviation from triplicate samples. Statistical significance was assessed by multiple t-tests **p<0.01, ***p<0.001. Results representative of three independent experiments.

3.2.2.6 SRPK1 is localised in the nucleus and cytoplasm

Next, we sought to determine the subcellular localisation of SRPK1. In the absence of influenza polymerase, SRPK1-flag could be observed in the cytoplasm of all cells in which it was expressed as well as the nucleus of a proportion of these cells **(Fig 40** top panel**)**. We looked to see whether expression of viral polymerase proteins altered its subcellular distribution. Expression of the trimeric polymerase complex did not alter the pattern of SRPK1 localisation **(Fig 40** middle panel**)**. Reconstitution of an active vRNP also did not affect the localisation of SRPK1 within cells **(Fig 40** bottom panel**)**. SRPK1 has previously been shown to be cytoplasmic, but can translocate into the nucleus due to specific signals (Aubol *et al.,* 2018; Zhou *et al.,* 2012). It is clear that in some cells, SRPK1 is nuclear, but this does not seem to be associated with presence of the viral polymerase.

Overall, SRPK1 has been identified as a novel host factor with the ability to support the activity of the influenza polymerase. The exact mechanism of this and whether the kinase activity of SRPK1 is needed for this activity remains to be investigated.

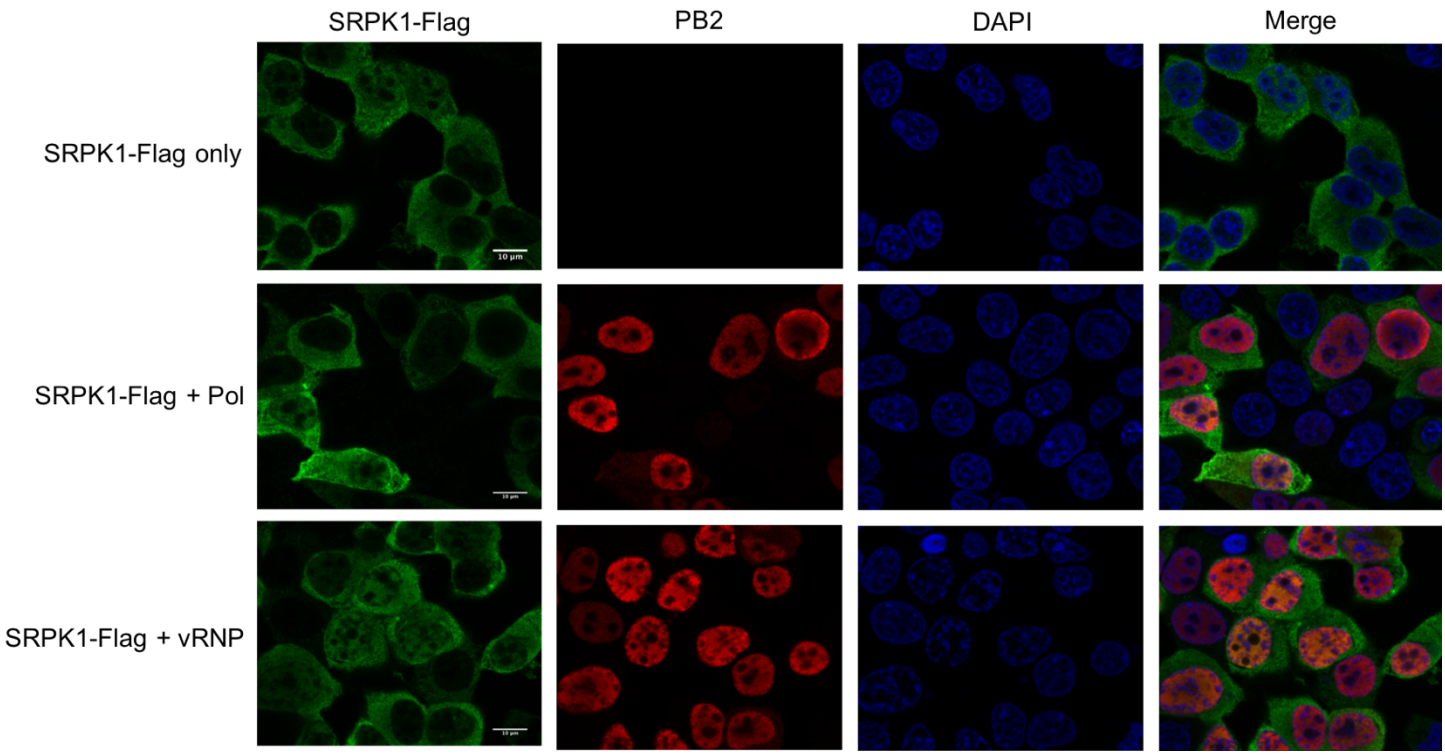


Fig 40: Localisation of SRPK1

HEK 293T cells were transfected with 100 ng SRPK1-flag and either empty (top panel), 50-92 PB2 627K, PB1 and PA (third panel) or PB2 627K, PB1, PA, NP and a polI plasmid for expression of a flu-like RNA (bottom panel). 24 hours after transfection, cells were fixed, permeabilised and stained for flag and PB2 using specific antibodies. Images were taken using confocal microscopy. Scale bars represent 10 μm.

3.2.3 Characterisation of the role of Importin α7 in influenza polymerase activity

3.2.3.1 Validation of mass spectrometry results-Importin α7

The results of the mass spectrometry experiments revealed that importin α7 was co-precipitated to a greater extent with the influenza polymerase when chANP32A was present compared to when it was absent. In the absence of chANP32A, importin α7 could still bind to a polymerase bearing either E or K at position 627 **(Fig 41a)**. Importin α7 has previously been implicated in influenza A host range and therefore we were interested in further exploring the significance of the interaction pattern observed in the mass spectrometry experiments. First, we validated that this pattern could be reproduced using immunoprecipitation followed by western blotting. In agreement with the mass spectrometry results, the greatest binding of importin α7 was seen to a 627E polymerase when chANP32A was present. Importin α7 also bound to both polymerases in the absence of chANP32A **(Fig 41b)**.

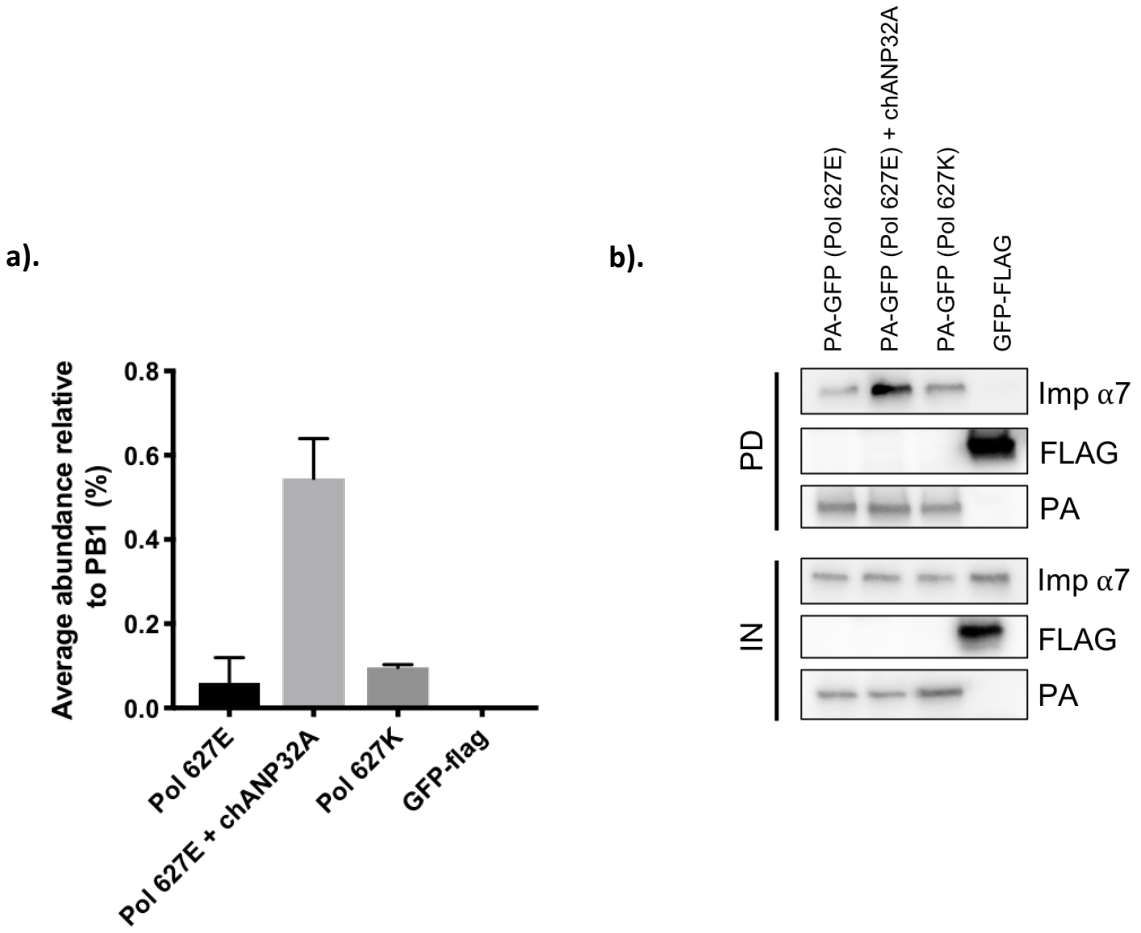


Fig 41: Validation of binding pattern of importin α7 revealed by mass spectrometry
a). Average abundance of importin α7 detected by mass spectrometry. Data is relative to abundance of PB1, which was set to 100%. **b).** HEK 293T cells were transfected with pCAGGs expression plasmids encoding PB1, PA-GFP, either PB2 627E or PB2 627K and chANP32 or an empty vector. GFP-flag was used as a negative control. 30 hours after transfection, PA-GFP was immunoprecipitated and endogenous importin α7 probed for on a western blot. Co-immunoprecipitation assay repeated twice.

3.2.3.2 Importin α7 is coprecipitated with ANP32A

Since the presence of chANP32A resulted in increased coprecipitation of importin α7 with the influenza polymerase, it is possible that this enhancement was a result of chANP32A binding to importin α7. To determine whether ANP32A could bind to importin α7 in the absence of influenza polymerase, we transfected 293T cells with chANP32A-flag or huANP32A-flag. The flag tagged ANP32A proteins were immunoprecipitated and co-precipitation of endogenous importin α7 was detected using western blotting. Results indicated that importin α7 was coprecipitated with both chANP32A-flag and huANP32A-flag **(Fig 42)**.

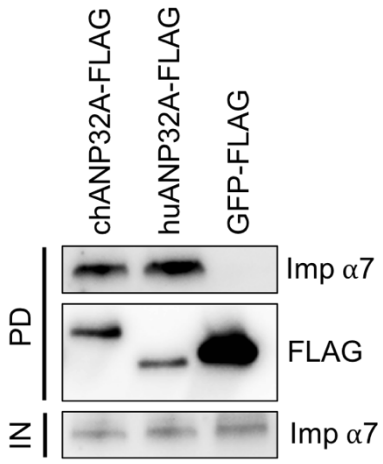


Fig 42: Importin α7 coprecipitates with ANP32A-flag
HEK 293T cells were transfected with either chANP32A-flag, huANP32A-flag or GFP-flag. 30 hours after transfection the flag tagged proteins were immunoprecipitated and coprecipitation of endogenous importin α7 was probed for on a western blot. Representative of three independent experiments.

3.2.3.3 Knockdown of importin α7 does not affect entry of ANP32A into the nucleus

Importin α7 is a protein involved in the nuclear import of many cellular proteins. Previous studies which have proposed a role for importin α7 in influenza A host restriction have used siRNA to knockdown importin α7. Knockdown down of importin α7 resulted in a decrease in polymerase activity of a PB2 627K containing polymerase, but not a polymerase containing PB2 627E (Hudjetz *et al.,* 2012). The subcellular distribution of vRNPs remained the same in importin α7 knockdown cells compared to controls indicating that the effect on polymerase activity was not due to changes in the localisation of the vRNP (Hudjetz *et al.,* 2012). However, since influenza A polymerase activity relies on the use of multiple cellular host factors, it is possible that the decrease in polymerase activity could be a result of limited nuclear entry of one of these proteins. We therefore used shRNA to knock down importin α7 in HEK 293T cells and investigated whether this affected the nuclear import of ANP32A. We observed that knockdown of importin α7 did not affect the accumulation of exogenously expressed chANP32A or huANP32A in the nucleus of human cells **(Fig 43a and b)**.

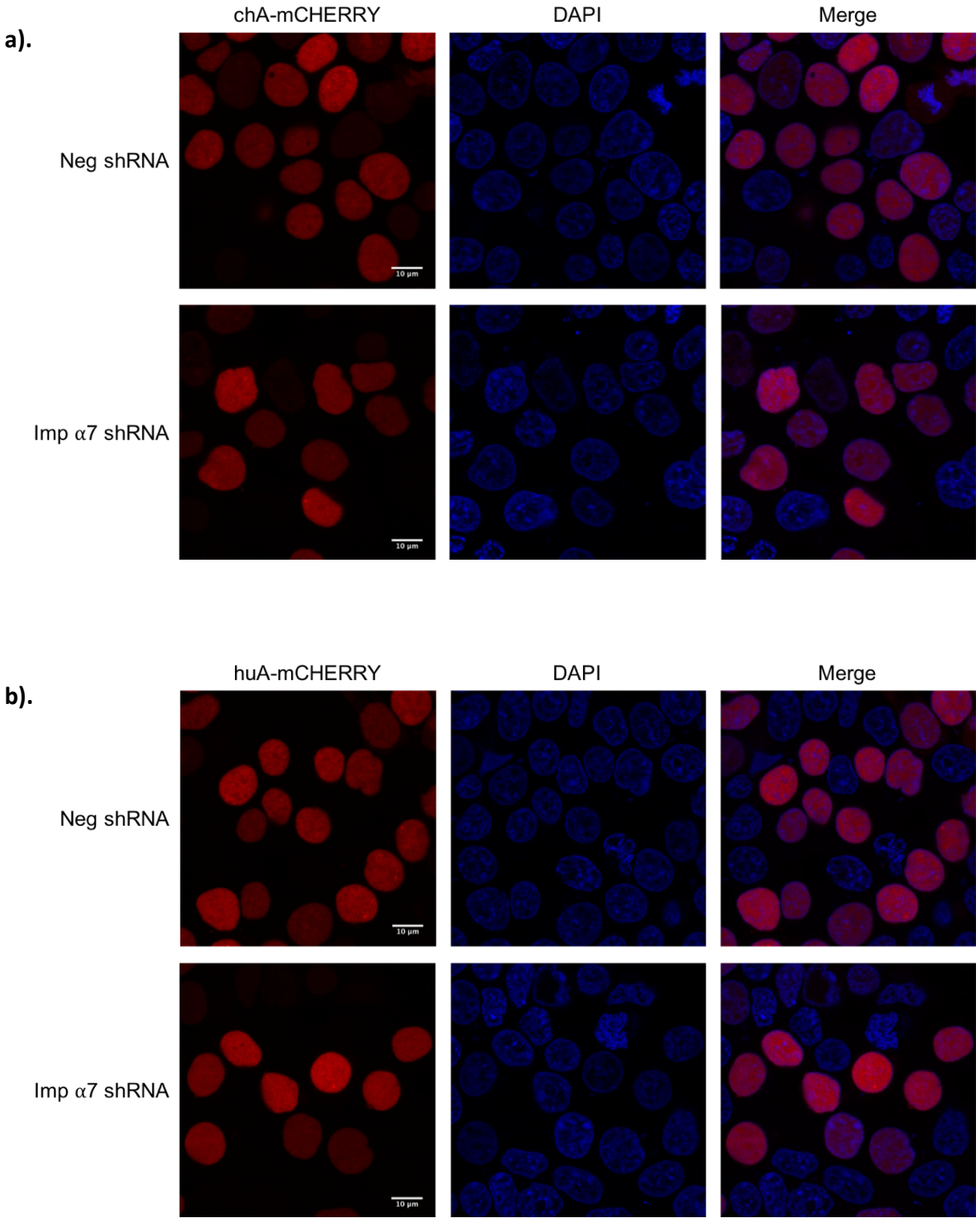


Fig 43: knockdown of importin α7 does not affect subcellular distribution of ANP32A
Control (neg) or importin α7 shRNA HEK 293T cells were transfected with **a).** chANP32A-mCHERRY or **b).** huANP32A-mCHERRY. 24 hours after transfection, cells were fixed and imaged using confocal microscopy. Scale bars represent 10 μm.

3.2.3.4 Effect of importin α7 on polymerase activity

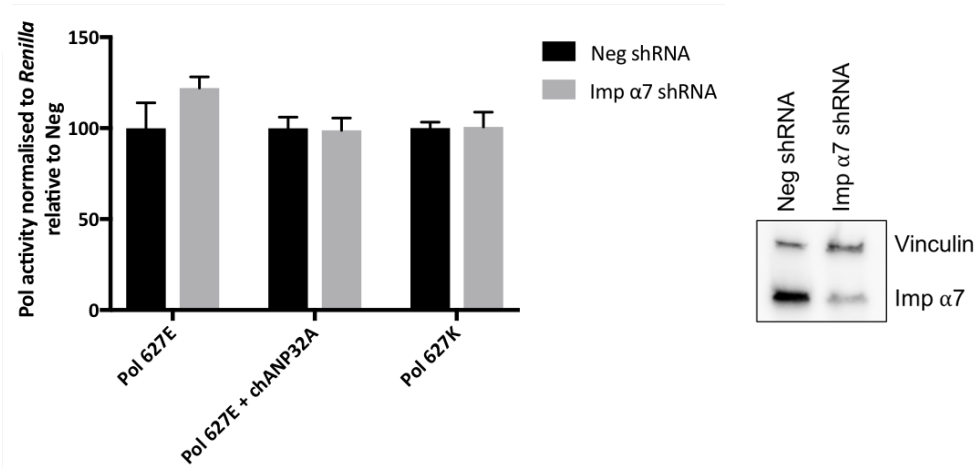
To assess the effect of importin α7 on polymerase activity, we knocked down importin α7 by shRNA in HEK 293T cells and assessed changes in activity of the 50-92 polymerase with either the PB2 627E or 627K signature and in the presence of chANP32A. shRNA induced knockdown of importin α7 did not significantly affect the polymerase activity of either a 627E or 627K containing polymerase or a PB2 627E polymerase in the presence of chANP32A, measured 24 hours after transfection **(Fig 44a)**. It is possible that the residual importin α7 in the shRNA knockdown cells could mask the effect of knocking down importin α7. We therefore measured polymerase activity after only 16 hours after transfection to see if this revealed any differences. After 16 hours, no differences in polymerase activity could be detected in the knockdown cells compared to controls **(Fig 44b)**.

This is in contrast to previous studies which showed that siRNA mediated knockdown of importin α7 caused a decrease in human adapted polymerase activity (Hudjetz *et al.,* 2012). In this study, they used the H1N1 A/WSN/1933 virus strain. We therefore, looked to see whether the effect of importin α7 knockdown was strain dependent. We measured polymerase activity from several different polymerases; H5N1 A/turkey/Turkey/05/2005 (Tky05), H9N2 A/chicken/Pakistan/UDL-01/2008 (UDL), pH1N1 A/England/195/2009 (Eng195), H3N2 A/Victoria/3/1975 (Vic) and H1N1 A/WSN/1933 (WSN). The activity of WSN polymerase only decreased slightly (13%) but the effect was significant. However, none of the other strains tested revealed any significant difference in polymerase activity compared to controls **(Fig 44c)**.

Another difference between this study and that published by Hudjetz *et al* is the expression vector used. Here, the polymerase components are cloned into pCAGGs vectors. The promoter region of these vectors is made up of a fusion between the chicken beta actin gene and rabbit beta globin gene, which together allows for very high expression of downstream genes. It is possible that any functional significance of knocking down importin α7 is masked by the high levels of polymerase expression. We therefore did a minigenome assay using A/WSN/33 polymerase components cloned into the pcDNA3 backbone. Using these plasmids, shRNA knockdown of importin α7 resulted in a 52% decrease in polymerase activity compared to controls **(Fig 44d)**.

Altogether this suggests that importin α7 is able to bind to the polymerase and this interaction is affected by the presence of chANP32A. Importin α7 can support the activity of a human adapted polymerase, but the need may be circumvented by high levels of polymerase expression. Western blot analysis should be used in the future to confirm this.

a).



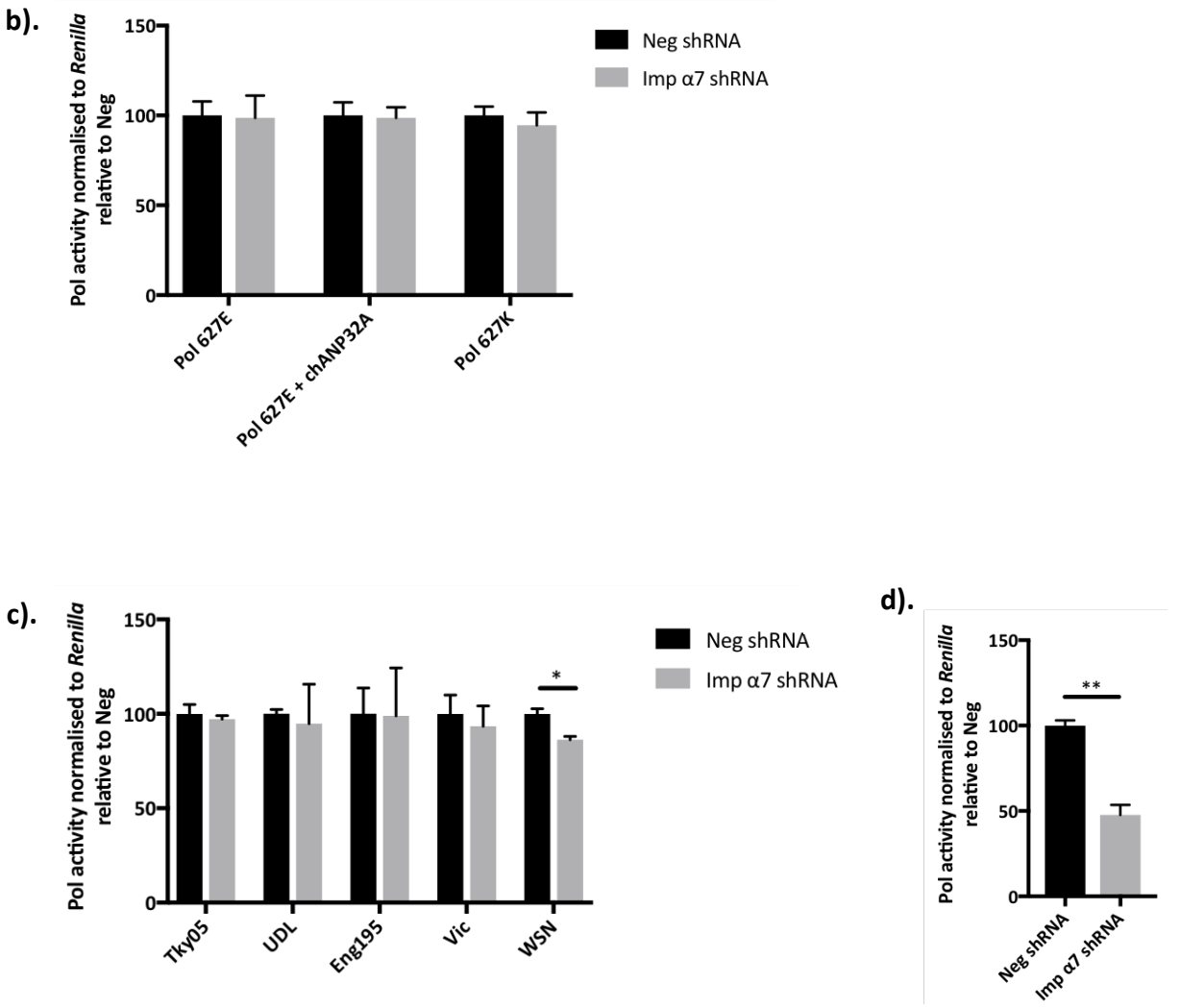


Fig 44: Functional effects of importin α7 on polymerase activity

a). Expression plasmids encoding 50-92 PB1, PB2 627E or 627K, PA, NP, *Renilla* luciferase and polI minigenome encoding firefly luciferase were transfected into negative or importin α7 shRNA HEK 293T cells. Either chANP32A or an empty plasmid was also transfected. Polymerase activity was measured 24 hours or **b).** 16 hours after transfection. Validation of importin α7 shRNA knockdown was validated by western blot (right). **c).** Negative or importin α7 shRNA HEK 293T cells were transfected with minigenome assay components including pCAGGs expression plasmids encoding PB1, PB2 627K, PA, NP from the indicated influenza A background. All PB2s naturally contain or were engineered to contain 627K, apart from Eng195 which has 627E **d).** Negative or SRPK1 shRNA HEK 293T cells were transfected with pcDNA3 expression plasmids encoding PB1, PB2 627K, PA, NP from the WSN/33 background as well as *Renilla* luciferase. The influenza mini genome encoding firefly luciferase was used to measure polymerase activity. Results are normalised to *Renilla* luciferase and represented relative to control (neg) shRNA cells, which were all set to 100%. Results shown are mean ± standard deviation from triplicate samples. Statistical significance was assessed by multiple t-tests, *p<0.05, **p<0.01. Non-significant results not indicated. Results representative of three independent experiments.

3.3 Discussion

In this chapter, we used label free LC-MS/MS to identify differences in the interactome of an avian origin influenza A polymerase in the presence or absence of chANP32A. We further characterised two proteins, SRPK1 and importin α7, which both increased in association with polymerase containing PB2 627E when chANP32A was present. Knockdown of SRPK1 resulted in reduced polymerase activity, however a relationship between SRPK1 and chANP32A could not be identified. Knockdown of importin α7 resulted in a reduction of polymerase activity but only when the polymerase was expressed from pcDNA3 vectors. Importin α7 was also found to co-precipitate with ANP32A in the absence of influenza polymerase.

Mass spectrometry has previously been used to identify proteins which bind to the influenza polymerase (Bradel-Trethway *et al.,* 2011; Fislova *et al.,* 2010; Jorba *et al.,* 2008a; Meyer *et al.,* 2007; Wang *et al.,* 2017; York *et al.,* 2014). Although there is some overlap, the interactomes presented by different studies are not completely redundant. This is most likely due to differences in methodology, influenza virus strain used and tags used to purify viral proteins prior to mass spectrometry analysis. Many of proteins identified as binding to the influenza polymerase in this study have been previously shown to bind to the polymerase and many have been further characterised. For example, RNA polymerase II (Lukarska *et al.,* 2017), PPP6 (York *et al.,* 2014), DDX17 (Bortz *et al.,* 2011), DNAJA1 (Cao *et al.,* 2014) as well as various importin isoforms (Gabriel *et al.,* 2011).

Label free mass spectrometry was used to quantify differences between the same protein in different samples. A more robust quantitative approach would have been to use SILAC (stable isotope labelling of amino acids in cell culture) based mass spectrometry (Chen *et al.,* 2015).

Nevertheless, the binding patterns of the proteins which were further characterised were validated using co-immunoprecipitation, indicating that label free mass spectrometry was a sufficient approach.

The mass spectrometry screen identified proteins which both increased and decreased in abundance in the presence of chANP32A. Those proteins which decreased in abundance were regarded as possible inhibitory factors since expression of chANP32A may allow the AIV polymerase to escape restriction by this factor. In line with this, it has previously been proposed that the restriction in activity of an AIV polymerase in human cells is due to an inhibitory factor (Mehle and Doudna, 2008). It is important to note however, that over expression of chANP32A could also displace endogenous proteins which actually support the AIV polymerase purely due to sheer abundance of chANP32A. For example, the abundance of hsp90 binding to the AIV polymerase decreased when chANP32A was expressed. However, there have been several reports of hsp90 having a supportive role in the activity of the influenza polymerase (Momose *et al.,* 2002; Naito *et al.,* 2007b). Nevertheless, exogenous expression of chANP32A, whilst perhaps displacing supportive host cell factors, is able to rescue the activity of the AIV polymerase in human cells (Long *et al.,* 2016).

Those proteins which increased in co-precipitation with AIV polymerase in the presence of chANP32A were regarded as possible positive factors. A SIM sequence has been identified at the beginning of the 33 amino acid insertion in chANP32A (Domingues and Hale, 2017). Therefore, the mechanism by which chANP32A supports the activity of the AIV polymerase may involve interactions with SUMOylated host or viral factors. Upon influenza infection, the SUMOylation state of many host proteins are altered (Domingues *et al.,* 2015). Furthermore,

SUMOylation of several viral proteins, including PB1, which is only SUMOylated upon co-expression of both PB2 and PA, has also been demonstrated (Pal *et al.,* 2011).

SRPK1 was identified as a factor which increased in abundance when chANP32A was present. SUMOplot prediction software (abgent) revealed 13 potential SUMOylation sites, three of which had a high probability of SUMOylation. It is therefore possible that the SIM domain of chANP32A may bind to SRPK1 via one of these SUMOylated sites. Although SRPK1 could not be coprecipitated with chANP32A alone, this does not exclude binding of the two proteins within the polymerase complex. However, knockdown of SRPK1 reduced activity of the influenza polymerase regardless of the nature of residue 627 of PB2 and regardless of the presence of chANP32A. This suggests that SRPK1 may act as a host factor which supports polymerase activity, but does not contribute to determining host range of influenza. The human and chicken SRPK1 proteins share 70% sequence identity. It would therefore be interesting to explore whether knockdown of this avian protein in avian cells had the same effect on influenza polymerase activity.

Despite being able to support the activity of the influenza polymerase regardless of the nature of the amino acid at position 627, results from mass spectrometry and co-immunoprecipitation experiments revealed greater binding between SRPK1 to a polymerase containing PB2 627K compared to PB2 627E, unless chANP32A was also expressed. It has previously been shown that a polymerase with PB2 627E is less dynamic in the nucleus of human cells (Foeglein *et al.,* 2011) and therefore may occupy different nuclear subdomains compared to a polymerase with PB2 627K. This could therefore suggest that SRPK1 is able to support both polymerases but that an AIV polymerase is less available to SRPK1. Alternatively,

a glutamic acid at residue 627 of PB2 may destabilise the interaction, but the activity of SRPK1 in supporting polymerase function may not depend on the extent of this interaction.

Immunofluorescence assays suggested that SRPK1 localises in the both the nucleus and the cytoplasm. This is consistent with previous findings (Aubol *et al.,* 2018; Wang *et al.,* 1998). It is not clear what triggers the nuclear translocation of SRPK1, although one study has proposed that EGF signalling may disrupt interactions between SRPK1 and chaperone proteins which otherwise retain this protein in the cytoplasm (Zhou *et al.,* 2012). SRPK1 could not be detected in the nucleus of some cells in which PB2 was also expressed suggesting that expression of PB2 does not affect the localisation of SRPK1. However, quantitative analysis to determine whether expression of PB2 increases the proportion of cells where SRPK1 can be observed in the nucleus could be carried out to confirm this.

SRPK1 has been implicated in supporting a number of viruses. SRPK1 phosphorylates the hepatitis B core protein (Daub *et al.,* 2002). Furthermore, knockdown or drug mediated inhibition of SRPK1 resulted in a decrease in hepatitis C replication (Karakama *et al.,* 2010). Phosphorylation of human papilloma virus type 1 E4 protein by SRPK1 is required for its replication cycle as well as that of coronavirus (Bell *et al.,* 2007; Peng *et al.,* 2008). SRPK1 has not previously been linked to influenza replication, neither has it been identified in any previous influenza proteomic experiments. We therefore present SRPK1 as a novel host factor capable of supporting influenza A polymerase activity. Whether the kinase activity of SRPK1 is needed for its ability to support the influenza polymerase is yet to be tested. Interestingly, a phosphorylation site at PB2 S742 has been detected (Hutchinson *et al.,* 2012). This site is conserved between influenza A, B and C and lies within the NLS domain of PB2. Phosphorylation is a known regulator of nuclear import (Poon and Jans, 2005) and therefore

phosphorylation at this site may affect binding to nuclear import factors (Hutchinson *et al.,* 2012). Whether nuclear import of PB2 is affected upon depletion of SRPK1 could be investigated in the future.

Importin α7 has been extensively implicated in host range of influenza. Avian viruses show dependency on importin α3, whilst human viruses show dependency on importin α7 (Gabriel *et al.,* 2011). This switch was mapped to mutations NP N319K and PB2 D701N, which enhanced binding of the viral proteins to importins resulting in increased transport into the nucleus (Gabriel *et al.,* 2008; Gabriel *et al.,* 2011). The relationship between the PB2 E627K mutation and importins has also been investigated. A viral polymerase with PB2 627K required importin α7 for polymerase activity, whereas that with PB2 627E did not (Hudjetz *et al.,* 2012). In this study, function of the polymerase was only affected when importin α7 was knocked down if the polymerase was expressed from pcDNA3 vectors. Previous studies have observed reduced polymerase activity of a PB2 627K polymerase in cells depleted of importin α7 when the polymerase was reconstituted from pHW2000 vectors (Hudjetz *et al.,* 2012). It is possible that the high expression levels obtained from pCAGGs vectors may overcome the effects of shRNA mediated knockdown of importin α7 on polymerase activity.

It is important to note that importin α proteins are responsible for the nuclear import of many proteins and therefore the effects of importin α7 knockdown on viral polymerase activity may be indirect through the reduced nuclear import of a different factor. We have demonstrated that knockdown of importin α7 does not prevent nuclear localisation of exogenously expressed ch- or huANP32A. However, the role of importin α7 on the nuclear localisation of endogenous huANP32A was not assessed. Previous studies have shown that mouse ANP32A is imported into the nuclei of adult mouse brain cells using importin isoforms (Fukumoto *et*

al., 2011). Nonetheless, further roles other than nuclear import have also been proposed to account for the effect of importin α7 knockdown on PB2 627K viral polymerase activity (Hudjetz *et al.,* 2012; Resa-Infante *et al.,* 2008). Substitution of the PB2 NLS with an exogenous NLS resulted in reduced polymerase activity despite full nuclear localisation of PB2 (Resa-Infante *et al.,* 2008).

We have shown that importin α7 is co-immunoprecipitated with the influenza polymerase and this interaction increases with an avian adapted polymerase in the presence of chANP32A. Importin α7 can also bind to ch- and huANP32A independently of the influenza polymerase. It is therefore possible that ANP32 proteins may bind to importin α7 within the polymerase complex. A crystal structure of the PB2 627 and NLS domains revealed that these domains can pack against each other (Tarendeau *et al.,* 2008). Using this structure and that of importin α5 bound to the PB2 NLS domain (Tarendeau *et al.,* 2007), it is predicted that the 627 domain and importin α5 would clash and therefore conformational changes in the PB2 domains would be required to allow importin α binding (Boivin and Hart, 2011; Tarendeau *et al.,* 2008). Binding of chANP32A to the AIV polymerase may aid this conformational change to allow importin α binding. Whether importin α7 can still be coprecipitated with the mammalian adapted influenza polymerase in the absence of huANP32A and -B would be interesting to explore. The generation of human cells in our laboratory that lack huANP32A and -B expression could facilitate this.

Overall, we have used LC-MS/MS to identify changes in the interactome of an avian origin polymerase in the presence or absence of chANP32A. In doing so, we have revealed SRPK1 as a potential novel host factor which supports activity of the influenza A polymerase. We have

also further characterised importin α7. However, further work is needed to be able to fully resolve the functions of these two proteins in the context of influenza.

Chapter 4: Differences between nuclear location of avian and human adapted viral polymerases visualised by widefield microscopy

4.1 Introduction

Influenza A virus requires the use of host cell machinery for each step of its life cycle, but how the virus coordinates the use of these host factors is not clear. The cell nucleus contains various substructures, often characterised by the identity and abundance of specific macromolecules in that subdomain (Dundr and Misteli, 2001). For example, cellular RNA is synthesised in 'transcription factories.' These are sites with a high concentration of proteins required for the synthesis and processing of RNAs. Mass spectrometry experiments revealed a wealth of proteins associated with the processing of mRNA in complex with RNAPII including helicases, transcription factors and splicing components (Melnik *et al.,* 2011).

Many studies suggest that viral processes take place in distinct subdomains of the nucleus and some of the host factors that regulate this have been identified. For example, binding of the influenza A polymerase to RNAPII puts it in close proximity to cap structures, as well as

mRNA processing proteins (Engelhardt and Fodor, 2006; Lukarska *et al*., 2017; Rialdi *et al.,* 2017). The localisation of NP changes throughout infection, first being dispersed throughout the nucleus, then being localised at the periphery of the nucleus at later time points (Elton *et al.,* 2005). vRNPs have been shown to undergo export from the nucleus in a process whereby transit through SC-35^{+} nuclear speckles is mediated by the host protein, CLUH (Ando *et al.,* 2016). Several viral proteins including M1, NS1 and NS2 have also been associated with Promyelocytic leukaemia (PML) nuclear bodies (Sato *et al.,* 2003). Furthermore, M1 mRNA is transported to SC-35^{+} nuclear speckles for splicing and this was dependent on viral NS1 as well as various host factors (Mor *et al.,* 2016). NS1 has also been reported to accumulate in the nucleolus, although this appears to be strain dependent in mammalian cells (Volmer *et al.,* 2012). The exact nuclear subdomain in which viral replication is carried out is unknown. Which host factors are involved in transporting the viral proteins to this location and how this is regulated is also unclear.

AIV polymerases are restricted in human cells. The well-known PB2 E627K mutation is able to overcome this restriction (Subbarao *et al*., 1993). Interestingly, studies indicate that RNA synthesis by a PB2 627E polymerase or that lacking the 627 domain is not impaired *in vitro* (Aggarwal *et al*., 2011; Nilsson *et al.,* 2017). Presence of host factors or differences in the spatial distribution of the polymerase within cells may therefore contribute to the restriction seen in mammalian cells. In line with this, position 627 of PB2 lies on a surface exposed region of the polymerase and is therefore accessible to host factors (Tarendeau *et al.,* 2008). Furthermore, it has been shown that a PB2 627E polymerase is less dynamic in human cells than that with the PB2 E627K mutation (Foeglein *et al.,* 2011). This could be a result of either

binding to an inhibitory factor or being unable to bind to a stimulatory factor which may direct it to the correct position within the nucleus.

In this chapter, we used widefield microscopy to investigate whether any differences between the nuclear localisation of a PB2 627E or PB2 627K polymerase could be observed in human cells. We found that the AIV polymerase forms speckles in the nuclei of human cells and these were seen less frequently in cells expressing 627K polymerase. Since ANP32A can bind and support viral polymerase activity, we also explored the relationship of these speckles with ANP32A.

Imaging in this chapter was carried out in collaboration with Adam Cawte and Prof David Rueda at Imperial College London.

4.2 Results

4.2.1 An avian origin polymerase forms speckles in the nuclei of human cells

In order to investigate whether any differences in intranuclear localization could be observed between a viral polymerase bearing either a glutamic acid or lysine residue at position 627 of PB2, we transfected HEK 293T cells with expression plasmids encoding the three viral polymerase components (including PB2 627E or that engineered to contain 627K) as well as NP. Again, viral proteins from the AIV A/Turkey/England/50-92/91 were used due to their avian origin. Polymerase activity was verified using an influenza like RNA encoding blue fluorescent protein tagged with a nuclear localisation sequence (BFP-NLS). In order to visualise the polymerase, PA was tagged with GFP at its C terminus.

As expected, there were more blue nuclei when using a polymerase bearing the PB2 E627K mutation compared to wildtype (PB2 627E), indicative of increased transcription and replication **(Fig 45a and b)**. In general, the PA-GFP was observed to localize diffusely throughout the nucleus regardless of whether the polymerase was active. Interestingly, when the polymerase was reconstituted using PB2 627E, the PA-GFP could be seen forming speckles in the nuclei of these cells. These speckles were present in only 8.4 % of PA-GFP expressing cells transfected with PB2 627K compared to 61.6 % of PA-GFP expressing cells transfected with PB2 627E **(Fig 45a and b)**. Although levels of expression of PA-GFP was heterogeneous between cells, overall expression of PA-GFP between conditions remained similar, as detected by western blotting **(Fig 45a)**.

Only two cells out of 140 with efficient replication also contained speckles (data not shown). This suggests that although efficient polymerase activity and the formation of speckles in the nuclei of human cells are not completely mutually exclusive, there is a strong negative relationship between the two occurrences.

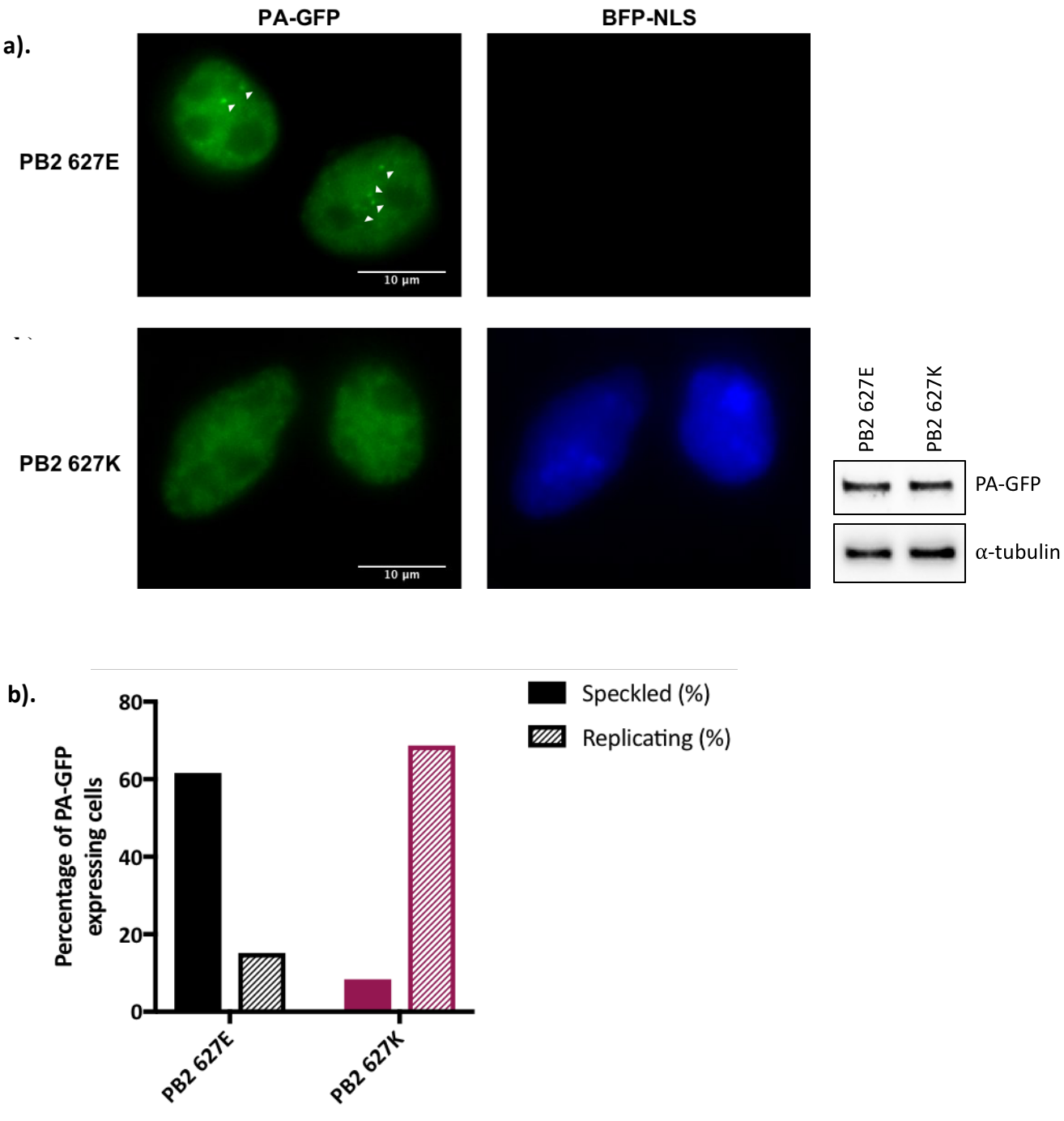


Fig 45: Speckles can be observed in cells expressing AIV polymerase
a). HEK 293T cells were transfected with 10 ng PA-GFP, 20 ng PB1, 40 ng NP, 20 ng polI-vRNA encoding BFP-NLS and 20 ng either PB2 627E or PB2 627K. 24 hours after transfection, cells were fixed and imaged using widefield microscopy. Prominent speckles are highlighted by white arrowheads. Scale bar is 10µm. Representative image for each condition shown. Expression of proteins detected by western blot. **b).** Percentage of speckled (solid bars) or replicating (diagonally striped bars) cells were counted from seven random fields of view of each condition. Percentage shown is relative to total number of PA-GFP expressing cells in these fields of view. n=112 for PB2 627E, n=179 for PB2 627K. Results representative of three independent experiments.

4.2.2 The trimeric polymerase complex is the minimal requirement for formation of speckles

Next, we wanted to decipher which components of the RNP are required for formation of the speckles. It is thought that both PA and PB1 enter the nucleus as a dimer (Deng *et al.,* 2005; Huet *et al.,* 2010). Therefore, if PA-GFP is located in the nucleus of cells, this indicates that at least PB1 has been co-expressed with it. It could be proposed that the PA-GFP - PB1 dimer always forms speckles, but the presence of PB2 627K allows the dimer to be released from these speckles, whereas addition of PB2 627E is not able to have this effect. However, we observed that transfection of only PA-GFP and PB1 did not result in the formation of speckles in the nuclei of human cells suggesting that this is not the case **(Fig 46a)**.

Since the nature of position 627 of PB2 seemed to determine the likelihood of speckles being observed, we investigated whether PB2 627E alone was able to form speckles. Expression of either PB2 627E-GFP or PB2-627K-GFP resulted in no observable speckles in the nuclei of human cells **(Fig 46b)**.

We next examined whether the trimeric polymerase complex was sufficient for formation of the speckles or whether NP and influenza-like viral RNA were also required. Expression of only the trimeric polymerase bearing PB2 627E resulted in the formation of speckles **(Fig 46c and d)**. Speckles were rarely observed in cells expressing the trimeric polymerase complex bearing PB2 627K **(Fig 46c and d)**. This suggests that the three viral polymerase subunits are the minimal components required for formation of the speckles.

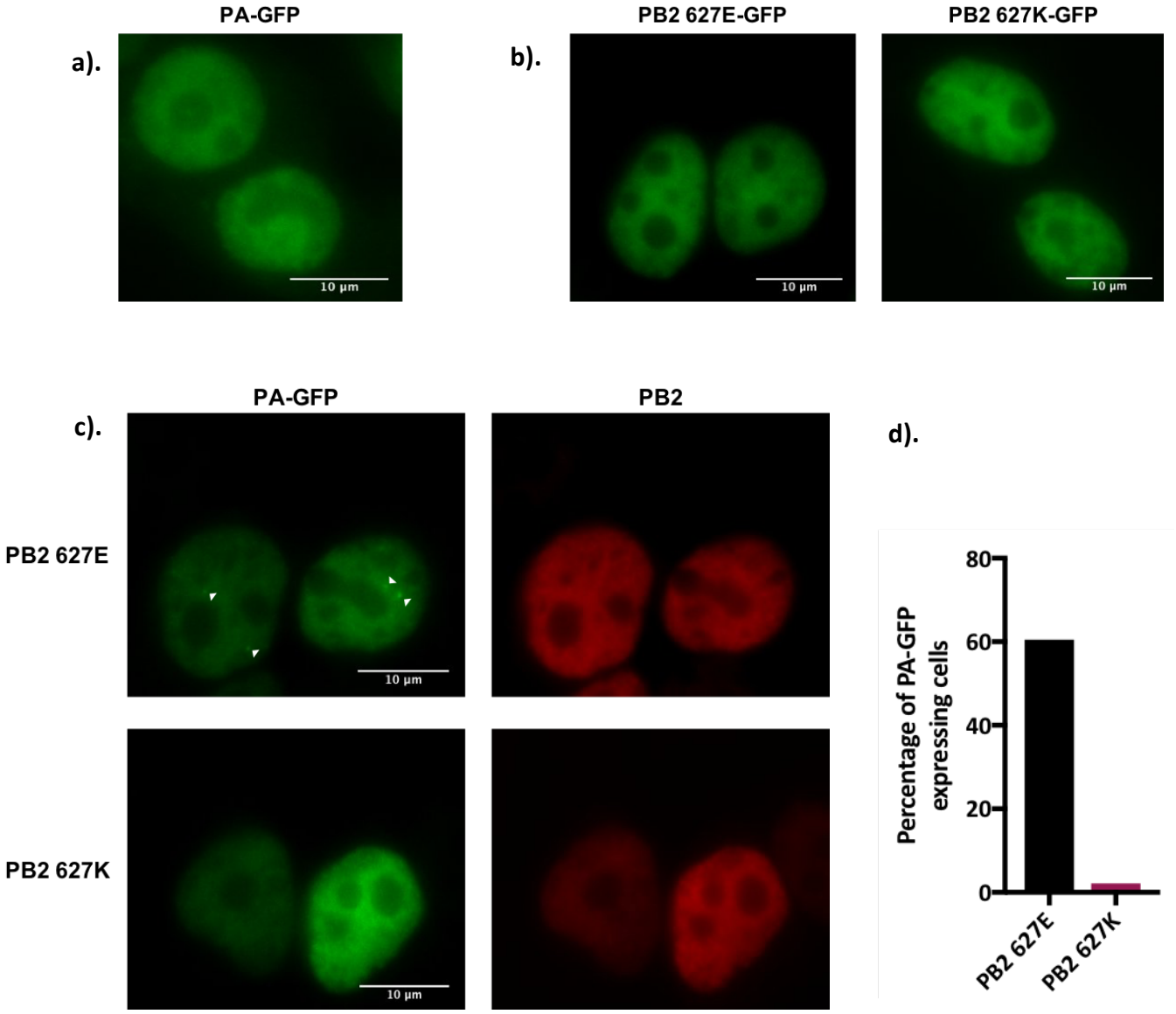


Fig 46: The trimeric polymerase is the minimum requirement for speckle formation
a). (Fig a). carried out by masters student, Eve Hopkins). HEK 293T cells were transfected with 10 ng PA-GFP and 20 ng PB1 or **b).** 20ng PB2 627E-GFP or 20 ng PB2-627K GFP. 24 hours after transfection, cells were fixed and imaged using widefield microscopy. **c).** HEK 293T cells were transfected with 10 ng PA-GFP, 20 ng PB1 and 20 ng either PB2 627E or PB2 627K. 24 hours after transfection, cells were fixed, permeabilised and PB2 detected using fluorescent antibodies. Cells were imaged using widefield microscopy. Prominent speckles are highlighted by white arrowheads. Scale bar is 10µm. Representative image for each condition shown. **d).** Percentage of speckled (solid bars) cells were counted from seven random fields of view of each condition. Percentage shown is relative to total number of PA-GFP expressing cells in these fields of view. n=76 for PB2 627E, n=93 for PB2 627K. Fig c and d representative of three independent experiments.

4.2.3 chANP32A decreases the proportion of speckled nuclei in cells expressing IAV polymerase

Since chANP32A can bind to the AIV trimeric polymerase complex and support its function (Long *et al.,* 2016), we investigated whether the presence of chANP32A would affect the proportion of speckled nuclei observed. Co-expression of chANP32A-mCHERRY with the 50-92 AIV polymerase (PB2 627E), resulted in a decrease in the percentage of speckled nuclei and an increase in replication, as measured by the number of blue cells **(Fig 47)**. Expression of huANP32A-mCHERRY, which cannot support the activity of AIV, only decreased the percentage of speckled nuclei by 16 % compared to chANP32A-mCHERRY, which decreased it by 36% **(Fig 47)**. If either chANP32A-mCHERRY or huANP32A-mCHERRY were co-expressed with the humanised polymerase, neither replication or percentage of speckled cells were affected **(Fig 47)**. This suggests that the presence of chANP32A can affect formation or stability of the AIV polymerase speckles. However, in 7 % of cells which displayed replication, even if chANP32A was expressed, speckles could still be observed. As suggested above, this indicates that the formation of speckles and replication are not absolutely mutually exclusive.

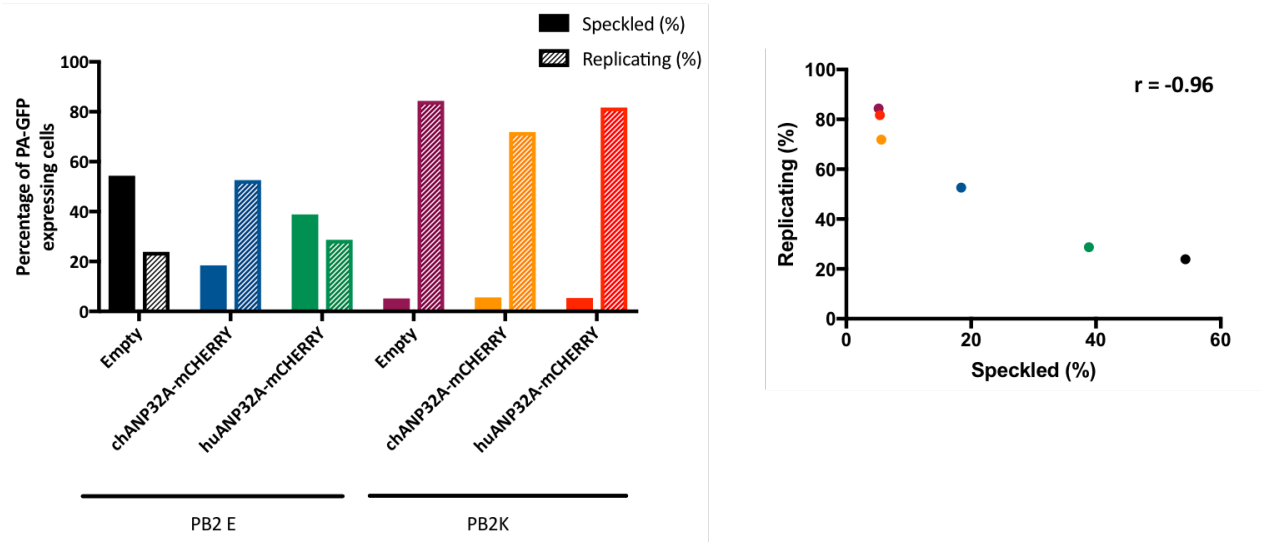


Fig 47: chANP32A decreases the proportion of speckled nuclei in cells expressing AIV polymerase

HEK 293T cells were transfected with 10 ng PA-GFP, 20 ng PB1, 40 ng NP, 20 ng polI-vRNA encoding BFP-NLS, 20 ng either PB2 627E or PB2 627K and 20 ng either an empty plasmid, chANP32A-mCHERRY or huANP32A-mCHERRY. 24 hours after transfection, cells were fixed and imaged using widefield microscopy. Percentage of speckled (solid bars) or replicating (diagonally striped bars) cells were counted from seven random fields of view of each condition. Percentage shown is relative to total number of PA-GFP expressing cells in these fields of view. Right: data plotted as scatter plot using same colour code as in bar graph. r value calculated using Pearsons correlation. n=92, n=114 and n=108 for PB2 627E empty, chANP32A-mCHERRY and huANP32A-mCHERRY, respectively. n= 77, n= 89 and n=93 for PB2 627K empty, chANP32A-mCHERRY and huANP32A-mCHERRY, respectively. Results representative of three independent experiments.

4.2.4 Reconstituted AIV polymerase from a different viral subtype also forms speckles in the nucleus of human cells

To ensure that the formation of speckles was not specific to the 50-92 AIV polymerase, we next examined whether the same effect occurred in the H9N2 avian strain A/Chicken/UDL-01/08 (UDL). The UDL polymerase formed speckles in the nuclei of 57 % of human cells expressing PA-GFP, whereas a UDL polymerase whose PB2 had been mutated to lysine at position 627 resulted in only 8.9 % of nuclei displaying speckles **(Fig 48a and b)**. Addition of chANP32A-mCHERRY, but not huANP32A-mCHERRY, resulted in a reduction in the percentage of speckled cells and increased replication of AIV polymerase **(Fig 48b)**. Addition of either ANP32A-mCHERRY proteins had a negligible effect on replication or formation of speckles in cells expressing UDL polymerase bearing PB2 627K **(Fig 48b)**. Overall, these results, using the UDL polymerase, corroborate those found using the 50-92 polymerase. This indicates that the observations are not specific to 50-92, but are likely to be universal across other avian virus strains.

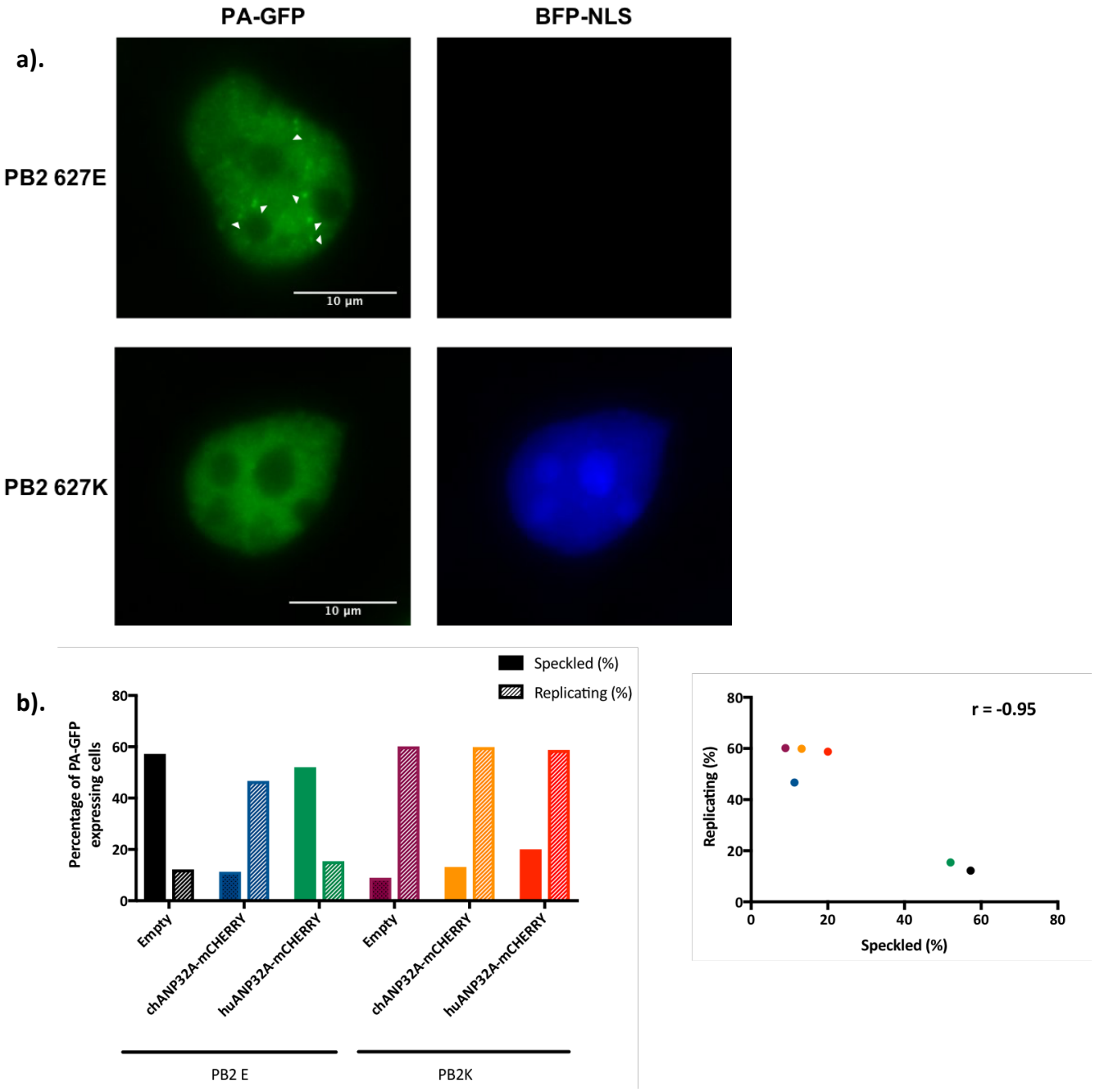


Fig 48: UDL viral polymerase displays same speckled pattern as 5092 viral polymerase
a). HEK 293T cells were transfected with 10 ng PA-GFP, 20 ng PB1, 40 ng NP, 20 ng polI-vRNA encoding BFP-NLS, 20 ng either PB2 627E or PB2 627K and 20 ng either an empty plasmid, chANP32A-mCHERRY or huANP32A-mCHERRY. 24 hours after transfection, cells were fixed and imaged using widefield microscopy. Scale bar is 10µm **b).** Percentage of speckled (solid bars) or replicating (diagonally striped bars) cells were counted from seven random fields of view of each condition. Percentage shown is relative to total number of PA-GFP expressing cells in these fields of view. Right: data plotted as scatter plot using same colour code as in bar graph. r value calculated using Pearsons correlation. n=131, n=150 and n=123 for PB2 627E empty, chANP32A-mCHERRY and huANP32A-mCHERRY, respectively. n= 123, n= 152 and n=160 for PB2 627K empty, chANP32A-mCHERRY and huANP32A-mCHERRY, respectively. Results representative of two independent experiments.

4.2.5 chANP32A 1-208 can affect the likelihood of speckled nuclei forming

In chapter 2 it was demonstrated that chANP32A lacking its LCAR domain (chANP32A 1-208), despite binding only poorly to polymerase, was still able to support the activity of an avian origin polymerase in human cells, albeit less than full length chANP32A. To further investigate the relationship between ANP32A and the speckles, we looked to see whether expression of chANP32A 1-208 affected the presence of the speckles. Expression of full length chANP32A resulted in 58 % fewer speckled nuclei compared to an empty vector control **(Fig 49)**. Expression of chANP32A 1-208 resulted in only a 19 % decrease in cells with speckled nuclei. Polymerase activity as measured by the number of cells detected with BFP expression in the nucleus increased by 58 % and 10 % when chANP32A and chANP32A 1-208 were expressed, respectively, compared to the control **(Fig 49)**. Overall, this suggests that as polymerase activity increases, less speckled cells can be observed.

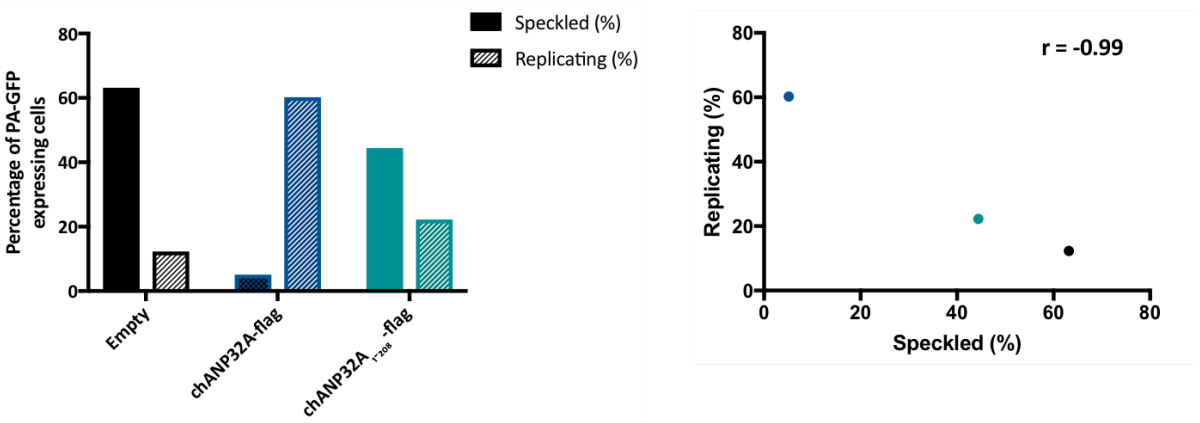


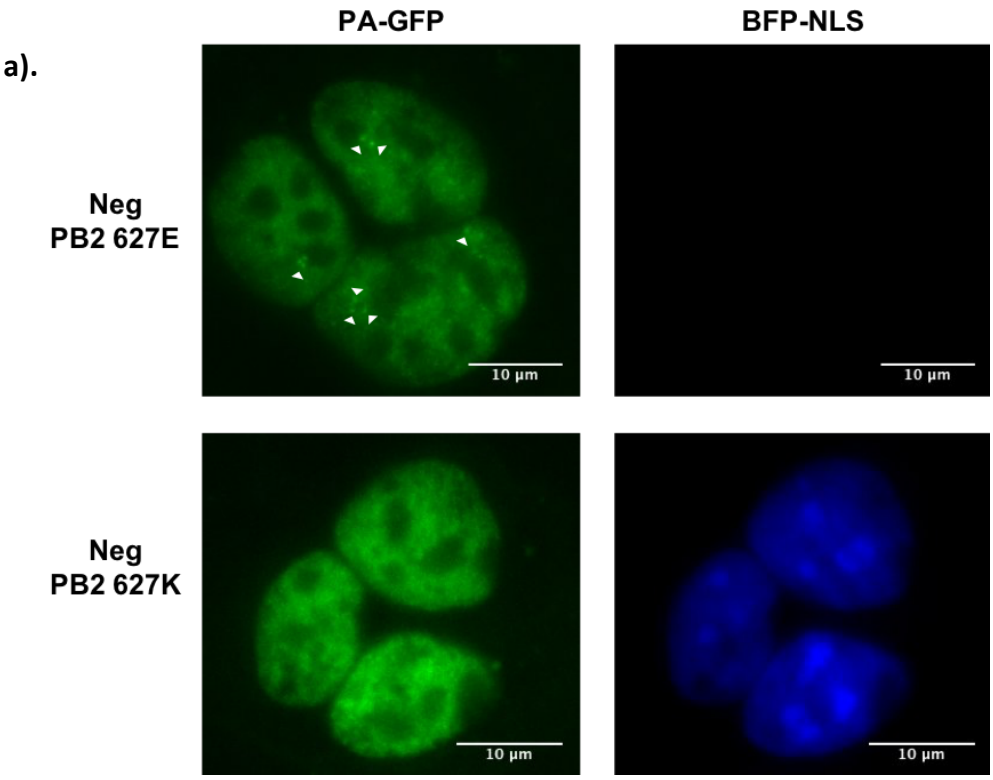
Fig 49: chANP32A$_{1-208}$ decreases the proportion of speckled nuclei in cells expressing AIV
HEK 293T cells were transfected with 10 ng PA-GFP, 20 ng PB1, 40 ng NP, 20 ng polI-vRNA encoding BFP-NLS, 20 ng PB2 627E 20 ng either an empty plasmid, chANP32A-flag or chANP32A 1-208-flag. 24 hours after transfection, cells were fixed, permeabilised and flag was detected using fluorescent antibodies. Samples were imaged using widefield microscopy. Percentage of speckled (solid bars) or replicating (diagonally striped bars) cells were counted from seven random fields of view of each condition. Percentage shown is relative to total number of PA-GFP expressing cells in these fields of view. Right: data plotted as scatter plot using same colour code as in bar graph. r value calculated using Pearsons correlation. n=57, n=78 and n=72 for empty, chANP32A-flag and chANP32A 1-208-flag, respectively. Results representative of one experiment.

4.2.6 The human adapted viral polymerase forms speckles in the absence of huANP32A and -B

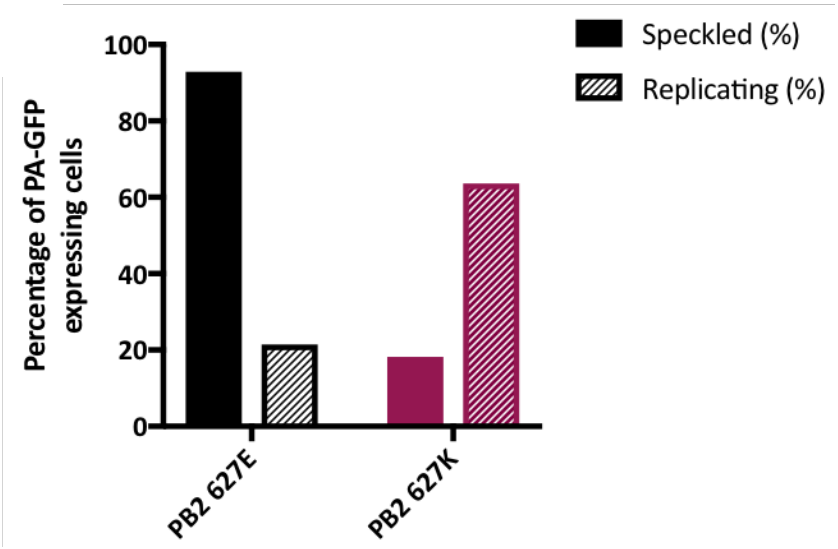
Work from another member of the lab and published data has revealed that huANP32A and huANP32B are essential for the replication of a viral polymerase bearing PB2 627K in human cells; eHAP1 cells engineered to lack expression of both proteins using CRISPR did not support polymerase activity (Staller, *in review*; Zhang *et al.,* 2019). We hypothesized that the absence of the ANP32 proteins in human cells would increase the proportion of PB2 627K expressing cells displaying speckled nuclei. It was first important to ensure that the wild type eHAP1 cells (neg) behaved in the same way as HEK 293T cells with regards to the formation of speckles. Expression of RNP components with PB2 bearing 627E resulted in a greater proportion of speckled nuclei and lower percentage of cells where efficient replication could be observed, compared to RNP components with PB2 bearing 627K **(Fig 50a and b)**. This indicates that the observed pattern is consistent between both cell types.

Absence of huANP32A and –B expression resulted in the appearance of speckles in nearly all cells expressing PA-GFP, regardless of the nature of the amino acid at position 627 of PB2 **(Fig 50c and d)**. As expected, viral polymerase activity, indicated by expression of BFP, was not visible in any cells. Addition of huANP32A to cells expressing a PB2 627K polymerase increased the proportion of BFP positive cells by 39 %. However, the proportion of speckled nuclei decreased by only 25 % **(Fig 50d)**. 50 % of the cells where active replication had taken place, were also speckled **(Fig 50c and d)**. Furthermore, no observable differences in the number of speckles per cell could be detected. This suggests that the presence of huANP32A was not sufficient to completely prevent or disperse all the speckles. However, due to limitations in transfection efficiency of the eHAP1 cells, the sample size was relatively small for this

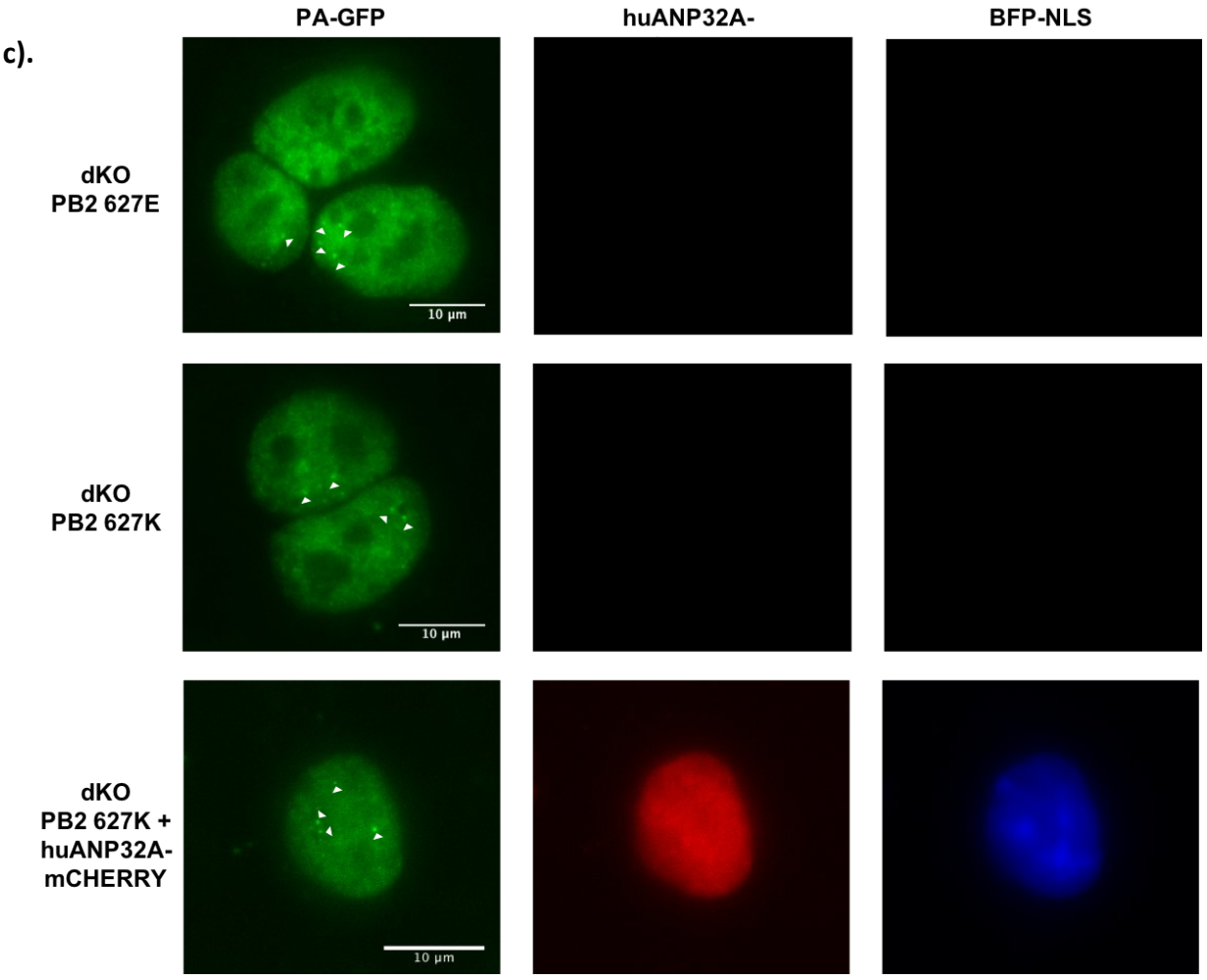
experiment. Moreover, the experiment should be repeated with the addition of both huANP32A and huANP32B since the latter orthologue has been shown to be very efficient at rescue of polymerase activity (Staller, *in review;* Zhang *et al.,* 2019).



b).


Speckled (%)
Replicating (%)
Percentage of PA-GFP expressing cells
100
80
60
40
20
0
PB2 627E
PB2 627K

c).


PA-GFP
huANP32A-
BFP-NLS
dKO PB2 627E
dKO PB2 627K
dKO PB2 627K + huANP32A-mCHERRY
10 µm
10 µm
10 µm

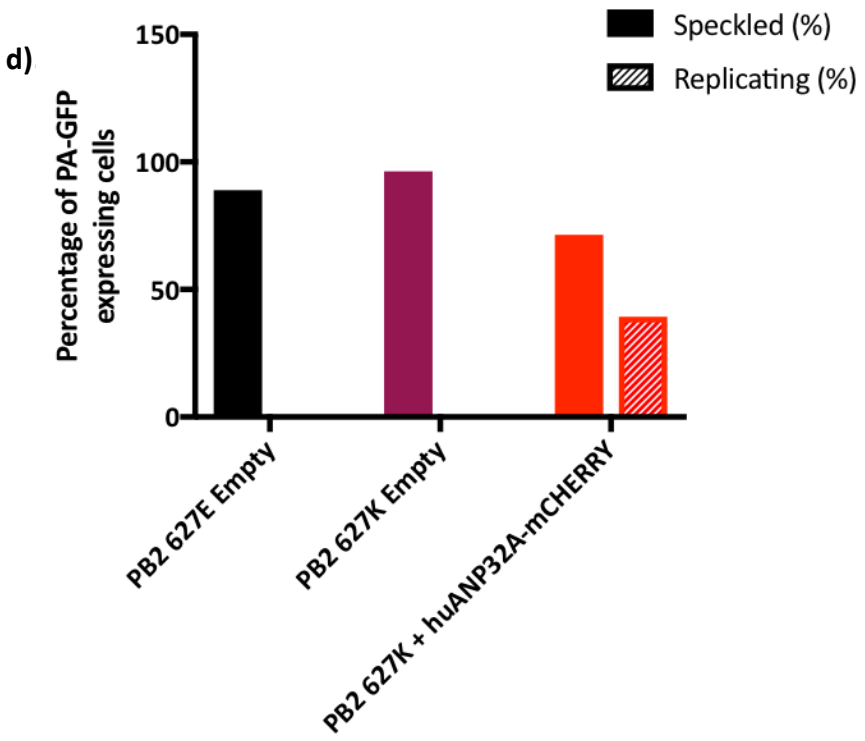
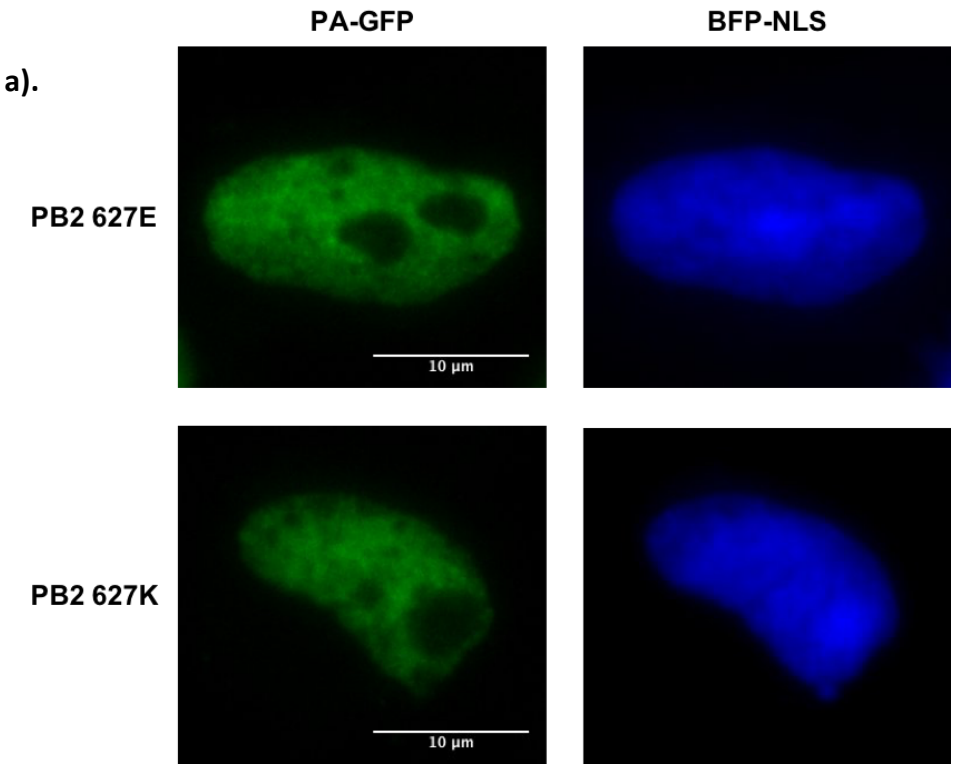


Fig 50: Influenza polymerase forms speckles in eHAP1 double knockout cells
a). Wildtype eHAP1 cells (neg) or **c).** huANP32A and -B double knockout cells were transfected with 10 ng 5092 PA-GFP, 20 ng PB1, 40 ng NP, 20 ng polI-vRNA encoding BFP-NLS and 20 ng either PB2 627E or PB2 627K. 20 ng huANP32A-mCHERRY was expressed in c). where indicated. 24 hours after transfection, cells were fixed and imaged using widefield microscopy. Prominent speckles are highlighted by white arrowheads. Scale bar is 10μm. Representative image for each condition shown. **b and d).** Percentage of speckled (solid bars) or replicating (diagonally striped bars) cells (**b**=wildtype**, d**=dko) were counted from seven random fields of view of each condition. Percentage shown is relative to total number of PA-GFP expressing cells in these fields of view. Neg: n=14 for PB2 627E, n=11 for PB2 627K. dKO: n=20 for PB2 627E, n=27 for PB2 627K, n=33 for PB2 627K + huANP32A. Results representative of one experiment.

4.2.7 Speckles in avian cells expressing the AIV polymerase form less frequently

A polymerase bearing a glutamic acid at position 627 of PB2 can function efficiently in the nucleus of avian cells. The E627K is also able to work efficiency in these cells and possesses no notable advantage over polymerase having 627E. To further explore the relationship between replication and the formation of speckles, we investigated whether any speckles could be observed in the chicken fibroblast cell line, DF-1. Transfection of DF-1 cells with a polymerase bearing either 627E or 627K resulted in a similar percentage of speckled and replicating cells as each other **(Fig 51a and b)**. The relatively small number of cells displaying polymerase activity may be due to the lower transfection efficiency of these cells. Only 8.8 % and 5.5 % of cells were speckled in DF-1 cells expressing PB2 627E or 627K polymerase, respectively. Of all the cells where efficient replication occurred, only 7 % of these were also speckled. Overall, in avian cells, where both an AIV polymerase and a polymerase with the 627K humanising mutation can carry out replication efficiently, these polymerases display the same pattern with regards to speckle formation. Although speckles can be observed in avian cells, they are only apparent in a small proportion of cells.



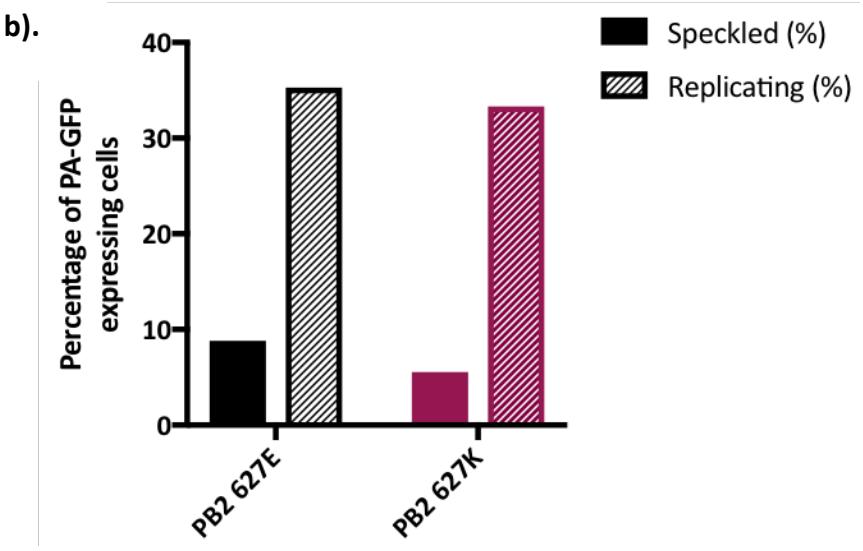


Fig 51: Speckles in avian cells are observed less frequently
a). DF-1 cells were transfected with 10 ng PA-GFP, 20 ng PB1, 40 ng NP, 20 ng polI-vRNA encoding BFP-NLS (with a chicken polymerase I promoter) and 20 ng either PB2 627E or PB2 627K. 24 hours after transfection, cells were fixed and imaged using widefield microscopy. Scale bar is 10µm. Representative image for each condition shown. **b).** Percentage of speckled (solid bars) or replicating (diagonally striped bars) cells were counted from seven random fields of view of each condition. Percentage shown is relative to total number of PA-GFP expressing cells in these fields of view. n=68 for PB2 627E, n=54 for PB2 627K. Results representative of two independent experiments.

4.2.8 The formation of speckles negatively correlates with replication efficiency directed by different PB2 mutants

Although the PB2 E627K mutation is the most common adaptive mutation in the polymerase of human adapted influenza viruses, there are also other mutations in the PB2 subunit which confer polymerase activity in human cells to different extents. Most notably, the 2009 swine flu pandemic H1N1 virus strain retained a glutamic acid at position 627. Instead, it bore GQ590/91SR and T271A mutations, which have been shown to aid polymerase activity in human cells (Bussey *et al.,* 2010; Mehle and Doudna, 2009). Since position 591 lies adjacent to 627 and arginine is positively charged, it has been proposed that this mutation may support polymerase activity through similar mechanisms as the E627K mutation (Mehle and Doudna, 2009). Other studies have revealed that the PB2 D701N mutation is also able to enhance replication in mammalian cells, probably through increased nuclear import of the polymerase (Gabriel *et al.,* 2008; Gabriel *et al.,* 2011). Finally, the PB2 E158G mutation has been shown to increase pathogenicity in mice as well as enhanced polymerase activity in mammalian cells (Zhou *et al.,* 2011). However, it has only been found in a single human isolate in nature (Zhou *et al.,* 2011).

We investigated whether these PB2 mutations affected the formation of speckles and their relationship with replication. Even though a glutamic acid was present at position 627, in cells expressing the other PB2 mutations, the proportion of speckles decreased as polymerase activity increased. Compared to wildtype, the proportion of speckled cells decreased by 57 % in cell expressing PB2 158G. The proportion of replicating cells increased by 42 %. The proportion of cells that were speckled or with active polymerase also decreased and increased, respectively, in cells expressing PB2 590/91SR or PB2 701N. Cells expressing PB2

271A saw an 8 % increase in cells expressing BFP compared to wildtype and consequently only a 7 % reduction in speckled cells **(Fig 52)**. Together, this indicates that it is not the nature of position 627 of PB2 specifically which determines the likelihood of a nucleus displaying speckles, but instead the degree of replication. Overall, we observed a negative correlation between the percentage of cells where efficient replication has occurred and the percentage of speckled nuclei observed.

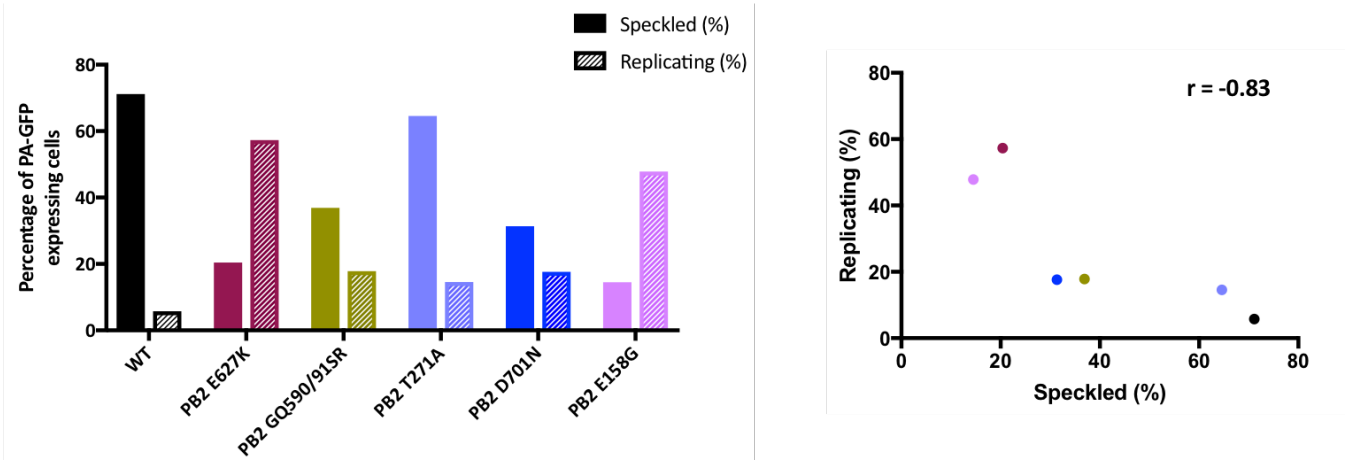


Fig 52: Other humanising mutations in PB2 affect speckle formation
HEK 293T cells were transfected with 10 ng 5092 PA-GFP, 20 ng PB1, 40 ng NP, 20 ng polI-vRNA encoding BFP-NLS and either 20 ng PB2 627E, 627K, GQ590/91SR, T271A, D701N or E158G. 24 hours after transfection, cells were fixed and imaged using widefield microscopy. Percentage of speckled (solid bars) or replicating (diagonally striped bars) cells were counted from seven random fields of view of each condition. Percentage shown is relative to total number of PA-GFP expressing cells in these fields of view. Right: data plotted as scatter plot using same colour code as in bar graph. r value calculated using Pearsons correlation. n=52 for WT, n=82 for E627K, n=84 for GQ590/9SR, n=48 for T271A, n=51 D701N, n=69 for E158G. Results representative of two independent experiments.

4.2.9 The speckles do not colocalise with previously described nuclear bodies

There are many known nuclear bodies which serve as sites for specific functions or storage of proteins (Zimber *et al.,* 2004). We investigated whether the polymerase speckles observed here colocalised with known nuclear bodies including Promyelocytic leukaemia (PML) nuclear bodies, Cajal bodies and SC-35^{+} nuclear speckles. Antibodies specific for proteins associated with each structure were obtained and immunofluorescence used to detect them along with the PA-GFP marked polymerase speckles in transfected cells. However, the IAV polymerase speckles did not colocalise with any of these nuclear structures **(Fig 53)**. It is therefore possible that either these speckles colocalise with one of the growing number of other nuclear bodies that are being discovered or perhaps they are able to form their own distinct structures.

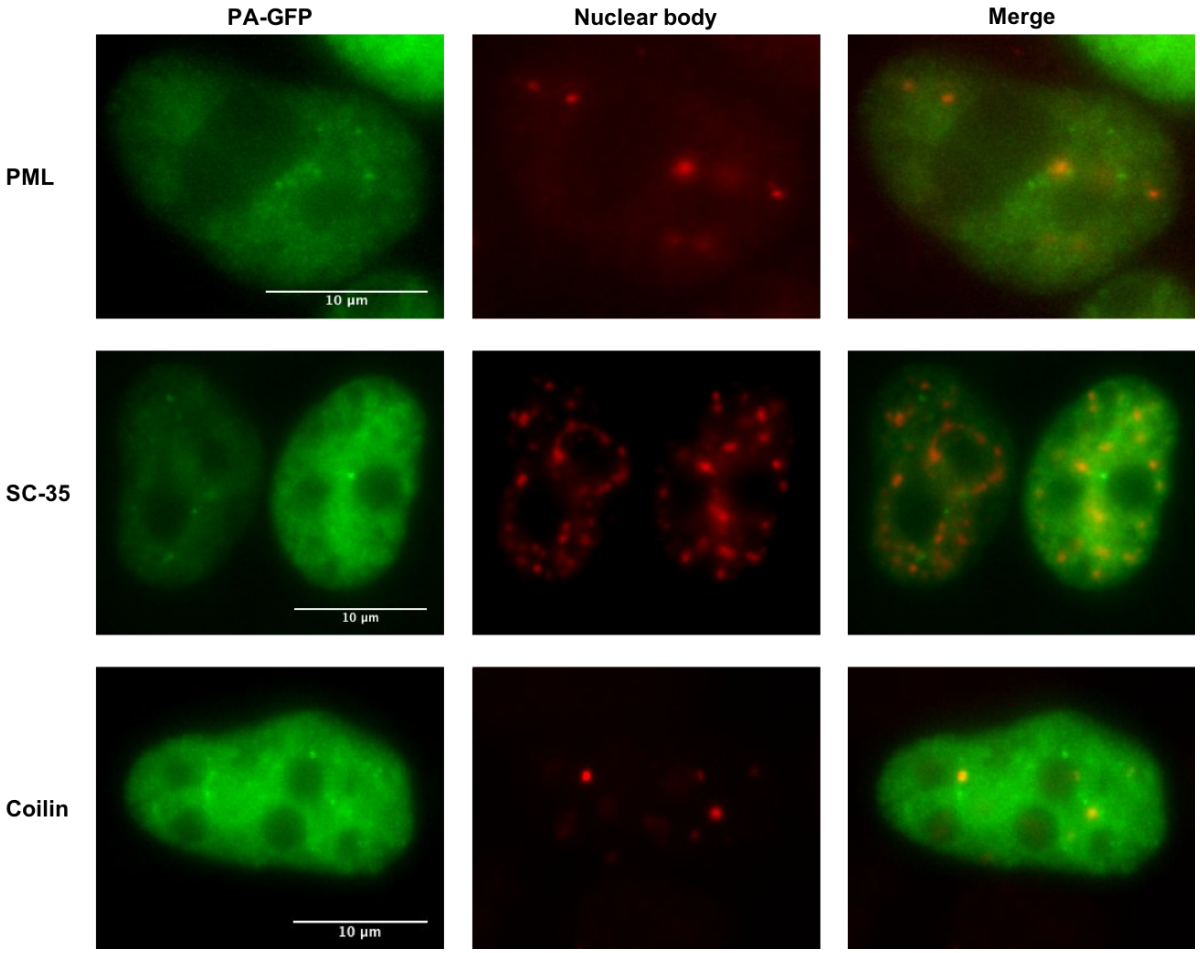


Fig 53: Polymerase speckles do not colocalise with other known nuclear bodies
a). HEK 293T cells were transfected with 10 ng PA-GFP, 20 ng PB1, 20 ng PB2 627E, 40 ng NP, 20 ng polI-vRNA encoding BFP-NLS. 24 hours after transfection, cells were fixed and permeabilised. Nuclear bodies detected using specific antibodies as indicated. Samples were imaged using widefield microscopy. Representative image for each condition shown.

4.3 Discussion

The AIV polymerase is not restricted *in vitro,* suggesting that the restriction seen in mammalian cells is due to interactions with host factors and/or is affected by the spatial distribution of the polymerase within the cell (Aggarwal *et al*., 2011; Nilsson *et al.,* 2017). The aim of this chapter was to investigate whether any differences between a PB2 627E viral polymerase and that with the PB2 E627K mutation could be visualised in the nucleus of human cells. We observed the formation of speckles in nuclei expressing a PB2 627E viral polymerase. These were seen only rarely in cells expressing a PB2 627K viral polymerase. Addition of chANP32A-mCHERRY, but not huANP32A-mCHERRY resulted in dispersal of the speckles formed by the PB2 627E viral polymerase. In avian cells where the PB2 627E polymerase is active, the speckles occurred rarely and independently of the nature of the residue at position 627 of PB2. Furthermore, speckles were observed frequently in human cells expressing PB2 627K polymerase that lacked expression of huANP32A and -B. Other humanising PB2 mutations also affected the frequency of speckled nuclei. Altogether, we observed a negative correlation between the formation of speckles and the ability of the viral polymerase to carry out replication.

These speckles were detected by transfection of viral polymerase components including PA-GFP. They were not as easily detected when using antibodies against viral proteins. This may

explain why these speckles have not been previously detected despite many studies in the literature in which imaging of the viral polymerase has been carried out. The speckles observed are unlikely to be an artefact of PA-GFP expression since their detection was determined by the nature of the PB2 subunit.

The speckles observed in these studies may represent oligomers of polymerase complexes. Given its size, the diffusion rate of the trimeric polymerase in the nucleus of human cells was predicted to be much faster than that measured (Huet *et al.,* 2010). This suggests that the polymerase may be bound to host factors or form oligomers or both. Indeed, several studies have demonstrated oligomerisation of the polymerase complex (Chang *et al.,* 2015; Digard *et al.,* 1989; Huet *et al.,* 2010; Jorba *et al.,* 2008a). Interestingly, Huet *et al.,* demonstrated that higher order structures were formed mostly by oligomerisation of the trimeric polymerase complex rather than when individual polymerase subunits or if combinations of two of the subunits were expressed (Huet *et al.,* 2010). In line with this, we discovered that the trimeric polymerase complex was the minimum requirement for the formation of speckles. Speckles could not be observed by expressing the PA-GFP -PB1 dimer or PB2-GFP alone.

The higher order structures detected by Huet *et al.,* represented only a fraction of the population, indicating that many of the polymerase subunits did not oligomerise (Huet *et al.,* 2010). Although speckles could be observed in human cells expressing AIV polymerase, the PA-GFP was not confined to these areas and was found dispersed around the nucleus. The dispersed PA-GFP may represent PA-GFP -PB1 dimers which have not bound to PB2 and therefore would not be displaying the speckled phenotype. Alternatively, perhaps not all of the trimeric polymerase complexes are bound in the putative higher order structures. The

existence of polymerase complexes not located in speckles may explain why replication was apparent in some nuclei where speckles could also be observed.

It has previously been suggested that the restriction of AIV polymerase in human cells is due to an inhibitory factor (Mehle and Doudna, 2008). In line with this, using FRAP experiments, the mobility of a 50-92 PB2 627E containing polymerase was shown to be slower than that harbouring PB2 627K (Foeglein *et al.,* 2011). This may be a consequence of specific interactions between the PB2 627E polymerase and an inhibitory host factor. The speckles observed in this study did not colocalise with any of the nuclear bodies tested. It is possible that they may colocalise with a different nuclear body or form distinct domains of their own. Other proteins such as the murine Mx1, which inhibits influenza A replication in mice, have previously been shown to form distinct domains in the nucleus (Engelhardt *et al.,* 2004). Although the human homologue of this protein, MxA, is cytoplasmic, other inhibitory factors may be present in the speckles observed in this study. One candidate for this inhibitory factor is DDX17. Compared to PB2 627K, greater co-precipitation of PB2 627E with DDX17-flag was detected (Bortz *et al.,* 2011). Furthermore, siRNA mediated knockdown resulted in upregulation of avian origin polymerase activity in human cells, but not that with PB2 627K (Bortz *et al.,* 2011). The factors shown to decrease in co-precipitation with PB2 627E polymerase in chapter 3 may also be potential inhibitory factors. For example, the chaperone protein, DNAJC7 identified in the screen co-precipitated with the PB2 627E polymerase but not when chANP32A was expressed or when the polymerase harboured the PB2 E627K mutation. This factor has been identified in other influenza proteomic screens (Rialdi *et al.,* 2017; Wang *et al.,* 2017; Watanabe *et al.,* 2014; York *et al.,* 2014) and also acts as a co-

chaperone for HSP70, which has been demonstrated to inhibit influenza virus replication (Li *et al.,* 2011).

In DF-1 cells, where the PB2 627E polymerase is able to replicate, the number of speckled nuclei observed was low regardless of the nature of the amino acid at position 627. Other human adaptive PB2 mutations aside from PB2 E627K, also affected the proportion of speckles in human cells and this was negatively correlated with how well the polymerase was able to replicate. Since the trimeric polymerase was discovered to be the minimum requirements for the formations of speckles, dispersion of speckles is unlikely to be a consequence of replication, but instead perhaps the formation of speckles dictates the ability of the polymerase to replicate. The activity of influenza polymerase with various humanising mutations in PB2 also correlated with the mobility of the polymerase (Foeglein *et al.,* 2011). It is possible that these two observations are connected. The speckles may represent polymerases which are bound to an inhibitory factor, slowing their diffusion and consequently resulting in reduced polymerase activity.

Another hypothesis for the formation of speckles is that they may be a consequence of not being able to bind sufficiently to a positive factor which could take the polymerase to the appropriate place in the nucleus. chANP32A is able to support the activity of the AIV polymerase, but huANP32A cannot (Long *et al.,* 2016). The frequency of speckles in cells expressing the AIV polymerase decreased upon expression of chANP32A-mCHERRY, but not huANP32A-mCHERRY. Furthermore, the LCAR truncated mutant, chANP32A 1-208, which can sub-optimally support AIV polymerase activity decreased the proportion of speckled cells but not to the same degree as full length chANP32A. In the absence of huANP32A and -B, the proportion of speckles in cells expressing the PB2 627K polymerase increased compared to

controls. It is unclear whether ANP32A is directly related to the formation of the speckles. Whether other PB2 humanising mutations allow the polymerase to co-opt huANP32A or -B also remains to be established.

Existence of both an inhibitory factor and stimulatory factor are not mutually exclusive. The formation of speckles may be transient and perhaps all polymerases form speckles at some stage, but a PB2 627E polymerase remains within these structures for longer. This could explain why some speckles were also found in cells expressing PB2 627K, but at a lower frequency than those expressing PB2 627E. The viral polymerase may be bound to an inhibitory factor or an immobile nuclear substructure. Failure to associate co-operatively with a stimulatory factor by an un-adapted polymerase would prevent it from being able to co-opt this factor, either by directly stimulating polymerase activity or transporting the polymerase into a region within the nucleus where it is able to carry out replication.

To summarise, we have observed speckles that the contain influenza polymerase complex in the nuclei of cells expressing the PB2 627E polymerase. These are observed less frequently in cells expressing the PB2 627K polymerase. Although ANP32A can affect the frequency of speckles detected in nuclei, it is unclear whether ANP32A is directly involved with the formation of these speckles. What is apparent is that the formation of speckles negatively correlates with polymerase activity Further investigation into the components of these speckles will aid understanding into the mechanisms by which the AIV polymerase is restricted in human cells.

Chapter 5: Discussion and summary

Influenza A is responsible for seasonal epidemics as well as occasional pandemics and as such represents a significant burden on both health and the economy. The natural reservoir of influenza A is wild aquatic birds. For successful zoonosis, the virus must acquire mutations in its genome which adapt it to the new host. The restriction in activity of an unadapted viral polymerase represents one of the main barriers determining host range. Adaptions such as the well studied PB2 E627K mutation allow the viral polymerase to overcome this restriction (Subbarao *et al.,* 1993). Why the avian origin polymerase is restricted and how specific mutations in the polymerase are able to overcome this restriction has eluded scientists for decades. When this study began, species differences in ANP32A were identified as being determinants for host range of influenza (Long *et al.,* 2016). Avian ANP32A can be co-opted by an avian or human adapted polymerase, whereas huANP32A can only be co-opted by a viral polymerase with humanising mutations (Long *et al.,* 2016; Long *et al., in* press; Sugiyama *et al.,* 2015; Zhang *et al.,* 2019). This study explored how ANP32A proteins are able to support the viral polymerase, why an avian origin polymerase is not able to co-opt huANP32A and how adaptive mutations in the polymerase enable it to be able to utilise huANP32A. To do this, we studied interactions between ANP32A and the viral polymerase (chapter 2), interactomes of the viral polymerase in the presence and absence of chANP32A (chapter 3) and the subcellular localisation of viral polymerases with various mammalian adaptions (chapter 4).

chANP32A harbors an avian specific 33 amino acids between its LRR and LCAR domains. These 33 amino acids are present in all avian species excluding ratites (which select for mammalian adaptions in the polymerase) and are vital for supporting activity of an influenza polymerase of avian origin (Long *et al.,* 2016). chANP32A was found to be responsible for supporting the activity of both avian and mammalian adapted polymerases in avian cells (Long *et al., in press;* Zhang *et al.,* 2019). Mammalian adapted polymerases are able to utilize shorter versions of ANP32 such as huANP32A and huANP32B (Long *et al.,* 2016; Sugiyama *et al.,* 2015). Interestingly, swine ANP32A, which does not contain the 33 amino acids, was shown to partially support the activity of a H7N9 virus harboring PB2 627E suggesting that swine ANP32A may enable pigs to act as an intermediate for influenza A between avian and human hosts and may be one reason why pigs are susceptible to infection from both avian and human adapted viruses (Zhang *et al.,* 2019). However, it is not only the 33 amino acids which determine whether ANP32 can support polymerase activity. 129N and 130D in the LLR domain were shown to be important for function. chANP32B which does not have the 33 amino acid insertion and also harbors 129I and 130N cannot support function of either avian or mammalian adapted viral polymerases (Long *et al., in press*; Zhang *et al.,* 2019). Murine ANP32A, which has 130A also does not support activity of influenza A polymerase (Zhang *et al.,* 2019). Instead, influenza A is able to replicate in murine cells by co-opting murine ANP32B, which harbors 130D (Staller *et al., in review*). Overall, ANP32 proteins appear to be essential for the replication of influenza A virus and therefore it is likely that species differences between these proteins drive adaptations in the polymerase.

ANP32A is able to interact with the influenza A polymerase regardless of the identity of position 627 of PB2 **(Fig 22)** (Domingues and Hale, 2017). Removal of the 33 amino acids or

the LCAR domain from chANP32A both resulted in reduced interactions **(Fig 21b)**. N129I and D130N mutations in the LRR domain of chANP32A have also recently been shown to reduce binding to viral polymerase (Long *et al., in press*; Zhang *et al* 2019). Although to differing extents, all of these modifications to chANP32A affect the function of the polymerase suggesting that binding of chANP32A is important for optimal polymerase function **(Fig 21c)** (Long *et al., in press*; Zhang *et al* 2019).

Sugiyama *et al.,* have demonstrated that huANP32A and -B enhance synthesis of vRNA from a cRNA template *in vitro,* but had little effect on synthesis of cRNA from vRNA templates in the same assay (Sugiyama *et al.,* 2015). As mentioned, vRNA synthesis differs from cRNA synthesis primarily by its mechanism of initiation (a prime and realign method where the ApG primer is synthesised at positions 4 and 5 and translocated back to positions 1 and 2) and also due to the requirement of either *trans*-acting or *trans*-activating polymerases (Deng *et al.,* 2006; Jorba *et al.,* 2009; York *et al.,* 2013). In line with this, we and others have shown that the interactions between ANP32A increase at inactive RNPs **(Fig 24)** (Baker *et al.,* 2018). The role of ANP32A in supporting the polymerase may therefore be to promote initiation, possibly through recruitment of a *trans*-acting or *trans*-activating polymerase. Since the polymerase can adopt multiple conformations (Hengrung *et al.,* 2015; Pflug *et al.,* 2014; Reich *et al.,* 2014; Reich *et al.,* 2017; Thierry *et al.,* 2016), binding to ANP32A may stabilise a specific conformation necessary for initiation. However, it is not clear why interactions between inactive polymerase and ANP32A increase in the presence of both v- and cRNA if huANP32A supports synthesis of vRNA from cRNA templates specifically.

When the polymerase is active, we observed a decrease in interaction between chANP32A and PB2 627E polymerase as well as huANP32A and PB2 627K polymerase **(Fig 25b and c)**. This suggests that the interaction is transient, but the precise time during replication that ANP32A dissociates is unclear. huANP32A does not dissociate from an AIV polymerase under the same conditions **(Fig 25d)**. Since huANP32A cannot support the activity of this polymerase, this may cause the huANP32A:PB2 627E polymerase interaction to remain intact. Alternatively, the lack of dissociation of huANP32A may lock the polymerase in an unfavourable conformation and consequently render it unable to support the activity of the AIV polymerase. In contrast, the PB2 E627K mutation may allow huANP32A to interact with the polymerase in a cooperative manner.

G3A, U5C and C8U mutations in the 3' vRNA can also overcome the restriction of AIV polymerase in human cells (Crescenzo-Chaigne *et al.,* 2002; Neumann and Hobom, 1995). This further suggests that the way in which the viral polymerase binds to viral RNA is important for function. Synthesis from a vRNA template containing 3' G3A, U5C and C8U mutations results in cRNA with a 5' promoter mirroring that of the 5' vRNA promoter. The crystal structures of influenza B bound to 5' vRNA differ from that bound to 5' cRNA (Thierry *et al.,* 2016). Furthermore, structural studies on bunyavirus polymerase, which functions similarly to that of influenza polymerase, demonstrate that binding of 5' vRNA induces changes in the active site of the polymerase by an allosteric mechanism (Gerlach *et al.,* 2015). chANP32A does not further potentiate the synthesis of this mutated RNA by the AIV polymerase (Baker *et al.,* 2018) and yet we showed that huANP32A and -B were still absolutely necessary for the activity of this polymerase **(Fig 26)**. This could suggest that mutations within the promoter of influenza viral RNA may promote a favourable conformation of the AIV polymerase, perhaps

overcoming the locked conformation imposed by huANP32A as suggested in the previous paragraph. This may instead allow the AIV polymerase to successfully co-opt huANP32A as a human adapted polymerase would.

It is important to note that how ANP32A supports viral polymerase function and how chANP32A is able to overcome the restriction imposed on the avian origin polymerase in human cells are two separate questions. Although it is likely that both ch- and huANP32A have similar mechanisms by which they support the viral polymerase, it seems likely that chANP32A has additional roles. The 33 amino acids and in particular the first four of these, as well as regions within the LRR domain are most important for function **(Fig 21c)** (Domingues and Hale, 2017; Long *et al., in press*; Zhang *et al.,* 2019). The important regions for function in the LRR domain are conserved between ch- and huANP32A and therefore are likely important for the role in supporting the viral polymerase. However, the 33 amino acids unique to chANP32A are important for overcoming the restriction imposed on an avian origin polymerase in human cells (Long *et al.,* 2016).

The discovery that chANP32A 1-208 could support the activity of the viral polymerase despite no detectable binding to the apo-polymerase was an intriguing find **(Fig 21)**. Whether binding can be detected between chANP32A 1-208 and the AIV polymerase in the presence of viral RNA will be important to investigate. In the presence of viral RNA, it may bind sufficiently to polymerase and function to stabilise a particular conformation as described above. Strong binding may not be absolutely necessary for function and this is further supported by the fact the PB2 E627K mutation did not significantly increase interactions with huANP32A, even though this human adapted polymerase is able to utilise huANP32A for its activity **(Fig 22)**.

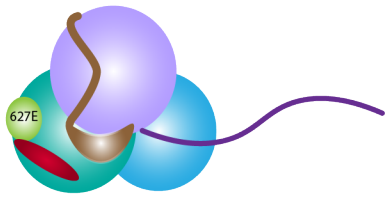
Alternatively, one could speculate that the way in which chANP32A 1-208 is able to overcome the restriction on AIV does not require it to bind to the viral polymerase at all. chANP32A 1-208 harbours the avian specific 33 amino acids important for function. The interaction between chANP32A and the AIV polymerase significantly decreased upon removal of the PB2 627 domain **(Fig 20a).** The interaction between AIV polymerase and huANP32A, which does not harbour this 33 amino acid insertion, was unaffected by the removal of the 627 domain **(Fig 20a and c)**. This is in line with a previous study which reported that PB2 residues 307-534, which are not within the 627 domain, were required for interaction with huANP32A (Wei *et al.,* 2019). In addition, we found a significant increase in binding to the viral polymerase was measured with chANP32A, but not huANP32A, upon mutation of PB2 residue 627 to lysine **(Fig 22a and d)**. Altogether, this suggests that binding of the 33 amino acids in chANP32A, to the polymerase, involves the 627 domain.

The role of the avian specific 33 amino acid insertion in chANP32A may be to prevent or alter binding of an inhibitory factor bound to the AIV polymerase due to PB2 627E **(Fig 54** second row**)**. In fact, the existence of an inhibitory factor has previously been suggested to account for the restriction on the PB2 627E polymerase in human cells (Mehle and Doudna, 2008). The LCAR domain of ANP32A is most important for binding to the viral polymerase **(Fig 21)** (Domingues and Hale, 2017; Wei *et al.,* 2019). chANP32A 1-208 does not contain the LCAR, but does harbour the avian specific 33 amino acids. chANP32A 1-208 may therefore support activity of the AIV polymerase, not by binding to the polymerase, but instead by binding to the inhibitory factor, preventing this factor from interacting with the polymerase. Free from inhibition, the AIV polymerase may be able to utilise other host factors to support its activity, perhaps even huANP32A **(Fig 54** third row**)**. Further support of this hypothesis comes from an

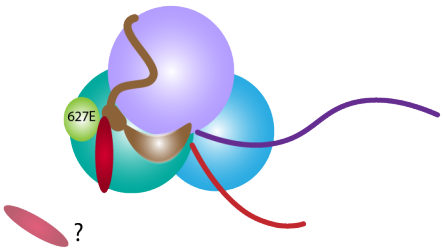
experiment where viral polymerase bearing either PB2 627E or 627K was pre-expressed in human cells, followed by infection of these cells with either a PB2 627E or PB2 627K virus in the presence of cycloheximide. Using this method, Mänz *et al* were able to demonstrate that a viral polymerase harbouring PB2 627E was capable of vRNA synthesis in human cells from intact cRNA templates (Mänz *et al*., 2012). As mentioned, it is vRNA synthesis which huANP32A and -B have been implicated in (Sugiyama *et al.,* 2015).

The PB2 E627K mutation may allow escape from inhibition by this putative factor altogether. Alternatively, it may alter the way in which it is bound to the polymerase to promote a more favourable orientation **(Fig 54** bottom row**)**. In line with this, human host factors implicated in host range of influenza such as DDX17 have previously been shown to bind to both a PB2 627E and PB2 627K polymerase (Bortz *et al.,* 2011). DDX17 was also identified as a factor interacting with polymerase in the mass spectrometry experiment carried out in chapter 3 (Appendix A). DDX17 inhibits the PB2 627E polymerase, but supports the activity of the PB2 627K polymerase in human cells (Bortz *et al.,* 2011). In other words, it may not be binding of the factor per se that makes it inhibitory, but rather the orientation in which it is bound. In the correct orientation, this factor could support the polymerase. In the model presented here, chANP32A 1-208 would prevent binding of this factor to the polymerase altogether, rather than change it to a supportive orientation. This might explain why although chANP32A 1-208 can support activity of the AIV polymerase, polymerase activity is not optimal.

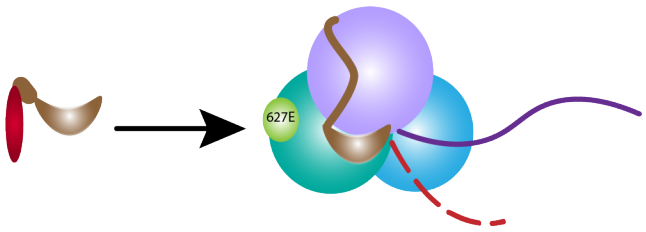
PB2 627E
+ huANP32A



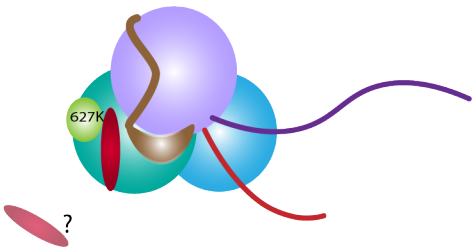
PB2 627E
+ chANP32A



PB2 627E
+ chANP32A 1-208



PB2 627K
+ huANP32A



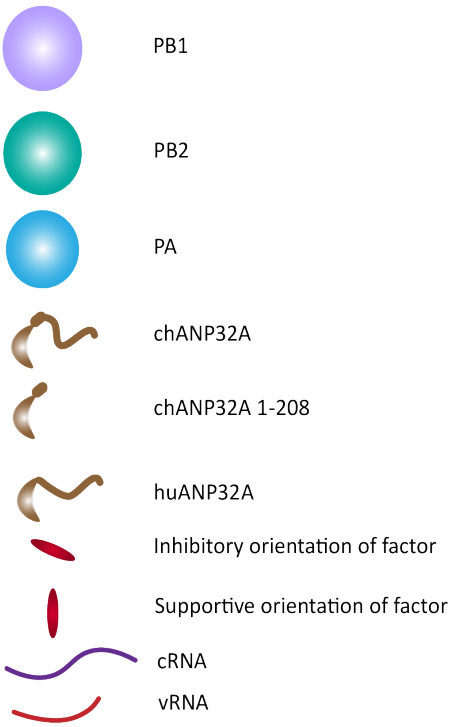


Fig 54: Model for the role of the avian specific 33 amino acids in chANP32A in preventing inhibition of AIV polymerase. Top: the PB2 627E polymerase is restricted in human cells due to an inhibitory factor. Second: chANP32A can change the orientation of the factor or possibly displace it. In the different orientation the factor supports PB2 627E polymerase activity. Third: chANP32A 1-208 binds the inhibitory factor with its avian specific 33 amino acids preventing it from binding to the PB2 627E polymerase. Free from inhibition, the polymerase can then utilise other host factors such as huANP32A to support its activity. Since the factor is not bound to the polymerase in the positive orientation, polymerase activity is sub-optimal. Bottom: The PB2 E627K mutation alters the orientation of the factor into a supportive orientation, or perhaps does not bind to this factor at all.

Further evidence for an inhibitory factor comes from chapter 4. We observed speckles in the nuclei of human cells transfected with an avian origin polymerase **(Fig 45)**. Although the trimeric polymerase complex was the minimal requirement for formation of the speckles, this does not exclude the possibility that NP and viral RNA are also within these structures. The formation of theses speckles negatively correlated with polymerase activity suggesting that dispersal of viral polymerase from these speckles is necessary for optimal replication. These speckles could be dispersed upon expression of chANP32A-mCHERRY, but not huANP32A-mCHERRY, suggesting that the avian specific 33 amino acids of chANP32A were involved in this **(Fig 47)**.

The identity of the putative inhibitory factor remains unknown. The proteins identified in **Fig 34c** highlight potential candidates since these proteins co-precipitated with an AIV polymerase and this co-precipitation was reduced in the presence of chANP32A. Examples include DNAJC7, which as mentioned in section 4.3 acts as a co-chaperone for HSP70, which has been shown to inhibit influenza replication (Li *et al.,* 2011). IFIT5 is another potential candidate. IFIT family members have been demonstrated to restrict a number of viruses including West Nile virus, vesicular stomatitis virus and influenza virus (reviewed in Fensterl

and Sen, 2015). Although humans express four evolutionary conserved members of the family, only IFIT5 is present in birds. Recent studies have demonstrated that stable expression of chicken IFIT5 in chicken fibroblasts or transgenic chicken embryos reduced Influenza A replication, whereas knocking out this gene increased viral replication (Santhakumar *et al.,* 2018). Overexpression of human IFIT5 was also able to suppress influenza A replication in chicken fibroblasts (Santhakumar *et al.,* 2018). IFIT5 recognises 5'triphosphate groups on single stranded RNA and although primarily found in the cytoplasm where it blocks translation, duck IFIT5 was shown to also localise in the nucleus suggesting it may also have other functions (Wang *et al.,* 2015).

PB2 E627K is not the only mutation which is able to overcome the restriction on an avian origin polymerase in mammalian cells. Most notably, the 2009 pandemic H1N1 virus retained 627E, but instead GQ590/91SR mutations were acquired, which enabled polymerase activity in human cells (Mehle and Doudna, 2009). Furthermore, Mänz *et al.,* were able to identify other polymerase stimulatory mutations, most of which were located near the RNA exit channel of the polymerase (Mänz *et al.,* 2016). In chapter 4 we assessed the effect of other PB2 mutations (T271A, GQ590/91SR, D701N and E158G) on the formation of speckles **(Fig 52)**. We found a negative correlation between the formation of speckles and the activity of the polymerase. This observation is reminiscent of a study by Foeglein *et al.,* who demonstrated that polymerase activity was correlated with the mobility of viral polymerase in human cells (Foeglein *et al.,* 2011).

Position 591 of PB2 lies adjacent to 627 and therefore these mutations may promote polymerase activity by the same mechanism (Mehle and Doudna, 2009). Position 701 is close to this region and lies within the PB2 627-NLS domain. This mutation was shown to disrupt a

salt bridge formed between D701 and R753 within the NLS, favoring enhanced binding to importin α and subsequently increased nuclear import (Taredeau *et al.,* 2007). Whether there are any other consequences of the D701N mutation is unknown. Position 271 and 158 are not within this region and therefore it is possible that these mutations adapt the polymerase to mammalian cells in different ways. All of these mutations are located on the surface of the polymerase complex and therefore all may bind to host factors. If the aim is to facilitate polymerase activity by stabilizing a specific conformation of the viral polymerase or alter binding of another host factor to the polymerase, it is possible that mutations located at different regions on the polymerase could achieve the same outcome, but perhaps via different strategies.

In chapter 3, we also identified putative positive factors which may support the influenza A polymerase. Further characterization of SRPK1 and importin α7 demonstrated that shRNA mediated silencing of these proteins results in decreased viral polymerase activity **(Fig 39 and Fig 44d)**. Importin α7 has previously been implicated in host range of influenza (Hudjetz *et al.,* 2012). A specific interaction between importin α and the PB2 NLS is required for viral polymerase activity (Resa-Infante *et al.,* 2008). The PB2 NLS has also been identified as a flexible region of the polymerase which is subject to large conformational shifts (Thierry *et al.,* 2016). Binding of importin α7 may therefore stabilize a specific conformation of the polymerase. A conserved phosphorylation site in the PB2 NLS has been identified (Hutchinson *et al.,* 2012). Whether phosphorylation of this site is carried out by SRPK1 or a different kinase is unknown. Phosphorylation at this site could regulate importin α7 binding and consequently viral polymerase activity. Whether importin α7 or SRPK1 are linked to the function of ANP32A is unclear.

Influenza A is a fast-evolving virus and therefore the threat of a novel virus gaining the ability to sustain transmission between humans is constant. An understanding of the mechanisms of viral replication in human cells, why certain viruses are restricted and how adaptive mutations enable them to overcome this restriction is therefore key to enabling an assessment of potential threats and the development of novel therapeutics to treat infection. Current treatments include neuraminidase inhibitors (oseltamivir, zanamivir and peramivir), M2 ion channel inhibitors (amantadine and rimantadine) and viral polymerase endonuclease activity inhibitors (baloxavir marboxil). Since these compounds all target viral proteins, mutations in the viral genome can be quickly acquired due the error prone viral polymerase, resulting in resistance. Indeed, resistant strains have emerged (Hussain *et al.,* 2017). Targeting host proteins may therefore be a favourable option. huANP32A and -B are essential for the replication of influenza A virus in human cells (Staller *et al., in review;* Zhang *et al.,* 2019). In this study, we developed a split luciferase complementation assay to measure interactions between ANP32A and the influenza polymerase (chapter 2). This has subsequently been used to screen for drugs which could inhibit this interaction with the hypothesis that they would also display antiviral activity due to decreased polymerase activity. A library of FDA approved drugs was acquired and the screen carried out by another lab member simultaneously with the studies presented here. Several compounds that could decrease the ANP32A:polymerase interaction were identified and these also showed a deleterious effect on the activity of the viral polymerase and on virus replication (Jocelyn Schreyer). The consequences of targeting host proteins as an antiviral strategy during virus infection are not clear since ANP32 proteins are important for a healthy cell. On the one hand mice that lack ANP32A have been generated and are viable (Opal *et al*., 2004), but the loss of ANP32B in mice appears to be deleterious or lethal depending on background strain (Reilly *et al*., 2011). huANP32A and -B have been

demonstrated to be redundant in their function in supporting viral polymerase activity and so compounds which target both of these proteins would be advantageous (Staller, *in review;* Zhang *et al.,* 2019). Murine ANP32B was shown to be the only murine ANP32 orthologue to be co-opted by influenza A polymerase (Staller, *in review*). Although knocking out ANP32B was demonstrated to be lethal in mice (Reilly *et al*., 2011), the recent development of conditional knockout mice lacking ANP32B may be able a useful tool to give insight into the role of ANP32B in viral infection *in vivo* (Chemnitz *et al.,* 2019).

In summary, we have characterised interactions between ANP32A proteins and the viral polymerase as well as explored deeper into why the viral polymerase is restricted and which human proteins it co-opts to support its activity. ANP32A can interact with the viral polymerase. This interaction increases at RNPs and decreases under conditions in which the polymerase is active. However, binding patterns alone are not sufficient to understand why the AIV polymerase is unable to co-opt huANP32A. It is possible that other host factors are involved in this process. We have identified human host proteins which bind to the viral polymerase in the presence and absence of chANP32A and further characterised SRPK1 and importin α7. Finally, we observed speckles in the nuclei of human cells, which negatively correlated with viral polymerase activity. Altogether, this study has provided insights into the mechanism by which ANP32A is able to support the activity of the polymerase furthering our understanding of influenza replication and host restriction.

Chapter 6 Materials and Methods

6.1 Materials

6.1.1 Cell lines

Cells	Notes	Source
HEK 293T	Human embryonic kidney cells expressing large T antigen of SV40	ATCC
eHAP1	Engineered haploid cells derived from Male chronic myelogenous leukaemia cell line- KBM7	Horizon Discovery
DF-1	Chicken fibroblast cell line	ATCC

Table 5: Cell lines used in this study

6.1.2 Antibodies

Antibody	Application	Source
Rabbit polyclonal anti-influenza A PB1	WB: 1:1000	ThermoFisher Scientific #PA5-34914

Rabbit polyclonal anti-influenza A PB2	WB: 1:4000 IF: 1:2000	GeneTex #GTX125926
Rabbit polyclonal anti-influenza A PA	WB: 1:1000	ThermoFisher Scientific #PA5-32223
Mouse monoclonal anti-FLAG M2	WB: 1:1000 IF: 1:1000	Sigma-Aldrich #F1804
Rabbit polyclonal anti-influenza NP	WB: 1:1000	Paul Digard (University of Edinburgh)
Mouse monoclonal anti-karyopherin α6 (importin α7)	WB: 1:1000	Santa Cruz Biotechnology #sc-390055
Mouse monoclonal anti-Srpk1	WB: 1:8000	BD Transduction Laboratories #611072
Rabbit polyclonal anti-Gaussia luciferase	WB: 1:1000	NEB #E8023
Rabbit polyclonal anti-PML	IF: 1:1000	Abcam #ab53773
Mouse monoclonal anti-Coilin	IF: 1:1000	Sigma-Aldrich #C1862
Mouse monoclonal anti-SC-35	IF: 1:1000	Abcam

		#ab11826
Rabbit monoclonal anti-Vinculin	WB: 1:1000	Abcam #EPR8185
Rabbit polyclonal anti-αTubulin	WB: 1:2000	Abcam #ab4074

Table 6: Primary antibodies used in this study

Antibody	**Application**	**Source**
Sheep polyclonal anti-Rabbit IgG, HRP	WB 1:20000	EMD Millipore #AP510P
Goat polyclonal anti-Mouse IgG, HRP	WB 1:10000	BioRad #STAR11P
Goat polyclonal anti-Mouse IgG (H+L), Alexa Fluor 488	IF: 1:1000	ThermoFisher Scientific #A11001
Goat polyclonal anti-Rabbit IgG (H+L), Alexa Fluor 594	IF: 1:1000	ThermoFisher Scientific #A11012
Goat polyclonal anti-Rabbit IgG (H+L), Alexa Fluor 647	IF: 1:1000	ThermoFisher Scientific #A21245

Goat polyclonal anti-Mouse IgG (H+L), Alexa Fluor 647	IF: 1:1000	ThermoFisher Scientific #A21235

Table 7: Secondary antibodies used in this study

6.1.3 Plasmids

Plasmid	Notes	Source
pCAGGS-50-92-PB1		Barclay lab
pCAGGS-50-92-PB1 D446Y	Expression plasmid encoding catalytic mutant of PB1	Anna Cauldwell (Barclay lab)
pCAGGS-50-92-PB2		Barclay lab
pCAGGS-50-92-PB2 E627K	Expression plasmid encoding PB2 with mammalian adaption	Barclay lab
pCAGGS-50-92-PB2 GQ590/91SR	Expression plasmid encoding PB2 with mammalian adaption	Anna Cauldwell (Barclay lab)
pCAGGS-50-92-PB2 T271A	Expression plasmid encoding PB2 with mammalian adaption	Anna Cauldwell (Barclay lab)
pCAGGS-50-92-PB2 D701N	Expression plasmid encoding PB2 with mammalian adaption	Anna Cauldwell (Barclay lab)

pCAGGS-50-92-PB2 E158G	Expression plasmid encoding PB2 with mammalian adaption	Anna Cauldwell (Barclay lab)
pCAGGS-50-92-PB2-GFP	Expression plasmid encoding PB2 tagged with GFP	Hayley Loy (Barclay lab)
pCAGGS-50-92-PB2 E627K-GFP	Expression plasmid encoding PB2 with mammalian adaption tagged with GFP	Hayley Loy (Barclay lab)
pCAGGS-50-92-PB2Δ535-667	Expression plasmid encoding PB2 lacking 627 domain	Jocelyn Schreyer (This study)
pCAGGS-50-92-PA		Barclay lab
pCAGGS-50-92-PA-GFP	Expression plasmid encoding PA tagged with GFP	Hayley Loy (Barclay lab)
pCAGGS-50-92-NP		Barclay lab
pCAGGS-Vic75-PB1		Barclay lab
pCAGGS-Vic75-PB2		Barclay lab
pCAGGS-Vic75-PB2 K627E	Expression plasmid encoding PB2 K627E mutation	Barclay lab
pCAGGS-Vic75-PA		Barclay lab
pCAGGS-Vic75-NP		Barclay lab

pCAGGS-UDL-PB1		Barclay lab
pCAGGS-UDL-PB2		Barclay lab
pCAGGS-UDL-PB2 E627K	Expression plasmid encoding PB2 with mammalian adaption	Barclay lab
pCAGGS-UDL-PA		Barclay lab
pCAGGS-UDL-NP		Barclay lab
pCAGGS-Tky05-PB1		Barclay lab
pCAGGS-Tky05-PB2		Barclay lab
pCAGGS-Tky05-PA		Barclay lab
pCAGGS-Tky05-NP		Barclay lab
pCAGGS-Eng195-PB1		Barclay lab
pCAGGS-Eng195-PB2		Barclay lab
pCAGGS-Eng195-PA		Barclay lab
pCAGGS-Eng195-NP		Barclay lab
pCAGGS-WSN-PB1		AJ te Velthuis (University of Cambridge)

pCAGGS-WSN-PB2		AJ te Velthuis (University of Cambridge)
pCAGGS-WSN-PA		AJ te Velthuis (University of Cambridge)
pCAGGS-WSN-NP		AJ te Velthuis (University of Cambridge) AJ te Velthuis (University of Cambridge)
pcDNA3-WSN-PB1		AJ te Velthuis (University of Cambridge)
pcDNA3-WSN-PB2		AJ te Velthuis (University of Cambridge)
pcDNA3-WSN-PA		AJ te Velthuis (University of Cambridge)
pcDNA3-WSN-NP		AJ te Velthuis (University of Cambridge)
pCAGGS-chANP32A		Jason Long (Barclay lab)
pCAGGS-huANP32A		Jason Long (Barclay lab)

pCAGGS-chANP32A-FLAG	Expression plasmid encoding chANP32A with single FLAG tag	Jason Long (Barclay lab)
pCAGGS-chANP32AΔ4-FLAG	Expression plasmid encoding chANP32A lacking amino acids VLSL from beginning of 33 amino acids, with single FLAG tag	Jason Long (Barclay lab)
pCAGGS-chANP32AΔ33-FLAG	Expression plasmid encoding chANP32A lacking 33 amino acid insertion, with single FLAG tag	Jason Long (Barclay lab)
pCAGGS-chANP32A 1-208-FLAG	Expression plasmid encoding chANP32A lacking LCAR domain but retaining 33 amino acid insertion as well as NLS, with single FLAG tag	Jason Long (Barclay lab)
pCAGGS-huANP32A-FLAG	Expression plasmid encoding huANP32A with single FLAG tag	Jason Long (Barclay lab)
pCAGGS-huANP32A+33-FLAG	Expression plasmid encoding huANP32A with 33 amino acid insertion usually found in avian genes, with single FLAG tag	Jason Long (Barclay lab)
pCAGGS-huANP32B-FLAG	Expression plasmid encoding huANP32B with single FLAG tag	Jason Long (Barclay lab)
pCAGGS-chANP32A-mCHERRY	Expression plasmid encoding chANP32A with mCHERRY tag	Jason Long (Barclay lab)

pCAGGS-huANP32A-mCHERRY	Expression plasmid encoding huANP32A with mCHERRY tag	Jason Long (Barclay lab)
pCAGGS-50-92-PB1$_{luc1}$	Expression plasmid encoding PB1 tagged with N terminus of Gaussia luciferase, on its C terminus	This study
pCAGGS-50-92-PB1 D446Y$_{luc1}$	Expression plasmid encoding PB1 catalytic mutant tagged with N terminus of Gaussia luciferase, on its C terminus	This study
pCAGGS-50-92-$_{luc1}$PB2	Expression plasmid encoding PB2 tagged with N terminus of Gaussia luciferase, on its N terminus	Jocelyn Schreyer (This study)
pCAGGS-50-92-$_{luc1}$PB2 E627K	Expression plasmid encoding PB2 with mammalian adaption tagged with N terminus of Gaussia luciferase, on its N terminus	Jocelyn Schreyer (This study)
pCAGGS-50-92-PB2$_{luc1}$	Expression plasmid encoding PB2 tagged with N terminus of Gaussia luciferase, on its C terminus	Jocelyn Schreyer (This study)
pCAGGS-50-92-PB2 E627K$_{luc1}$	Expression plasmid encoding PB2 with mammalian adaption tagged with N terminus of Gaussia luciferase, on its C terminus	Jocelyn Schreyer (This study)
pCAGGS-50-92-PB2$_{luc2}$	Expression plasmid encoding PB2 tagged with C terminus of	This study

	Gaussia luciferase, on its C terminus	
pCAGGS-50-92-PB2 E627K$_{luc2}$	Expression plasmid encoding PB2 with mammalian adaption tagged with C terminus of Gaussia luciferase, on its C terminus	This study
pCAGGS-50-92-PA$_{luc1}$	Expression plasmid encoding PA tagged with N terminus of Gaussia luciferase, on its C terminus	This study
pCAGGS-50-92-PA$_{luc2}$	Expression plasmid encoding PA tagged with C terminus of Gaussia luciferase, on its C terminus	This study
pCAGGS-Vic75-$_{luc1}$PB1	Expression plasmid encoding PB1 tagged with N terminus of Gaussia luciferase, on its N terminus	This study
pCAGGS- Vic75-PB1$_{luc1}$	Expression plasmid encoding PB1 tagged with N terminus of Gaussia luciferase, on its C terminus	This study
pCAGGS- Vic75-$_{luc1}$PB2	Expression plasmid encoding PB2 tagged with N terminus of Gaussia luciferase, on its N terminus	This study
pCAGGS- Vic75-$_{luc2}$PB2	Expression plasmid encoding PB2 tagged with C terminus of Gaussia luciferase, on its N terminus	This study

pCAGGS- Vic75-PB2$_{luc1}$	Expression plasmid encoding PB2 tagged with N terminus of Gaussia luciferase, on its C terminus	This study
pCAGGS- Vic75-PB2 627E$_{luc1}$	Expression plasmid encoding PB2 with avian back mutation tagged with N terminus of Gaussia luciferase, on its C terminus	This study
pCAGGS- Vic75-PB2$_{luc2}$	Expression plasmid encoding PB2 tagged with C terminus of Gaussia luciferase, on its C terminus	This study
pCAGGS- Vic75-PB2 627E$_{luc2}$	Expression plasmid encoding PB2 with avian back mutation tagged with C terminus of Gaussia luciferase, on its C terminus	This study
pCAGGS- Vic75-PA$_{luc1}$	Expression plasmid encoding PA tagged with N terminus of Gaussia luciferase, on its C terminus	This study
pCAGGS- Vic75-PA$_{luc2}$	Expression plasmid encoding PA tagged with C terminus of Gaussia luciferase, on its C terminus	Jocelyn Schreyer (This study)
pCAGGS- Vic75-$_{luc1}$NP	Expression plasmid encoding NP tagged with N terminus of Gaussia luciferase, on its N terminus	This study
pCAGGS- Vic75-NP$_{luc1}$	Expression plasmid encoding NP tagged with N terminus of	This study

	Gaussia luciferase, on its C terminus	
pCAGGS-chANP32A$_{luc2}$	Expression plasmid encoding chANP32A tagged with C terminus of Gaussia luciferase, on its C terminus	This study
pCAGGS-chANP32AΔ33$_{luc2}$	Expression plasmid encoding chANP32A lacking 33 amino acid insertion tagged with C terminus of Gaussia luciferase, on its C terminus	This study
pCAGGS-huANP32A$_{luc2}$	Expression plasmid encoding huANP32A tagged with C terminus of Gaussia luciferase, on its C terminus	This study
pCAGGS-huANP32A+33$_{luc2}$	Expression plasmid encoding huANP32A with 33 amino acid insertion tagged with C terminus of Gaussia luciferase, on its C terminus	This study
pCAGGS-Luc1	Expression plasmid encoding N terminus of Gaussia luciferase	This study
pCAGGS-Luc2	Expression plasmid encoding C terminus of Gaussia luciferase	This study
pCAGGS-50-92-PB1-VN	Expression plasmid encoding PB1 tagged with N terminus of Venus on its C terminus	This study

pCAGGS-chANP32A-VC	Expression plasmid encoding chANP32A tagged with C terminus of Venus on its C terminus	This study
pCAGGS-huANP32A-VC	Expression plasmid encoding huANP32A tagged with C terminus of Venus on its C terminus	This study
pCAGGS-SRPK1-FLAG	Expression plasmid encoding SRPK1 with N terminal flag tag	This study
pCAGGS-Importin α7-FLAG	Expression plasmid encoding importin α7 with C terminal flag tag	This study
pCAGGS-eGFP-Strep-FLAG		Olivier Moncorge (Barclay lab)
pCAGGS-Empty		(Barclay lab)
pCAGGS-Renilla Luciferase	Expression plasmid encoding Renilla luciferase used as control in minigenome assays	(Barclay lab)
pPOL1-Firefly Luciferase	Human polI negative sense minigenome reporter encoding firefly luciferase	Olivier Moncorge (Barclay lab)
pPOL1-Firefly Luciferase (pos sense)	Human polI positive sense minigenome reporter encoding firefly luciferase	Olivier Moncorge (Barclay lab)

pPOL1-Firefly Luciferase 358	Human polI negative sense minigenome reporter with G3A, U5C and C8U mutations in 3' promoter sequence encoding firefly luciferase	Anna Cauldwell (Barclay lab)
pPOL1-BFPNLS	Human polI negative sense reporter encoding blue fluorescent protein with an NLS	Hayley Loy (Barclay lab)
pPOL1-76NP	Human polI negative sense minigenome reporter of 76 nt (Non coding regions from NP)	Ervin Fodor (University of Oxford)
pPolI (chicken)-Firefly luciferase	Chicken minigenome luciferase reporter	Dr Laurence Tiley, Cambridge University
pPOL1-Empty		Barclay lab

Table 8: Main plasmids used in this study

6.1.4 Oligonucleotides

Oligonucleotides were synthesised by Eurofins.

Oligonucleotide sequence	**Notes**
AAAAAAGCGGCCGCGCCACCATGGATGTCAATCCGACTTTAC	Fwd primer for amplifying pCAGGS-50-92-PB1 and pCAGGS-Vic75-PB1 for fusion constructs with PB1 at N terminus

CCCCCCCTCGAGCTATTATTTTTGCCGTCTGAGTTCTTC	Rev Primer for amplifying pCAGGS-Vic75-PB1 for fusion constructs with PB1 at C terminus
AAAAAAGCGGCCGCGCCACCATGGAGAGAATAAAAGAAC	Fwd primer for amplifying pCAGGS-50-92-PB2 for fusion constructs with PB2 at N terminus
CCCCCCCTCGAGTCACTAATTGATGGCCATCCGAATTC	Rev primer for amplifying pCAGGS-50-92-PB2 for fusion constructs with PB2 at C terminus
AAAAAAGCGGCCGCGCCACCATGGAAAGAATAAAAGAACTAC	Fwd primer for amplifying pCAGGS-Vic75-PB2 for fusion constructs with PB2 at N terminus
CCCCCCCTCGAGCTATTATAAGATGGCCATCCGAATTC	Fwd primer for amplifying pCAGGS-Vic75-PB2 for fusion constructs with PB2 at C terminus
AAAAAAGCGGCCGCGCCACCATGGAAGACTTTGTGCG	Fwd primer for amplifying pCAGGS-50-92-PA for fusion constructs with PA at N terminus
AAAAAAGCGGCCGCGCCACCATGGAAGATTTTGTGCGACAATG	Fwd primer for amplifying pCAGGS-Vic75-PA for fusion constructs with PA at N terminus

AAAAAAGCGGCCGCGCCACCATGGCGTCCC AAGGCACCAAAC	Fwd primer for amplifying pCAGGS-Vic75-NP for fusion constructs with NP at N terminus
CCCCCCCTCGAGCTATTAATTGTCGTACTCCT CTGCATTG	Rev primer for amplifying pCAGGS-Vic75-NP for fusion constructs with NP at C terminus
GCCCGCGGCTGCCTGTTTTTGCCGTCTGAGC TC	Rev primer for amplifying pCAGGS-50-92-PB1$_{luc1}$ and pCAGGS-50-92-PB1 D446Y$_{luc1}$ primary PCR product
CGGCAAAAACAGGCAGCCGCGGGCGGGGG AGGC	Fwd primer for amplifying pCAGGS-50-92-PB1$_{luc1}$ and pCAGGS-50-92-PB1 D446Y$_{luc1}$ primary PCR product
CTTTTATTCTCTCCATTGAACCACCGCCACCG GAGCCTCC	Rev primer for amplifying pCAGGS-50-92-$_{luc1}$PB2 and pCAGGS-50-92-$_{luc1}$PB2 E627K primary PCR product
GGCGGTGGTTCAATGGAGAGAATAAAAGAA CTAAGAG	Fwd primer for amplifying pCAGGS-50-92-$_{luc1}$PB2 and pCAGGS-50-92-$_{luc1}$PB2 E627K primary PCR product
GCCCGCGGCTGCATTGATGGCCATCCGAATT CTTTTGG	Rev primer for pCAGGS-50-92-PB2$_{luc1}$ and pCAGGS-50-92-PB2 E627K$_{luc1}$ primary PCR product

GATGGCCATCAATGCAGCCGCGGGCGGGGGAGG	Fwd primer for pCAGGS-50-92-PB2$_{luc1}$, pCAGGS-50-92-PB2 E627K$_{luc1}$, pCAGGS-50-92-PB2$_{luc2}$ and pCAGGS-50-92-PB2 E627K$_{luc2}$ primary PCR product
GCCCGCGGCTGCATTGATGGCCATCCGAATTC	Rev primer for pCAGGS-50-92-PB2$_{luc2}$ and pCAGGS-50-92-PB2 E627K$_{luc2}$ primary PCR product
GCCCGCGGCTGCTTTCAGTGCATGTGTGAGGAAGGAG	Rev primer for pCAGGS-50-92-PA$_{luc1}$ primary PCR product
CATGCACTGAAAGCAGCCGCGGGCGGGGGAGGCTCCGG	Fwd primer for pCAGGS-50-92-PA$_{luc1}$ primary PCR product
GCCCGCGGCTGCTTTCAGTGCATGTGTGAGGAAGGAG	Rev primer for pCAGGS-50-92-PA$_{luc2}$ primary PCR product
CATGCACTGAAAGCAGCCGCGGGCGGGGGAGGCTCCGG	Fwd primer for pCAGGS-50-92-PA$_{luc2}$ primary PCR product
GTAAAGTCGGATTGACATCCATTGAACCACCGCC	Rev primer for pCAGGS-Vic75-$_{luc1}$PB1 primary PCR product

GGCTCCGGTGGCGGTGGTTCAATGGATGTCAAT	Fwd primer for pCAGGS-Vic75-$_{luc1}$PB1 primary PCR product
GCCCGCGGCTGCTTTTTGCCGTCTGAGTTCTTC	Rev primer for pCAGGS- Vic75-PB1$_{luc1}$ primary PCR product
AGACGGCAAAAAGCAGCCGCGGGCGGGGGAGGC	Fwd primer for pCAGGS- Vic75-PB1$_{luc1}$ primary PCR product
TATTCTTTCCATTGAACCACCGCCACCGGAGCC	Rev primer for pCAGGS- Vic75-$_{luc1}$PB2 primary PCR product
GGCGGTGGTTCAATGGAAAGAATAAAAGAACTAC	Fwd primer for pCAGGS- Vic75-$_{luc1}$PB2 primary PCR product
TATTCTTTCCATACCACCGCCACCGGAGCCTCC	Rev primer for pCAGGS- Vic75-$_{luc2}$PB2 primary PCR product
GGTGGCGGTGGTATGGAAAGAATAAAAGAACTAC	Fwd primer for pCAGGS- Vic75-$_{luc2}$PB2 primary PCR product

GCCCGCGGCTGCTAAGATGGCCATCCGAATTC	Rev primer for pCAGGS- Vic75-PB2$_{luc1}$ and pCAGGS- Vic75-PB2 K627E$_{luc1}$ primary PCR product
ATGGCCATCTTAGCAGCCGCGGGCGGGGGAGGC	Fwd primer for pCAGGS- Vic75-PB2$_{luc1}$ and pCAGGS- Vic75-PB2 K627E$_{luc1}$ primary PCR product
GCCCGCGGCTGCTAAGATGGCCATCCGAATTC	Rev primer for pCAGGS- Vic75-PB2$_{luc2}$ and pCAGGS- Vic75-PB2 K627E$_{luc2}$ primary PCR product
GATGGCCATCTTAGCAGCCGCGGGCGGGGGAGG	Fwd primer for pCAGGS- Vic75-PB2$_{luc2}$ and pCAGGS- Vic75-PB2 K627E$_{luc2}$ primary PCR product
GCCCGCGGCTGCTCTTAATGCATGTGTTAGGAAG	Rev primer for pCAGGS- Vic75-PA$_{luc1}$ primary PCR product
CATGCATTAAGAGCAGCCGCGGGCGGGGGAGGC	Fwd primer for pCAGGS- Vic75-PA$_{luc1}$ primary PCR product
GCCCGCGGCTGCTCTTAATGCATGTGTTAGGAAGGAGTTG	Rev primer for pCAGGS- Vic75-PA$_{luc2}$ primary PCR product
CATGCATTAAGAGCAGCCGCGGGCGGGGGAGGCTCCGG	Fwd primer for pCAGGS- Vic75-PA$_{luc2}$ primary PCR product
TTGGGACGCCATTGAACCACCGCCACCGGAGCC	Rev primer for pCAGGS- Vic75-$_{luc1}$NP primary PCR product

GGCGGTGGTTCAATGGCGTCCCAAGGCACCAAAC	Fwd primer for pCAGGS- Vic75-$_{luc1}$NP primary PCR product
GCCCGCGGCTGCATTGTCGTACTCCTCTGCATTG	Rev primer for pCAGGS- Vic75-NP$_{luc1}$ primary PCR product
GAGTACGACAATGCAGCCGCGGGCGGGGGAGGC	Fwd primer for pCAGGS- Vic75-NP$_{luc1}$ primary PCR product
AAAAAAGCGGCCGCGCCACCATGGACATGAAGAAGCGGATC	Fwd primer for pCAGGS- chANP32A$_{luc1}$ and pCAGGS- chANP32A$_{VC}$
AAAAAAGCGGCCGCGCCACCATGGAAATGGGCAGACGGATC	Fwd primer for pCAGGS- huANP32A$_{luc1}$ and pCAGGS- huANP32A$_{VC}$
GCCCGCGGCTGCGTCATCCTCGTCGCCTTCGTC	Rev primer for pCAGGS-chANP32A$_{luc2}$ and pCAGGS-chANP32AΔ33$_{luc2}$ primary PCR product
GACGAGGATGACGCAGCCGCGGGCGGGGGAGGC	Fwd primer for pCAGGS-chANP32A$_{luc2}$ and pCAGGS-chANP32AΔ33$_{luc2}$ primary PCR product
GCCCGCGGCTGCGTCGTCATCCTCGCCCTCGTC	Rev primer for pCAGGS-huANP32A$_{luc2}$ and pCAGGS-huANP32A+33$_{luc2}$ primary PCR product
GCCCGCGGCTGCGTCGTCATCCTCGCCCTCGTC	Fwd primer for pCAGGS-huANP32A$_{luc2}$ and pCAGGS-huANP32A+33$_{luc2}$ primary PCR product

AAAAAAGCGGCCGCATGGGCATCTCCAAGC CCACCGAGAACAACGAAGAC	Fwd primer for pCAGGS-Luc1 and all fusion plasmids with luc1 at their N terminus
CCCCCCCTCGAGTTATCAGCCTATGCCGCCC TGTGCGG	Rev primer for pCAGGS-Luc1and all fusion plasmids with luc1 at their C terminus
AAAAAAGCGGCCGCATGGGCATCTCCGAGG CGATCGTCGACATTCCTGAG	Fwd primer for pCAGGS-Luc2 and all fusion plasmids with luc2 at their N terminus
CCCCCCCTCGAGCTATTAGTCACCACCGGCC CCCTTGATC	Rev primer for pCAGGS-Luc2 and all fusion plasmids with luc2 at their C terminus
CCCGCCACCTCCCTGTTTTTGCCGTCTGAGCT CTTC	Rev primer for pCAGGS-50-92-PB1-VN primary PCR product
CGGCAAAAACAGGGAGGTGGCGGGAGCGG AGG	Fwd primer for pCAGGS-50-92-PB1-VN primary PCR product
GGGGGGCTCGAGTCAGGCGGTGAGATAGA CGTTGTGG	Rev primer for pCAGGS-50-92-PB1-VN
GATTTTGCACGCCGGACGGCCACCAGAGCC GTCATCCTCGTCGCC	Rev primer for pCAGGS-chANP32A-VC
GGCGACGAGGATGACGGCTCTGGTGGCCGT CCGGCGTGCAAAATC	Fwd primer for pCAGGS-chANP32A-VC
GATTTTGCACGCCGGACGGCCACCAGAGCC GTCGTCATCCTCGCCC	Rev primer for pCAGGS-huANP32A-VC primary PCR product

GGGCGAGGATGACGACGGCTCTGGTGGCC GTCCGGCGTGCAAAATC	Fwd primer for pCAGGS-huANP32A-VC primary PCR product
GGGGGCTCGAGTTACTTGTACAGCTCGTCC	Rev primer for pCAGGS-chANP32A-VC and pCAGGS-huANP32A-VC
AAAAAAGCGGCCGCGCCACCATGGACTACA AGGATGACGATGACAAGGGCTCAGGGGAG CGGAAAGTGCTTGC	Fwd primer for FLAG-Srpk1
CCCCCCACGCGTCTATTAGGAGTTAAGCCAA GGG	Rev primer for FLAG-Srpk1
AAAAAGCGGCCGCGCCACCATGGAGACCAT GGCGAGC	Fwd primer for pCAGGS-Importin α7-FLAG
CCCCCCTCGAGCTATTACTTGTCATCGTCATC CTTGTAGTCTCCGCTGCCTAGCTGGAAGCCC TCCATG	Rev primer for pCAGGS-Importin α7-FLAG
GGCCGTCATGGTGGCGAATAGCAAAAGCAG GGTAGATAATC	Reverse transcription of 76 nt vRNA
CTTTACTACTGATTTCGATGTC	qPCR of 76 nt vRNA
ATTCGCCACCATGACGGCC	qPCR of 76 nt vRNA (primer against tag which is incorporated in RT step).
GCAAATTACCCACTCCCG	qPCR of 18S rRNA Fwd
CTGCAGCAACTTTAATATACGC	qPCR of 18S rRNA Rev
GCTAACCATGTTCATGCCTTC	pCAGGS Fwd sequencing primer

GGTATTTGTGAGCCAGGGCATTG	pCAGGS Rev sequencing primer

Table 9: Oligonucleotides used in this study

6.1.5 Buffers

Name	Recipe	Description
TAE buffer	40mM Tris-acetate pH 8 1mM EDTA	DNA gel electrophoresis
Tris glycine SDS buffer	0.025 M Tris 0.192 M Glycine 0.1 % w/v SDS Distilled water	Running SDS PAGE gels
Transfer buffer	0.025 M Tris 0.192 M Glycine Distilled water	Transferring proteins from gel to membrane
TBS	0.02 M Tris 0.137 M NaCl Distilled water Adjusted to pH 7.6	Washing flag beads
TBS Tween	0.02 M Tris 0.137 M NaCl	Washing western blots

	0.1 % Tween (Sigma Aldrich) Distilled water Adjusted to pH 7.6	
5 % Milk blocking buffer	0.02 M Tris 0.137 M NaCl 0.1 % Tween 20 5 % w/v skim milk powder (Sigma Alrich) Distilled water Adjusted to pH 7.6	Blocking western blots and diluting antibodies for western blots
Lysis buffer	50mM Tris-HCl pH 7.8 (sigma) 100mM NaCl 50mM KCl 0.5% Triton X-100 (sigma) cOmplete EDTA free Protease inhibitor cocktail tablet (Roche).	Lysis of cells for co-immunoprecipitation and western blots
Wash buffer	50mM Tris-HCl pH 7.8 100mM NaCl 50mM KCl cOmplete EDTA free Protease inhibitor cocktail tablet	Washing of gfp beads during coimmunoprecipitations

Permeabilization buffer	0.2 % Triton-x100 PBS (Gibco)	Permeabilising cells for IF
IF wash buffer	0.1 % Tween 20 PBS	Wash steps for IF
IF blocking buffer	5 % BSA (Sigma Aldrich) PBS	Blocking stage for IF
IF dilution buffer	1 % BSA 0.1 % Tween 20 PBS	Dilution of antibodies during IF

Table 10: Buffers used in this study

6.2 Methods

6.2.1 Cloning

Primer design

Forward primers were designed to include restriction sites, a Kozak sequence to aid translation followed by approximately 20 nt of the gene of interest.

Reverse primers were designed to include 20 nt of the gene of interest, two stop codons followed by a restriction site.

Internal primers for overlapping PCR were designed to include 20 nt of the gene to be amplified followed by 12 nt complimentary to the sequence to be fused. Primary PCR products therefore encompass an overlapping region of 24 nt.

Polymerase chain reaction

PCR was carried out using the KOD hot start polymerase kit (Novagen). 10 ng template DNA was mixed with a final concentration of 0.3 μM gene specific forward and reverse primers, 1.5 mM $MgSO_4$, 0.2 mM dNTPs, 0.02 U/μl KOD hot start DNA polymerase and 10X KOD hot start buffer. The mix was made to up 50 μl with PCR grade water. Thermocycling conditions were based on manufacturer's instructions. Annealing temperatures were based on melting temperature of specific primers used. Extension time was based on length of amplicon. 30-35 cycles were performed.

Overlapping PCR was carried out to generate fusion constructs. Equimolar amounts of the two overlapping primary PCR products were added to the mix above, excluding primers. Five cycles were performed before addition of the primers. A further 30 cycles were then carried out.

Gaussia luciferase was synthesised by gene synthesis (GeneArt, ThermoFisher) and used as a template to make luc1 and luc2.

Generation of cDNA from cellular mRNA

Templates for cloning of Srpk1-flag and Importin α7-flag were generated by reverse transcription of cellular mRNA using superscript III (ThermoFisher Scientific). Briefly, 1 μg cellular RNA (see section 6.2.3 for RNA extraction protocol) was mixed with 0.5 μl OligodT primer (ThermoFisher Scientific), 1 μl dNTPs and made up to a total volume of 12 μl with nuclease free water. Mixes were heated to 65 °C for five minutes followed by incubation on ice. 4 μl 5X first strand buffer, 1 μl 0.1M DTT and 1 μl superscript III were added to the mix and heated to 50 °C for 50 minutes followed by 70 °C for 15 minutes. The cDNA produced was then used as a template for PCR using the KOD polymerase as described above under the heading 'polymerase chain reaction' using gene specific primers listed in table 9.

Gel electrophoresis

Agarose gel electrophoresis was used to separate DNA. Gels were made using 0.5 %, 1 % or 2 % agarose (Invitrogen) in Tris-acetate-EDTA (TAE), depending on DNA size. Gel red (Biotium) was added to the agarose solution to visualise DNA. DNA was mixed with 6x loading dye (NEB) and gels were run for approximately 30 minutes at 135 V in 0.5X TAE buffer. 1 kb or 100 bp ladder (NEB) was used to estimate DNA size. Gels were visualised using the gel doc XR+ imaging system (Bio-Rad).

DNA purification

DNA bands of the correct size were excised from the gel under UV light. DNA was purified using the Monarch gel extraction kit (NEB). Briefly, 4 volumes of gel dissolving buffer were added to the excised gel slice and incubated at 50 °C until the gel had dissolved. The solution was then loaded onto the provided columns and centrifuged, followed by two washes and elution using 20 μl nuclease free water.

Digestion

Purified DNA fragments generated by PCR were digested with HF-NotI (NEB) and either HF-XhoI (NEB) or MluI (NEB). 1 μl of each enzyme was added to 1 μg DNA, along with 5 μl 10X CutSmart buffer (NEB) in a total volume of 50 μl with nuclease free water. The mixture was incubated at 37 °C for 1 hour followed by 20 minutes at 65 °C to inactivate the enzymes. Digestion of vector backbones were carried out using the same enzymes, but with an additional incubation period of 16 hours at room temperature before 37 °C for 1 hour and 20 minutes at 65 °C.

Ligation

Digested inserts and vectors were ligated together using T4 DNA ligase (NEB). 1 μl T4 DNA ligase, 2 μl 10X DNA ligase buffer (NEB) and DNA were added together and made up to a total volume of 20 μl with nuclease free water. Amount of vector and insert used depended on size. All plasmids made in this study were ligated to pCAGGS vectors.

Transformation

Plasmids were transformed using 5-alpha competent *E. coli* (NEB). Briefly, 5 μl of ligated products or 10 ng of plasmid DNA was incubated with 5-alpha competent *E. coli* for 30 minutes, followed by heat shock at 42 °C for 30 seconds and recovery on ice. *E. coli* were then incubated at 37 °C in SOC medium (NEB) for one hour whilst shaking. An appropriate volume of bacteria was spread on prewarmed agar plates supplemented with 100 μg/ml ampicillin (Sigma Aldrich) and incubated overnight at 37 °C to facilitate growth of colonies.

Minipreps

Bacterial cells were grown in 5 ml LB supplemented with 100 μg/ml ampicillin for 16 hours at 37 °C. Cells were then pelleted, supernatant discarded and DNA purified using the Monarch miniprep kit (NEB) following manufacturer's instructions. DNA was eluted in 36 μl nuclease free water.

Maxipreps

Bacterial cells were grown in 250 ml LB supplemented with 100 μg/ml ampicillin for 16 hours at 37 °C. Cells were then pelleted, supernatant discarded and DNA purified using the QIAGEN plasmid maxi kit following manufacturer's instructions. DNA was eluted in 1 ml nuclease free water.

DNA concentration measurement and Sequencing

DNA concentration was measured using the Nanodrop Lite spectrophotometer (ThermoFisher Scientific).

To verify sequences of DNA, plasmids were mixed with appropriate primers and sequencing was performed by GATC Biotech.

6.2.2 Cell culture, transfections and complementation assays

Cell culture

HEK 293T cells were cultured in Dulbecco's Modified Eagle Medium (DMEM) (Gibco) supplemented with 10 % FCS (Biosera), 1 % penstrep (Gibco) and 1 % non essential amino acids (Sigma Aldrich). eHAP1 cells were cultured in Iscove's Modified Dulbecco's Medium (IMDM) (Gibco) supplemented with 10 % FCS, 1 % penstrep and 1 % non-essential amino acids. DF-1 cells were cultured in DMEM supplemented with 10 % FCS, 5 % tryptose phosphate broth (Sigma Aldrich), 1 % penstrep and 1 % non-essential amino acids. 293T and eHAP1 cells were maintained at 37 °C and 5 % CO_2. DF-1 cells were maintained at 39 °C and 5 % CO_2. All cells were maintained at 90% confluency by splitting every 2-3 days using 0.05% trypsin (Gibco) and phosphate buffered saline (PBS) (Gibco) to wash cells.

Transfections

Transfections were carried out using lipofectamine 3000 (Invitrogen) following manufacturers instructions. Briefly, cells were seeded to 70-90 % confluency unless otherwise stated. Separate solutions of P3000 and L3000 with opti-mem (Gibco) were prepared. DNA mixes were incubated with the p3000 solution for 5 minutes after which the L3000 solution was added. 15 minutes after addition of L3000/opti-mem, solutions were added dropwise to cells. Quantity of reagents used varied depending on number of cells to be transfected.

Minigenome assays

HEK 293T or Ehap1 cells were seeded to approximately 80 % confluency in 48 well plates (VWR). 20 ng pCAGGS-PB1, 20 ng pCAGGS-PB2, 10 ng pCAGGS-PA, 40 ng pCAGGS-NP, and 20 ng pPolI-firefly luciferase, a plasmid encoding firefly luciferase flanked by the non-coding regions of NS, were transfected into cells using lipofectamine 3000. 10 ng pCAGGS-*Renilla* luciferase was also transfected as an internal control. 24 hours after transfection, media was removed and cells were lysed in 50 μl passive lysis buffer (Promega) for 20 minutes at room temperature. Firefly and *Renilla* luciferase activities were measured simultaneously from 10 μl of each sample by addition of substrates using the dual luciferase kit (Promega). Substrates were injected and activity measured using the FLUOstar Omega plate reader (BMG Labtech). Minigenome assays carried out in bigger wells were scaled up accordingly.

Split luciferase complementation assay

HEK 293T or Ehap1 cells were seeded to approximately 65 % confluency in 48 well plates. 25 ng pCAGGS-PB1$_{luc1}$, 25 ng either pCAGGS-PB2 627E or 627K, 12.5 ng pCAGGS-PA and 12.5 ng either pCAGGS-chANP32A$_{luc2}$ or huANP32A$_{luc2}$ was transfected into 293T or eHAP1 cells. For assays comparing different tagged polymerase constructs, 25 ng tagged or untagged pCAGGS-PB1, 25 ng tagged or untagged pCAGGS-PB2 and 12.5 ng tagged or untagged pCAGGS-PA was transfected into 293T cells depending on which constructs interactions were being measured between. For assays including viral like RNA, 10 ng pCAGGS-PB1$_{luc1,}$ 10 ng pCAGGS-PB2 627E or 627K, 5 ng pCAGGS-PA and 5 ng pCAGGS-chANP32A$_{luc2}$ or huANP32A$_{luc2}$ were transfected into 293T cells in 24 well plates (Greiner bio-one). 0 ng, 10 ng, 100 ng, 200 ng, 300 ng or 400 ng viral like RNA was transfected in assays measuring interactions between ANP32 and polymerase under non-replicating conditions. 0 ng, 0.625 ng, 1.25 ng, 2.5 ng, 5 ng or 10 ng viral like RNA was transfected in assays measuring interactions between ANP32 and polymerase under conditions that permitted replication. Samples substituting pCAGGS-PB1$_{luc1}$ with pCAGGS-luc1 and pCAGGS-ANP32A$_{luc2}$ with pCAGGS-luc2 were used as controls. Untagged proteins were kept constant between samples containing interacting partners of interest and controls. Untagged PB1 or ANP32A was also added to control samples where it has been substituted for by pCAGGS-luc1 or pCAGGs-luc2. Equivalent controls were used in experiments in which different luc-tagged constructs were used. Total DNA was kept constant between samples using an empty vector. 24 hours after transfections, media was removed and 50 μl (for 48 well plate) or 100 μl (for 24 well plate) *Renilla* lysis buffer (Promega) was added for 1 hour at room temperature. Signal was measured from 10 μl of the sample using the FLUOstar Omega plate reader (BMG Labtech) after injection of the *Renilla* luciferase

substrate from the *Renilla* luciferase kit (Promega). Normalised luminescence ratios were calculated by dividing the signal measured from the two interacting partners of interest by the sum of the two controls containing pCAGGS-luc1 or pCAGGS-luc2 as described above and in Cassonnet *et al.,* 2011.

Bimolecular fluorescence complementation assay

HEK 293T cells were seeded onto glass bottomed 8 well chamber μ-slides (Ibidi). 80 ng pCAGGS 5092 $PB1_{VN}$, 40 ng pCAGGS 5092 PA, 80 ng either pCAGGS 5092 PB2 627E or PB2 627K and either 40 ng $chANP32A_{VC}$ or $huANP32A_{VC}$ were transfected into cells. 20 hours after transfection, cells were fixed using 4 % paraformaldehyde (Alfa Aesar) for 10 minutes. Cells were then permeabilised using 0.2 % triton (Sigma-Aldrich) for 10 minutes followed by 4',6-Diamidino-2-Phenylindole (DAPI) staining for 4 minutes. Images were acquired using the Leica SP5 inverted confocal microscope described in section 6.2.6.

Flow cytometry

HEK 293T cells were transfected as for BiFC assays. Cells were washed, trypsinised, centrifuged and resuspended in PBS supplemented with 2 % FBS. After washing, cells were fixed with 4 % paraformaldehyde for 10 minutes. Following fixing, cells were washed and fluorescence was quantified using the LSRFortessa Cell analyser (BD Biosciences). Viable cells were gated by plotting SSC-Area vs FSC-Area. Single cells were gated by plotting FSC-Height

vs FSC-Area. 10000 events were measured for each sample and mean fluorescent intensity of YFP^+ cells (480-530 nm) calculated. Analysis was performed using FlowJo version 9 software.

6.2.3 RNA extraction and qRTPCR

RNA extraction

RNA was extracted from HEK 293T cells using the RNeasy mini kit (QIAGEN) following manufacturer's instructions. RNA was eluted in 36 μl nuclease free water.

qRTPCR

Reverse transcription was performed using the Revertaid H minus reverse transcriptase kit (ThermoFisher Scientific) following manufacturers protocol. Briefly, 1 μg extracted RNA was mixed with 20 pmol specific primers towards vRNA of pPolI-76nt viral like RNA (GGCCGTCATGGTGGCGAATAGCAAAAGCAGGGTAGATAATC) up to a volume of 13 μl. Primer incorporates tag onto cDNA product as described in Kawakami *et al.,* 2011. To reduce formation of secondary structure, this mixture was heated to 65 °C for 5 minutes followed by incubation on ice. 4 μl 5X reaction buffer, 2 μl 10mM dNTPs and 1 μl Revertaid H minus reverse transcriptase was added and heated to 42 °C for one hour followed by 70 °C for 10 minutes. Random hexamers (Invitrogen) were used to reverse transcribe RNA to cDNA. This cDNA was used to amplify housekeeping control, 18S ribosomal RNA.

For qPCR, 20 ng cDNA was mixed with 10 μl Sybr green (ThermoFisher Scientific) and 4 μl gene specific forward and 4 μl reverse primer up to a total volume of 20 μl with nuclease free water. Primers used for amplification of 76 nt vRNA are: Fwd- CTTTACTACTGATTTCGATGTC, Rev- ATTCGCCACCATGACGGCC. Primers used for amplification of 18S are Fwd- GCAAATTACCCACTCCCG and Rev- CTGCAGCAACTTTAATATACGC. 76 nt vRNA C_T values were normalised to 18S rRNA C_T values and plotted relative to pol 627E + empty. qPCR was carried out using Applied Biosystems ViiA 7 Real Time PCR System (ThermoFisher Scientific) and ViiA 7 software.

6.2.4 shRNA induced silencing

Generation of lentivirus for shRNA mediated silencing

Silencing of SRPK1 or importin α7 in 293T cells was achieved using lentiviral transduction of specific shRNAs. shRNA sequences were: srpk1-CCGGGAACAACACATTAGCCAACTTCTCGAGAAGTTGGCTAATGTGTTGTTCTTTTT, importin α7-CCGGCGGAGAAATGTGGAGCTGATTCTCGAGAATCAGCTCCACATTTCTCCGTTTTTG cloned into TRC1.5-pLKO.1-puro vectors (MISSION Sigma Aldrich). The non-mammalian shRNA control (MISSION Sigma Aldrich) was used as a negative control. To generate lentiviruses, 293T cells were transfected with TRC1.5-pLKO.1-puro shRNA vector, pCAGGS-VSV G and pCMV-delta8.2 at a ratio of 1:0.25:1 using lipofectamine 3000 (Invitrogen) in 10cm dishes (Greiner bio-one). 16 hours after transfection, media was replaced with 10ml fresh media. 36 hours after transfection, supernatant was collected, passed through a 0.45 μm filter (Merck Millipore), aliquoted and stored at -80 °C.

Lentivirus transduction of 293T cells was performed in six well plates (Greiner bio-one). Media was removed from cells and lentivirus added after washing with PBS. Lentivirus was replaced with DMEM media after 16 hours and incubated for a further 48 hours at 37 °C before splitting and selection using 0.5 μg/ml puromycin (Gibco). Selection was confirmed by cell death of mock cells which had not been transduced. Cells were incubated with 0.5 μg/ml puromycin for at least 72 hours before analysis. Knockdown was confirmed by western blotting.

6.2.5 Co-immunoprecipitations, western blotting and mass spectrometry

Cell lysis

Cells in 24 well plates were washed three times in cold phosphate buffered saline (PBS) at 0.5 x g for three minutes at 4 °C and pellets were resuspended in 100 μl lysis buffer. Cells were left to lyse for 20 minutes on ice, followed by centrifugation for 30 minutes at 4 °C at full speed to collect cell debris. Supernatant was collected and cell debris discarded.

For co-immunoprecipitation experiments, cells in 10 cm dishes were transfected with up to 15 μg total DNA. 24 hours after transfection, cells were washed three times in cold phosphate buffered saline (PBS) at 0.5 x g for three minutes at 4 °C and pellets were resuspended in 500 μl lysis buffer. Cells were left to lyse for 20 minutes on ice, followed by centrifugation for 30 minutes at 4 °C at full speed to separate cell debris. Supernatant was collected and cell debris discarded. 450 μl of cell lysate was subjected to flag or GFP immunoprecipitation, whilst the remaining lysate was retained for assessing protein expression from whole cell lysate. All protein samples were stored at -80 °C.

FLAG immunoprecipitation

Anti-flag M2 affinity agarose gel (Sigma Aldrich) was used to immunoprecipitate flag tagged proteins. After sufficient mixing, 40 μl Anti-flag M2 affinity gel per sample was washed three times in cold Tris-buffered saline (TBS) by centrifugation at 8200 x g at 4 °C for 30 seconds. Cell lysates were added and the tubes incubated on a rotator at 4 °C overnight. Following binding, the anti-flag M2 affinity gel was washed three times in TBS at 8200 x g at 4 °C for 30 seconds. Proteins were eluted by competition with 100 μl 3X flag peptide (Sigma Aldrich) at a concentration of 150 ng/μl. Samples were incubated with 3X flag peptide for 30 minutes. After centrifugation, eluted proteins were collected.

GFP immunoprecipitation

GFP-trap agarose beads (Chromotek) were used to immunoprecipitate GFP fusion proteins. After sufficient mixing, 25 μl GFP-trap beads per sample were added to 500 μl cold wash buffer. Beads were washed three times at 2500 x g for two minutes at 4 °C in wash buffer. Cell lysate was added to beads and left to bind at 4 °C overnight on a rotator. Following binding, the GFP-trap beads were washed three times in wash buffer at 2500 x g for two minutes at 4 °C. Proteins were eluted by heating samples to 95 °C for 10 minutes in 100 μl 2X laemlli buffer (Sigma Aldrich). After heating, samples were centrifuged to pellet beads and eluted proteins were collected.

Samples for LC-MS/MS analysis were prepared using a scaled-up version of the GFP immunoprecipitation method described above. Briefly, two 145mm plates (Greiner bio-one)

per sample were seeded with HEK 293T cells to 80 % confluency. 7 μg pCAGGS-5092 PB1, 7 μg pCAGGS-5092-PB2 627E or 627K, 3.5 μg PA-GFP and 7 μg pCAGGS-chANP32A or pCAGGS-empty was transfected into cells using lipofectamine 3000 (Invitrogen). 3.5 μg GFP-FLAG was used as a negative control. 24 hours after transfection, cells were washed three times in PBS. Cells from the two plates for each sample were pooled together. Cells were lysed in 3 ml lysis buffer for 30 minutes on ice followed by centrifugation to separate cell debris and lysate was collected. 50 μl GFP trap beads per sample was washed three times in wash buffer before addition of cell lysate. Proteins were allowed to bind to beads on a rotator at 4 °C overnight. Samples were then washed three times in 1 ml wash buffer and finally resuspended in 110 μl 2X laemlli buffer and heated to 95 °C for 10 minutes. After a final centrifugation step, eluted proteins were collected.

Western blotting

Lysates were mixed with 2X laemmli buffer and incubated at 95 °C for 10 minutes to denature proteins. Samples were loaded onto 4-20 % mini-PROTEAN TXG precast protein gels (Bio-Rad). Novex Pre stained protein ladder (Invitrogen) was used to estimate size of proteins. Gels were run at 180 V for 40 minutes in running buffer to separate proteins. Proteins were transferred onto 0.2 μm PVDF membranes by semi-dry transfer (Bio-Rad) at 15 V for 20 minutes in transfer buffer. Membranes were then blocked in 5 % milk for one hour at room temperature, followed by incubation with appropriate primary antibodies for 1 hour at room temperature. Membranes were washed for five minutes in TBS- 1 % Tween. Wash steps were repeated five times followed by incubation with appropriate secondary antibodies

conjugated to horseradish peroxidase for 1 hour at room temperature. After a further five washes, membranes were incubated for five minutes with Amersham ECL prime western blotting detection reagents (GE Healthcare). Protein bands were imaged using the Fusion Fx imaging system (Vilber Lourmat).

Preparation of samples for label free mass spectrometry

15 μl of each sample was run on NuPAGE 4-12 % Bis-Tris Protein gels (ThermoFisher Scientific) in MES buffer (ThermoFisher Scientific) for eight minutes until bands had run approximately 1 cm down the gel. Proteins were stained with colloidal Coomassie Blue G-250 (Simply BlueTM, ThermoFisher Scientific) following manufacturer's instructions. Each gel lane was excised into small pieces and destained in 50% acetonitrile/50 mM ammonium bicarbonate (pH~8). Proteins were then reduced with 10 mM dithiothreitol (Sigma) in 50 mM ammonium bicarbonate for 30 minutes at 37 °C followed by alkylation with 55 mM iodoacetamide (Sigma) in 50 mM ammonium bicarbonate for 30 minutes at room temperature in the dark. 50 mM ammonium bicarbonate was then used to wash the gel pieces for 15 minutes before they were dehydrated using 100% acetonitrile. Proteins were then trypsinsed overnight at 37 °C with 0.01 μg/μl proteomic grade trypsin (Sigma) diluted in 50 mM ammonium bicarbonate. Digested peptides were extracted from the gel pieces by repeated incubations with 50% (v/v) acetonitrile 0.1% (v/v) TFA for 15 minutes. Solutions were pooled and lyophilised using a centrifugal evaporator (Eppendorf concentrator plus). Finally, peptides were re-suspended in 5% (v/v) acetonitrile, 0.1% (v/v) TFA for analysis by mass spectrometry. Description of method

and preparation of samples was carried out with the help of Stuart Armstrong, University of Liverpool.

NanoLCMS ESI MS/MS analysis

Mass spectrometry experiments were performed using the Ultimate 3000 nano HPLC system (Dionex/Thermo Fisher Scientific) with a Q-Exactive mass spectrometer (Thermo Fisher Scientific). Samples were loaded onto the trap column (Acclaim PepMap 100, 2 cm × 75 µm inner diameter, C18, 3 µm, 100 Å) at 5 µl min−1. The column was connected in-line to an analytical column (Easy-Spray PepMap® RSLC 50 cm × 75 µm inner diameter, C18, 2 µm, 100 Å) which was fused to a silica nano-electrospray emitter (Dionex). Peptides were separated by a linear gradient of 3.8 – 50 % 80% acetonitrile in 0.1% formic acid. The Q-Exactive was operated in a top 10 data-dependent mode. Survey scans were acquired at a resolution of 70,000 and scan range of 300-2000 m/z. The ion injection time was 250 ms and ion target value was set to 1E6. Charge state +2 to +5 ions from the survey scan were selected with an isolation window of 2.0 Th. These were then fragmented by higher energy collisional dissociation with normalized collision energies of 30. The ion injection time for the MS/MS scans was 100 ms and the ion target value was set to 1E5. MS/MS scans were acquired at a resolution of 35,000. Dynamic exclusion for 20 seconds was enabled. Description of and implementation of this analysis was carried out by Stuart Armstrong, University of Liverpool.

Mass spectrometry data analysis

PEAKS software was used to search the mass spectrometry data against a human protein database (Uniprot reviewed, release-2017_07; 20,207 sequences) and the relevant bait protein sequences. The following search parameters were set; Enzyme-trypsin, precursor mass tolerance- 10 ppm, fragment mass tolerance- 0.05 Da. Two missed cleavage events were allowed and false discovery rate for peptide-spectrum matches was set at 1%. Only proteins with −10 lgP ≥ 20 and unique peptides ≥ 1 were included. This analysis was carried out by Stuart Armstrong, University of Liverpool.

6.2.6 Immunofluorescence

Immunofluorescence

For images where visualisation via the use of fluorescently tagged proteins were not used, proteins were visualised using fluorescently labelled antibodies. After transfection, cells were fixed with 4 % paraformaldehyde for 10 minutes, followed by three washes in PBS. Cells were permeabilised with 0.2 % triton for 10 minutes followed by a further three washes in PBS with 0.1 % Tween. Cells were blocked for one hour with 5 % bovine serum albumin (BSA) in PBS followed by three washes in PBS with 0.1 % Tween. Primary antibodies were diluted in 1 % BSA in PBS and added to cells for one hour. Following three washes in PBS with 0.1 % Tween, cells were incubated with fluorescently labelled secondary antibodies diluted in 1 % BSA in PBS and then subjected to a further three washes in PBS with 0.1 % Tween. Nuclei were stained using DAPI for four minutes followed by three washes.

Images were acquired for BiFC assays (chapter 2) and imaging of SRPK1 and ANP32A-mCHERRY (chapter 3) using the Leica SP5 inverted confocal microscope using a Plan-Apochromat 63.0x 1.40 numerical aperture objective. Fluorescence was detected using excitation at 405 nm with 420-480 nm emission bandwidth for DAPI. Fluorescence was detected using excitation at 514 nm with 525-650 nm emission bandwidth for Venus. Fluorescence was detected using excitation at 488 nm with 493-555 nm emission bandwidth for Alexa Fluor 488. Fluorescence was detected using excitation at 543 nm with 600-680 nm emission bandwidth for Alexa Fluor 594. Images were taken with the help of the FILM facility at Imperial College London. Images were processed using FIJI software.

For image acquisition with widefield microscopy, see 'blue fluorescent reporter assay' below.

Blue fluorescent protein reporter assay

Cells were transfected with 20 ng pCAGGS-PB1, 20 ng pCAGGS-PB2 627E or 627K, 10 ng pCAGGS-PA-GFP, 40 ng pCAGGS-NP and 20 ng pPolI-BFP-NLS as well as pCAGGS-chANP32A-mCHERRY, pCAGGS-huANP32A-mCHERRY or pCAGGS-empty in glass bottomed 8 well chamber μ-slides (Ibidi). 24 hours after transfection cells were fixed for 10 minutes with 4 % paraformaldehyde and washed three times in PBS before image acquisition. Images were acquired using a Zeiss Elya widefield microscope. Laser excitation at 405 nm, 488 nm, 561 nm and 642 nm and bandwidth filters at 420-280 nm, 495-550 nm, 570-640 nm and a long pass filter >650 nm were used, respectively. Emission was detected with a 63.0x 1.40 numerical aperture objective and Immersol TM 518F immersion oil (Zeiss). 5 mW of power and 200 ms

exposure time was used to acquire each image. Imaging was carried out in collaboration with Adam Cawte, Imperial College London.

Speckle analysis

Images were analysed and prepared using FIJI software. Number of PA-GFP expressing cells were counted from seven random fields of view of each condition. PA-GFP expressing cells with speckles were counted and calculated as a percentage of total PA-GFP expressing cells in those fields of view.

6.2.7 Statistical analysis

Statistical analysis

Statistical analysis, including t-tests one-way Anovas and Pearsons correlation were carried out using Prism 7 software (GraphPad). P-values less than 0.05 were considered significant.

References

Aggarwal, S., Dewhurst, S., Takimoto, T. and Kim, B. (2011) 'Biochemical Impact of the Host Adaptation-associated PB2 E627K Mutation on the Temperature-dependent RNA Synthesis Kinetics of Influenza A Virus Polymerase Complex', *Journal of Biological Chemistry*, 286(40), pp. 34504-34513.

Almond, J. W. (1977) 'A single gene determines the host range of influenza virus', *Nature*, 270(5638), pp. 617-8.

Amorim, M. J., Bruce, E. A., Read, E. K. C., Foeglein, A., Mahen, R., Stuart, A. D. and Digard, P. (2011) 'A Rab11-and Microtubule-Dependent Mechanism for Cytoplasmic Transport of Influenza A Virus Viral RNA', *Journal of Virology*, 85(9), pp. 4143-4156.

Ando, T., Yamayoshi, S., Tomita, Y., Watanabe, S., Watanabe, T. and Kawaoka, Y. (2016) 'The host protein CLUH participates in the subnuclear transport of influenza virus ribonucleoprotein complexes', *Nature Microbiology*, 1(8), 16062

Arranz, R., Coloma, R., Chichon, F. J., Conesa, J. J., Carrascosa, J. L., Valpuesta, J. M., Ortin, J. and Martin-Benito, J. (2012) 'The Structure of Native Influenza Virion Ribonucleoproteins', *Science*, 338(6114), pp. 1634-1637.

Aubol, B. E., Keshwani, M. M., Fattet, L. and Adams, J. A. (2018) 'Mobilization of a splicing factor through a nuclear kinase-kinase complex', *Biochemical Journal*, 475, pp. 677-690.

Badham, M. D. and Rossman, J. S. (2016) 'Filamentous Influenza Viruses', *Current Clinical Microbiology Reports*, 3(3), pp. 155-161.

Bai, J. N., Brody, J. R., Kadkol, S. H. S. and Pasternack, G. R. (2001) 'Tumor suppression and potentiation by manipulation of pp32 expression', *Oncogene*, 20(17), pp. 2153-2160.

Baker, S. F., Ledwith, M. P. and Mehle, A. (2018) 'Differential Splicing of ANP32A in Birds Alters Its Ability to Stimulate RNA Synthesis by Restricted Influenza Polymerase', *Cell Reports*, 24(10), pp. 2581-2588.

Banerjee, I., Miyake, Y., Nobs, S. P., Schneider, C., Horvath, P., Kopf, M., Matthias, P., Helenius, A. and Yamauchi, Y. (2014) 'Influenza A virus uses the aggresome processing machinery for host cell entry', *Science*, 346(6208), pp. 473-477.

Baudin, F., Bach, C., Cusack, S. and Ruigrok, R. W. H. (1994) 'Structure of influenza -virus RNP .1. Influenza-virus nucleoprotein melts secondary structure in panhandle RNA and exposes the bases to the solvent', *Embo Journal*, 13(13), pp. 3158-3165.

Bauer, A., Neumann, S., Karger, A., Henning, A. K., Maisner, A., Lamp, B., Dietzel, E., Kwasnitschka, L., Balkema-Buschmann, A., Keil, G. M. and Finke, S. (2014) 'ANP32B Is a Nuclear Target of Henipavirus M Proteins', *Plos One*, 9(5), e97233.

Beaton, A. R. and Krug, R. M. (1981) 'Selected host cell capped RNA fragments prime influenza viral RNA transcription in vivo', *Nucleic Acids Res*, 9(17), pp. 4423-36.

Bell, I., Martin, A. and Roberts, S. (2007) 'The E1 boolean AND E4 protein of human papillomavirus interacts with the serine-arginine-specific protein kinase SRPK1', *Journal of Virology*, 81(11), pp. 5437-5448.

Benfield, C. T. O., Lyall, J. W., Kochs, G. and Tiley, L. S. (2008) 'Asparagine 631 variants of the chicken Mx protein do not inhibit influenza virus replication in primary chicken embryo fibroblasts or in vitro surrogate assays', *Journal of Virology*, 82(15), pp. 7533-7539.

Bertram, S., Thiele, S., Dreier, C., Resa-Infante, P., Preuss, A., van Riel, D., Mok, C. K. P., Schwalm, F., Peiris, J. S. M., Klenk, H. D. and Gabriel, G. (2017) 'H7N9 Influenza A Virus Exhibits Importin-alpha 7-Mediated Replication in the Mammalian Respiratory Tract', *American Journal of Pathology*, 187(4), pp. 831-840.

Bier, K., York, A. and Fodor, E. (2011) 'Cellular cap-binding proteins associate with influenza virus mRNAs', *Journal of General Virology*, 92, pp. 1627-1634.

Biswas, S. K., Boutz, P. L. and Nayak, D. P. (1998) 'Influenza virus nucleoprotein interacts with influenza virus polymerase proteins', *Journal of Virology*, 72(7), pp. 5493-5501.

Biswas, S. K. and Nayak, D. P. (1994) 'Mutational analysis of the conserved motifs of influenza A virus polymerase basic protein 1', *Journal of Virology*, 68(3), pp. 1819-1826.

Blumenkrantz, D., Roberts, K. L., Shelton, H., Lycett, S. and Barclay, W. S. (2013) 'The Short Stalk Length of Highly Pathogenic Avian Influenza H5N1 Virus Neuraminidase Limits Transmission of Pandemic H1N1 Virus in Ferrets', *Journal of Virology*, 87(19), pp. 10539-10551.

Bodem, J., Schied, T., Gabriel, R., Rammling, M. and Rethwilm, A. (2011) 'Foamy Virus Nuclear RNA Export Is Distinct from That of Other Retroviruses', *Journal of Virology*, 85(5), pp. 2333-2341.

Boivin, S. and Hart, D. J. (2011) 'Interaction of the Influenza A Virus Polymerase PB2 C-terminal Region with Importin alpha Isoforms Provides Insights into Host Adaptation and Polymerase Assembly', *Journal of Biological Chemistry*, 286(12), pp. 10439-10448.

Bortz, E., Westera, L., Maamary, J., Steel, J., Albrecht, R. A., Manicassamy, B., Chase, G., Martinez-Sobrido, L., Schwemmle, M. and Garcia-Sastre, A. (2011) 'Host- and Strain-Specific Regulation of Influenza Virus Polymerase Activity by Interacting Cellular Proteins', *Mbio*, 2(4), e00151-11.

Bouloy, M., Plotch, S. J. and Krug, R. M. (1978) 'Globin messenger-RNAs are primers for transcription of influenza viral RNA in vitro', *Proceedings of the National Academy of Sciences of the United States of America*, 75(10), pp. 4886-4890.

Bouvier, N. M. and Palese, P. (2008) 'The biology of influenza viruses', *Vaccine*, 26, pp. D49-D53.

Bradel-Tretheway, B. G., Mattiacio, J. L., Krasnoselsky, A., Stevenson, C., Purdy, D., Dewhurst, S. and Katze, M. G. (2011) 'Comprehensive Proteomic Analysis of Influenza Virus Polymerase Complex Reveals a Novel Association with Mitochondrial Proteins and RNA Polymerase Accessory Factors', *Journal of Virology*, 85(17), pp. 8569-8581.

Brennan, C. M., Gallouzi, I. E. and Steitz, J. A. (2000) 'Protein ligands to HuR modulate its interaction with target mRNAs in vivo', *Journal of Cell Biology*, 151(1), pp. 1-13.

Brody, J. R., Kadkol, S. S., Mahmoud, M. A., Rebel, J. M. J. and Pasternack, G. R. (1999) 'Identification of sequences required for inhibition of oncogene-mediated transformation by pp32', *Journal of Biological Chemistry*, 274(29), pp. 20053-20055.

Brunotte, L., Flies, J., Bolte, H., Reuther, P., Vreede, F. and Schwemmle, M. (2014) 'The Nuclear Export Protein of H5N1 Influenza A Viruses Recruits Matrix 1 (M1) Protein to the Viral Ribonucleoprotein to Mediate Nuclear Export', *Journal of Biological Chemistry*, 289(29), pp. 20067-20077.

Bui, M., Wills, E. G., Helenius, A. and Whittaker, G. R. (2000) 'Role of the influenza virus M1 protein in nuclear export of viral ribonucleoproteins', *Journal of Virology*, 74(4), pp. 1781-1786.

Bussey, K. A., Bousse, T. L., Desmet, E. A., Kim, B. and Takimoto, T. (2010) 'PB2 Residue 271 Plays a Key Role in Enhanced Polymerase Activity of Influenza A Viruses in Mammalian Host Cells', *Journal of Virology*, 84(9), pp. 4395-4406.

Callebaut, C., Blanco, J., Benkirane, N., Krust, B., Jacotot, E., Guichard, G., Seddiki, N., Svab, J., Dam, E., Muller, S., Briand, J. P. and Hovanessian, A. G. (1998) 'Identification of V3 loop-binding proteins as potential receptors implicated in the binding of HIV particles to CD4(+) cells', *Journal of Biological Chemistry*, 273(34), pp. 21988-21997.

Cao, M. M., Wei, C. D., Zhao, L. L., Wang, J. F., Jia, Q. N., Wang, X., Jin, Q. and Deng, T. (2014) 'DnaJA1/Hsp40 Is Co-Opted by Influenza A Virus To Enhance Its Viral RNA Polymerase Activity', *Journal of Virology*, 88(24), pp. 14078-14089.

Cassonnet, P., Rolloy, C., Neveu, G., Vidalain, P. O., Chantier, T., Pellet, J., Jones, L., Muller, M., Demeret, C., Gaud, G., Vuillier, F., Lotteau, V., Tangy, F., Favre, M. and Jacob, Y. (2011) 'Benchmarking a luciferase complementation assay for detecting protein complexes', *Nature Methods*, 8(12), pp. 990-992.

Cauldwell, A. V., Long, J. S., Moncorge, O. and Barclay, W. S. (2014) 'Viral determinants of influenza A virus host range', *Journal of General Virology*, 95, pp. 1193-1210.

Chai, G. S., Feng, Q., Wang, Z. H., Hu, Y., Sun, D. S., Li, X. G., Ke, D., Li, H. L., Liu, G. P. and Wang, J. Z. (2017) 'Downregulating ANP32A rescues synapse and memory loss via chromatin remodelling in Alzheimer model', *Molecular Neurodegeneration*, 12, 34.

Chan, W. H., Ng, A. K. L., Robb, N. C., Lam, M. K. H., Chan, P. K. S., Au, S. W. N., Wang, J. H., Fodor, E. and Shaw, P. C. (2010) 'Functional Analysis of the Influenza Virus H5N1 Nucleoprotein Tail Loop Reveals Amino Acids That Are Crucial for Oligomerization and Ribonucleoprotein Activities', *Journal of Virology*, 84(14), pp. 7337-7345.

Chang, C. K., Chen, C. J., Wu, C. C., Chen, S. W., Shih, S. R. and Kuo, R. L. (2017) 'Cellular hnRNP A2/B1 interacts with the NP of influenza A virus and impacts viral replication', *Plos One*, 12(11), e0188214.

Chang, J., Liu, Y., Zhang, D. D., Zhang, D. J., Wu, C. T., Wang, L. S. and Cui, C. P. (2010) 'Hepatopoietin Cn suppresses apoptosis of human hepatocellular carcinoma cells by up-regulating myeloid cell leukemia-1', *World Journal of Gastroenterology*, 16(2), pp. 193-200.

Chang, S. H., Sun, D. P., Liang, H. H., Wang, J., Li, J., Guo, L., Wang, X. L., Guan, C. C., Boruah, B. M., Yuan, L. M., Feng, F., Yang, M. R., Wang, L. L., Wang, Y., Wojdyla, J., Li, L. J., Wang, J. W., Wang, M. T., Cheng, G. H., Wang, H. W. and Liu, Y. F. (2015) 'Cryo-EM Structure of Influenza Virus RNA Polymerase Complex at 4.3 angstrom Resolution', *Molecular Cell*, 57(5), pp. 925-935.

Chemnitz, J., Pieper, D., Stich, L., Schumacher, U., Balabanov, S., Spohn, M., Grundhoff, A., Steinkasserer, A., Hauber, J. and Zinser, E. (2019) 'The acidic protein rich in leucines Anp32b is an immunomodulator of inflammation in mice', *Scientific Reports*, 9 (1), 4853.

Chen, H., Bright, R. A., Subbarao, K., Smith, C., Cox, N. J., Katz, J. M. and Matsuoka, Y. (2007) 'Polygenic virulence factors involved in pathogenesis of 1997 Hong Kong H5N1 influenza viruses in mice', *Virus Research*, 128(1-2), pp. 159-163.

Chen, H., Smith, G. J. D., Zhang, S. Y., Qin, K., Wang, J., Li, K. S., Webster, R. G., Peiris, J. S. M. and Guan, Y. (2005) 'H5N1 virus outbreak in migratory waterfowl', *Nature*, 436(7048), pp. 191-192.

Chen, S., Li, B., Grundke-Iqbal, I. and Iqbal, K. (2008) 'I-1(PP2A) affects Tau phosphorylation via association with the catalytic subunit of protein phosphatase 2A', *Journal of Biological Chemistry*, 283(16), pp. 10513-10521.

Chen, S. C., Jeng, K. S. and Lai, M. M. C. (2017) 'Zinc Finger-Containing Cellular Transcription Corepressor ZBTB25 Promotes Influenza Virus RNA Transcription and Is a Target for Zinc Ejector Drugs', *Journal of Virology*, 91(20), e00842-17.

Chen, T. H., Brody, J. R., Romantsev, R. E., Yu, J. G., Kayler, A. E., Voneiff, E., Kuhajda, F. P. and Pasternack, G. R. (1996) 'Structure of pp32, an acidic nuclear protein which inhibits oncogene-induced formation of transformed foci', *Molecular Biology of the Cell*, 7(12), pp. 2045-2056.

Chen, W. S., Calvo, P. A., Malide, D., Gibbs, J., Schubert, U., Bacik, I., Basta, S., O'Neill, R., Schickli, J., Palese, P., Henklein, P., Bennink, J. R. and Yewdell, J. W. (2001) 'A novel influenza A virus mitochondrial protein that induces cell death', *Nature Medicine*, 7(12), pp. 1306-1312.

Chua, M. A., Schmid, S., Perez, J. T., Langlois, R. A. and tenOever, B. R. (2013) 'Influenza A Virus Utilizes Suboptimal Splicing to Coordinate the Timing of Infection', *Cell Reports*, 3(1), pp. 23-29.

Crescenzo-Chaigne, B., van der Werf, S. and Naffakh, N. (2002) 'Differential effect of nucleotide substitutions in the 3 ' arm of the influenza A virus vRNA promoter on transcription/replication by avian and human polymerase complexes is related to the nature of PB2 amino acid 627', *Virology*, 303(2), pp. 240-252.

Cui, C. P., Zhang, D. J., Shi, B. X., Du, S. J., Wu, D. L., Wei, P., Zhong, G. S., Guo, Z. K., Liu, Y., Wang, L. S. and Wu, C. T. (2008) 'Isolation and functional identification of a novel human hepatic growth factor: Hepatopoietin Cn', *Hepatology*, 47(3), pp. 986-995.

Cui, L., Mahesutihan, M., Zheng, W. N., Meng, L. J., Fan, W. H., Li, J., Ye, X., Liu, W. J. and Sun, L. (2018) 'CDC25B promotes influenza A virus replication by regulating the phosphorylation of nucleoprotein', *Virology*, 525, pp. 40-47.

Cvetanovic, M., Rooney, R. J., Garcia, J. J., Toporovskaya, N., Zoghbi, H. Y. and Opal, P. (2007) 'The role of LANP and ataxin 1 in E4F-mediated transcriptional repression', *Embo Reports*, 8(7), pp. 671-677.

Daub, H., Blencke, S., Habenberger, P., Kurtenbach, A., Dennenmoser, J., Wissing, J., Ullrich, A. and Cotten, M. (2002) 'Identification of SRPK1 and SRPK2 as the major cellular protein kinases phosphorylating hepatitis B virus core protein', *Journal of Virology*, 76(16), pp. 8124-8137.

de Chiara, C., Menon, R. P. and Pastore, A. (2008) 'Structural bases for recognition of Anp32/LANP proteins', *Febs Journal*, 275(10), pp. 2548-2560.

Deng, T., Sharps, J., Fodor, E. and Brownlee, G. G. (2005) 'In vitro assembly of PB2 with a PB1-PA dimer supports a new model of assembly of influenza A virus polymerase subunits into a functional trimeric complex', *Journal of Virology*, 79(13), pp. 8669-8674.

Deng, T., Vreede, F. T. and Brownlee, G. G. (2006) 'Different de novo initiation strategies are used by influenza virus RNA polymerase on its cRNA and viral RNA promoters during viral RNA replication', *Journal of Virology*, 80(5), pp. 2337-2348.

Detjen, B. M., Stangelo, C., Katze, M. G. and Krug, R. M. (1987) 'THE 3 INFLUENZA-VIRUS POLYMERASE (P) PROTEINS NOT ASSOCIATED WITH VIRAL NUCLEOCAPSIDS IN THE INFECTED CELL ARE IN THE FORM OF A COMPLEX', Journal of Virology, 61(1), pp. 16-22.

Digard, P., Blok, V. C. and Inglis, S. C. (1989) 'Complex formation between influenza virus polymerase proteins expressed in Xenopus oocytes', Virology, 171(1), pp. 162-9.

Dittmann, J., Stertz, S., Grimm, D., Steel, J., Garcia-Sastre, A., Haller, O. and Kochs, G. (2008) 'Influenza A virus strains differ in sensitivity to the antiviral action of Mx-GTPase', *Journal of Virology*, 82(7), pp. 3624-3631.

Domingues, P., Golebiowski, F., Tatham, M. H., Lopes, A. M., Taggart, A., Hay, R. T. and Hale, B. G. (2015) 'Global Reprogramming of Host SUMOylation during Influenza Virus Infection', *Cell Reports*, 13(7), pp. 1467-1480.

Domingues, P. and Hale, B. G. (2017) 'Functional Insights into ANP32A-Dependent Influenza A Virus Polymerase Host Restriction', *Cell Reports*, 20(11), pp. 2538-2546.

Dou, D., Revol, R., Ostbye, H., Wang, H. and Daniels, R. (2018) 'Influenza A Virus Cell Entry, Replication, Virion Assembly and Movement', *Frontiers in Immunology*, 9, 1581.

Dundr, M. and Misteli, T. (2001) 'Functional architecture in the cell nucleus', *Biochemical Journal*, 356, pp. 297-310.

Eisfeld, A. J., Neumann, G. and Kawaoka, Y. (2015) 'At the centre: influenza A virus ribonucleoproteins', *Nature Reviews Microbiology*, 13(1), pp. 28-41.

Elton, D., Amorim, M. J., Medcalf, L. and Digard, P. (2005) ''Genome gating'; polarized intranuclear trafficking of influenza virus RNPs', *Biology Letters*, 1(2), pp. 113-117.

Elton, D., Medcalf, L., Bishop, K., Harrison, D. and Digard, P. (1999) 'Identification of amino acid residues of influenza virus nucleoprotein essential for RNA binding', *Journal of Virology*, 73(9), pp. 7357-7367.

Engelhardt, O. G., Smith, M. and Fodor, E. (2005) 'Association of the influenza A virus RNA-dependent RNA polymerase with cellular RNA polymerase II', J Virol, 79(9), pp. 5812-8.

Engelhardt, O. G. and Fodor, E. (2006) 'Functional association between viral and cellular transcription during influenza virus infection', *Reviews in Medical Virology*, 16(5), pp. 329-345.

Engelhardt, O. G., Sirma, H., Pandolfi, P. P. and Haller, O. (2004) 'Mx1 GTPase accumulates in distinct nuclear domains and inhibits influenza A virus in cells that lack promyelocytic leukaemia protein nuclear bodies', *Journal of General Virology*, 85, pp. 2315-2326.

Fensterl, V. and Sen, G. C. (2015) 'Interferon-Induced Ifit Proteins: Their Role in Viral Pathogenesis', *Journal of Virology*, 89(5), pp. 2462-2468.

Ferhadian, D., Contrant, M., Printz-Schweigert, A., Smyth, R. P., Paillart, J. C. and Marquet, R. (2018) 'Structural and Functional Motifs in Influenza Virus RNAs', *Frontiers in Microbiology*, 9, 559.

Fislova, T., Thomas, B., Graef, K. M. and Fodor, E. (2010) 'Association of the Influenza Virus RNA Polymerase Subunit PB2 with the Host Chaperonin CCT', *Journal of Virology*, 84(17), pp. 8691-8699.

Flick, R., Neumann, G., Hoffmann, E., Neumeier, E. and Hobom, G. (1996) 'Promoter elements in the influenza vRNA terminal structure', *Rna*, 2(10), pp. 1046-1057.

Fodor, E., Pritlove, D. C. and Brownlee, G. G. (1994) 'The influenza-virus panhandle is involved in the initiation of transcription', *Journal of Virology*, 68(6), pp. 4092-4096.

Fodor, E. and Smith, M. (2004) 'The PA subunit is required for efficient nuclear accumulation of the PB1 subunit of the influenza A virus RNA polymerase complex', *Journal of Virology*, 78(17), pp. 9144-9153.

Foeglein, A., Loucaides, E. M., Mura, M., Wise, H. M., Barclay, W. S. and Digard, P. (2011) 'Influence of PB2 host-range determinants on the intranuclear mobility of the influenza A virus polymerase', *Journal of General Virology*, 92, pp. 1650-1661.

Fournier, G., Chiang, C., Munier, S., Tomoiu, A., Demeret, C., Vidalain, P. O., Jacob, Y. and Naffakh, N. (2014) 'Recruitment of RED-SMU1 Complex by Influenza A Virus RNA Polymerase to Control Viral mRNA Splicing', *Plos Pathogens*, 10(6), e1004164.

Fries, B., Heukeshoven, J., Hauber, I., Gruttner, C., Stocking, C., Kehlenbach, R. H., Hall, J. and Chemnitz, J. (2007) 'Analysis of nucleocytoplasmic trafficking of the HuR ligand APRIL and its influence on CD83 expression', *Journal of Biological Chemistry*, 282(7), pp. 4504-4515.

Fujioka, Y., Nishide, S., Ose, T., Suzuki, T., Kato, I., Fukuhara, H., Fujioka, M., Horiuchi, K., Satoh, A. O., Nepal, P., Kashiwagi, S., Wang, J., Horiguchi, M., Sato, Y., Paudel, S., Nanbo, A., Miyazaki, T., Hasegawa, H., Maenaka, K. and Ohba, Y. (2018) 'A Sialylated Voltage-Dependent Ca2+ Channel Binds Hemagglutinin and Mediates Influenza A Virus Entry into Mammalian Cells', *Cell Host & Microbe*, 23(6), pp. 809-818.

Fujioka, Y., Tsuda, M., Nanbo, A., Hattori, T., Sasaki, J., Sasaki, T., Miyazaki, T. and Ohba, Y. (2013) 'A Ca2+-dependent signalling circuit regulates influenza A virus internalization and infection', *Nature Communications*, 4, 2763.

Fukumoto, M., Sekimoto, T. and Yoneda, Y. (2011) 'Proteomic Analysis of Importin alpha-interacting Proteins in Adult Mouse Brain', *Cell Structure and Function*, 36(1), pp. 57-67.

Gabriel, G., Herwig, A. and Klenk, H. D. (2008) 'Interaction of polymerase subunit PB2 and NP with importin alpha 1 is a determinant of host range of influenza a virus', *Plos Pathogens*, 4(2), e11.

Gabriel, G., Klingel, K., Otte, A., Thiele, S., Hudjetz, B., Arman-Kalcek, G., Sauter, M., Shmidt, T., Rother, F., Baumgarte, S., Keiner, B., Hartmann, E., Bader, M., Brownlee, G. G., Fodor, E. and Klenk, H. D. (2011) 'Differential use of importin-alpha isoforms governs cell tropism and host adaptation of influenza virus', *Nature Communications*, 2, 156.

Garcia-Dorival, I., Wu, W. N., Dowall, S., Armstrong, S., Touzelet, O., Wastling, J., Barr, J. N., Matthews, D., Carroll, M., Hewson, R. and Hiscox, J. A. (2014) 'Elucidation of the Ebola Virus VP24 Cellular Interactome and Disruption of Virus Biology through Targeted Inhibition of Host-Cell Protein Function', *Journal of Proteome Research*, 13(11), pp. 5120-5135.

Gavazzi, C., Yver, M., Isel, C., Smyth, R. P., Rosa-Calatrava, M., Lina, B., Moules, V. and Marquet, R. (2013) 'A functional sequence-specific interaction between influenza A virus genomic RNA segments', *Proceedings of the National Academy of Sciences of the United States of America*, 110(41), pp. 16604-16609.

Gerlach, P., Malet, H., Cusack, S. and Reguera, J. (2015) 'Structural Insights into Bunyavirus Replication and Its Regulation by the vRNA Promoter', *Cell*, 161(6), pp. 1267-1279.

Giannakouros, T., Nikolakaki, E., Mylonis, I. and Georgatsou, E. (2011) 'Serine-arginine protein kinases: a small protein kinase family with a large cellular presence', *Febs Journal*, 278(4), pp. 570-586.

Gonzalez, S. and Ortin, J. (1999) 'Distinct regions of influenza virus PB1 polymerase subunit recognize vRNA and cRNA templates', *Embo Journal*, 18(13), pp. 3767-3775.

Gotz, V., Magar, L., Dornfeld, D., Giese, S., Pohlmann, A., Hoeper, D., Kong, B. W., Jans, D. A., Beer, M., Haller, O. and Schwemmle, M. (2016) 'Influenza A viruses escape from MxA restriction at the expense of efficient nuclear vRNP import', *Scientific Reports*, 6, 23138.

Gu, W. F., Gallagher, G. R., Dai, W. W., Liu, P., Li, R. D., Trombly, M. I., Gammon, D. B., Mello, C. C., Wang, J. P. and Finberg, R. W. (2015) 'Influenza A virus preferentially snatches noncoding RNA caps', *Rna*, 21(12), pp. 2067-2075.

Harada, J. N., Shevchenko, A., Pallas, D. C. and Berk, A. J. (2002) 'Analysis of the adenovirus E1B-55K-anchored proteome reveals its link to ubiquitination machinery', *Journal of Virology*, 76(18), pp. 9194-9206.

Hatakeyama, D., Shoji, M., Yamayoshi, S., Hirota, T., Nagae, M., Yanagisawa, S., Nakano, M., Ohmi, N., Noda, T., Kawaoka, Y. and Kuzuhara, T. (2014) 'A Novel Functional Site in the PB2 Subunit of Influenza A Virus Essential for Acetyl-CoA Interaction, RNA Polymerase Activity, and Viral Replication', *Journal of Biological Chemistry*, 289(36), pp. 24980-24994.

Hatakeyama, D., Shoji, M., Yamayoshi, S., Yoh, R., Ohmi, N., Takenaka, S., Saitoh, A., Arakaki, Y., Masuda, A., Komatsu, T., Nagano, R., Nakano, M., Noda, T., Kawaoka, Y. and Kuzuhara, T. (2018) 'Influenza A virus nucleoprotein is acetylated by histone acetyltransferases PCAF and GCN5', *Journal of Biological Chemistry*, 293(19), pp. 7126-7138.

Hatta, M., Gao, P., Halfmann, P. and Kawaoka, Y. (2001) 'Molecular basis for high virulence of Hong Kong H5N1 influenza A viruses', *Science*, 293(5536), pp. 1840-1842.

Hay, A. J., Skehel, J. J. and McCauley, J. (1982) 'Characterization of influenza virus RNA complete transcripts', Virology, 116(2), pp. 517-22.

Hedestam, G. B. K., Fouchier, R. A. M., Phogat, S., Burton, D. R., Sodroski, J. and Wyatt, R. T. (2008) 'The challenges of eliciting neutralizing antibodies to HIV-1 and to influenza virus', *Nature Reviews Microbiology*, 6(2), pp. 143-155.

Hengrung, N., El Omari, K., Martin, I. S., Vreede, F. T., Cusack, S., Rambo, R. P., Vonrhein, C., Bricogne, G., Stuart, D. I., Grimes, J. M. and Fodor, E. (2015) 'Crystal structure of the RNA-dependent RNA polymerase from influenza C virus', *Nature*, 527(7576), pp. 114-117.

Herfst, S., Schrauwen, E. J. A., Linster, M., Chutinimitkul, S., de Wit, E., Munster, V. J., Sorrell, E. M., Bestebroer, T. M., Burke, D. F., Smith, D. J., Rimmelzwaan, G. F., Osterhaus, A. and Fouchier, R. A. M. (2012) 'Airborne Transmission of Influenza A/H5N1 Virus Between Ferrets', *Science*, 336(6088), pp. 1534-1541.

Higashino, F., Aoyagi, M., Takahashi, A., Ishino, M., Taoka, M., Isobe, T., Kobayashi, M., Totsuka, Y., Kohgo, T. and Shindoh, M. (2005) 'Adenovirus E4orf6 targets pp32/LANP to control the fate of ARE-containing mRNAs by perturbing the CRM1-dependent mechanism', *Journal of Cell Biology*, 170(1), pp. 15-20.

Hoffmann, T. W., Munier, S., Larcher, T., Soubieux, D., Ledevin, M., Esnault, E., Tourdes, A., Croville, G., Guerin, J. L., Quere, P., Volmer, R., Naffakh, N. and Marc, D. (2012) 'Length Variations in the NA Stalk of an H7N1 Influenza Virus Have Opposite Effects on Viral Excretion in Chickens and Ducks', *Journal of Virology*, 86(1), pp. 584-588.

Honda, A., Ueda, K., Nagata, K. and Ishihama, A. (1988) 'RNA-Polymerase of influenza-viruses – Role of NP in RNA chain elongation', *Journal of Biochemistry*, 104(6), pp. 1021-1026.

Hsu, M. T., Parvin, J. D., Gupta, S., Krystal, M. and Palese, P. (1987) 'Genomic RNAS of Influenza-viruses are held in a circular conformation in virions and in infected cells by a terminal panhandle', *Proceedings of the National Academy of Sciences of the United States of America*, 84(22), pp. 8140-8144.

Hsu, S. F., Su, W. C., Jeng, K. S. and Lai, M. M. C. (2015) 'A Host Susceptibility Gene, DR1, Facilitates Influenza A Virus Replication by Suppressing Host Innate Immunity and Enhancing Viral RNA Replication', *Journal of Virology*, 89(7), pp. 3671-3682.

Hudjetz, B. and Gabriel, G. (2012) 'Human-like PB2 627K Influenza Virus Polymerase Activity Is Regulated by Importin-alpha 1 and -alpha 7', *Plos Pathogens*, 8(1), e1002488.

Huet, S., Avilov, S. V., Ferbitz, L., Daigle, N., Cusack, S. and Ellenberg, J. (2010) 'Nuclear Import and Assembly of Influenza A Virus RNA Polymerase Studied in Live Cells by Fluorescence Cross-Correlation Spectroscopy', *Journal of Virology*, 84(3), pp. 1254-1264.

Hussain, M., Galvin, H. D., Haw, T. Y., Nutsford, A. N. and Husain, M. (2017) 'Drug resistance in influenza A virus: the epidemiology and management', *Infection and Drug Resistance*, 10, pp. 121-134.

Hutchinson, E. C., Charles, P. D., Hester, S. S., Thomas, B., Trudgian, D., Martinez-Alonso, M. and Fodor, E. (2014) 'Conserved and host-specific features of influenza virion architecture', *Nature Communications*, 5, 4816.

Hutchinson, E. C., Denham, E. M., Thomas, B., Trudgian, D. C., Hester, S. S., Ridlova, G., York, A., Turrell, L. and Fodor, E. (2012) 'Mapping the Phosphoproteome of Influenza A and B Viruses by Mass Spectrometry', *Plos Pathogens*, 8(11).

Hutchinson, E. C., von Kirchbach, J. C., Gog, J. R. and Digard, P. (2010) 'Genome packaging in influenza A virus', *Journal of General Virology*, 91, pp. 313-328.

Huyton, T. and Wolberger, C. (2007) 'The crystal structure of the tumor suppressor protein pp32 (Anp32a): Structural insights into Anp32 family of proteins', *Protein Science*, 16(7), pp. 1308-1315.

Jagger, B. W., Wise, H. M., Kash, J. C., Walters, K. A., Wills, N. M., Xiao, Y. L., Dunfee, R. L., Schwartzman, L. M., Ozinsky, A., Bell, G. L., Dalton, R. M., Lo, A., Efstathiou, S., Atkins, J. F., Firth, A. E., Taubenberger, J. K. and Digard, P. (2012) 'An Overlapping Protein-Coding Region in Influenza A Virus Segment 3 Modulates the Host Response', *Science*, 337(6091), pp. 199-204.

Jiang, X. J., Kim, H. E., Shu, H. J., Zhao, Y. M., Zhang, H. C., Kofron, J., Donnelly, J., Burns, D., Ng, S. C., Rosenberg, S. and Wang, X. D. (2003) 'Distinctive roles of PHAP proteins and prothymosin-alpha in a death regulatory pathway', *Science*, 299(5604), pp. 223-226.

Jorba, N., Area, E. and Ortin, J. (2008a) 'Oligomerization of the influenza virus polymerase complex in vivo', *Journal of General Virology*, 89, pp. 520-524.

Jorba, N., Coloma, R. and Ortin, J. (2009) 'Genetic trans-Complementation Establishes a New Model for Influenza Virus RNA Transcription and Replication', *Plos Pathogens*, 5(5), e1000462.

Jorba, N., Juarez, S., Torreira, E., Gastaminza, P., Zamarreno, N., Albar, J. P. and Ortin, J. (2008b) 'Analysis of the interaction of influenza virus polymerase complex with human cell factors', *Proteomics*, 8(10), pp. 2077-2088.

Kadkol, S. S., Brody, J. R., Epstein, J. I., Kuhajda, F. P. and Pasternack, G. R. (1998) 'Novel nuclear phosphoprotein pp32 is highly expressed in intermediate- and high-grade prostate cancer', *Prostate*, 34(3), pp. 231-237.

Kadota, S. and Nagata, K. (2011) 'pp32, an INHAT component, is a transcription machinery recruiter for maximal induction of IFN-stimulated genes', *Journal of Cell Science*, 124(6), pp. 892-899.

Karakama, Y., Sakamoto, N., Itsui, Y., Nakagawa, M., Tasaka-Fujita, M., Nishimura-Sakurai, Y., Kakinuma, S., Oooka, M., Azuma, S., Tsuchiya, K., Onogi, H., Hagiwara, M. and Watanabe, M. (2010) 'Inhibition of Hepatitis C Virus Replication by a Specific Inhibitor of Serine-Arginine-Rich Protein Kinase', *Antimicrobial Agents and Chemotherapy*, 54(8), pp. 3179-3186.

Kawaguchi, A. and Nagata, K. (2007) 'De novo replication of the influenza virus RNA genome is regulated by DNA replicative helicase, MCM', *Embo Journal*, 26(21), pp. 4566-4575.

Khaperskyy, D. A. and McCormick, C. (2015) 'Timing Is Everything: Coordinated Control of Host Shutoff by Influenza A Virus NS1 and PA-X Proteins', *Journal of Virology*, 89(13), pp. 6528-6531.

Khaperskyy, D. A., Schmaling, S., Larkins-Ford, J., McCormick, C. and Gaglia, M. M. (2016) 'Selective Degradation of Host RNA Polymerase II Transcripts by Influenza A Virus PA-X Host Shutoff Protein', *Plos Pathogens*, 12(2), e1005427.

Kobe, B. and Kajava, A. V. (2001) 'The leucine-rich repeat as a protein recognition motif', *Current Opinion in Structural Biology*, 11(6), pp. 725-732.

Komarnitsky, P., Cho, E. J. and Buratowski, S. (2000) 'Different phosphorylated forms of RNA polymerase II and associated mRNA processing factors during transcription', *Genes & Development*, 14(19), pp. 2452-2460.

Kuo, S. M., Chen, C. J., Chang, S. C., Liu, T. J., Chen, Y. H., Huang, S. Y. and Shih, S. R. (2017) 'Inhibition of Avian Influenza A Virus Replication in Human Cells by Host Restriction Factor TUFM Is Correlated with Autophagy', *Mbio*, 8(3), e00481-17.

Labadie, K., Afonso, E. D., Rameix-Welti, M. A., van der Werf, S. and Naffakh, N. (2007) 'Host-range determinants on the PB2 protein of influenza A viruses control the interaction between the viral polymerase and nucleoprotein in human cells', *Virology*, 362(2), pp. 271-282.

Lam, S. S., Martell, J. D., Kamer, K. J., Deerinck, T. J., Ellisman, M. H., Mootha, V. K. and Ting, A. Y. (2015) 'Directed evolution of APEX2 for electron microscopy and proximity labeling', *Nature Methods*, 12(1), pp. 51-54.

Lamb, R. A., Lai, C. J. and Choppin, P. W. (1981) 'Sequences of mRNAs derived from genome RNA segment 7 of influenza virus: colinear and interrupted mRNAs code for overlapping proteins', *Proc Natl Acad Sci U S A*, 78(7), pp. 4170-4.

Landeras-Bueno, S., Jorba, N., Perez-Cidoncha, M. and Ortin, J. (2011) 'The Splicing Factor Proline-Glutamine Rich (SFPQ/PSF) Is Involved in Influenza Virus Transcription', *Plos Pathogens*, 7(11), e1002397.

Leser, G. P. and Lamb, R. A. (2005) 'Influenza virus assembly and budding in raft-derived microdomains: A quantitative analysis of the surface distribution of HA, NA and M2 proteins', *Virology*, 342(2), pp. 215-227.

Li, C. F., Wang, Z. N., Cao, Y., Wang, L. L., Ji, J. Y., Chen, Z. G., Deng, T., Jiang, T. J., Cheng, G. H. and Qin, X. F. (2017) 'Screening for Novel Small-Molecule Inhibitors Targeting the Assembly of Influenza Virus Polymerase Complex by a Bimolecular Luminescence Complementation-Based Reporter System', *Journal of Virology*, 91(5), e02282-16.

Li, G., Zhang, J. J., Tong, X. M., Liu, W. J. and Ye, X. (2011) 'Heat Shock Protein 70 Inhibits the Activity of Influenza A Virus Ribonucleoprotein and Blocks the Replication of Virus In Vitro and In Vivo', *Plos One*, 6(2), e16546.

Li, J., Yu, M., Zheng, W. N. and Liu, W. J. (2015) 'Nucleocytoplasmic Shuttling of Influenza A Virus Proteins', *Viruses-Basel*, 7(5), pp. 2668-2682.

Li, M., Guo, H. and Damuni, Z. (1995) 'Purification and characterisation of 2 potent heat-stable protein inhibitors of protein phosphatase 2A from bovine kidney', *Biochemistry*, 34(6), pp. 1988-1996.

Lin, Y. C., Jeng, K. S. and Lai, M. M. C. (2017) 'CNOT4-Mediated Ubiquitination of Influenza A Virus Nucleoprotein Promotes Viral RNA Replication', *Mbio*, 8(3), e00597-17.

Linster, M., Boheemen, S., de Graaf, M., Schrauwen, E. J. A., Lexmond, P., Manz, B., Bestebroer, T. M., Baumann, J., van Riel, D., Rimmelzwaan, G. F., Osterhaus, A., Matrosovich, M., Fouchier, R. A. M. and Herfst, S. (2014) 'Identification, Characterization, and Natural Selection of Mutations Driving Airborne Transmission of A/H5N1 Virus', *Cell*, 157(2), pp. 329-229.

Long, J. S., Giotis, E. S., Moncorge, O., Frise, R., Mistry, B., James, J., Morisson, M., Iqbal, M., Vignal, A., Skinner, M. A. and Barclay, W. S. (2016) 'Species difference in ANP32A underlies influenza A virus polymerase host restriction', *Nature*, 529(7584), pp. 101-104.

Long, J. S., Mistry, B., Haslam, S. M. and Barclay, W. S. (2019) 'Host and viral determinants of influenza A virus species specificity', *Nature Reviews Microbiology*, 17(2), pp. 67-81.

Long, J.S., Idoko-Akoh, A., Mistry, B. Goldhill, D.H., Staller, E., Schreyer, J., Ross, Craig., Goodbourn, Steve., Shelton, H., Skinner, M., Sang, H.M., McGrew, M.J and Barclay, W.S. 'Species specific differences in use of ANP32 proteins by influenza A virus,' *eLife. In press.*

Lukarska, M., Fournier, G., Pflug, A., Resa-Infante, P., Reich, S., Naffakh, N. and Cusack, S. (2017) 'Structural basis of an essential interaction between influenza polymerase and Pol II CTD', *Nature*, 541(7635), pp. 117-121.

Manz, B., Brunotte, L., Reuther, P. and Schwemmle, M. (2012) 'Adaptive mutations in NEP compensate for defective H5N1 RNA replication in cultured human cells', *Nature Communications*, 3, 802.

Manz, B., de Graaf, M., Mogling, R., Richard, M., Bestebroer, T. M., Rimmelzwaan, G. F. and Fouchier, R. A. M. (2016) 'Multiple Natural Substitutions in Avian Influenza A Virus PB2 Facilitate Efficient Replication in Human Cells', *Journal of Virology*, 90(13), pp. 5928-5938.

Manz, B., Dornfeld, D., Gotz, V., Zell, R., Zimmermann, P., Haller, O., Kochs, G. and Schwemmle, M. (2013) 'Pandemic Influenza A Viruses Escape from Restriction by Human MxA through Adaptive Mutations in the Nucleoprotein', *Plos Pathogens*, 9(3), e1003279.

Manzoor, R., Kuroda, K., Yoshida, R., Tsuda, Y., Fujikura, D., Miyamoto, H., Kajihara, M., Kida, H. and Takada, A. (2014) 'Heat Shock Protein 70 Modulates Influenza A Virus Polymerase Activity', *Journal of Biological Chemistry*, 289(11), pp. 7599-7614.

Marcos-Villar, L., Pazo, A. and Nieto, A. (2016) 'Influenza Virus and Chromatin: Role of the CHD1 Chromatin Remodeler in the Virus Life Cycle', *Journal of Virology*, 90(7), pp. 3694-3707.

Marjuki, H., Alam, M. I., Ehrhardt, C., Wagner, R., Planz, O., Klenk, H. D., Ludwig, S. and Pleschka, S. (2006) 'Membrane accumulation of influenza A virus hemagglutinin triggers nuclear export of the viral genome via protein kinase C alpha-mediated activation of ERK signaling', *Journal of Biological Chemistry*, 281(24), pp. 16707-16715.

Martin, K. and Helenius, A. (1991a) 'Nuclear transport of influenza-virus ribonucleoproteins-the viral matrix protein (M1) promotes export and inhibits import', *Cell*, 67(1), pp. 117-130.

Martin, K. and Helenius, A. (1991b) 'Transport of incoming influenza-virus nucleocapsids into the nucleus', *Journal of Virology*, 65(1), pp. 232-244.

Martinez-Alonso, M., Hengrung, N. and Fodor, E. (2016) 'RNA-Free and Ribonucleoprotein-Associated Influenza Virus Polymerases Directly Bind the Serine-5-Phosphorylated Carboxyl-Terminal Domain of Host RNA Polymerase II', *Journal of Virology*, 90(13), pp. 6014-6021.

Martinvalet, D., Zhu, P. C. and Lieberman, J. (2005) 'Granzyme A induces caspase-independent mitochondrial damage, a required first step for apoptosis', *Immunity*, 22(3), pp. 355-370.

Massin, P., van der Werf, S. and Naffakh, N. (2001) 'Residue 627 of PB2 is a determinant of cold sensitivity in RNA replication of avian influenza viruses', *Journal of Virology*, 75(11), pp. 5398-5404.

Matilla, A., Koshy, B. T., Cummings, C., Isobe, T., Orr, H. T. and Zoghbi, H. Y. (1997) 'The cerebellar leucine-rich acidic nuclear protein interacts with ataxin-1', *Nature*, 389(6654), pp. 974-978.

Matilla, A. and Radrizzani, M. (2005) 'The Anp32 family of proteins containing leucine-rich repeats', *Cerebellum*, 4(1), pp. 7-18.

Matlin, K. S., Reggio, H., Helenius, A. and Simons, K. (1981) 'Infectious entry pathway of influenza-virus in a canine kidney-cell line', *Journal of Cell Biology*, 91(3), pp. 601-613.

Matrosovich, M., Tuzikov, A., Bovin, N., Gambaryan, A., Klimov, A., Castrucci, M. R., Donatelli, I. and Kawaoka, Y. (2000) 'Early alterations of the receptor-binding properties of H1, H2, and H3 avian influenza virus hemagglutinins after their introduction into mammals', *Journal of Virology*, 74(18), pp. 8502-8512.

Mayer, D., Molawi, K., Martinez-Sobrido, L., Ghanem, A., Thomas, S., Baginsky, S., Grossmann, J., Garcia-Sastre, A. and Schwemmle, M. (2007) 'Identification of cellular interaction partners of the influenza virus ribonucleoprotein complex and polymerase complex using proteomic-based approaches', *Journal of Proteome Research*, 6(2), pp. 672-682.

Mehle, A. and Doudna, J. A. (2008) 'An inhibitory activity in human cells restricts the function of an avian-like influenza virus polymerase', *Cell Host & Microbe*, 4(2), pp. 111-122.

Mehle, A. and Doudna, J. A. (2009) 'Adaptive strategies of the influenza virus polymerase for replication in humans', *Proceedings of the National Academy of Sciences of the United States of America*, 106(50), pp. 21312-21316.

Melnik, S., Deng, B. W., Papantonis, A., Baboo, S., Carr, I. M. and Cook, P. R. (2011) 'The proteomes of transcription factories containing RNA polymerases I, II or III', *Nature Methods*, 8(11), pp. 963-968.

Minakuchi, M., Sugiyama, K., Kato, Y., Naito, T., Okuwaki, M., Kawaguchi, A. and Nagata, K. (2017) 'Pre-mRNA Processing Factor Prp18 Is a Stimulatory Factor of Influenza Virus RNA Synthesis and Possesses Nucleoprotein Chaperone Activity', *Journal of Virology*, 91(3), e01398-16.

Miyake, Y., Keusch, J., Decamps, L., Ho-Xuan, H., Iketani, S., Gut, H., Kutay, U., Helenius, A. and Yamauchi, Y. (2019) 'Influenza virus uses transportin 1 for vRNP debundling during cell entry', *Nature Microbiology*, 4(4), pp. 578-586.

Moeller, A., Kirchdoerfer, R. N., Potter, C. S., Carragher, B. and Wilson, I. A. (2012) 'Organization of the Influenza Virus Replication Machinery', *Science*, 338(6114), pp. 1631-1634.

Momose, F., Basler, C. F., O'Neill, R. E., Iwamatsu, A., Palese, P. and Nagata, K. (2001) 'Cellular splicing factor RAF-2p48/NPI-5/BAT1/UAP56 interacts with the influenza virus nucleoprotein and enhances viral RNA synthesis', *Journal of Virology*, 75(4), pp. 1899-1908.

Momose, F., Naito, T., Yano, K., Sugimoto, S., Morikawa, Y. and Nagata, K. (2002) 'Identification of Hsp90 as a stimulatory host factor involved in influenza virus RNA synthesis', *Journal of Biological Chemistry*, 277(47), pp. 45306-45314.

Moncorge, O., Mura, M. and Barclay, W. S. (2010) 'Evidence for Avian and Human Host Cell Factors That Affect the Activity of Influenza Virus Polymerase', *Journal of Virology*, 84(19), pp. 9978-9986.

Mondal, A., Dawson, A. R., Potts, G. K., Freiberger, E. C., Baker, S. F., Moser, L. A., Bernard, K. A., Coon, J. J. and Mehle, A. (2017) 'Influenza virus recruits host protein kinase C to control assembly and activity of its replication machinery', *Elife*, 6, e26910.

Mor, A., White, A., Zhang, K., Thompson, M., Esparza, M., Munoz-Moreno, R., Koide, K., Lynch, K. W., Garcia-Sastre, A. and Fontoura, B. M. A. (2016) 'Influenza virus mRNA trafficking through host nuclear speckles', *Nature Microbiology*, 1(7), 16069.

Munemasa, Y., Suzuki, T., Aizawa, K., Miyamoto, S., Imai, Y., Matsumura, T., Horikoshi, M. and Nagai, R. (2008) 'Promoter region-specific histone incorporation by the novel histone chaperone ANP32B and DNA-binding factor KLF5', *Molecular and Cellular Biology*, 28(3), pp. 1171-1181.

Munier, S., Rolland, T., Diot, C., Jacob, Y. and Naffakh, N. (2013) 'Exploration of Binary Virus-Host Interactions Using an Infectious Protein Complementation Assay', *Molecular & Cellular Proteomics*, 12(10), pp. 2845-2855.

Muramoto, Y., Noda, T., Kawakami, E., Akkina, R. and Kawaoka, Y. (2013) 'Identification of Novel Influenza A Virus Proteins Translated from PA mRNA', *Journal of Virology*, 87(5), pp. 2455-2462.

Naito, T., Kiyasu, Y., Sugiyama, K., Kimura, A., Nakano, R., Matsukage, A. and Nagata, K. (2007a) 'An influenza virus replicon system in yeast identified Tat-SF1 as a stimulatory host factor for viral RNA synthesis', *Proceedings of the National Academy of Sciences of the United States of America*, 104(46), pp. 18235-18240.

Naito, T., Momose, F., Kawaguchi, A. and Nagata, K. (2007b) 'Involvement of Hsp90 in assembly and nuclear import of influenza virus RNA polymerase subunits', *Journal of Virology*, 81(3), pp. 1339-1349.

Nakajima, K., Desselberger, U. and Palese, P. (1978) 'Recent human influenza-A (H1N1) viruses are closely related genetically to strains isolated in 1950', *Nature*, 274(5669), pp. 334-339.

Neumann, G. and Hobom, G. (1995) 'Mutational analysis of Influenza-virus promoter elements in vivo', *Journal of General Virology*, 76, pp. 1709-1717.

Neumann, G. and Kawaoka, Y. (2015) 'Transmission of influenza A viruses', *Virology*, 479, pp. 234-246.

Ng, A. K. L., Chan, W. H., Choi, S. T., Lam, M. K. H., Lau, K. F., Chan, P. K. S., Au, S. W. N., Fodor, E. and Shaw, P. C. (2012) 'Influenza Polymerase Activity Correlates with the Strength of Interaction between Nucleoprotein and PB2 through the Host-Specific Residue K/E627', *Plos One*, 7(5), e36415.

Nilsson, B. E., te Velthuis, A. J. W. and Fodor, E. (2017) 'Role of the PB2 627 Domain in Influenza A Virus Polymerase Function', *Journal of Virology*, 91(7), e02467-16.

Ninpan, K., Suptawiwat, O., Boonarkart, C., Phuangphung, P., Sathirareuangchai, S., Uiprasertkul, M. and Auewarakul, P. (2016) 'Expression of importin-alpha isoforms in human nasal mucosa: implication for adaptation of avian influenza A viruses to human host', *Virology Journal*, 13, 90.

Noble, E., Mathews, D. H., Chen, J. L., Turner, D. H., Takimoto, T. and Kim, B. (2011) 'Biophysical Analysis of Influenza A Virus RNA Promoter at Physiological Temperatures', *Journal of Biological Chemistry*, 286(26), pp. 22965-22970.

Noda, T., Murakami, S., Nakatsu, S., Imai, H., Muramoto, Y., Shindo, K., Sagara, H. and Kawaoka, Y. (2018) 'Importance of the 1+7 configuration of ribonucleoprotein complexes for influenza A virus genome packaging', *Nature Communications*, 9(1), 54.

Noda, T., Sagara, H., Yen, A., Takada, A., Kida, H., Cheng, R. H. and Kawaoka, Y. (2006) 'Architecture of ribonucleoprotein complexes in influenza A virus particles', *Nature*, 439(7075), pp. 490-492.

Nturibi, E., Bhagwat, A. R., Coburn, S., Myerburg, M. M. and Lakdawala, S. S. (2017) 'Intracellular Colocalization of Influenza Viral RNA and Rab11A Is Dependent upon Microtubule Filaments', *Journal of Virology*, 91(19), e001179-17.

O'Neill, R. E., Jaskunas, R., Blobel, G., Palese, P. and Moroianu, J. (1995) 'Nuclear import of influenza virus RNA can be mediated by viral nucleoprotein and transport factors required for protein import', *J Biol Chem*, 270(39), pp. 22701-4.

Obri, A., Ouararhni, K., Papin, C., Diebold, M. L., Padmanabhan, K., Marek, M., Stoll, I., Roy, L., Reilly, P. T., Mak, T. W., Dimitrov, S., Romier, C. and Hamiche, A. (2014) 'ANP32E is a histone chaperone that removes H2A.Z from chromatin', *Nature*, 505(7485), pp. 648-653.

O'Neill, R. E., Talon, J. and Palese, P. (1998) 'The influenza virus NEP (NS2 protein) mediates the nuclear export of viral ribonucleoproteins', EMBO J, 17(1), pp. 288-96.

Opal, P., Garcia, J. J., McCall, A. E., Xu, B. S., Weeber, E. J., Sweatt, J. D., Orr, H. T. and Zoghbi, H. Y. (2004) 'Generation and characterization of LANP/pp32 null mice', *Molecular and Cellular Biology*, 24(8), pp. 3140-3149.

Ortega, J., Martin-Benito, J., Zurcher, T., Valpuesta, J. M., Carrascosa, J. L. and Ortin, J. (2000) 'Ultrastructural and functional analyses of recombinant influenza virus ribonucleoproteins suggest dimerization of nucleoprotein during virus amplification', *Journal of Virology*, 74(1), pp. 156-163.

Paine, P. L., Moore, L. C. and Horowitz, S. B. (1975) 'NUCLEAR-ENVELOPE PERMEABILITY', *Nature*, 254(5496), pp. 109-114.

Pal, S., Santos, A., Rosas, J. M., Ortiz-Guzman, J. and Rosas-Acosta, G. (2011) 'Influenza A virus interacts extensively with the cellular SUMOylation system during infection', *Virus Research*, 158(1-2), pp. 12-27.

Pan, W., da Graca, L. S., Shao, Y. F., Yin, Q., Wu, H. and Jiang, X. J. (2009) 'PHAPI/pp32 Suppresses Tumorigenesis by Stimulating Apoptosis', *Journal of Biological Chemistry*, 284(11), pp. 6946-6954.

Paterson, D., te Velthuis, A. J. W., Vreede, F. T. and Fodor, E. (2014) 'Host Restriction of Influenza Virus Polymerase Activity by PB2 627E Is Diminished on Short Viral Templates in a Nucleoprotein-Independent Manner', *Journal of Virology*, 88(1), pp. 339-344.

Pegoraro, G., Marcello, A., Myers, M. P. and Giacca, M. (2006) 'Regulation of adeno-associated virus DNA replication by the cellular TAF-I/Set complex', *Journal of Virology*, 80(14), pp. 6855-6864.

Peng, T. Y., Lee, K. R. and Tarn, W. Y. (2008) 'Phosphorylation of the arginine/serine dipeptide-rich motif of the severe acute respiratory syndrome coronavirus nucleocapsid protein modulates its multimerization, translation inhibitory activity and cellular localization', *Febs Journal*, 275(16), pp. 4152-4163.

Peng, W. J., de Vries, R. P., Grant, O. C., Thompson, A. J., McBride, R., Tsogtbaatar, B., Lee, P. S., Razi, N., Wilson, I. A., Woods, R. J. and Paulson, J. C. (2017) 'Recent H3N2 Viruses Have Evolved Specificity for Extended, Branched Human-type Receptors, Conferring Potential for Increased Avidity', *Cell Host & Microbe*, 21(1), pp. 23-34.

Perez, J. T., Varble, A., Sachidanandam, R., Zlatev, I., Manoharan, M., Garcia-Sastre, A. and tenOever, B. R. (2010) 'Influenza A virus-generated small RNAs regulate the switch from transcription to replication', *Proceedings of the National Academy of Sciences of the United States of America*, 107(25), pp. 11525-11530.

Perez, J. T., Zlatev, I., Aggarwal, S., Subramanian, S., Sachidanandam, R., Kim, B., Manoharan, M. and Tenoever, B. R. (2012) 'A Small-RNA Enhancer of Viral Polymerase Activity', *Journal of Virology*, 86(24), pp. 13475-13485.

Pflug, A., Guilligay, D., Reich, S. and Cusack, S. (2014) 'Structure of influenza A polymerase bound to the viral RNA promoter', *Nature*, 516(7531), pp. 355-360.

Pflug, A., Lukarska, M., Resa-Infante, P., Reich, S. and Cusack, S. (2017) 'Structural insights into RNA synthesis by the influenza virus transcription-replication machine', *Virus Research*, 234, pp. 103-117.

Poon, I. K. H. and Jans, D. A. (2005) 'Regulation of nuclear transport: Central role in development and transformation?', *Traffic*, 6(3), pp. 173-186.

Poon, L. L. M., Pritlove, D. C., Fodor, E. and Brownlee, G. G. (1999) 'Direct evidence that the poly(A) tail of influenza A virus mRNA is synthesized by reiterative copying of a U track in the virion RNA template', *Journal of Virology*, 73(4), pp. 3473-3476.

Portela, A. and Digard, P. (2002) 'The influenza virus nucleoprotein: a multifunctional RNA-binding protein pivotal to virus replication', *Journal of General Virology*, 83, pp. 723-734.

Potter, C. W. (2001) 'A history of influenza', *Journal of Applied Microbiology*, 91(4), pp. 572-579.

Radrizzani, M., Vila-Ortiz, G., Cafferata, E. G. A., Di Tella, M. C., Gonzalez-Guerrico, A., Perandones, C., Pivetta, O. H., Carminatti, H., Vargas, V. P. I. and Santa-Coloma, T. A. (2001) 'Differential expression of CPD1 during postnatal development in the mouse cerebellum', *Brain Research*, 907(1-2), pp. 162-174.

Reich, S., Guilligay, D. and Cusack, S. (2017) 'An in vitro fluorescence based study of initiation of RNA synthesis by influenza B polymerase', *Nucleic Acids Research*, 45(6), pp. 3353-3368.

Reich, S., Guilligay, D., Pflug, A., Malet, H., Berger, I., Crepin, T., Hart, D., Lunardi, T., Nanao, M., Ruigrok, R. W. H. and Cusack, S. (2014) 'Structural insight into cap-snatching and RNA synthesis by influenza polymerase', *Nature*, 516(7531), pp. 361-366.

Reilly, P. T., Afzal, S., Gorrini, C., Lui, K., Bukhman, Y. V., Wakeham, A., Haight, J., Ling, T. W., Cheung, C. C., Elia, A. J., Turner, P. V. and Mak, T. W. (2011) 'Acidic nuclear phosphoprotein 32kDa (ANP32)B-deficient mouse reveals a hierarchy of ANP32 importance in mammalian development', *Proceedings of the National Academy of Sciences of the United States of America*, 108(25), pp. 10243-10248.

Reilly, P. T., Afzal, S., Wakeham, A., Haight, J., You-Ten, A., Zaugg, K., Dembowy, J., Young, A. and Mak, T. W. (2010) 'Generation and Characterization of the Anp32e-Deficient Mouse', *Plos One*, 5(10), e13597.

Reilly, P. T., Yu, Y., Hamiche, A. and Wang, L. S. (2014) 'Cracking the ANP32 whips: Important functions, unequal requirement, and hints at disease implications', *Bioessays*, 36(11), pp. 1062-1071.

Remy, I. and Michnick, S. W. (2006) 'A highly sensitive protein-protein interaction assay based on Gaussia luciferase', *Nature Methods*, 3(12), pp. 977-979.

Resa-Infante, P. and Gabriel, G. (2013) 'The nuclear import machinery is a determinant of influenza virus host adaptation', *Bioessays*, 35(1), pp. 23-27.

Resa-Infante, P., Jorba, N., Zamarreno, N., Fernandez, Y., Juarez, S. and Ortin, J. (2008) 'The Host-Dependent Interaction of alpha-Importins with Influenza PB2 Polymerase Subunit Is Required for Virus RNA Replication', *Plos One*, 3(12), e3904.

Reuther, P., Giese, S., Gotz, V., Kilb, N., Manz, B., Brunotte, L. and Schwemmle, M. (2014) 'Adaptive Mutations in the Nuclear Export Protein of Human-Derived H5N1 Strains Facilitate a Polymerase Activity-Enhancing Conformation', *Journal of Virology*, 88(1), pp. 263-271.

Rialdi, A., Hultquist, J., Jimenez-Morales, D., Peralta, Z., Campisi, L., Fenouil, R., Moshkina, N., Wang, Z. Z., Laffleur, B., Kaake, R. M., McGregor, M. J., Haas, K., Pefanis, E., Albrecht, R. A., Pache, L., Chanda, S., Jen, J., Ochando, J., Byun, M., Basu, U., Garcia-Sastre, A., Krogan, N., van Bakel, H. and Marazzi, I. (2017) 'The RNA Exosome Syncs IAV-RNAPII Transcription to Promote Viral Ribogenesis and Infectivity', *Cell*, 169(4), pp. 679-692.

Robb, N. C., Smith, M., Vreede, F. T. and Fodor, E. (2009) 'NS2/NEP protein regulates transcription and replication of the influenza virus RNA genome', *Journal of General Virology*, 90, pp. 1398-1407.

Robb, N. C., te Velthuis, A. J. W., Wieneke, R., Tampe, R., Cordes, T., Fodor, E. and Kapanidis, A. N. (2016) 'Single-molecule FRET reveals the pre-initiation and initiation conformations of influenza virus promoter RNA', *Nucleic Acids Research*, 44(21), pp. 10304-10315.

Rodriguez, A., Perez-Gonzalez, A. and Nieto, A. (2011) 'Cellular Human CLE/C14orf166 Protein Interacts with Influenza Virus Polymerase and Is Required for Viral Replication', *Journal of Virology*, 85(22), pp. 12062-12066.

Rossman, J. S. and Lamb, R. A. (2011) 'Influenza virus assembly and budding', *Virology*, 411(2), pp. 229-236.

Rossman, J. S., Leser, G. P. and Lamb, R. A. (2012) 'Filamentous Influenza Virus Enters Cells via Macropinocytosis', *Journal of Virology*, 86(20), pp. 10950-10960.

Santhakumar, D., Rohaim, M., Hussein, H. A., Hawes, P., Ferreira, H. L., Behboudi, S., Iqbal, M., Nair, V., Arns, C. W. and Munir, M. (2018) 'Chicken Interferon-induced Protein with Tetratricopeptide Repeats 5 Antagonizes Replication of RNA Viruses', *Scientific Reports*, 8 (1), 6794.

Sato, Y., Yoshioka, K., Suzuki, C., Awashima, S., Hosaka, Y., Yewdell, J. and Kuroda, K. (2003) 'Localization of influenza virus proteins to nuclear dot 10 structures in influenza virus-infected cells', *Virology*, 310(1), pp. 29-40.

Selman, M., Dankar, S. K., Forbes, N. E., Jia, J. J. and Brown, E. G. (2012) 'Adaptive mutation in influenza A virus non-structural gene is linked to host switching and induces a novel protein by alternative splicing', *Emerging Microbes & Infections*, 1(11), e42.

Seo, S. B., Macfarlan, T., McNamara, P., Hong, R., Mukai, Y., Heo, S. and Chakravarti, D. (2002) 'Regulation of histone acetylation and transcription by nuclear protein pp32, a subunit of the INHAT complex', *Journal of Biological Chemistry*, 277(16), pp. 14005-14010.

Shapiro, G. I., Gurney, T. and Krug, R. M. (1987) 'Influenza-virus gene expression- control mechanisms at early and late times of infection and nuclear-cytoplasmic transport of virus-specific RNAs', *Journal of Virology*, 61(3), pp. 764-773.

Shaw, M. L., Stone, K. L., Colangelo, C. M., Gulcicek, E. E. and Palese, P. (2008) 'Cellular proteins in influenza virus particles', *Plos Pathogens*, 4(6), e1000085.

Shen, S. M., Yu, Y., Wu, Y. L., Cheng, J. K., Wang, L. S. and Chen, G. Q. (2010) 'Downregulation of ANP32B, a novel substrate of caspase-3, enhances caspase-3 activation and apoptosis induction in myeloid leukemic cells', *Carcinogenesis*, 31(3), pp. 419-426.

Shi, Y., Wu, Y., Zhang, W., Qi, J. X. and Gao, G. F. (2014) 'Enabling the 'host jump': structural determinants of receptor-binding specificity in influenza A viruses', *Nature Reviews Microbiology*, 12(12), pp. 822-831.

Shih, S. R. and Krug, R. M. (1996) 'Novel exploitation of a nuclear function by influenza virus: The cellular SF2/ASF splicing factor controls the amount of the essential viral M2 ion channel protein in infected cells', *Embo Journal*, 15(19), pp. 5415-5427.

Shih, S. R., Suen, P. C., Chen, Y. S. and Chang, S. C. (1998) 'A novel spliced transcript of influenza A/WSN/33 virus', *Virus Genes*, 17(2), pp. 179-183.

Shinya, K., Hamm, S., Hatta, M., Ito, H., Ito, T. and Kawaoka, Y. (2004) 'PB2 amino acid at position 627 affects, replicative efficiency, but not cell tropism, of Hong Kong H5N1 influenza A viruses in mice', *Virology*, 320(2), pp. 258-266.

Shinya, K., Makino, A., Ozawa, M., Kim, J. H., Sakai-Tagawa, Y., Ito, M., Quynh, M. L. and Kawaoka, Y. (2009) 'Ostrich Involvement in the Selection of H5N1 Influenza Virus Possessing Mammalian-Type Amino Acids in the PB2 Protein', *Journal of Virology*, 83(24), pp. 13015-13018.

Sieczkarski, S. B. and Whittaker, G. R. (2002) 'Influenza virus can enter and infect cells in the absence of clathrin-mediated endocytosis', *Journal of Virology*, 76(20), pp. 10455-10464.

Sikora, D., Rocheleau, L., Brown, E. G. and Pelchat, M. (2017) 'Influenza A virus cap-snatches host RNAs based on their abundance early after infection', *Virology*, 509, pp. 167-177.

Smith, G. L. and Hay, A. J. (1982) 'Replication of the influenza-virus genome', *Virology*, 118(1), pp. 96-108.

Staller, E., Neasham. P.J., Sheppard, C.M., Mistry, B., Peacock, T.P., Goldhill, D.H., Long, J.S and Barclay, W.S. 'ANP32 proteins are essential for influenza virus replication in human cells.' *In review.*

Steel, J., Lowen, A. C., Mubareka, S. and Palese, P. (2009) 'Transmission of Influenza Virus in a Mammalian Host Is Increased by PB2 Amino Acids 627K or 627E/701N', *Plos Pathogens*, 5(1), e1000252.

Su, W. C., Hsu, S. F., Lee, Y. Y., Jeng, K. S. and Lai, M. M. C. (2015) 'A Nucleolar Protein, Ribosomal RNA Processing 1 Homolog B (RRP1B), Enhances the Recruitment of Cellular mRNA in Influenza Virus Transcription', *Journal of Virology*, 89(22), pp. 11245-11255.

Subbarao, E. K., London, W. and Murphy, B. R. (1993) 'A single amino-acid in the PB2 gene of influenza A virus is a determinant of host range', *Journal of Virology*, 67(4), pp. 1761-1764.

Sugiyama, K., Kawaguchi, A., Okuwaki, M. and Nagata, K. (2015) 'pp32 and APRIL are host cell-derived regulators of influenza virus RNA synthesis from cRNA', *Elife*, 4, e08939.

Sun, W., Kimura, H., Hattori, N., Tanaka, S., Matsuyama, S. and Shiota, K. (2006) 'Proliferation related acidic leucine-rich protein PAL31 functions as a caspase-3 inhibitor', *Biochemical and Biophysical Research Communications*, 342(3), pp. 817-823.

Sutton, T. C. (2018) 'The Pandemic Threat of Emerging H5 and H7 Avian Influenza Viruses', *Viruses-Basel*, 10(9), e461.

Tarendeau, F., Boudet, J., Guilligay, D., Mas, P. J., Bougault, C. M., Boulo, S., Baudin, F., Ruigrok, R. W. H., Daigle, N., Ellenberg, J., Cusack, S., Simorre, J. P. and Hart, D. J. (2007) 'Structure and nuclear import function of the C-terminal domain of influenza virus polymerase PB2 subunit', *Nature Structural & Molecular Biology*, 14(3), pp. 229-233.

Tarendeau, F., Crepin, T., Guilligay, D., Ruigrok, R. W. H., Cusack, S. and Hart, D. J. (2008) 'Host determinant residue lysine 627 lies on the surface of a discrete, folded domain of influenza virus polymerase PB2 subunit', *Plos Pathogens*, 4(8), e1000136.

te Velthuis, A. J. W. and Fodor, E. (2016a) 'Influenza virus RNA polymerase: insights into the mechanisms of viral RNA synthesis', *Nature Reviews Microbiology*, 14(8), pp. 479-493.

te Velthuis, A. J. W., Robb, N. C., Kapanidis, A. N. and Fodor, E. (2016b) 'The role of the priming loop in influenza A virus RNA synthesis', *Nature Microbiology*, 1(5), 16029.

Thierry, E., Guilligay, D., Kosinski, J., Bock, T., Gaudon, S., Round, A., Pflug, A., Hengrung, N., El Omari, K., Baudin, F., Hart, D. J., Beck, M. and Cusack, S. (2016) 'Influenza Polymerase Can Adopt an Alternative Configuration Involving a Radical Repacking of PB2 Domains', *Molecular Cell*, 61(1), pp. 125-137.

Tochio, N., Umehara, T., Munemasa, Y., Suzuki, T., Sato, S., Tsuda, K., Koshiba, S., Kigawa, T., Nagai, R. and Yokoyama, S. (2010) 'Solution Structure of Histone Chaperone ANP32B: Interaction with Core Histones H3-H4 through Its Acidic Concave Domain', *Journal of Molecular Biology*, 401(1), pp. 97-114.

Tong, S. X., Li, Y., Rivailler, P., Conrardy, C., Castillo, D. A. A., Chen, L. M., Recuenco, S., Ellison, J. A., Davis, C. T., York, I. A., Turmelle, A. S., Moran, D., Rogers, S., Shi, M., Tao, Y., Weil, M. R., Tang, K., Rowe, L. A., Sammons, S., Xu, X. Y., Frace, M., Lindblade, K. A., Cox, N. J., Anderson, L. J., Rupprecht, C. E. and Donis, R. O. (2012) 'A distinct lineage of influenza A virus from bats', *Proceedings of the National Academy of Sciences of the United States of America*, 109(11), pp. 4269-4274.

Tong, S. X., Zhu, X. Y., Li, Y., Shi, M., Zhang, J., Bourgeois, M., Yang, H., Chen, X. F., Recuenco, S., Gomez, J., Chen, L. M., Johnson, A., Tao, Y., Dreyfus, C., Yu, W. L., McBride, R., Carney, P. J., Gilbert, A. T., Chang, J., Guo, Z., Davis, C. T., Paulson, J. C., Stevens, J., Rupprecht, C. E., Holmes, E. C., Wilson, I. A. and Donis, R. O. (2013) 'New World Bats Harbor Diverse Influenza A Viruses', *Plos Pathogens*, 9(10), e1003657.

Tsai, P. L., Chiou, N. T., Kuss, S., Garcia-Sastre, A., Lynch, K. W. and Fontoura, B. M. A. (2013) 'Cellular RNA Binding Proteins NS1-BP and hnRNP K Regulate Influenza A Virus RNA Splicing', *Plos Pathogens*, 9(6), e1003460.

Tscherne, D. M. and Garcia-Sastre, A. (2011) 'Virulence determinants of pandemic influenza viruses', *Journal of Clinical Investigation*, 121(1), pp. 6-13.

Tsujio, I., Zaidi, T., Xu, J. L., Kotula, L., Grundke-Iqbal, I. and Iqbal, K. (2005) 'Inhibitors of protein phosphatase-2A from human brain structures, immunocytological localization and activities towards dephosphorylation of the Alzheimer type hyperphosphorylated tau', *Febs Letters*, 579(2), pp. 363-372.

Turrell, L., Hutchinson, E. C., Vreede, F. T. and Fodor, E. (2015) 'Regulation of Influenza A Virus Nucleoprotein Oligomerization by Phosphorylation', *Journal of Virology*, 89(2), pp. 1452-1455.

Ulitzur, N., Humbert, M. and Pfeffer, S. R. (1997a) 'Mapmodulin: A possible modulator of the interaction of microtubule-associated proteins with microtubules', *Proceedings of the National Academy of Sciences of the United States of America*, 94(10), pp. 5084-5089.

Ulitzur, N., Rancano, C. and Pfeffer, S. R. (1997b) 'Biochemical characterization of mapmodulin, a protein that binds microtubule-associated proteins', *Journal of Biological Chemistry*, 272(48), pp. 30577-30582.

van Riel, D., Leijten, L. M. E., de Graaf, M., Siegers, J. Y., Short, K. R., Spronken, M. I. J., Schrauwen, E. J. A., Fouchier, R. A. M., Osterhaus, A. and Kuiken, T. (2013) 'Novel Avian-Origin Influenza A (H7N9) Virus Attaches to Epithelium in Both Upper and Lower Respiratory Tract of Humans', *American Journal of Pathology*, 183(4), pp. 1137-1143.

Ver, L. S., Marcos-Villar, L., Landeras-Bueno, S., Nieto, A. and Ortin, J. (2015) 'The Cellular Factor NXP2/MORC3 Is a Positive Regulator of Influenza Virus Multiplication', *Journal of Virology*, 89(19), pp. 10023-10030.

Vidic, J., Noiray, M., Bagchi, A. and Slama-Schwok, A. (2016) 'Identification of a Novel Complex between the Nucleoprotein and PA(1-27) of Influenza A Virus Polymerase', *Biochemistry*, 55(31), pp. 4259-4262.

Volmer, R., Mazel-Sanchez, B., Volmer, C., Soubies, S. M. and Guerin, J. L. (2010) 'Nucleolar localization of influenza A NS1: striking differences between mammalian and avian cells', *Virology Journal*, 7, 63.

Vreede, F. T. and Brownlee, G. G. (2007) 'Influenza virion-derived viral ribonucleoproteins synthesize both mRNA and cRNA in vitro', *Journal of Virology*, 81(5), pp. 2196-2204.

Vreede, F. T. and Fodor, E. (2010) 'Mechanisms and functional implications of the degradation of host RNA polymerase II in influenza virus infected cells', *Virulence*, 1(5), pp. 436-439.

Vreede, F. T., Jung, T. E. and Brownlee, G. G. (2004) 'Model suggesting that replication of influenza virus is regulated by stabilization of replicative intermediates', *Journal of Virology*, 78(17), pp. 9568-9572.

Wang, B., Chen, Y., Mu, C. Y., Su, Y. H., Liu, R., Huang, Z. Y., Li, Y., Yu, Q. M., Chang, G. B., Xu, Q. and Chen, G. H. (2015) 'Identification and Expression Analysis of the Interferon-Induced Protein with Tetratricopeptide Repeats 5 (IFIT5) Gene in Duck (Anas platyrhynchos domesticus)', *Plos One*, 10(3), e0121065.

Wang, H. Y., Lin, W., Dyck, J. A., Yeakley, J. M., Zhou, S. Y., Cantley, L. C. and Fu, X. D. (1998) 'SRPK2: A differentially expressed SR protein-specific kinase involved in mediating the interaction and localization of pre-mRNA splicing factors in mammalian cells', *Journal of Cell Biology*, 140(4), pp. 737-750.

Wang, J., Wang, Y. J., Zhou, R., Zhao, J. Y., Zhang, Y. X., Yi, D. R., Li, Q. J., Zhou, J. M., Guo, F., Liang, C., Li, X. Y. and Cen, S. (2018) 'Host Long Noncoding RNA lncRNA-PAAN Regulates the Replication of Influenza A Virus', *Viruses-Basel*, 10(6), 330.

Wang, L. Y., Fu, B. S., Li, W. J., Patil, G., Liu, L., Dorf, M. E. and Li, S. T. (2017) 'Comparative influenza protein interactomes identify the role of plakophilin 2 in virus restriction', *Nature Communications*, 8, 13876.

Wang, P., Palese, P. and Oneill, R. E. (1997) 'The NPI-1/NPI-3 (Karyopherin alpha) binding site on the influenza A virus nucleoprotein NP is a nonconventional nuclear localization signal', *Journal of Virology*, 71(3), pp. 1850-1856.

Watanabe, T., Kawakami, E., Shoemaker, J. E., Lopes, T. J. S., Matsuoka, Y., Tomita, Y., Kozuka-Hata, H., Gorai, T., Kuwahara, T., Takeda, E., Nagata, A., Takano, R., Kiso, M., Yamashita, M., Sakai-Tagawa, Y., Katsura, H., Nonaka, N., Fujii, H., Fujii, K., Sugita, Y., Noda, T., Goto, H., Fukuyama, S., Watanabe, S., Neumann, G., Oyama, M., Kitano, H. and Kawaoka, Y. (2014) 'Influenza Virus-Host Interactome Screen as a Platform for Antiviral Drug Development', *Cell Host & Microbe*, 16(6), pp. 795-805.

Weber, M., Sediri, H., Felgenhauer, U., Binzen, I., Banfer, S., Jacob, R., Brunotte, L., Garcia-Sastre, A., Schmid-Burgk, J. L., Schmidt, T., Hornung, V., Kochs, G., Schwemmle, M., Klenk, H. D. and Weber, F. (2015) 'Influenza Virus Adaptation PB2-627K Modulates Nucleocapsid Inhibition by the Pathogen Sensor RIG-I', *Cell Host & Microbe*, 17(3), pp. 309-319.

Wei, X. L., Liu, Z. X., Wang, J. J., Yang, R. P., Yang, J., Guo, Y., Tan, H. B., Chen, H. Y., Liu, Q. and Liu, L. (2019) 'The interaction of cellular protein ANP32A with influenza A virus polymerase component PB2 promotes vRNA synthesis', Archives of Virology, 164(3), pp. 787-798.

White, S. K., Ma, W. J., McDaniel, C. J., Gray, G. C. and Lednicky, J. A. (2016) 'Serologic evidence of exposure to influenza D virus among persons with occupational contact with cattle', *Journal of Clinical Virology*, 81, pp. 31-33.

Whittaker, G., Bui, M. and Helenius, A. (1996) 'Nuclear trafficking of influenza virus ribonucleoproteins in heterokaryons', *Journal of Virology*, 70(5), pp. 2743-2756.

Wise, H. M., Foeglein, A., Sun, J. C., Dalton, R. M., Patel, S., Howard, W., Anderson, E. C., Barclay, W. S. and Digard, P. (2009) 'A Complicated Message: Identification of a Novel PB1-Related Protein Translated from Influenza A Virus Segment 2 mRNA', *Journal of Virology*, 83(16), pp. 8021-8031.

Wise, H. M., Hutchinson, E. C., Jagger, B. W., Stuart, A. D., Kang, Z. H., Robb, N., Schwartzman, L. M., Kash, J. C., Fodor, E., Firth, A. E., Gog, J. R., Taubenberger, J. K. and Digard, P. (2012) 'Identification of a Novel Splice Variant Form of the Influenza A Virus M2 Ion Channel with an Antigenically Distinct Ectodomain', *Plos Pathogens*, 8(11), e1002998.

World Health Organisation. www.who.int/en/news-room/fact-sheets/detail/influenza-(avian-and-other-zoonotic) Accessed Feb 2019

Xiong, Z. C., Ye, L. P., He, Z. Y., Li, F. Y., Xiong, Y. H., Lin, C. Y., Wu, X. Q., Deng, G. Z., Shi, W., Song, L. B., Yuan, Z. Y. and Wang, X. (2018) 'ANP32E induces tumorigenesis of triple-negative breast cancer cells by upregulating E2F1', *Molecular Oncology*, 12(6), pp. 896-912.

Xue, Y. M., Johnson, J. S., Ornelles, D. A., Lieberman, J. and Engel, D. A. (2005) 'Adenovirus protein VII functions throughout early phase and interacts with cellular proteins SET and pp32', *Journal of Virology*, 79(4), pp. 2474-2483.

Yamayoshi, S., Watanabe, M., Goto, H. and Kawaoka, Y. (2016) 'Identification of a Novel Viral Protein Expressed from the PB2 Segment of Influenza A Virus', *Journal of Virology*, 90(1), pp. 444-456.

Yan, W., Bai, Z., Wang, J. A., Li, X. M., Chi, B. X. and Chen, X. (2017) 'ANP32A modulates cell growth by regulating p38 and Akt activity in colorectal cancer', *Oncology Reports*, 38(3), pp. 1605-1612.

Yang, C., Liu, X. K., Gao, Q. X., Cheng, T. L., Xiao, R., Ming, F., Zhang, S. S., Jin, M. L., Chen, H. C., Ma, W. J. and Zhou, H. B. (2018a) 'The Nucleolar Protein LYAR Facilitates Ribonucleoprotein Assembly of Influenza A Virus', *Journal of Virology*, 92(23), e01042-18.

Yang, X. J., Lu, B., Sun, X. Q., Han, C. J., Fu, C. L., Xu, K. L., Wang, M., Li, D. J., Chen, Z. C., Opal, P., Wen, Q., Crispino, J. D., Wang, Q. F. and Huang, Z. (2018b) 'ANP32A regulates histone H3 acetylation and promotes leukemogenesis', *Leukemia*, 32(7), pp. 1587-1597.

Yanguez, E. and Nieto, A. (2011) 'So similar, yet so different: Selective translation of capped and polyadenylated viral mRNAs in the influenza virus infected cell', *Virus Research*, 156(1-2), pp. 1-12.

Ye, Q. Z., Krug, R. M. and Tao, Y. Z. J. (2006) 'The mechanism by which influenza A virus nucleoprotein forms oligomers and binds RNA', *Nature*, 444(7122), pp. 1078-1082.

York, A., Hengrung, N., Vreede, F. T., Huiskonen, J. T. and Fodor, E. (2013) 'Isolation and characterization of the positive-sense replicative intermediate of a negative-strand RNA virus', *Proceedings of the National Academy of Sciences of the United States of America*, 110(45), pp. E4238-E4245.

York, A., Hutchinson, E. C. and Fodor, E. (2014) 'Interactome Analysis of the Influenza A Virus Transcription/Replication Machinery Identifies Protein Phosphatase 6 as a Cellular Factor Required for Efficient Virus Replication', *Journal of Virology*, 88(22), pp. 13284-13299.

Zamarin, D., Ortigoza, M. B. and Palese, P. (2006) 'Influenza A virus PB1-F2 protein contributes to viral pathogenesis in mice', *Journal of Virology*, 80(16), pp. 7976-7983.

Zamora-Caballero, S., Siauciunaite-Gaubard, L. and Bravo, J. (2015) 'High-resolution crystal structure of the leucine-rich repeat domain of the human tumour suppressor PP32A (ANP32A)', *Acta Crystallographica Section F-Structural Biology Communications*, 71, pp. 684-687.

Zhang, H., Zhang, Z., Wang, Y., Wang, M., Wang, X., Zhang, X., Ji, S., Du, C. and Chen, H. (2019) 'Fundamental contribution and host range determination of ANP32A and ANP32B in influenza A virus polymerase activity', *J Virol*, 93(13), e00174-19

Zhang, J. J., Li, G. and Ye, X. (2010) 'Cyclin T1/CDK9 Interacts with Influenza A Virus Polymerase and Facilitates Its Association with Cellular RNA Polymerase II', *Journal of Virology*, 84(24), pp. 12619-12627.

Zhang, S. P., Tian, H. Y., Cui, J. M., Xiao, J., Wang, M. and Hu, Y. X. (2016) 'The c-Jun N-terminal kinase (JNK) is involved in H5N1 influenza A virus RNA and protein synthesis', *Archives of Virology*, 161(2), pp. 345-351.

Zhirnov, O. P., Poyarkov, S. V., Vorob'eva, I. V., Safonova, O. A., Malyshev, N. A. and Klenk, H. D. (2007) 'Segment NS of influenza a virus contains an additional gene NSP in positive-sense orientation', *Doklady Biochemistry and Biophysics*, 414(1), pp. 127-133.

Zhou, B., Li, Y., Halpin, R., Hine, E., Spiro, D. J. and Wentworth, D. E. (2011) 'PB2 Residue 158 Is a Pathogenic Determinant of Pandemic H1N1 and H5 Influenza A Viruses in Mice', *Journal of Virology*, 85(1), pp. 357-365.

Zhou, Z., Cao, M. M., Guo, Y., Zhao, L. L., Wang, J. F., Jia, X., Li, J. G., Wang, C. H., Gabriel, G., Xue, Q. H., Yi, Y. H., Cui, S., Jin, Q., Wang, J. W. and Deng, T. (2014) 'Fragile X mental retardation protein stimulates ribonucleoprotein assembly of influenza A virus', *Nature Communications*, 5, 3259.

Zhou, Z. H., Qiu, J. S., Liu, W., Zhou, Y., Plocinik, R. M., Li, H., Hu, Q. D., Ghosh, G., Adams, J. A., Rosenfeld, M. G. and Fu, X. D. (2012) 'The Akt-SRPK-SR Axis Constitutes a Major Pathway in Transducing EGF Signaling to Regulate Alternative Splicing in the Nucleus', *Molecular Cell*, 47(3), pp. 422-433.

Zhu, B. D., Li, X. L., Liu, Y., Chang, J., Zhang, D. D., Wang, Q. A., Ren, J. and Cui, C. P. (2010) 'Involvement of Hepatopoietin Cn in the development of human hepatocellular carcinoma', *Clinical & Experimental Metastasis*, 27(8), pp. 571-580.

Zimber, A., Nguyen, Q. D. and Gespach, C. (2004) 'Nuclear bodies and compartments: Functional roles and cellular signalling in health and disease', *Cellular Signalling*, 16(10), pp. 1085-1104.

Appendices

Appendix A

Proteins interacting with viral polymerase identified by mass spectrometry. Values represent abundance of each protein calculated by the sum of the area under the curve for each peptide for that protein. A linear discriminative function score was calculated to measure the probability of accurate protein identification using PEAKS software. This value was converted to -10lgP. Only proteins with −10lgP ≥ 20 (p<0.01) were included.

Accession	Pol 627E	Pol 627E	Pol 627E + chANP32A	Pol 627E + chANP32A	Pol 627K	Pol 627K	GFP-flag	GFP-flag	Significance (-10lgP)
5092_PA-GFP	9.99E+08	1.07E+09	1.11E+09	1.01E+09	9.73E+07	2.21E+08	1.53E+06	1.39E+06	200
5092_PB1	7.26E+08	7.08E+08	6.29E+08	7.84E+08	5.15E+08	6.56E+08	7.91E+05	5.92E+05	200
5092_PB2	7.41E+08	5.77E+08	6.67E+08	6.52E+08	2.95E+08	4.19E+08	1.69E+06	8.21E+05	200
P19338|NUCL_HUMAN	6.71E+07	6.74E+07	7.02E+07	7.67E+07	4.71E+07	1.51E+08	6.82E+05	5.45E+05	200
Q04837|SSBP_HUMAN	6.89E+07	6.70E+07	4.96E+07	6.65E+07	6.29E+07	1.37E+08	1.78E+05	1.52E+05	200
P06748|NPM_HUMAN	2.94E+07	3.09E+07	2.24E+07	3.75E+07	6.43E+07	7.38E+07	0	0	200
P18124|RL7_HUMAN	2.36E+07	1.88E+07	2.38E+07	3.50E+07	4.70E+07	6.32E+07	1.89E+04	1.28E+04	200
P36578|RL4_HUMAN	2.05E+07	1.73E+07	2.29E+07	3.17E+07	4.71E+07	5.67E+07	0	1.91E+04	200
P52272|HNRPM_HUMAN	2.62E+07	1.56E+07	2.54E+07	2.99E+07	4.65E+07	6.21E+07	1.83E+05	8.91E+04	200
P05388|RLA0_HUMAN	2.20E+07	1.61E+07	2.18E+07	2.66E+07	3.74E+07	5.25E+07	1.25E+05	8.98E+04	200
P30050|RL12_HUMAN	1.71E+07	1.65E+07	1.79E+07	2.24E+07	4.93E+07	5.23E+07	1.45E+05	1.08E+05	200
P62424|RL7A_HUMAN	1.64E+07	1.37E+07	1.54E+07	1.46E+07	4.03E+07	3.71E+07	0	0	200
P62913|RL11_HUMAN	1.68E+07	1.29E+07	1.30E+07	1.91E+07	3.45E+07	4.53E+07	1.69E+05	5.47E+04	200
P62906|RL10A_HUMAN	1.57E+07	1.29E+07	1.50E+07	2.07E+07	3.18E+07	4.31E+07	0	0	200
P55084|ECHB_HUMAN	3.76E+07	3.52E+07	2.40E+07	2.71E+07	3.56E+07	4.11E+07	0	0	200
Q07020|RL18_HUMAN	1.22E+07	1.03E+07	1.32E+07	2.13E+07	3.28E+07	3.30E+07	0	0	200
O00505|IMA4_HUMAN	2.74E+07	1.99E+07	2.18E+07	2.79E+07	2.63E+07	3.41E+07	1.06E+05	4.17E+04	200

P50914|RL14_HUMAN	1.24E+07	1.29E+07	1.64E+07	2.55E+07	2.40E+07	2.74E+07	0	0	200
P09651|ROA1_HUMAN	9.59E+06	6.91E+06	8.52E+06	9.39E+06	2.66E+07	2.82E+07	0	0	200
P26373|RL13_HUMAN	1.16E+07	1.24E+07	1.36E+07	1.74E+07	2.75E+07	2.49E+07	0	0	200
P62888|RL30_HUMAN	1.12E+07	1.32E+07	1.16E+07	1.84E+07	2.38E+07	2.74E+07	5.91E+04	4.70E+04	200
P35268|RL22_HUMAN	7.48E+06	9.06E+06	8.26E+06	1.12E+07	2.48E+07	2.29E+07	0	0	200
P62917|RL8_HUMAN	9.99E+06	8.40E+06	1.04E+07	1.59E+07	2.41E+07	2.22E+07	0	0	200
P15880|RS2_HUMAN	1.23E+07	1.36E+07	1.09E+07	1.40E+07	1.45E+07	2.24E+07	0	0	200
P62263|RS14_HUMAN	1.32E+07	1.09E+07	9.35E+06	8.42E+06	1.84E+07	2.43E+07	3.76E+04	2.02E+04	200
P62280|RS11_HUMAN	1.11E+07	9.85E+06	8.27E+06	1.07E+07	1.91E+07	2.02E+07	0	0	200
P34741|SDC2_HUMAN	9.88E+06	7.17E+06	4.75E+06	5.08E+06	1.71E+07	1.98E+07	0	0	200
P08865|RSSA_HUMAN	1.30E+07	7.84E+06	6.95E+06	7.36E+06	1.37E+07	2.75E+07	0	0	200
GFP-strep-flag	1.41E+06	3.50E+06	3.43E+06	3.83E+06	3.34E+07	2.01E+07	1.59E+09	1.77E+09	200
P60866|RS20_HUMAN	1.34E+07	6.74E+06	8.60E+06	1.09E+07	1.87E+07	2.18E+07	2.70E+04	1.44E+04	200
P62829|RL23_HUMAN	8.77E+06	9.80E+06	7.28E+06	1.10E+07	1.60E+07	1.82E+07	3.45E+04	5.19E+04	200
P62899|RL31_HUMAN	1.07E+07	6.62E+06	1.33E+07	1.51E+07	1.75E+07	2.84E+07	0	0	200
P62277|RS13_HUMAN	1.10E+07	9.03E+06	7.98E+06	1.08E+07	1.84E+07	1.52E+07	0	0	200
P52597|HNRPF_HUMAN	8.45E+06	9.92E+06	4.23E+06	8.32E+06	1.80E+07	1.59E+07	6.97E+04	6.49E+04	200
P46778|RL21_HUMAN	7.43E+06	3.71E+06	6.62E+06	1.07E+07	1.55E+07	1.42E+07	0	0	200
P83731|RL24_HUMAN	8.56E+06	5.55E+06	7.05E+06	9.45E+06	1.26E+07	1.84E+07	0	0	200
Q86V81|THOC4_HUMAN	4.69E+06	4.71E+06	6.53E+06	8.84E+06	1.62E+07	1.55E+07	2.44E+04	1.27E+04	200
P46779|RL28_HUMAN	8.30E+06	5.11E+06	6.50E+06	1.08E+07	1.19E+07	1.73E+07	0	0	200
Q8IZL8|PELP1_HUMAN	8.35E+06	8.90E+06	6.36E+06	7.71E+06	1.08E+07	1.54E+07	0	0	200
P61247|RS3A_HUMAN	1.52E+07	1.37E+07	1.40E+07	1.82E+07	1.43E+07	2.23E+07	1.75E+05	1.55E+05	200
P62269|RS18_HUMAN	1.47E+07	6.24E+06	1.08E+07	1.47E+07	1.19E+07	2.45E+07	3.25E+04	6.45E+03	200
P61353|RL27_HUMAN	9.29E+06	1.06E+07	7.96E+06	1.39E+07	1.61E+07	1.93E+07	0	0	200
P31943|HNRH1_HUMAN	7.83E+06	7.28E+06	4.58E+06	4.72E+06	1.34E+07	1.40E+07	0	0	200
P62701|RS4X_HUMAN	1.01E+07	9.29E+06	8.74E+06	1.12E+07	1.60E+07	1.73E+07	0	0	200
P05387|RLA2_HUMAN	2.91E+06	6.36E+06	4.75E+06	9.97E+06	1.71E+07	1.11E+07	0	0	200
P62910|RL32_HUMAN	5.59E+06	3.05E+06	5.02E+06	8.23E+06	1.58E+07	1.28E+07	1.05E+04	0	200
P62750|RL23A_HUMAN	6.04E+06	6.24E+06	7.59E+06	9.99E+06	1.02E+07	1.70E+07	0	5.18E+03	200

P62851|RS25_HUMAN	9.28E+06	9.27E+06	7.16E+06	8.69E+06	1.31E+07	1.17E+07	0	0	200
P49207|RL34_HUMAN	5.86E+06	5.69E+06	5.17E+06	8.10E+06	1.14E+07	1.25E+07	0	0	200
P23396|RS3_HUMAN	1.42E+07	1.15E+07	9.90E+06	1.31E+07	1.25E+07	1.72E+07	8.44E+04	8.80E+04	200
Q02543|RL18A_HUMAN	5.60E+06	4.12E+06	5.09E+06	7.78E+06	1.30E+07	1.19E+07	0	0	200
P17844|DDX5_HUMAN	4.82E+06	6.16E+06	6.77E+06	7.90E+06	1.24E+07	1.15E+07	1.72E+04	0	200
P61513|RL37A_HUMAN	5.10E+06	4.50E+06	4.82E+06	6.57E+06	1.26E+07	1.10E+07	0	0	200
P46783|RS10_HUMAN	8.50E+06	8.64E+06	6.72E+06	7.04E+06	1.20E+07	1.54E+07	1.43E+04	1.46E+04	200
P39023|RL3_HUMAN	2.01E+07	1.65E+07	1.72E+07	1.84E+07	1.22E+07	1.50E+07	0	0	200
P40429|RL13A_HUMAN	7.38E+06	9.05E+06	9.54E+06	1.57E+07	1.13E+07	1.12E+07	0	0	200
P62249|RS16_HUMAN	1.16E+07	6.16E+06	7.44E+06	8.86E+06	1.20E+07	1.39E+07	1.88E+04	1.06E+04	200
P42766|RL35_HUMAN	3.46E+06	2.05E+06	3.21E+06	5.87E+06	1.10E+07	1.15E+07	0	0	200
Q02878|RL6_HUMAN	4.73E+06	4.50E+06	5.84E+06	1.04E+07	1.24E+07	1.38E+07	0	0	200
P61313|RL15_HUMAN	5.93E+06	5.33E+06	7.77E+06	1.18E+07	1.40E+07	1.06E+07	0	0	200
P62753|RS6_HUMAN	1.28E+07	1.03E+07	1.10E+07	1.42E+07	9.18E+06	1.18E+07	0	0	200
Q7L2E3|DHX30_HUMAN	6.33E+06	6.85E+06	5.12E+06	7.51E+06	9.61E+06	1.11E+07	0	0	200
P46781|RS9_HUMAN	6.45E+06	6.77E+06	5.23E+06	9.13E+06	1.22E+07	7.62E+06	0	0	200
P08708|RS17_HUMAN	7.56E+06	6.18E+06	6.47E+06	7.23E+06	1.51E+07	1.07E+07	0	0	200
P11940|PABP1_HUMAN	8.71E+06	4.59E+06	2.95E+06	2.28E+06	8.60E+06	1.07E+07	0	0	200
Q9NZI8|IF2B1_HUMAN	4.31E+06	3.47E+06	4.32E+06	5.95E+06	8.08E+06	1.05E+07	1.00E+04	3.90E+03	200
P62244|RS15A_HUMAN	5.14E+06	4.33E+06	3.93E+06	4.59E+06	9.55E+06	8.85E+06	0	0	200
Q9H0D6|XRN2_HUMAN	5.24E+06	5.31E+06	5.01E+06	5.54E+06	7.86E+06	9.04E+06	0	0	200
P39019|RS19_HUMAN	6.32E+06	6.91E+06	3.75E+06	7.08E+06	9.29E+06	1.15E+07	0	1.37E+04	200
O15355|PPM1G_HUMAN	1.22E+07	1.48E+07	1.03E+07	1.35E+07	6.61E+06	8.65E+06	0	0	200
Q96PK6|RBM14_HUMAN	3.61E+06	3.41E+06	3.04E+06	3.81E+06	8.11E+06	7.92E+06	0	0	200
P32969|RL9_HUMAN	5.10E+06	4.53E+06	4.81E+06	7.45E+06	5.76E+06	1.19E+07	0	0	200
Q9H0A0|NAT10_HUMAN	6.99E+06	7.58E+06	5.68E+06	7.38E+06	9.58E+06	7.98E+06	3.79E+04	0	200
Q8WV44|TRI41_HUMAN	6.40E+06	6.91E+06	4.32E+06	5.18E+06	7.66E+06	7.90E+06	4.98E+04	2.93E+04	200
Q12905|ILF2_HUMAN	5.77E+06	5.60E+06	2.83E+06	7.72E+06	1.16E+07	7.74E+06	7.44E+05	0	200
P62854|RS26_HUMAN	5.02E+06	6.59E+06	4.54E+06	6.54E+06	8.99E+06	8.09E+06	0	0	200
P25398|RS12_HUMAN	4.04E+06	6.68E+06	2.94E+06	7.64E+06	6.02E+06	1.08E+07	0	0	200

260

P67809|YBOX1_HUMAN	4.56E+06	6.92E+06	4.19E+06	5.55E+06	8.03E+06	9.33E+06	0	0	200
P27635|RL10_HUMAN	5.42E+06	5.37E+06	6.22E+06	7.94E+06	7.20E+06	1.07E+07	0	0	200
P16104|H2AX_HUMAN	5.74E+06	3.17E+06	5.86E+06	8.26E+06	6.83E+06	7.98E+06	0	0	200
P78347|GTF2I_HUMAN	1.10E+07	8.24E+06	5.98E+06	4.77E+06	6.44E+06	1.03E+07	7.18E+04	0	200
P62081|RS7_HUMAN	1.03E+07	1.03E+07	1.42E+07	1.69E+07	4.73E+06	1.34E+07	6.75E+04	7.50E+04	200
P63272|SPT4H_HUMAN	3.31E+06	2.35E+06	2.16E+06	3.30E+06	5.95E+06	7.28E+06	2.89E+04	2.07E+04	200
P84103|SRSF3_HUMAN	5.24E+06	4.11E+06	3.66E+06	5.11E+06	6.82E+06	8.11E+06	0	0	200
O00410|IPO5_HUMAN	1.20E+07	1.03E+07	8.96E+06	9.08E+06	4.88E+06	1.20E+07	0	0	200
Q16778|H2B2E_HUMAN	3.65E+06	3.30E+06	4.73E+06	5.31E+06	6.90E+06	6.55E+06	1.35E+04	1.10E+04	200
P83881|RL36A_HUMAN	4.40E+06	3.92E+06	4.26E+06	4.46E+06	6.12E+06	6.29E+06	0	0	200
Q9Y230|RUVB2_HUMAN	4.67E+06	4.54E+06	3.72E+06	3.72E+06	6.31E+06	6.23E+06	3.68E+03	0	200
P10644|KAP0_HUMAN	4.70E+06	4.11E+06	1.75E+06	2.08E+06	5.60E+06	7.13E+06	0	0	200
Q15365|PCBP1_HUMAN	2.75E+06	2.70E+06	2.44E+06	3.09E+06	5.34E+06	5.91E+06	9.62E+04	1.72E+04	200
P46087|NOP2_HUMAN	2.60E+06	3.03E+06	2.60E+06	3.40E+06	6.19E+06	5.68E+06	1.11E+05	0	200
Q12899|TRI26_HUMAN	4.10E+06	4.35E+06	5.63E+06	7.76E+06	3.84E+06	8.61E+06	0	0	200
P62841|RS15_HUMAN	3.48E+06	3.66E+06	2.69E+06	3.93E+06	6.29E+06	4.78E+06	0	0	200
Q12906|ILF3_HUMAN	4.17E+06	3.93E+06	5.08E+06	5.57E+06	4.67E+06	7.57E+06	0	0	200
P61254|RL26_HUMAN	3.66E+06	2.93E+06	3.79E+06	3.05E+06	6.18E+06	6.84E+06	1.81E+04	1.44E+04	200
O15371|EIF3D_HUMAN	4.60E+06	4.50E+06	2.63E+06	2.76E+06	4.41E+06	5.76E+06	7.34E+04	5.08E+04	200
Q92896|GSLG1_HUMAN	3.26E+06	3.18E+06	2.52E+06	2.48E+06	5.23E+06	5.51E+06	0	0	200
Q13610|PWP1_HUMAN	3.00E+06	1.61E+06	7.03E+05	4.19E+06	2.93E+06	7.38E+06	2.42E+05	0	200
Q9ULX6|AKP8L_HUMAN	4.53E+06	4.85E+06	3.29E+05	7.10E+05	4.67E+06	5.50E+06	0	0	200
Q9NR30|DDX21_HUMAN	5.67E+06	5.76E+06	9.67E+06	8.66E+06	5.47E+06	5.76E+06	0	0	200
Q9BQ67|GRWD1_HUMAN	1.93E+06	2.42E+06	2.42E+06	3.46E+06	3.54E+06	5.13E+06	1.37E+04	2.22E+04	200
P42677|RS27_HUMAN	4.59E+06	4.32E+06	2.55E+06	3.56E+06	5.53E+06	4.62E+06	0	0	200
P16403|H12_HUMAN	1.09E+06	1.42E+06	1.10E+06	1.93E+06	4.61E+06	4.22E+06	0	0	200
P31689|DNJA1_HUMAN	3.79E+06	2.94E+06	7.63E+05	1.64E+06	7.85E+06	3.71E+06	0	1.33E+05	200
O00571|DDX3X_HUMAN	5.06E+06	5.70E+06	4.44E+06	6.30E+06	2.24E+06	1.05E+07	0	3.54E+04	200
P17480|UBF1_HUMAN	2.53E+06	1.74E+06	1.72E+06	4.64E+06	4.03E+06	5.48E+06	0	0	200
P63244|RACK1_HUMAN	1.65E+06	1.23E+06	1.19E+05	6.03E+05	3.87E+06	5.12E+06	0	0	200

P61978|HNRPK_HUMAN	2.24E+06	1.61E+06	1.40E+06	1.56E+06	3.07E+06	5.05E+06	0	0	200
Q14974|IMB1_HUMAN	5.15E+06	4.61E+06	2.30E+06	3.42E+06	3.78E+06	5.11E+06	2.86E+04	4.49E+04	200
Q00839|HNRPU_HUMAN	5.81E+06	7.24E+06	9.20E+06	2.09E+07	3.61E+06	5.73E+06	0	0	200
Q14257|RCN2_HUMAN	7.21E+06	6.99E+06	2.87E+06	5.02E+06	5.21E+06	4.09E+06	0	0	200
Q9BZF1|OSBL8_HUMAN	6.61E+06	5.30E+06	3.62E+06	3.20E+06	3.87E+06	4.91E+06	0	0	200
Q99459|CDC5L_HUMAN	3.41E+06	3.64E+06	3.00E+06	4.08E+06	4.48E+06	4.00E+06	0	0	200
P62847|RS24_HUMAN	3.99E+06	3.86E+06	3.17E+06	5.39E+06	4.15E+06	3.99E+06	0	0	200
P31431|SDC4_HUMAN	5.21E+06	3.40E+06	1.96E+06	2.17E+06	2.19E+06	6.31E+06	0	0	200
Q13243|SRSF5_HUMAN	1.20E+06	5.88E+05	1.63E+06	1.90E+06	2.43E+06	3.35E+06	0	0	200
P22626|ROA2_HUMAN	3.16E+06	3.14E+06	2.80E+06	3.65E+06	2.90E+06	6.73E+06	0	0	200
P52294|IMA5_HUMAN	1.96E+06	2.01E+06	2.77E+06	4.88E+06	3.24E+06	3.82E+06	0	0	200
Q9UMS4|PRP19_HUMAN	3.14E+06	3.10E+06	3.03E+06	2.99E+06	3.51E+06	3.99E+06	0	0	200
Q9BV38|WDR18_HUMAN	4.49E+06	4.72E+06	4.01E+06	2.82E+06	3.40E+06	3.17E+06	0	0	200
Q9BVP2|GNL3_HUMAN	1.77E+06	2.56E+06	2.88E+06	4.14E+06	2.71E+06	4.81E+06	0	0	200
Q7Z2W4|ZCCHV_HUMAN	1.89E+06	1.85E+06	1.45E+06	2.16E+06	2.81E+06	4.05E+06	0	0	200
Q92841|DDX17_HUMAN	1.78E+06	1.96E+06	9.22E+05	9.78E+05	3.70E+06	3.51E+06	0	0	200
P26368|U2AF2_HUMAN	2.22E+06	2.46E+06	2.31E+06	2.93E+06	3.69E+06	5.15E+06	2.13E+04	1.21E+04	200
P50402|EMD_HUMAN	2.62E+06	3.37E+06	5.31E+05	1.05E+06	3.67E+06	3.03E+06	0	0	200
Q99613|EIF3C_HUMAN	3.95E+06	2.37E+06	0	1.96E+06	2.60E+06	3.56E+06	0	0	200
P60228|EIF3E_HUMAN	2.92E+06	2.90E+06	1.23E+06	1.32E+06	3.80E+06	3.23E+06	2.62E+04	0	200
Q16531|DDB1_HUMAN	1.23E+07	1.79E+07	2.95E+07	2.22E+07	1.96E+06	4.89E+06	8.23E+04	5.01E+04	200
O43390|HNRPR_HUMAN	1.71E+06	1.07E+06	1.94E+06	2.45E+06	2.72E+06	4.04E+06	1.83E+05	0	200
Q13310|PABP4_HUMAN	3.68E+06	2.36E+06	1.69E+06	2.03E+06	1.45E+06	4.72E+06	1.74E+04	0	200
Q8NC51|PAIRB_HUMAN	1.09E+06	2.30E+06	2.43E+06	4.38E+06	2.86E+06	2.69E+06	3.20E+03	1.14E+04	200
Q14498|RBM39_HUMAN	1.74E+06	1.93E+06	1.40E+06	2.25E+06	2.94E+06	2.89E+06	0	0	200
O95831|AIFM1_HUMAN	3.82E+06	3.50E+06	9.14E+05	9.33E+05	3.44E+06	2.89E+06	0	0	200
P55209|NP1L1_HUMAN	6.64E+06	9.02E+06	3.59E+06	3.52E+06	2.67E+06	3.98E+06	3.43E+04	1.70E+04	200
P62979|RS27A_HUMAN	3.09E+06	3.05E+06	2.84E+06	2.95E+06	2.84E+06	2.95E+06	0	0	200
Q9H0S4|DDX47_HUMAN	1.00E+06	1.42E+06	1.55E+06	1.98E+06	2.05E+06	2.46E+06	0	0	200
Q13501|SQSTM_HUMAN	1.39E+06	1.20E+06	4.81E+05	4.30E+05	2.85E+06	2.82E+06	0	0	200

Q13151|ROA0_HUMAN	1.11E+06	7.55E+05	1.05E+06	1.17E+06	2.58E+06	2.71E+06	0	0	200
P62318|SMD3_HUMAN	1.48E+06	1.44E+06	8.55E+05	1.62E+06	2.57E+06	2.83E+06	1.82E+04	6.92E+03	200
P49411|EFTU_HUMAN	1.68E+06	2.65E+06	2.01E+06	2.23E+06	2.15E+06	2.92E+06	0	0	200
P04637|P53_HUMAN	2.05E+06	1.33E+06	0	3.37E+05	2.09E+06	3.43E+06	0	0	200
O76021|RL1D1_HUMAN	1.54E+06	1.01E+06	1.06E+06	2.74E+06	3.14E+06	3.15E+06	0	0	200
P17812|PYRG1_HUMAN	2.21E+06	1.84E+06	1.54E+06	1.68E+06	2.13E+06	2.64E+06	0	2.41E+04	200
P12004|PCNA_HUMAN	1.92E+06	2.07E+06	1.38E+06	1.12E+06	2.28E+06	2.24E+06	7.35E+04	7.83E+04	200
Q13347|EIF3I_HUMAN	3.60E+06	2.99E+06	1.34E+06	1.78E+06	1.48E+06	3.78E+06	0	1.58E+04	200
Q99848|EBP2_HUMAN	4.48E+05	3.01E+05	2.70E+05	4.68E+05	1.77E+06	3.08E+06	0	0	200
Q9BW61|DDA1_HUMAN	1.22E+06	1.98E+06	6.61E+05	2.17E+06	2.80E+06	1.75E+06	0	0	200
P05455|LA_HUMAN	2.45E+06	3.23E+06	2.34E+06	3.79E+06	1.47E+06	3.21E+06	0	0	200
P67870|CSK2B_HUMAN	0	1.22E+06	1.67E+06	2.09E+06	1.78E+06	1.59E+06	0	0	200
P18827|SDC1_HUMAN	1.40E+06	1.14E+06	1.04E+06	0	1.93E+06	2.17E+06	0	0	200
Q9Y265|RUVB1_HUMAN	4.10E+06	3.00E+06	1.78E+06	2.17E+06	2.47E+06	2.60E+06	1.65E+04	9.10E+03	200
Q14137|BOP1_HUMAN	1.94E+06	1.56E+06	8.51E+05	1.04E+06	1.83E+06	1.62E+06	0	0	200
O43823|AKAP8_HUMAN	1.34E+06	1.44E+06	6.73E+05	5.30E+05	1.64E+06	2.12E+06	0	0	200
P62266|RS23_HUMAN	5.37E+06	7.19E+06	4.09E+06	5.14E+06	2.36E+06	2.73E+06	0	1.28E+05	200
Q9NVI7|ATD3A_HUMAN	2.83E+06	4.51E+06	1.44E+06	1.99E+06	1.68E+06	2.99E+06	9.85E+03	1.59E+04	200
Q9BWF3|RBM4_HUMAN	7.24E+05	8.98E+05	1.27E+06	1.94E+05	1.82E+06	1.85E+06	0	0	200
P48643|TCPE_HUMAN	1.66E+06	1.35E+06	6.26E+05	2.28E+05	2.25E+06	2.01E+06	0	0	200
P11387|TOP1_HUMAN	4.78E+05	3.86E+05	4.99E+05	7.03E+05	1.54E+06	1.65E+06	0	0	200
Q04637|IF4G1_HUMAN	2.26E+06	2.70E+06	0	5.57E+05	1.60E+06	2.83E+06	0	0	200
Q9H501|ESF1_HUMAN	3.48E+06	2.78E+06	2.81E+06	4.18E+06	1.49E+06	4.07E+06	0	0	200
Q9BUJ2|HNRL1_HUMAN	2.93E+06	1.81E+06	2.69E+06	3.53E+06	2.05E+06	2.09E+06	0	0	200
O15226|NKRF_HUMAN	1.03E+06	8.93E+05	9.25E+05	1.07E+06	2.14E+06	1.83E+06	0	0	200
Q9Y5A9|YTHD2_HUMAN	8.73E+05	1.34E+06	1.03E+06	9.75E+05	1.54E+06	1.72E+06	0	0	200
P43243|MATR3_HUMAN	1.11E+06	3.25E+05	1.36E+05	1.94E+05	1.57E+06	2.52E+06	0	0	200
Q9NPD3|EXOS4_HUMAN	7.37E+05	2.60E+05	1.04E+06	1.21E+06	1.55E+06	1.74E+06	0	0	200
Q9UJS0|CMC2_HUMAN	2.42E+06	2.70E+06	8.09E+05	2.19E+05	1.73E+06	2.27E+06	0	0	200
P55795|HNRH2_HUMAN	1.41E+06	1.48E+06	1.53E+06	7.08E+05	1.51E+06	1.55E+06	0	0	200

P07910|HNRPC_HUMAN	1.59E+06	7.54E+05	3.60E+05	3.01E+05	1.30E+06	1.57E+06	0	0	200
P30876|RPB2_HUMAN	2.67E+06	1.61E+06	6.55E+05	1.95E+05	1.45E+06	1.76E+06	0	0	200
Q8TDN6|BRX1_HUMAN	1.21E+06	1.41E+06	2.07E+06	2.27E+06	1.16E+06	2.94E+06	0	0	200
P38159|RBMX_HUMAN	1.14E+06	0	2.99E+05	7.72E+04	2.19E+06	4.90E+05	0	0	200
Q9BRJ6|CG050_HUMAN	0	6.31E+05	9.39E+05	1.10E+06	1.28E+06	1.41E+06	0	0	200
O75934|SPF27_HUMAN	2.75E+05	5.50E+05	1.80E+06	8.59E+05	1.66E+06	1.35E+06	0	0	200
Q00325|MPCP_HUMAN	3.49E+06	3.58E+06	2.01E+06	1.79E+06	1.72E+06	1.71E+06	0	0	200
P19388|RPAB1_HUMAN	1.08E+06	7.50E+05	4.52E+05	6.34E+05	1.65E+06	1.50E+06	0	0	200
P07900|HS90A_HUMAN	2.24E+06	2.08E+06	1.29E+05	1.90E+05	4.93E+05	2.55E+06	0	0	200
Q9H4L4|SENP3_HUMAN	2.56E+06	1.63E+06	1.90E+06	2.03E+06	1.66E+06	1.37E+06	0	0	200
Q9UJV9|DDX41_HUMAN	8.56E+05	1.25E+06	1.24E+06	1.48E+06	9.90E+05	1.99E+06	0	0	200
P46060|RAGP1_HUMAN	1.00E+06	6.10E+05	6.92E+05	5.86E+05	6.06E+05	1.86E+06	3.20E+04	1.71E+04	200
Q9UNK9|ANGE1_HUMAN	2.45E+06	9.65E+05	1.28E+06	8.46E+05	8.35E+05	1.92E+06	0	0	200
P11586|C1TC_HUMAN	1.68E+06	5.38E+06	4.04E+06	5.72E+06	7.25E+05	1.58E+06	3.99E+04	2.27E+04	200
O00743|PPP6_HUMAN	1.11E+06	1.05E+06	3.70E+05	2.97E+05	7.42E+05	1.77E+06	0	0	200
O43143|DHX15_HUMAN	2.61E+06	1.99E+06	1.49E+06	1.89E+06	1.09E+06	1.20E+06	0	0	200
O15372|EIF3H_HUMAN	2.51E+06	1.68E+06	9.80E+05	1.04E+06	7.64E+05	2.19E+06	0	0	200
O00303|EIF3F_HUMAN	2.19E+06	6.94E+05	5.02E+05	9.28E+05	1.22E+06	1.64E+06	0	0	200
P36542|ATPG_HUMAN	1.53E+06	1.45E+06	9.54E+05	1.16E+06	7.66E+05	1.29E+06	4.13E+04	4.55E+04	200
Q9Y262|EIF3L_HUMAN	1.31E+06	1.52E+06	3.64E+05	5.46E+05	5.68E+05	1.39E+06	0	0	200
P13639|EF2_HUMAN	1.03E+06	2.29E+06	9.86E+05	9.12E+05	1.60E+05	2.25E+06	0	0	200
O75821|EIF3G_HUMAN	3.99E+06	4.83E+06	1.48E+06	2.94E+06	2.47E+05	3.25E+06	0	0	200
P61964|WDR5_HUMAN	9.76E+05	7.15E+05	3.69E+05	6.87E+05	1.57E+06	2.38E+05	0	0	200
P12236|ADT3_HUMAN	2.94E+06	2.31E+06	1.31E+06	1.56E+06	1.05E+06	1.19E+06	2.12E+04	2.19E+04	200
P55072|TERA_HUMAN	3.05E+06	7.65E+05	6.09E+05	7.69E+05	1.29E+06	1.17E+06	0	0	200
P41091|IF2G_HUMAN	4.47E+05	5.42E+05	4.91E+05	3.80E+05	1.51E+06	7.82E+05	0	0	200
Q9Y285|SYFA_HUMAN	8.95E+05	1.09E+06	8.96E+05	9.31E+05	8.38E+05	1.52E+06	1.82E+04	4.02E+03	200
Q01780|EXOSX_HUMAN	6.36E+05	3.56E+05	6.57E+05	6.96E+05	9.44E+05	1.37E+06	0	0	200
P52434|RPAB3_HUMAN	1.33E+06	2.43E+06	5.78E+05	7.16E+05	9.74E+05	8.56E+05	0	0	200
P60891|PRPS1_HUMAN	5.51E+06	6.00E+05	2.13E+06	4.07E+06	1.21E+06	5.86E+05	0	0	200

Q13685|AAMP_HUMAN	0	6.97E+05	0	3.39E+05	1.01E+06	5.47E+05	0	0	200
O00425|IF2B3_HUMAN	4.21E+05	3.21E+05	1.10E+06	2.42E+05	5.59E+05	7.18E+05	0	3.82E+04	200
Q15020|SART3_HUMAN	2.06E+05	2.81E+05	2.03E+05	2.36E+05	8.06E+05	9.23E+05	0	0	200
P55884|EIF3B_HUMAN	4.87E+06	3.24E+06	1.58E+06	6.46E+05	5.45E+05	1.91E+06	2.02E+04	0	200
Q9NXV6|CARF_HUMAN	3.40E+05	5.87E+05	1.34E+05	1.35E+05	7.44E+05	7.91E+05	0	0	200
Q5RKV6|EXOS6_HUMAN	1.56E+05	9.55E+04	1.51E+05	6.50E+05	1.03E+06	3.95E+05	0	0	200
Q5JSZ5|PRC2B_HUMAN	1.99E+06	9.02E+05	4.38E+05	2.71E+05	7.33E+05	1.25E+06	0	0	200
P82650|RT22_HUMAN	2.34E+05	1.86E+05	1.24E+05	2.23E+05	9.45E+05	1.03E+06	0	0	200
Q9Y5Q8|TF3C5_HUMAN	1.16E+06	7.82E+05	3.85E+05	5.26E+05	5.33E+05	1.45E+06	0	0	200
O75190|DNJB6_HUMAN	1.46E+06	1.43E+06	8.21E+05	8.41E+05	1.40E+06	6.75E+05	0	0	200
P17987|TCPA_HUMAN	2.05E+06	1.53E+06	7.52E+05	1.71E+06	2.24E+05	1.39E+06	4.04E+04	2.54E+04	200
O15084|ANR28_HUMAN	1.18E+05	0	0	0	5.16E+05	1.00E+06	0	0	200
Q9Y2R4|DDX52_HUMAN	9.89E+05	1.03E+06	1.16E+06	1.53E+06	4.99E+05	1.42E+06	0	0	200
P14923|PLAK_HUMAN	5.83E+05	2.23E+05	1.59E+06	2.41E+05	7.41E+05	1.08E+06	1.08E+04	1.46E+04	200
P63220|RS21_HUMAN	3.50E+05	3.09E+05	0	0	3.06E+05	6.37E+05	0	0	200
P13010|XRCC5_HUMAN	3.52E+05	4.02E+05	8.09E+05	7.97E+05	5.29E+05	1.67E+06	0	0	200
Q9BSD7|NTPCR_HUMAN	4.28E+05	1.87E+05	2.01E+05	8.02E+05	8.81E+05	5.27E+05	1.79E+04	8.50E+03	200
O75643|U520_HUMAN	7.79E+04	5.55E+05	2.02E+05	9.12E+05	7.87E+05	1.15E+06	0	0	200
P61927|RL37_HUMAN	5.33E+05	5.38E+05	3.04E+05	7.91E+05	1.06E+06	5.40E+05	0	0	200
Q9UG63|ABCF2_HUMAN	2.84E+06	1.69E+05	1.74E+06	3.17E+06	4.99E+05	1.49E+06	0	0	200
Q9BYG3|MK67I_HUMAN	1.23E+05	2.58E+05	0	3.42E+05	3.96E+05	1.15E+06	0	0	200
Q9NVP1|DDX18_HUMAN	0	9.35E+05	7.94E+05	1.09E+06	4.01E+05	4.77E+05	0	0	200
Q6DKI1|RL7L_HUMAN	7.94E+05	1.24E+05	2.13E+05	0	1.08E+06	3.87E+05	0	0	200
Q9Y3I0|RTCB_HUMAN	8.71E+05	8.22E+05	1.02E+05	3.01E+05	6.03E+05	6.37E+05	0	0	200
Q15029|U5S1_HUMAN	1.61E+05	5.32E+05	0	1.92E+05	6.38E+05	3.51E+05	0	0	200
O60684|IMA7_HUMAN	0	8.20E+05	2.81E+06	5.01E+06	4.76E+05	7.14E+05	0	0	200
P50991|TCPD_HUMAN	1.27E+06	3.03E+05	3.99E+05	5.21E+05	9.96E+04	1.29E+06	0	4.95E+03	200
P36954|RPB9_HUMAN	3.55E+05	4.99E+05	5.79E+05	5.88E+05	4.34E+05	7.37E+05	0	0	200
Q5SY16|NOL9_HUMAN	2.91E+06	1.31E+06	6.73E+05	9.54E+05	2.76E+05	9.25E+05	0	0	200
P11177|ODPB_HUMAN	4.68E+05	2.57E+05	1.43E+05	3.58E+04	5.73E+05	7.56E+05	0	0	200

O95071|UBR5_HUMAN	7.24E+05	6.16E+05	2.62E+05	1.79E+05	2.85E+05	7.81E+05	0	0	200
P43686|PRS6B_HUMAN	2.11E+05	1.27E+05	5.97E+04	8.26E+04	3.40E+04	1.41E+06	0	0	200
P42285|SK2L2_HUMAN	6.57E+05	2.28E+05	7.14E+05	2.10E+03	4.82E+05	3.13E+05	0	0	200
Q9C0C9|UBE2O_HUMAN	8.75E+05	9.84E+05	3.33E+05	8.51E+05	1.28E+05	6.14E+05	0	0	200
Q99832|TCPH_HUMAN	5.20E+05	5.20E+05	9.14E+05	7.95E+05	3.39E+04	6.09E+05	0	0	200
Q8NB90|SPAT5_HUMAN	1.48E+05	4.03E+05	1.65E+05	2.07E+05	2.72E+05	2.04E+05	0	0	200
P27708|PYR1_HUMAN	8.50E+05	5.15E+05	2.24E+05	0	8.66E+04	3.57E+05	0	0	200
O75400|PR40A_HUMAN	2.12E+04	3.74E+05	0	6.32E+04	4.23E+05	0	0	0	200
Q06265|EXOS9_HUMAN	4.02E+05	3.75E+05	3.45E+05	2.68E+05	0	0	0	0	200
O14654|IRS4_HUMAN	1.33E+06	2.98E+06	6.90E+05	1.56E+05	1.13E+06	1.99E+06	0	0	139.81
P62241|RS8_HUMAN	1.29E+07	7.73E+06	1.00E+07	1.17E+07	1.15E+07	1.27E+07	3.16E+05	1.83E+05	135.6
O00267|SPT5H_HUMAN	2.51E+07	8.46E+06	5.27E+06	5.15E+06	3.55E+06	3.67E+06	0	0	133.79
P46782|RS5_HUMAN	1.30E+07	1.19E+07	1.25E+07	1.88E+07	7.55E+06	2.16E+07	6.31E+04	5.68E+04	121.92
P06730|IF4E_HUMAN	1.78E+06	2.84E+05	2.87E+05	7.18E+05	5.19E+05	1.96E+06	1.81E+04	0	120.93
Q92688|AN32B_HUMAN	4.88E+06	7.67E+06	7.20E+06	1.11E+07	3.20E+06	4.89E+06	0	0	118.88
P46776|RL27A_HUMAN	6.04E+06	2.13E+06	1.06E+07	2.25E+07	1.03E+07	9.88E+06	0	0	115.82
Q7Z6Z7|HUWE1_HUMAN	1.18E+06	2.68E+05	0	5.13E+05	6.24E+05	8.51E+05	0	0	110.16
P10412|H14_HUMAN	2.05E+06	2.26E+06	1.60E+06	2.80E+06	6.41E+06	7.63E+06	1.85E+04	0	93.11
P49368|TCPG_HUMAN	1.08E+06	3.00E+05	2.88E+05	0	1.36E+06	1.95E+06	0	0	92.92
O95816|BAG2_HUMAN	1.55E+06	1.26E+06	0	6.48E+05	6.31E+05	1.55E+06	0	0	92.15
P17980|PRS6A_HUMAN	4.15E+05	1.73E+05	0	0	2.18E+05	6.70E+05	0	0	90.37
Q96EY1|DNJA3_HUMAN	1.08E+06	5.46E+05	0	8.06E+05	2.75E+06	3.25E+06	0	0	87.69
P05386|RLA1_HUMAN	1.97E+07	2.35E+07	4.60E+07	6.46E+07	2.63E+07	7.54E+07	1.97E+05	2.62E+05	86.38
Q8NDA2|HMCN2_HUMAN	1.21E+06	2.58E+06	1.89E+06	2.11E+06	2.99E+05	1.75E+05	0	0	84.04
Q96HN2|SAHH3_HUMAN	1.19E+06	1.24E+06	0	0	4.50E+04	0	0	0	81.89
Q9P258|RCC2_HUMAN	1.48E+06	4.39E+05	1.19E+06	4.12E+05	4.28E+05	8.47E+05	1.71E+04	1.28E+04	81.48
Q08211|DHX9_HUMAN	4.66E+06	6.26E+06	1.68E+07	1.18E+07	1.87E+06	3.19E+06	0	0	78.44
Q9BPZ3|PAIP2_HUMAN	0	5.84E+05	2.20E+05	3.52E+05	2.94E+05	1.11E+06	0	0	68.92
Q9UBQ5|EIF3K_HUMAN	3.01E+06	1.21E+06	6.66E+05	9.07E+05	2.37E+06	3.33E+06	0	0	67.05
O95905|ECD_HUMAN	0	2.73E+05	8.64E+04	7.38E+04	0	0	0	0	61.8

Q92522|H1X_HUMAN	7.20E+06	9.57E+05	1.51E+06	2.50E+06	8.60E+06	3.97E+06	0	0	57.37
O75487|GPC4_HUMAN	9.78E+05	4.31E+05	3.46E+05	2.53E+05	3.04E+06	4.68E+06	0	0	51.84
P18621|RL17_HUMAN	6.31E+06	3.40E+06	6.04E+06	8.30E+06	8.92E+06	8.64E+06	0	0	51.54
Chicken_ANP32A_flag	1.05E+06	2.83E+06	3.92E+07	7.41E+07	0	0	2.29E+05	7.45E+04	50.62
O95373|IPO7_HUMAN	3.06E+05	3.11E+05	0	5.38E+04	4.50E+04	1.78E+05	0	0	50.51
Q5T9A4|ATD3B_HUMAN	3.58E+06	1.72E+06	1.28E+06	0	1.88E+06	4.20E+06	0	0	50.26
Q9Y3U8|RL36_HUMAN	2.76E+06	2.54E+06	3.55E+06	5.68E+06	1.01E+07	8.95E+06	0	0	49.01
O15027|SC16A_HUMAN	1.15E+06	2.36E+06	3.04E+05	1.03E+05	2.18E+06	1.80E+06	0	0	47.98
P62861|RS30_HUMAN	1.09E+06	5.32E+05	4.81E+05	9.61E+05	1.77E+06	2.26E+06	0	0	47.78
P07814|SYEP_HUMAN	1.36E+06	5.83E+05	9.14E+05	5.77E+05	0	5.82E+05	0	0	47.33
Human_ANP32A_+33_flag	6.19E+05	1.35E+06	1.30E+06	3.28E+06	7.44E+05	3.66E+06	0	0	47.31
Q9Y5V3|MAGD1_HUMAN	9.04E+06	2.16E+07	1.02E+07	1.20E+07	7.57E+06	1.08E+07	0	0	47.15
Q9UKA4|AKA11_HUMAN	7.67E+05	1.65E+06	2.24E+05	4.87E+05	7.35E+05	3.36E+05	0	0	46.8
P33993|MCM7_HUMAN	1.52E+06	7.56E+05	6.82E+05	1.31E+06	8.23E+05	2.37E+06	2.21E+04	1.63E+04	46.2
P68363|TBA1B_HUMAN	2.38E+06	1.56E+07	1.09E+07	1.00E+07	1.54E+07	2.21E+07	5.26E+05	3.94E+05	45.88
P84098|RL19_HUMAN	1.31E+06	1.28E+06	3.00E+06	5.69E+06	7.71E+06	6.40E+06	0	0	45.84
Q00577|PURA_HUMAN	7.93E+04	3.52E+05	2.65E+05	0	8.17E+05	1.46E+06	0	0	45.32
O43719|HTSF1_HUMAN	1.11E+06	5.37E+05	8.05E+05	1.14E+06	8.17E+05	5.17E+05	0	0	44.44
Q07955|SRSF1_HUMAN	1.22E+06	1.13E+06	9.17E+05	1.79E+06	3.53E+06	3.10E+06	0	0	43.34
Q14684|RRP1B_HUMAN	6.81E+05	8.82E+05	1.26E+06	1.27E+06	3.39E+06	3.77E+06	0	0	42.71
P47914|RL29_HUMAN	1.04E+06	7.80E+05	1.65E+06	2.31E+06	4.37E+06	3.25E+06	0	0	42.33
Q99729|ROAA_HUMAN	8.63E+05	1.59E+06	1.12E+06	1.83E+06	1.23E+06	2.10E+06	3.10E+03	0	41.74
P04259|K2C6B_HUMAN	6.61E+05	2.84E+06	0	0	0	6.05E+05	0	3.46E+04	41.59
Q13263|TIF1B_HUMAN	1.43E+06	1.55E+06	1.27E+06	1.38E+06	3.37E+06	5.57E+06	0	0	41.05
Q14103|HNRPD_HUMAN	1.28E+06	1.08E+06	2.00E+06	2.34E+06	3.20E+06	4.41E+06	0	0	41.05
O60884|DNJA2_HUMAN	1.40E+06	3.31E+06	2.94E+06	2.98E+06	2.07E+06	1.96E+06	6.69E+04	3.70E+04	38.07
Q6PKG0|LARP1_HUMAN	1.31E+06	1.66E+06	1.51E+06	1.34E+06	1.05E+06	3.49E+06	0	0	37.35
Q9Y3B9|RRP15_HUMAN	0	0	6.55E+04	3.67E+05	1.28E+06	1.28E+06	0	0	37.11
Q9NVN8|GNL3L_HUMAN	9.30E+04	7.72E+05	7.59E+05	1.27E+06	1.24E+05	2.48E+05	0	0	37.05
Q96CS3|FAF2_HUMAN	2.12E+05	7.20E+05	0	0	0	2.34E+05	0	0	36.97

P09661|RU2A_HUMAN	1.25E+06	1.73E+06	1.87E+06	2.53E+06	1.57E+06	1.75E+06	0	0	36.68
Q9BTT0|AN32E_HUMAN	2.16E+05	1.51E+05	7.44E+05	2.05E+06	0	6.73E+05	0	0	35.93
O60506|HNRPQ_HUMAN	7.33E+05	9.52E+05	1.05E+06	9.58E+05	7.04E+05	2.27E+06	1.45E+04	8.72E+03	35.87
Q9H7E9|CH033_HUMAN	1.52E+06	1.57E+06	3.09E+06	3.43E+06	4.60E+06	6.07E+06	0	0	35.58
Q15233|NONO_HUMAN	4.03E+05	3.04E+05	9.46E+05	1.65E+06	8.29E+05	8.95E+05	0	0	35.24
P05089|ARGI1_HUMAN	0	0	0	0	0	4.76E+06	0	0	34.94
P04406|G3P_HUMAN	5.42E+05	0	0	0	0	4.14E+06	0	0	34.16
Q5JTC6|AMER1_HUMAN	0	2.24E+05	0	0	6.39E+05	2.04E+06	0	0	33.52
Q9NW13|RBM28_HUMAN	6.27E+05	4.14E+05	6.03E+05	8.44E+05	1.52E+06	1.78E+06	0	0	33.2
P30153|2AAA_HUMAN	6.30E+05	5.19E+05	4.44E+05	9.94E+05	5.01E+05	8.80E+05	0	0	33.15
Q96SB4|SRPK1_HUMAN	0	0	3.17E+05	4.62E+05	5.36E+05	5.44E+05	0	0	33.08
Q9UKN8|TF3C4_HUMAN	1.64E+05	1.54E+05	0	0	3.79E+05	5.24E+05	0	0	33
Q8IXB1|DJC10_HUMAN	2.29E+05	4.41E+05	3.80E+04	0	6.60E+05	8.69E+05	1.40E+04	0	32.96
P35251|RFC1_HUMAN	3.01E+05	2.31E+05	5.95E+05	4.88E+05	7.20E+05	9.28E+05	0	0	32.93
P19387|RPB3_HUMAN	4.54E+05	2.41E+05	9.64E+05	6.86E+05	1.21E+06	1.19E+06	0	0	32.68
P13995|MTDC_HUMAN	8.76E+05	1.79E+06	8.13E+05	1.67E+06	1.81E+06	3.42E+06	0	0	32.58
Q13868|EXOS2_HUMAN	9.49E+04	6.83E+04	4.32E+05	2.85E+05	2.11E+05	4.15E+05	0	0	32.43
P41252|SYIC_HUMAN	4.04E+05	5.86E+05	2.66E+05	5.56E+05	1.58E+05	3.23E+05	0	0	31.64
Q9UPY3|DICER_HUMAN	3.30E+05	3.32E+05	8.58E+05	3.89E+05	0	0	0	0	31.48
Q13325|IFIT5_HUMAN	5.94E+05	1.51E+06	1.60E+05	5.14E+05	7.76E+04	7.53E+04	0	0	31.47
Q9Y2R5|RT17_HUMAN	5.50E+05	6.37E+05	6.11E+05	5.67E+05	4.33E+05	1.68E+06	0	1.91E+04	31.26
Q969S3|ZN622_HUMAN	2.06E+05	2.49E+05	0	4.35E+05	7.81E+04	2.74E+04	0	0	31.24
Q13148|TADBP_HUMAN	5.58E+05	2.07E+05	2.60E+05	1.64E+05	1.16E+05	6.26E+05	0	0	30.86
Q02413|DSG1_HUMAN	1.40E+05	4.38E+05	1.04E+06	4.97E+05	4.33E+05	2.88E+05	1.94E+04	0	30.8
P49790|NU153_HUMAN	1.18E+05	8.73E+04	1.92E+05	1.69E+05	0	3.16E+05	0	0	30.77
Q8IY81|SPB1_HUMAN	0	1.64E+05	2.31E+05	4.93E+05	6.54E+05	1.47E+06	0	0	30.73
Q12849|GRSF1_HUMAN	1.60E+05	1.82E+06	2.92E+06	3.90E+06	1.74E+06	7.86E+05	0	0	30.23
P16989|YBOX3_HUMAN	1.40E+06	2.26E+06	1.06E+06	1.16E+06	1.65E+06	1.66E+06	0	0	30.21
Q9NXF1|TEX10_HUMAN	8.96E+05	4.19E+05	3.07E+05	1.62E+06	7.00E+05	2.43E+06	0	0	30.21
Q2NL82|TSR1_HUMAN	2.79E+05	5.28E+05	7.14E+05	1.18E+06	6.84E+05	1.68E+06	0	0	30

Q9UNS2|CSN3_HUMAN	1.17E+06	4.12E+05	6.43E+05	2.86E+05	3.26E+05	1.58E+06	0	0	29.37
P56192|SYMC_HUMAN	2.39E+05	1.50E+05	0	1.32E+05	2.75E+05	2.09E+06	0	0	29.29
Q9HC36|MRM3_HUMAN	0	0	0	0	1.90E+05	0	0	0	29.12
Q5T3I0|GPTC4_HUMAN	1.04E+06	7.49E+05	2.05E+06	2.02E+05	3.25E+06	9.06E+05	0	0	28.78
P23246|SFPQ_HUMAN	1.13E+06	4.64E+05	7.43E+05	9.55E+05	8.61E+05	9.29E+05	1.05E+05	0	28.78
Q8IXW5|RPAP2_HUMAN	1.28E+06	1.37E+06	0	0	1.63E+06	2.04E+06	0	1.12E+05	28.69
Q9Y3D9|RT23_HUMAN	0	1.81E+05	6.12E+04	1.61E+05	7.16E+05	3.07E+05	0	0	28.42
P41250|GARS_HUMAN	2.34E+05	0	0	8.27E+04	2.10E+05	3.34E+05	0	0	28.06
P17612|KAPCA_HUMAN	4.94E+05	5.30E+05	2.02E+05	8.08E+04	3.24E+05	1.36E+06	0	0	27.74
Q6P1J9|CDC73_HUMAN	5.46E+05	3.12E+05	2.99E+05	5.58E+05	3.79E+05	5.90E+05	0	0	27.22
P33176|KINH_HUMAN	7.34E+05	4.75E+05	2.51E+05	2.30E+05	4.85E+05	6.71E+05	0	0	27.18
Q99615|DNJC7_HUMAN	6.66E+05	3.87E+05	0	0	0	0	0	0	26.39
Q02978|M2OM_HUMAN	1.64E+06	1.24E+06	7.70E+05	8.88E+05	1.88E+06	1.77E+06	0	0	25.78
Q7L2H7|EIF3M_HUMAN	2.26E+06	2.35E+06	2.23E+06	1.85E+06	1.08E+06	2.46E+06	0	0	24.42
Q9UN86|G3BP2_HUMAN	9.06E+05	1.13E+06	5.88E+05	5.40E+05	1.02E+06	1.21E+06	0	0	24.27
P20042|IF2B_HUMAN	0	0	0	0	4.46E+05	1.03E+05	0	0	24.2
Q8TEX9|IPO4_HUMAN	1.88E+05	1.13E+05	0	0	8.79E+04	6.05E+04	0	0	23.84
Q9UHX1|PUF60_HUMAN	1.84E+05	2.50E+05	2.92E+05	1.55E+06	7.10E+05	9.34E+05	0	0	23.75
P22087|FBRL_HUMAN	0	6.22E+04	9.25E+04	1.28E+05	1.19E+06	1.08E+06	0	0	23.7
P25205|MCM3_HUMAN	8.15E+05	2.04E+06	2.49E+06	6.16E+05	1.05E+06	2.83E+06	0	0	23.27
Q9BQ39|DDX50_HUMAN	2.37E+05	1.65E+05	1.51E+05	6.87E+05	4.00E+05	1.96E+06	0	0	22.84
Q9UKD2|MRT4_HUMAN	1.10E+06	9.90E+05	2.43E+06	2.47E+06	1.98E+05	1.77E+06	0	0	22.82
P09038|FGF2_HUMAN	1.92E+05	1.37E+05	1.48E+05	0	5.95E+05	2.95E+05	0	0	22.48
P23588|IF4B_HUMAN	0	7.37E+05	6.41E+05	0	8.84E+05	1.45E+05	0	0	22.15
Q96B26|EXOS8_HUMAN	0	0	7.01E+05	7.32E+05	1.17E+06	1.29E+06	0	0	21.83
Q01130|SRSF2_HUMAN	5.32E+05	4.54E+05	6.59E+05	8.18E+05	1.17E+06	4.74E+05	0	3.40E+03	21.8
Q9H2U1|DHX36_HUMAN	1.34E+05	1.36E+05	1.97E+05	3.85E+04	5.79E+04	0	0	0	21.76
Q16629|SRSF7_HUMAN	4.26E+05	0	0	0	1.17E+06	9.06E+05	0	0	21.55
Q9Y3Y2|CHTOP_HUMAN	0	7.77E+04	3.44E+05	6.01E+05	1.38E+06	1.10E+06	0	0	21.39
Q9BY77|PDIP3_HUMAN	1.79E+05	2.63E+05	0	2.59E+05	4.09E+05	4.59E+05	0	0	20.59

Appendix B

List of proteins represented in each section of the Venn diagram in Figure 32.

Pol 627E = Pol 627E chANP32A = Pol 627K		
P55084|ECHB_HUMAN	P62979|RS27A_HUMAN	P09661|RU2A_HUMAN
O00505|IMA4_HUMAN	P49411|EFTU_HUMAN	P30153|2AAA_HUMAN
P15880|RS2_HUMAN	P17812|PYRG1_HUMAN	P41252|SYIC_HUMAN
P61247|RS3A_HUMAN	P05455|LA_HUMAN	P23246|SFPQ_HUMAN
P23396|RS3_HUMAN	Q9Y265|RUVB1_HUMAN	Q6P1J9|CDC73_HUMAN
P39023|RL3_HUMAN	P62266|RS23_HUMAN	Q7L2H7|EIF3M_HUMAN
P40429|RL13A_HUMAN	Q9H501|ESF1_HUMAN	
P62753|RS6_HUMAN	Q9BUJ2|HNRL1_HUMAN	
O15355|PPM1G_HUMAN	Q9H4L4|SENP3_HUMAN	
Q9H0A0|NAT10_HUMAN	Q9UJV9|DDX41_HUMAN	
O00410|IPO5_HUMAN	O43143|DHX15_HUMAN	
P83881|RL36A_HUMAN	P36542|ATPG_HUMAN	
Q12906|ILF3_HUMAN	P12236|ADT3_HUMAN	
Q9NR30|DDX21_HUMAN	Q9Y285|SYFA_HUMAN	
O00571|DDX3X_HUMAN	Q9Y2R4|DDX52_HUMAN	
Q14974|IMB1_HUMAN	P36954|RPB9_HUMAN	
Q9BZF1|OSBL8_HUMAN	P62241|RS8_HUMAN	
Q99459|CDC5L_HUMAN	P46782|RS5_HUMAN	
P62847|RS24_HUMAN	Q92688|AN32B_HUMAN	
Q9UMS4|PRP19_HUMAN	O43719|HTSF1_HUMAN	
Q9BV38|WDR18_HUMAN	Q99729|ROAA_HUMAN	

Pol 627E > Pol 627E chANP32A AND Pol 627K	Pol 627E chANP32A > Pol 627E AND Pol 627K	Pol 627K > Pol 627E AND Pol 627E chANP32A	
Q96HN2|SAHH3_HUMAN	O60684|IMA7_HUMAN	P06748|NPM_HUMAN	Q16629|SRSF7_HUMAN
P04259|K2C6B_HUMAN	Q9BTT0|AN32E_HUMAN	P18124|RL7_HUMAN	Q7Z2W4|ZCCHV_HUMAN
Q96CS3|FAF2_HUMAN		P36578|RL4_HUMAN	Q13151|ROA0_HUMAN
Q13325|IFIT5_HUMAN		P52272|HNRPM_HUMAN	P62318|SMD3_HUMAN
Q99615|DNJC7_HUMAN		P05388|RLA0_HUMAN	Q99848|EBP2_HUMAN
		P30050|RL12_HUMAN	P11387|TOP1_HUMAN
		P62424|RL7A_HUMAN	P62258|1433E_HUMAN
		P62913|RL11_HUMAN	O15226|NKRF_HUMAN
		P62906|RL10A_HUMAN	P38159|RBMX_HUMAN
		Q07020|RL18_HUMAN	P19388|RPAB1_HUMAN
		P09651|ROA1_HUMAN	Q15020|SART3_HUMAN
		P35268|RL22_HUMAN	P82650|RT22_HUMAN
		P62280|RS11_HUMAN	O15084|ANR28_HUMAN
		P34741|SDC2_HUMAN	Q9BYG3|MK67I_HUMAN
		P08865|RSSA_HUMAN	P10412|H14_HUMAN
		P83731|RL24_HUMAN	Q96EY1|DNJA3_HUMAN
		Q86V81|THOC4_HUMAN	Q9BPZ3|PAIP2_HUMAN
		P31943|HNRH1_HUMAN	P62861|RS30_HUMAN
		P61513|RL37A_HUMAN	Q00577|PURA_HUMAN
		P42766|RL35_HUMAN	Q07955|SRSF1_HUMAN
		Q9NZI8|IF2B1_HUMAN	Q14684|RRP1B_HUMAN
		P62244|RS15A_HUMAN	Q13263|TIF1B_HUMAN
		Q96PK6|RBM14_HUMAN	Q5JTC6|AMER1_HUMAN
		P63272|SPT4H_HUMAN	Q9NW13|RBM28_HUMAN
		Q15365|PCBP1_HUMAN	P48047|ATPO_HUMAN
		P46087|NOP2_HUMAN	P20042|IF2B_HUMAN
		P61254|RL26_HUMAN	P22087|FBRL_HUMAN
		P16403|H12_HUMAN	Q9BQ39|DDX50_HUMAN

Pol 627E AND Pol 627E chANP32A > Pol 627K	Pol 627E AND Pol 627K > Pol 627E chANP32A		Pol 627E chANP32A AND pol 627K > pol 627E
Q16531|DDB1_HUMAN	P11940|PABP1_HUMAN	Q5T9A4|ATD3B_HUMAN	P46776|RL27A_HUMAN
Q06265|EXOS9_HUMAN	Q9ULX6|AKP8L_HUMAN	O15027|SC16A_HUMAN	P05386|RLA1_HUMAN
Q8NDA2|HMCN2_HUMAN	P31689|DNJA1_HUMAN	Q9UKN8|TF3C4_HUMAN	P84098|RL19_HUMAN
Q9UPY3|DICER_HUMAN	P63244|RACK1_HUMAN	Q8IXB1|DJC10_HUMAN	Q9Y3B9|RRP15_HUMAN
	P50402|EMD_HUMAN	Q8IXW5|RPAP2_HUMAN	Q15233|NONO_HUMAN
	P60228|EIF3E_HUMAN	P17612|KAPCA_HUMAN	Q96SB4|SRPK1_HUMAN
	O95831|AIFM1_HUMAN	P33176|KINH_HUMAN	P19387|RPB3_HUMAN
	Q13501|SQSTM_HUMAN	Q8TEX9|IPO4_HUMAN	Q13868|EXOS2_HUMAN
	P04637|P53_HUMAN		Q8IY81|SPB1_HUMAN
	P48643|TCPE_HUMAN		Q2NL82|TSR1_HUMAN
	Q04637|IF4G1_HUMAN		Q96B26|EXOS8_HUMAN
	Q9UJS0|CMC2_HUMAN		Q9Y3Y2|CHTOP_HUMAN
	P60842|IF4A1_HUMAN		
	P07910|HNRPC_HUMAN		
	P30876|RPB2_HUMAN		
	P07900|HS90A_HUMAN		
	O00743|PPP6_HUMAN		
	Q9NXV6|CARF_HUMAN		
	Q5JSZ5|PRC2B_HUMAN		
	P63220|RS21_HUMAN		
	Q6DKI1|RL7L_HUMAN		
	Q9Y3I0|RTCB_HUMAN		
	Q15029|U5S1_HUMAN		
	P11177|ODPB_HUMAN		
	P49368|TCPG_HUMAN		
	O95816|BAG2_HUMAN		
	P17980|PRS6A_HUMAN		
	O95373|IPO7_HUMAN		

Pol 627E > Pol 627E chANP32A only	**Pol 627E > Pol 627K only**	**Pol 627E chANP32A > Pol 627E only**	**Pol 627E chANP32A > Pol 627K only**
Q9Y262|EIF3L_HUMAN P55884|EIF3B_HUMAN O95071|UBR5_HUMAN P27708|PYR1_HUMAN Q9UKA4|AKA11_HUMAN O75400|PR40A_HUMAN P55884|EIF3B_HUMAN	O00267|SPT5H_HUMAN Q13148|TADBP_HUMAN Q9H2U1|DHX36_HUMAN	Q9UKD2|MRT4_HUMAN	P11586|C1TC_HUMAN Q08211|DHX9_HUMAN O95905|ECD_HUMAN Q9NVN8|GNL3L_HUMAN

Pol 627K > Pol 627E only	Pol 627K > Pol 627E chANP32A only
P50914|RL14_HUMAN	Q8IZL8|PELP1_HUMAN
P26373|RL13_HUMAN	P46783|RS10_HUMAN
P62888|RL30_HUMAN	Q9Y230|RUVB2_HUMAN
P62917|RL8_HUMAN	O15371|EIF3D_HUMAN
P62910|RL32_HUMAN	Q92896|GSLG1_HUMAN
P62750|RL23A_HUMAN	Q13610|PWP1_HUMAN
P49207|RL34_HUMAN	Q92841|DDX17_HUMAN
Q02543|RL18A_HUMAN	Q99613|EIF3C_HUMAN
Q02878|RL6_HUMAN	P12004|PCNA_HUMAN
P61313|RL15_HUMAN	P18827|SDC1_HUMAN
Q16778|H2B2E_HUMAN	O43823|AKAP8_HUMAN
Q9BQ67|GRWD1_HUMAN	O00303|EIF3F_HUMAN
Q13243|SRSF5_HUMAN	P41091|IF2G_HUMAN
P52294|IMA5_HUMAN	Q13685|AAMP_HUMAN
P26368|U2AF2_HUMAN	O14654|IRS4_HUMAN
O43390|HNRPR_HUMAN	P06730|IF4E_HUMAN
Q9NPD3|EXOS4_HUMAN	Q9UBQ5|EIF3K_HUMAN
Q9BRJ6|CG050_HUMAN	P56192|SYMC_HUMAN
O75934|SPF27_HUMAN	Q9Y3D9|RT23_HUMAN
Q01780|EXOSX_HUMAN	Q02978|M2OM_HUMAN
Q5RKV6|EXOS6_HUMAN	Q9UN86|G3BP2_HUMAN
O75643|U520_HUMAN	
Q9Y3U8|RL36_HUMAN	
Q9UHX1|PUF60_HUMAN	